Eindhoven University of Technology

MASTER

Timber Concrete composite floor slab on point supports

van Maanen, Jan-Willem

Award date:
2024

Link to publication

Disclaimer
This document contains a student thesis (bachelor's or master's), as authored by a student at Eindhoven University of Technology. Student theses are made available in the TU/e repository upon obtaining the required degree. The grade received is not published on the document as presented in the repository. The required complexity or quality of research of student theses may vary by program, and the required minimum study period may vary in duration.

General rights
Copyright and moral rights for the publications made accessible in the public portal are retained by the authors and/or other copyright owners and it is a condition of accessing publications that users recognise and abide by the legal requirements associated with these rights.

- Users may download and print one copy of any publication from the public portal for the purpose of private study or research.
- You may not further distribute the material or use it for any profit-making activity or commercial gain

EINDHOVEN UNIVERSITY OF TECHNOLOGY

Department of the Built Environment
Structural Engineering

Timber Concrete composite floor slab on point supports

Master Thesis Report

ing. Jan-Willem van Maanen

Supervisors:
dr.ir. Faas S.P.G. Moonen
ir. Arjan P.H.W. Habraken
ir. Anton I.A. van der Esch

04-11-2023

LIST OF SYMBOLS AND ABBREVIATIONS

Symbols

Latin, lowercase letters

a	Distance of the center of the layer to the calculated center
a_c	Distance of the center of the concrete to the calculated center
a_t	Distance of the center of the timber to the calculated center
b	Width of the individual layer
h_c	Height of the concrete
h_i	Height of the individual layer
h_t	Height of the timber
k_i	Slip modulus of layer i
k_s	Slip modulus
l	Length of the TCC floor slab
s_{eff}	Effective center-to-center distance of the connector
s_i	Center-to-center distance of the connector
v_{04}	Slip measurement at 40% of the maximum estimated load
v_{01}	Slip measurement at 10% of the maximum estimated load
$v_{i,i}$	Factor of the influence of layer and the shear connection or perpendicular combined
$v_{i+1,i}$	Factor of the influence of the shear connection or perpendicular combined above this layer
$v_{i,i+1}$	Factor of the influence of the shear connection or perpendicular combined below this layer
$v_{i,mod}$	Modified initial slip

Latin, capital letters

A_c	Area of concrete
A_i	Area of layer i
$C_{j,k}$	Distributed stiffness of the shear connector or the perpendicular layer
D_i	Stiffness of the layer parallel to the span of the floor
EA_c	Bending stiffness of the concrete
E_c	Elastic modulus of concrete
E_i	Young's modulus of the i-th layer
EI_{CLT}	Bending stiffness of the CLT floor slab
EI_c	Bending stiffness of the concrete
EI_{eff}	Effective bending stiffness of the entire TCC floor slab
EI_i	Bending stiffness of the individual layer i

EI_{layer}	Effective bending stiffness of the individual layer of the TCC floor slab
EI_t	Bending stiffness of the timber
F_{est}	The estimated maximum load
G_r	Rolling shear of the layer perpendicular to the main direction
I_i	Moment of inertia of the layer i
S_i	Influence of the shear connector or perpendicular layer on this layer

Greek symbols

γ	Gamma factor
γ_i	Gamma factor of the i layer of the TCC floor slab
γ_c	Gamma factor of the concrete
γ_t	Gamma factor of the timber

Abstract

The timber concrete composite (TCC) floor slab is usually a floor type with a connection between concrete and timber, primarily a one-directional spanning floor. In order to explore how this floor could be further applied, a study was prepared with the research question: How can a timber concrete composite floor slab be designed when it is point supported on four corners? The timber in this floor type, cross-laminated timber (CLT), has a stronger direction and is, therefore, mainly used in one direction, which is why it has not been researched before. The stronger direction makes designing a TCC floor slab in multiple directions, which will happen with a point supported floor slab, challenging. An analytical and numerical study is set up to check whether stresses and shear forces do not exceed maximum values and the ideal arrangement for the connection between the two materials. This research will inform structural engineers of the critical aspects that change during the design between a one-directional floor slab and a point-supported floor slab.

Contents

Chapter 1

Introduction

Timber-concrete composite floors consist of a timber floor, typically timber beams or a timber slab, with a layer of concrete on top. This type of floor is unique because of the collaboration between the concrete and the underlying timber structure. Through connectors, these materials work together to enhance the overall stiffness of the floor. In addition to the benefits of regular timber floors, applying these composite floors also provides other advantages. One advantage is the increased fire resistance achieved by adding the concrete layer. The concrete acts as a protective barrier, delaying the timber's exposure to fire. Furthermore, the concrete layer enhances sound insulation. Zhang et al. [1] also discuss that the sound insulation is significantly higher than a CLT (Cross-Laminated Timber) floor slab. However, it still needs to catch up to the prescribed values set by European and American regulations without further measures.

The main objective of this research is to design a point-supported timber concrete composite floor with an optimal connection between the two materials in the multiple directions of the internal forces. The research question following this objective is: *How can a timber concrete composite floor slab be designed when it is point supported on four corners?*

The research question will be answered by first conducting a literature review on the current compositions of the timber-concrete composite floor and the calculation methods that have been applied. The calculation methods found during this literature review will be a basis for the numerical investigation. These calculation methods will verify the connections and the timber-concrete composite floors to be applied.

Chapter 2

Literature

The literature review focused on several topics within timber-concrete composite floors relevant to the subsequent research. Firstly, research was conducted on the history of these floors and how research has evolved over the years, leading to the development of a calculation method. Setting up a calculation method also requires researching the possible connections and whether existing applications allow multi-directional connections.

2.1 State-of-the-art

The first developments of timber-concrete floors were caused by a scarcity of steel that could be used in concrete, which occurred after the Second World War. Van der Linden et al. [2] mention that in 1922, a patent was filed for a structure that involved reinforcing existing timber beams. This structure was reusing the timber beams and enhancing them with a concrete plate. In addition, the beams were connected using nails and steel, facilitating the collaboration between the two materials.

In the same study by Van der Linden et al.[2], research was conducted on this type of floor, examining the connection types between concrete and timber and the overall floor stiffness with different connections. This research resulted in the development of a calculation method. Additionally, the study discusses the beam length's influence on the stiffness of the connections.

These investigations have also led to research on alternative methods of connecting timber-concrete composite floors. These alternative methods involved exploring the possibility of using timber floor slabs to connect concrete and timber instead of only researching the structure with timber beams.

In further research on timber-concrete composite floors, the structure exists of CLT and a concrete top layer. The floors are typically spanned in

one direction, and the differences in the research are in the use of connectors, timber quality, concrete quality, or floor dimensions. Jiang et al. [3] and Lamothe et al. [4] discuss timber-concrete composite floors with a notch connection. The difference between these two papers primarily lies in the specific floor configurations. The variation is mainly in the Cross-Laminated Timber (CLT) layers, connector spacing, and concrete quality. Jiang et al. [3] primarily focus on utilizing the notch connection and a calculation method to approximate the floor stiffness. On the other hand, Lamothe et al. [4] mainly concentrate on using high-strength concrete on these floors.

Another commonly used method for connecting timber to concrete is using screws. Bao et al. [5] and Mai et al. [6] explore applying these screw connections to timber-concrete composite floors. Mai et al. investigate the effect of utilizing connections where the screws are placed at a 45-degree angle. On the other hand, Bao et al. focus on examining the possibility of using straight or angled screws and varying the screw configuration, such as different quantities placed in different locations, to optimize the floor stiffness with fewer screws.

Other methods that are utilized include adhesives. Kanócz et al. [7] discuss this method, where the adhesive is applied to the CLT. This process must be executed carefully and quickly to prevent compromising the connection between the CLT and concrete. However, it results in a fully integrated and cooperative floor system. Furthermore, other methods include steel plates that act as connectors perpendicular to the span and steel meshes that align with the span of the floor. Shahnewaz et al. [8] investigated these approaches to explore using stiffer elements as connectors instead of screws.

Previous research has mainly focused on single-span floors in the context of timber-concrete composite floors. However, in Loebus et al. [9], an investigation was conducted on how a floor slab can span in multiple directions. The span in two directions was achieved by supporting the floor on each side with line supports. The study also examined the torsional behavior of the floor slab in both the uncracked and cracked states. The torsional behavior of the TCC floor has been researched by placing the floor slab on three-point supports at each corner, with force applied at the unsupported corner. The research also explored different methods of connection. For the notch connections, the study examined situations where the floor experiences forces when the CLT is oriented in the strongest direction and when it is rotated 90 degrees. The stiffness of the connection and the influence of notch depth were investigated. For the screw connections, the study analyzed how the stiffness of the connection decreases when the screws are loaded in a direction different from their placement. This research allows for optimized screw placement to manipulate the stiffness where needed.

2.2 Calculation methods

This paragraph discusses the calculations involved in these types of floors. Three types of calculations are applied in various studies. It is important to note that all these calculation methods are based on the NEN-EN 1995-1-1 Annex B: mechanical fasteners [10]. This standard provides a simplified calculation method for connecting timber elements and determining the combined stiffness. Equation 1 defines the stiffness of an individual layer. The first part represents the stiffness of the floor, while the second part accounts for eccentricity. Depending on the collaboration of the connectors, a factor called the Gamma factor needs to be considered. Equation 2 provides a more detailed explanation of this Gamma factor. Its value depends on the slip modulus of the connection, the spacing between the connections, and the length of the beam.

$$EI_{eff} = EI_{layer} + \gamma EA_{layer}a^2 \tag{1}$$

$$\gamma_i = (1 + \frac{\pi^2 E_i A_i s_i}{K_i l^2})^{-1} \tag{2}$$

The literature study observed that the determination of stiffness, as described in Equation 1, is interpreted differently, resulting in three main possibilities. As employed by Bao et al.[5], one approach involves calculating the Cross-Laminated Timber (CLT) and the concrete top layer separately and then combining their stiffness values. The layers γ_1, γ_2 and γ_3 in Fig. 2.1 will be combined to calculate the stiffness of the CLT. The Gamma method for the CLT layers is determined using Equation 3. This equation considers the layer's height in the CLT's spanning direction, the layer's rolling shear strength perpendicular to the CLT floor's spanning direction, and the floor width. Once the bending stiffness is determined for the CLT floor, the timber-concrete composite floor calculation is performed by determining the median of both materials and applying the Gamma method to both materials, as defined by Equation 2. The resulting bending stiffness is then calculated using Equation 1. In some studies, the Gamma method used for the CLT is either equal to 1 or predetermined, giving different results than the abovementioned method.

$$\gamma_i = (1 + \frac{\pi^2 E_i A_i h_i}{G_R b l^2})^{-1} \tag{3}$$

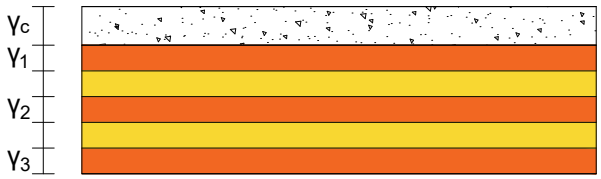

Figure 2.1: Cross-section for the combined calculation method

Jiang et al.[3] discussed a calculation method that involves combining the concrete and the CLT directly in the calculation using the Gamma method. Rather than calculating the CLT individually, both materials are combined. The first step is to determine the median, typically located in the top layer of the CLT. From there, the gamma factor for each layer can be determined. The γ_c for the concrete layer can be determined using Equation 2, while the Gamma factor for the CLT layers, can be determined using Equation 3.

The paper of Jiang et al. also mentioned the third calculation method found during the literature study. The Gamma method is limited to 3 layers of CLT, so the calculation method above is limited to a TCC floor with a CLT slab of 3 layers. To still apply the Gamma method for TCC floors with 5 layers of CLT, a method is suggested that doesn't consider the top layer of CLT, γ_1, because the median of the floor is in that layer and does not have an eccentricity that contributes to the stiffness of the floor. So, this layer will be calculated separately. Also, the gamma factor for the connectors and the timber is combined to get a Gamma factor that includes both layers.

2.3 Connections

The last paragraph explains the connectors' relation to the bending stiffness of the entire floor. In this paragraph, the stiffness of these connectors is determined and which data is available upfront about the different types of connectors. The stiffness of the connectors will be evaluated through a shear test, utilizing a test setup similar to that shown in Fig. 2.2. On top of one material, the timber for this example, a load will be applied. The material on which the load is applied is supported vertically to prevent it from creating an eccentric moment. The material to which the shear force is transferred will be prevented from moving at the bottom. Because one material is prevented from moving along the direction of the applied force, the connectors will be

activated. This activation will allow us to evaluate the connectors' behavior and stiffness.

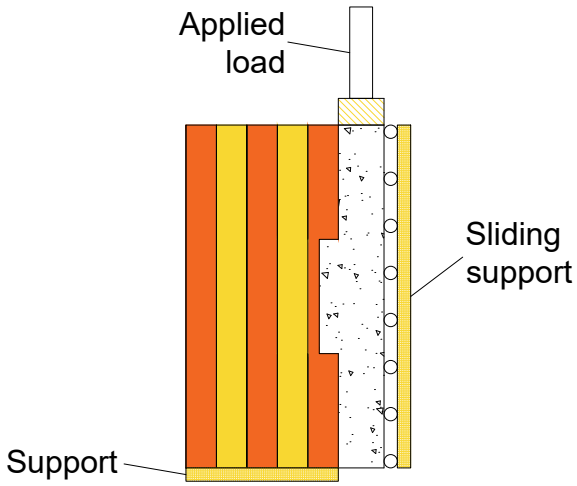

Figure 2.2: Standard shear test setup

The evaluation of this material will follow the guidelines outlined in ISO 6891 [11], which specify the principles for determining the strength and slip characteristics of these joints using mechanical fasteners. Stated in this standard is the loading procedure that is based on an estimated maximum load, which is based on experience or earlier tests. Then, the connection is loaded until 40 percent of the estimated maximum load is reached, which will be reduced to 10 percent. The load will then be increased until the ultimate load is reached or the slip reaches 15 mm.

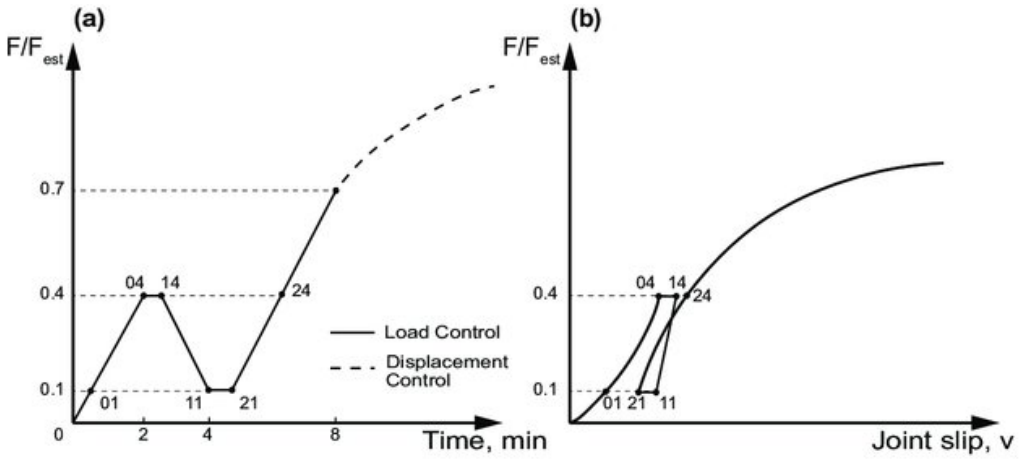

Figure 2.3: Loading procedure [12]

After the test results are obtained using the standard to set up the tests, the slip modules can also be calculated according to this standard. For determining the deformation elasticity stiffness, the modified elastic slip of the joint is determined by taking the slip at 0.1 and 0.4 of the estimated maximum strength of the connection and using a multiplication factor of 4/3, like in Equation 4. The slip modulus is then determined using the force applied at 0.4 of the maximum estimated force, like in Equation 5. The ultimate stresses in the floor must be determined at 0.7 of the maximum force. Also, the slip has to be determined based on 0.7 of the maximum force, which gives a reduced slip module that increases the stresses in the concrete top layer and the timber.

$$v_{i,mod} = \frac{4}{3}\left(v_{04} - v_{01}\right) \tag{4}$$

$$k_s = 0.4\frac{F_{est}}{v_{i,mod}} \tag{5}$$

As mentioned in paragraph 2.2, the bending stiffness of the floor slab is influenced by different types of connections. Dias et al. conducted a comprehensive literature study on various connectors used in shear tests, and the results are presented in Fig. 2.4. The graph illustrates that connectors such as glued and notched joints generally exhibit higher resistance to shear force and lower slip, leading to a higher slip modulus. These connections also display a brittle failure mechanism, evident from the sharp increase in shear force until a sudden failure occurs. In contrast, dowel-type fasteners exhibit different behavior. They are subjected to loading, and at a certain

point, the force does not increase further, but the slip continues to increase. This behavior demonstrates the ductile connection between the timber and the concrete.

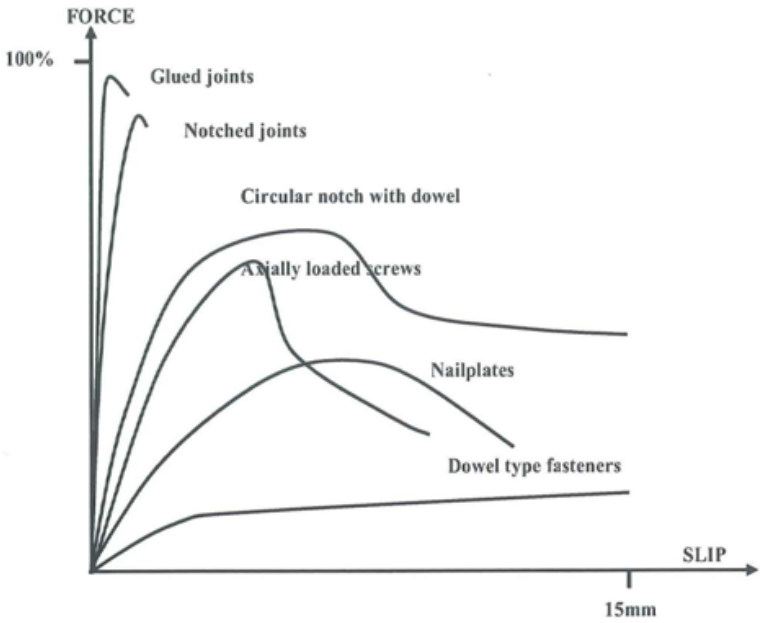

Figure 2.4: Comparisons of different connection systems [13]

Chapter 3

Calculation method

3.1 One-direction supported TCC floor slab

As mentioned in paragraph 2.2, various calculation methods are used for one-directional span floor slabs in different research studies. All the different calculation methods have been identified to establish a reliable benchmark for the upcoming numerical calculations later in this research. The test results from the papers that conducted experiments have been normalized to determine the most suitable calculation methods for timber-concrete composite floors.

3.1.1 Separate gamma method

The first method to calculate the bending stiffness involves considering the bending stiffness of the timber and the concrete. The stiffness of the concrete and timber are considered separately, and then the combined stiffness is determined. This calculation method is also mentioned in paragraph 2.1.

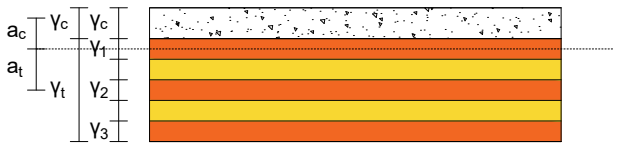

Figure 3.1: TCC floor which is calculated based on the separated calculation method

$$EI_{eff} = EI_c + \gamma EA_c a_c^2 + EI_t + \gamma EA_t a_t^2 \tag{6}$$

$$EI_t = EI_{clt} = EI_1 + EA_1 a^2 + EI_2 + EA_2 a^2 + EI_3 + EA_3 a^2 \tag{7}$$

$$A_i = b_i h_i, I_i = \frac{1}{12} b_i h_i^3 \tag{8}$$

$$\gamma_c = (1 + \frac{\pi^2 E_c A_c s_i}{k_i l^2})^{-1} \tag{9}$$

$$\gamma_t = 1 \tag{10}$$

$$a_t = \frac{\gamma_t E_t b_t h_t (\frac{(h_t + h_c)}{2})}{\gamma_t E_t b_t h_t + \gamma_c E_c b_c h_c} \tag{11}$$

$$a_c = \frac{h_c + h_t}{2} - a_t \tag{12}$$

Considering a symmetrical CLT floor slab, the TCC floor slab can be determined as follows. In Equation 6, the total stiffness is determined. The bending stiffness of the CLT floor slab can be determined according to Equation 8, so only the effective layers are considered. In Equations 9 and 10, the Gamma factors are determined. In this case, the gamma value is one since the median is within the CLT, indicating no stiffness reduction within the material. From that, the eccentricity from the median can be determined. What has to be considered is that in Equations 6 and 11, the area for the timber is only the effective layers and not the entire timber area.

3.1.2 Combined gamma method

The other method discussed in the papers is combining the concrete and timber immediately for calculating the Gamma method. In the paper of Jiang et al., this calculation method is explained, and what happens in this case, a TCC floor of 3 layers of CLT is considered a CLT floor of 5 layers. The top 2 layers will be removed and replaced by concrete. The Gamma factor calculated for the perpendicular layer will be rewritten as a Gamma factor for the slip modulus. The downside is that this method is only possible for TCC floors with 3 layers of CLT. When more layers are applied, some adjustments have to be made, like not considering a layer because it is on the median and does not contribute to the eccentricity.

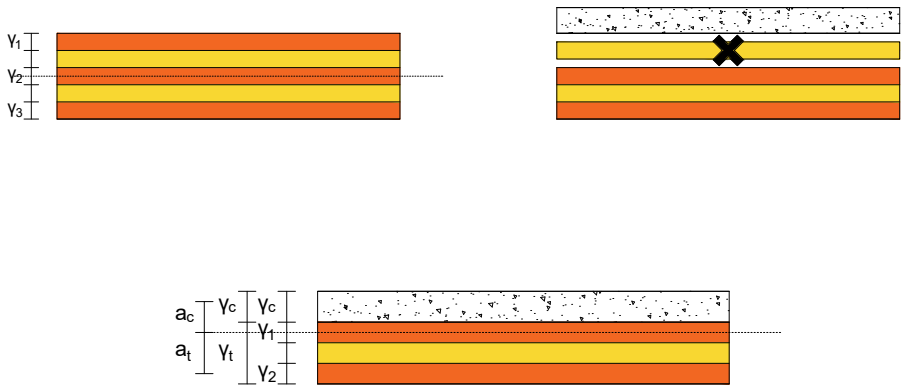

Figure 3.2: Applied combined Gamma method with the perpendicular CLT layer that will be transformed in the calculation to a slip modulus based resistance

Proposed calculation method

This research will suggest a calculation method based on the extended Gamma method proposed by Wallner et al.[14]. The extended Gamma method is proposed to calculate multiple layers of CLT without restriction to the number of layers and can be non-symmetrical. This method determines the gamma values via a linear equation system. The system is based on a sinusoidally distributed load, the respective deformation shape, and the assumption that all cross-section parts remain planar in the sections [14].The curvature-moment-relation will result in the equation system shown in Equation 13.

$$\begin{pmatrix} v_{1,1} & v_{1,2} & 0 \\ v_{2,1} & v_{2,2} & v_{2,3} \\ 0 & v_{3,2} & v_{3,3} \end{pmatrix}^{-1} \begin{pmatrix} S_1 \\ S_2 \\ S_3 \end{pmatrix} = \begin{pmatrix} \gamma_1 \\ \gamma_2 \\ \gamma_3 \end{pmatrix} \tag{13}$$

In Equation 18, the shear resistance of the perpendicular layers is considered. On the other hand, Equation 19 deals with the stiffness of layers that work in the direction parallel to the span. The factors $v_{i,i}$, obtained from Equation 14, determine the contribution of the main layer, while $v_{i,i-1}$ and $v_{i,i+1}$, derived from Equation 15 and 16, respectively, calculate the factors for layers perpendicular to the span.

$$v_{i,i} = (C_{i-1,i} + C_{i,i+1} + -D_i)\ a_i \tag{14}$$

$$v_{i,i-1} = -C_{i-1,i}\ a_{i-1} \tag{15}$$

$$v_{i,i+1} = -C_{i,i+1}\ a_{i+1} \tag{16}$$

$$S_i = -C_{i,i+1}\ (a_{i+1} - a_i) + -C_{i-1,i}\ (a_i - a_{i-1}) \tag{17}$$

$$C_{j,k} = \frac{b_i G_{R,jk}}{d_{j,k}} \tag{18}$$

$$D_i = \frac{\pi^2 E_i b_i d_i}{l_{ref}^2} \tag{19}$$

The suggested difference is to include the concrete top layer instead of only considering the CLT with the extended Gamma method. So, the matrix in Equation 13, which generally would be used for a CLT of 5 layers, can be rewritten to the matrix of 4 Gamma factors in Equation 20. A problem with this is that between the top layer of the CLT and the concrete, a connector is applied instead of a perpendicular that can be calculated with a shear resistance. Therefore, Equation 18 can be rewritten to the formula used in Equation 21. This one uses the Slip modules and the effective spacing between the connectors instead of the shear modules.

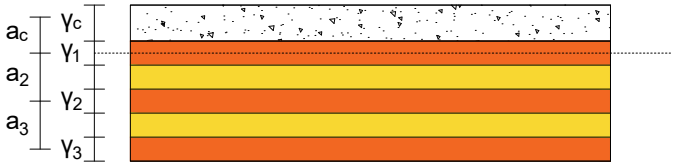

Figure 3.3: TCC floor cross-section and values applicable for the extended Gamma method

$$\begin{pmatrix} v_{1,1} & v_{1,2} & 0 & 0 \\ v_{2,1} & v_{2,2} & v_{2,3} & 0 \\ 0 & v_{3,2} & v_{3,3} & v_{3,4} \\ 0 & 0 & v_{4,3} & v_{4,4} \end{pmatrix}^{-1} \begin{pmatrix} S_1 \\ S_2 \\ S_3 \\ S_4 \end{pmatrix} = \begin{pmatrix} \gamma_1 \\ \gamma_2 \\ \gamma_3 \\ \gamma_4 \end{pmatrix} \tag{20}$$

$$C_{j,k} = \frac{k_i}{s} \tag{21}$$

Other direction

What also has to be remembered is that the final result is a timber-concrete composite floor in multiple directions spanning in multiple directions. So, it is also necessary to check what happens when the CLT is placed in the other direction, as shown in Fig.reffig:extgammetothdir.

Jiang et al.[3] also provided a solution for determining the Gamma factor in this other direction. This Gamma factor, applicable between the concrete layer and the top layer of the CLT, is influenced by two factors. The first factor is the connection between the concrete and the CLT, which is similar to every normal situation. The second factor is the effect of the shear resistance that typically exists between the two layers of CLT spanning parallel to the floor's span. The suggested approach to calculate the combined distributed stiffness is presented in Equation 22, wherein the connection is modeled as a spring in series. All the other steps in the calculation method can be kept the same. However, it is essential to consider that when using Equation 20, the bottom outer layer, which is perpendicular to the span of the floor, does not contribute to the deformation of the floor in the formula. That is because the shear resistance in that direction does not affect the equation.

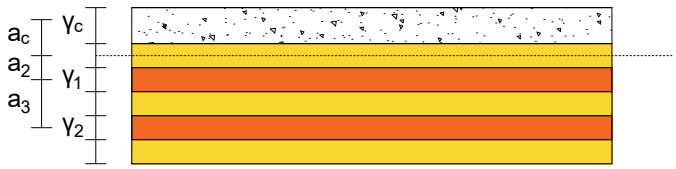

Figure 3.4: TCC floor cross-section of a rotated floor slab and values applicable for the extended Gamma method

$$(\frac{k}{s})_c = \frac{\frac{K_i}{s_{eff}} \times \frac{G_R b}{h}}{\frac{K_i}{s_{eff}} + \frac{G_R b}{h}} \tag{22}$$

3.1.3 Comparison

As stated in the previous paragraphs, various calculation methods can be applied to evaluate timber-concrete composite floors. These methods were compared with existing studies to facilitate a comparative analysis. The data from the tests conducted on timber-concrete floor slabs were collected to find

the appropriate calculation methods for further numerical computations. A challenging aspect involves determining a standard approach to uniformly assess the stiffness of floors. Prior works have employed diverse methodologies to determine stiffness at deflection during the testing phase. One of the methods used is to measure the deflection at the center of the floor based on the deflection. The range of 10 - 40 percent of the maximum load capacity is used to determine the stiffness of the floors, as used by Mai et al. Kanócz et al. took 40 percent of the maximum load capacity and used the load against deflection to determine the stiffness. Jiang et al. calculated from the predetermined stiffness of the floor what the maximum load is on the floor and took the stiffness of the floor at 40 percent of that. Bao et al. then again take the maximum deflection as the starting point to determine the stiffness. The required values for determining the calculated bending stiffnesses of these floors are derived from the data provided in the papers. When specific values are unavailable, data is estimated based on the described class or type of materials. Additionally, to ensure a uniform approach in determining the stiffness of the connectors, the slip modules are calculated using the method outlined in ISO 6891 [11]. For the comparison, the floors were categorized into different types based on their connectors, including those utilizing notches or adhesives, exhibiting brittle behaviour, and screw connections. Regarding the notch and adhesive connectors, seven distinct types of floors were tested, but the tests were not equally distributed, amounting to 14 tests in total [3] [7] [4]. The results depicted in Fig. 3.5a reveal that the Separated calculation method overestimated the bending stiffness of the floor, ranging from 99.1 to 121.7 percent with an average of 110.1 percent. The Combined calculation method overestimates it ranges from 91.4 to 126.3 percent with an average of 106.0 percent. Fig. 3.5b illustrates the outcomes of the calculation methods for the screw connectors. These connectors were tested using ten different setups, with 22 tests conducted[5] [6] [8]. It becomes apparent that both calculation methods result in bending stiffness values that remain below those observed in the experimental floors. The Separated calculation method underestimated the bending stiffness of the floor, ranging from 61.9 to 79.2 percent with an average of 67.3 percent. The Combined calculation method underestimates it ranges from 56.8 to 73.6 percent with an average of 63.1 percent.

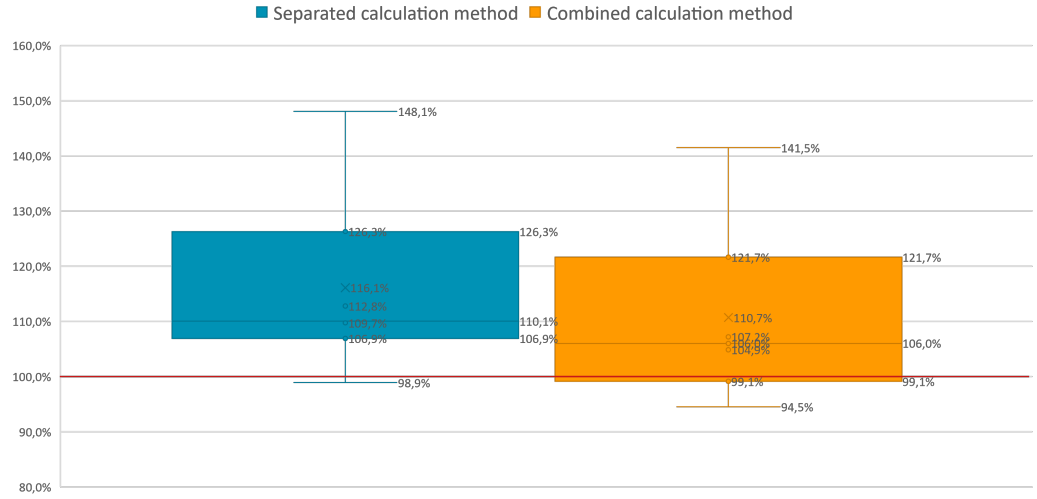

(a) Notch and Adhesive - Brittle behavior

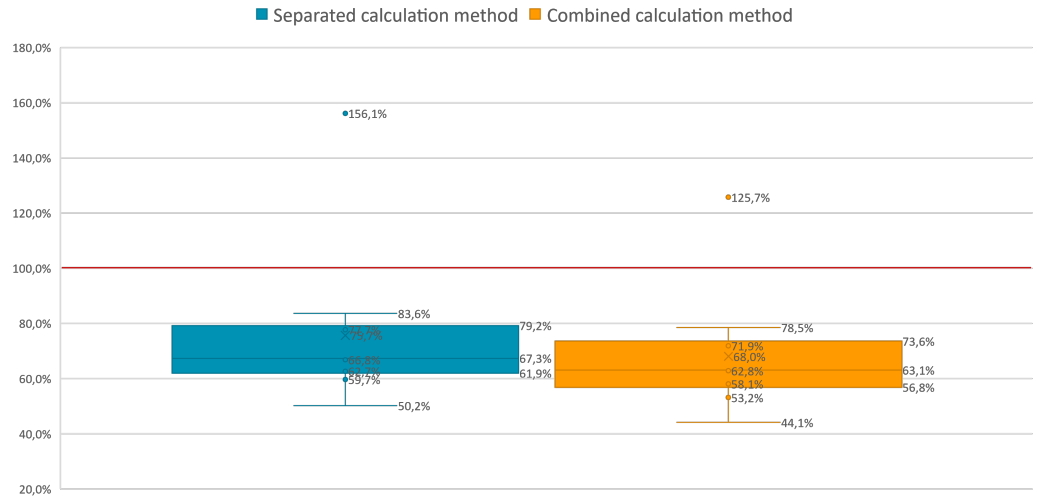

(b) Screws - Ductile behavior

Figure 3.5: (a) This graph compares the bending stiffness according to the test results with those acquired with the calculation methods for the one-directional supported TCC floors with brittle connectors. (b) as for (a) this graph shows the difference in bending stiffness with the ductile failure methods of screws

What can be observed from these comparisons is that both calculation methods overestimate the TCC floors that have brittle behavior connectors and underestimate the same type of floors with ductile behavior. The difference between the two calculation methods is insignificant, but the bending

stiffness obtained from Combined calculation method values are in a smaller range of results and are more conservative. The combined calculation method will be used to check the numerical results for further calculations.

3.2 FEM verification floor slabs

With the determination of the calculation method of the TCC floors, the change in behavior of the floors is determined from the one-directional spanning TCC floor slab to the point-supported floor slab. There is no FEM program available to check these types of floors, so what is done for this research is that Dlubal RFEM is used. This program can calculate CLT floor slabs, which determine the change in deformation, stresses, and the flow of forces.

The boundary condition has to be the same to compare the results between the floors, so a five-layer CLT floor with each layer a thickness of 40 mm is used. The floor dimensions are chosen to have a width of 3 meters and a length of 6 meters with only a load of 10 kN/m2 applied.

As the results are considered, it can be noted that the deformation increases from 30.9 to 48.5 mm for this CLT. The most significant increase is found when the stresses are considered. The bending stresses increase in the span direction, almost 2 times than for the one-directional CLT plate. Moreover, in the perpendicular direction, the CLT in the weaker direction will be activated, causing an increase of around 6 times. The most significant increase is in the shear stresses that will increase due to a concentration of forces towards the point support instead of the line support at the edge. In the case of the CLT floor slab, the shear stresses are the governing part of the structure, so also, for the TCC floor slabs, it must be considered when the point-supported structure is checked.

Considering the flow of forces in the floor slab to create a starting point for further cooperation to be made on the floor. In Fig. 3.6a, the forces in the floor run parallel to the course of the CLT. The flow of these forces makes sense because it can only go in a straight direction. The point-supported floor in Fig. 3.6b shows that the forces are still mainly straight but rotate as they progress toward the support point. It follows a smooth circular angle around the support. This circular angle must be considered necessary for further research on this type of floor because it will determine the pattern in which the connectors must be placed.

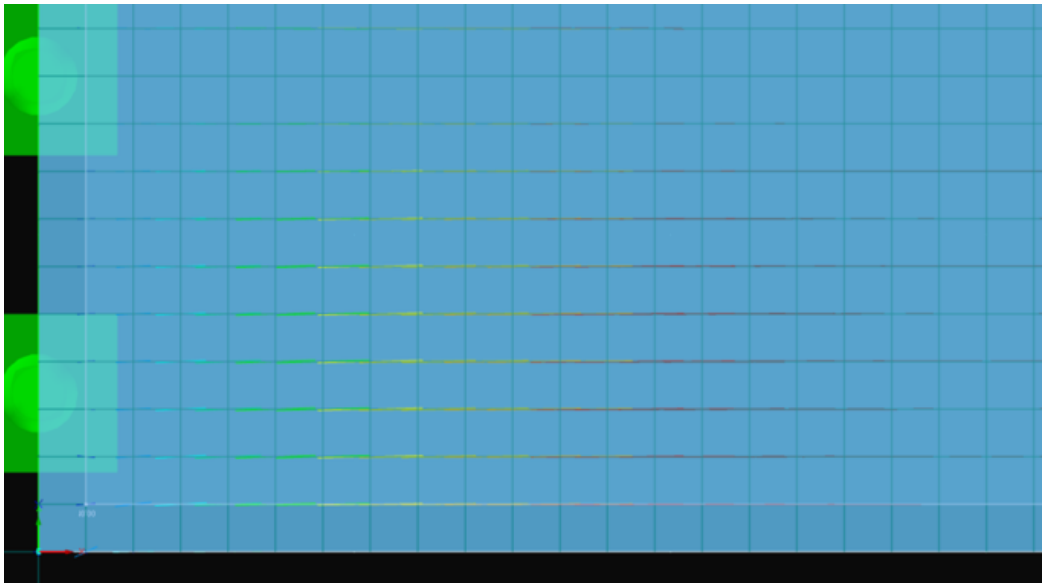

(a) Flow of forces one-directional line supported CLT floor slab

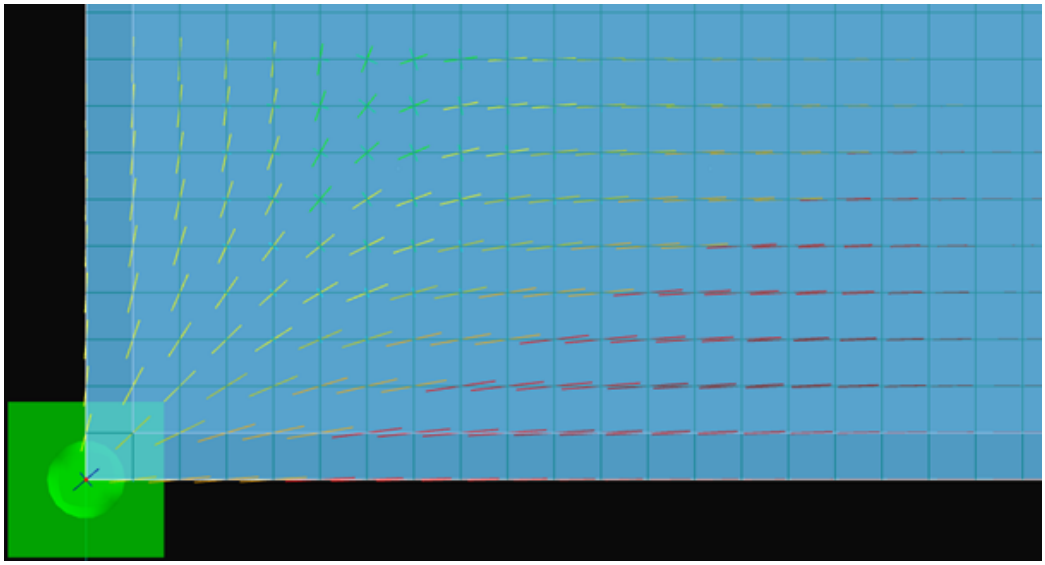

(b) Flow of forces point supported CLT floor slab

Figure 3.6: (a) This Figure shows the flow of forces for the one-directional line supported CLT floor slab (b) as (a) shows it for the Point supported CLT floor slab.

Chapter 4

Guiding principles

Before starting the numerical study, it is good to list the main assumptions for these numerical calculations. This chapter will clarify which materials have been chosen, which loads are assumed, which connection will be used between the timber and concrete, and which inputs have been done in the model.

4.1 Materials

Timber is an orthotropic material with one stronger main direction, which, generally, timber beams can use. The difficulty of this research is that a floor must be designed which spans multiple directions. Moreover, from what can be seen in paragraph 3.2, the forces will flow through different directions. Therefore, a timber floor that can be used in multiple directions must be used. CLT (Cross laminated timber) and LVL (Laminated Veneer Lumber) are among these possibilities because these types are also used in previous research mentioned in Chapter 2.1, which chose to use the CLT floor slab for further calculations.

To avoid too many variables between the numerical models, a CLT floor that consists of 5 layers and has a thickness of 40 mm per layer with a total thickness of 200 mm is used for this research. This floor thickness was chosen to investigate a floor that is a standard size so that no special CLT flooring needs to be applied to enable TCC floors. Moreover, it should contribute to the resistance to the bending and shear stresses in the floor slab.

For the concrete, it was decided to go for a standard available concrete quality already widely used. Therefore, concrete grade C30/37 was chosen to be used for this study. A thickness of 60 mm as a top layer is used in this research.

4.2 Dimensions & loads

A standard floor is used during the calculations unless it is mentioned. This standard floor consists of CLT of 5 layers with a thickness of 40 mm, a total thickness of 200 mm, and a concrete layer of 60 mm. The floor will have a width of 3 meters and a length of 6 meters. The dimensions and setup of this TCC floor are visualized in Fig. 4.1. For the Models in Abaqus, only 1/4 of the plate is modeled because it is symmetrical and reduces the calculation time significantly.

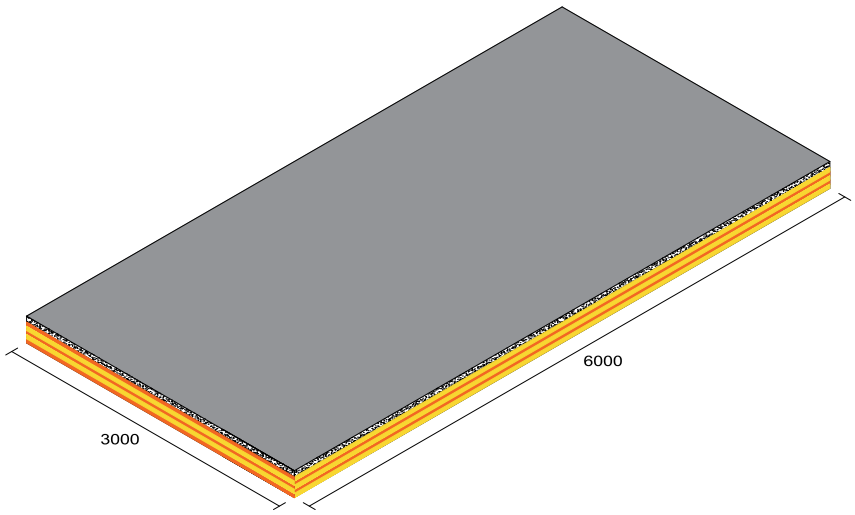

(a) 3D view of the TCC floor

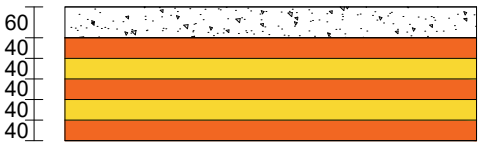

(b) TCC floor cross-section in the main direction

Figure 4.1: Visualization of the TCC floor with the dimensions

For these floors, a load was determined based on the Eurocode to make comparing the upcoming different setups of these floors easier. The floors are determined to be used in an office which, based on the Eurocode, should be

Class B, and the building has been determined as Consequence Class 2. With the loads of Table 4.1, a characteristic value of 5.12 kN/m^2 and a variable load of 6.89 kN/m^2 is placed on these kinds of floors.

Type Load	Load	Value	Unit
Permanent Load	Finishing	0.20	kN/m^2
	Timber	0.92	kN/m^2
	Concrete	1.50	kN/m^2
Variable Load	Class B	2.50	kN/m^2

Table 4.1: Loads

4.3 Connection

A choice was also made as to which connection to choose for the remainder of the study. Three main choices can be made to connect the timber and concrete. As mentioned in chapter 2.3, these are screws, notches, or adhesives. How the chosen connection should be applied has also been determined to create a standard for the rest of the research.

When the application of a screw joint in the timber concrete floor is considered, it can be seen that it is already commonly used in one-directional floors. For a multi-directional floor, the paper by Loeb et al. [9] established a model to determine the contributions of the screws to the stiffness of the floor at the angle that the force flows through the screw. This model was translated into a specimen that was tested. As the connection is examined further, it provides an advantage by allowing the screws to be placed in the direction of the flow of forces. The disadvantages are that this connection is ductile, so that it will fail first with a warning, but it is not known how the spring stiffness of each screw affects the whole system and which screw becomes the normative screw for this failure. This connection is also the connection with the lowest contribution to the overall stiffness of the structure.

The adhesive connection is glue applied on top of the CLT floor slab. Relatively short after the glue is applied on the CLT, the concrete has to be poured on top of the glue. Applying the glue should create a floor that theoretically lets the concrete and timber optically work together in both directions. The downside of this method is that it needs to be ensured that the connection between the concrete and timber is applied well enough and that the concrete can push the glue away while pouring it on the floor. Also,

the adhesive is not readily available and expensive. The research is also limited to these connections for the TCC floors.

The connection method chosen in this study is that of a notch. This notch connection has already been the subject of much research. The only research on this type of connection in multiple directions has been done by Loeb et al. [9]. The advantage of applying this connection is that it should lead to a rigid connection in the floor. It only needs to be cut in the CLT and is a relatively cheap solution. It is also easier to predict the behavior of this connection than by using screws, as this can be done more efficiently with numerical programs. The disadvantages are that the notches will weaken the CLT locally as part of it will be removed and that it is a brittle connection that does not show when it fails.

The design for the notch connection is shown in Fig. 4.2. It shows that the connection in the top layer of the CLT will have a depth of 25 mm instead of over the entire height of the layer. Loeb et al. describe that if a notch is not applied over the entire layer height, the connection's slip modulus will increase for the main direction. The downside is that the shear stress in the timber will locally slightly increase at the notch. This system of not using the entire depth will still be chosen to avoid sawing through boards completely and leaving some small pieces of planks separately on the layer beneath it.

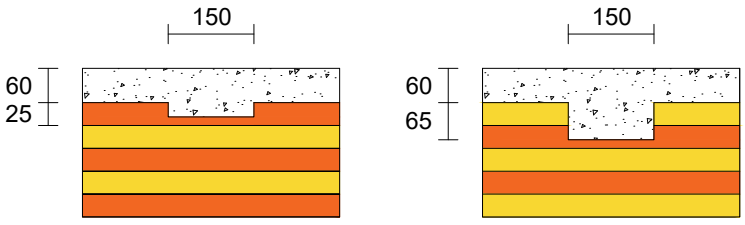

Figure 4.2: Dimensions of the notches, respectively, parallel and perpendicular to the span of the TCC floor slab

4.4 Input model

In this paragraph, the inputs in the Abaqus model are discussed per input parameter.

Materials: As discussed earlier, it was decided to apply concrete with a strength of C30/37. A concrete damage plasticity model is used according to Hafezolghorani et al. [15] to apply the concrete class in the Abaqus model. The material properties for concrete in class B40 were chosen here. For the

timber, the same timber model as in Jiang et al. has been used, which incorporates the orthotropic yield criterion proposed by Hill, capable of predicting the plasticity of the timber. The model also applies specific stresses in the different directions of the timber.

Parts: The model consists of mainly 3 different elements. A top layer of concrete, a timber layer working in the strongest and weakest direction. Later, the notch pattern was added under the concrete layer, and with this, notches were made in the timber. Also used at the point-supported floors is a column consisting of a steel plate that is fully supported where the CLT is supported.

Steps: For the load of the model, only the load acting on the floor is used for the model of the floors. For shear calculations, a displacement is used. It is set that the calculation starts at 0.01 of the displacement and is finally set until this displacement is reached or the joint is only calculated plastically.

Interaction and properties: 3 interaction properties have been used. The first one is for the connection between the CLT and the concrete. It was established using a friction coefficient of 0.57 for the tangential behavior and hard contact for the expected behavior. For the connection between the CLT, a cohesive behavior was used with the default contact enforcement method, which assumes that the connection between the layers is almost rigid. As a final proportion, an interaction was made for the connection between the CLT and the steel support by using a penalty of 0.35 for the tangential behavior and hard contact for the expected behavior. The friction coefficient changes because this involves wood with steel instead of concrete with wood, as in the beginning.

Boundary conditions: The Different models used different boundary conditions. For shear, a displacement of up to 5 mm was used on the concrete. At the same time, the timber was prohibited from moving. For the TCC floors in one direction, line support was used at the location of the support, and since only half of the model was applied, a symmetry axis was applied to model only half of it. For the model of the floor that spans in several directions, 1/4 of the floor was simulated, so two symmetry axes were applied. A support was also applied to this floor using a steel plate. A support was applied to this steel plate, preventing it from moving in all directions.

Chapter 5

Numerical calculation of the connections

By examining the flow of forces from Chapter 3.2, it can be seen that for a point-supported floor slab, the forces go partly through the top layer of the CLT in the direction and partly through the second layer, perpendicular to the strongest direction. The multiple directions the connection can work in are researched to optimize the connection. As earlier mentioned, there is already made a check in a Fem model for notches with 0 and 90 degrees angles in the top two layers by Loeb et al. [9] In this chapter, the Abaqus model created to research the different angles of the shear test is verified by Jiang et al. [3] research results. The verified shear test model checks multiple angles between 0 and 90 degrees on the maximum applicable force and the slip modules.

5.1 Verification

Initially, a model was created in Abaqus using the ISO 6892 [11]. A comparison is made between the paper by Jiang et al. [3] to verify the Abaqus model. This comparison uses the exact dimensions and material properties of the paper. Instead of a notch length of 150 mm, a notch length of 200 mm is used. Also, the self-compacting concrete is stronger than the concrete class C30/37 concrete used in this research. The other difference with the report's model is that no stirrup reinforcement was applied in the notches to transfer additional transverse force and reinforce the angle of the notch connection in the concrete. The stirrups were left out to avoid applying as little reinforcement as possible. Fig. 5.1 shows the test setup and the model translation to Abaqus.

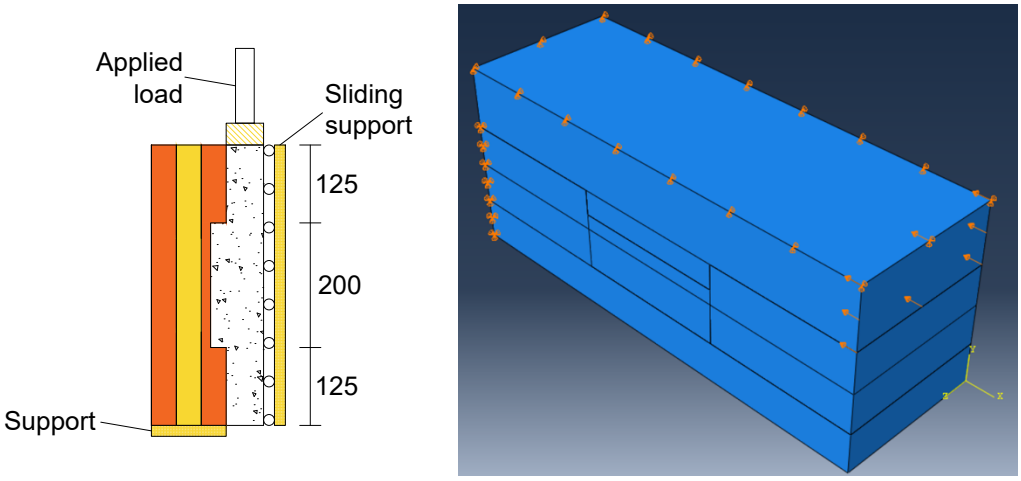

(a) Test setup (b) Test setup in Abaqus

Figure 5.1: (a) shows the test setup. (b) shows the translation from that test setup to an abaqus model.

As the exterior of the specimen is checked and the failure mechanism described in the model described by Jiang et al. with this Abaqus model, it can be seen that there is an initial failure at the corner of the notch of the concrete, as shown in Fig. 5.2. In the Abaqus model, shown in Fig. 5.3, it can be seen that at the edge of the concrete notch, the tension stress will reach its maximum before the compressive stresses in the timber reach it.

Figure 5.2: Test setup by Jiang et al. [3]

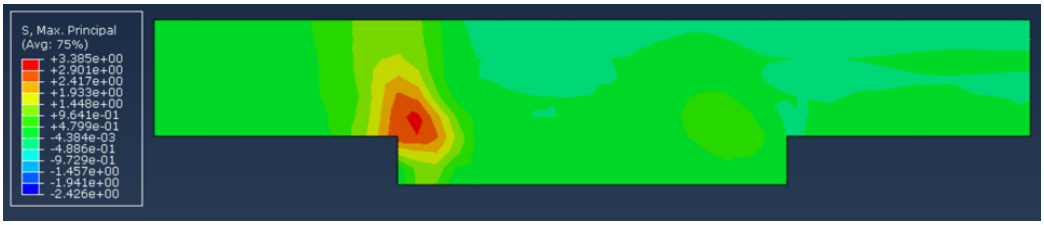

(a) Max. principal stresses in concrete top part

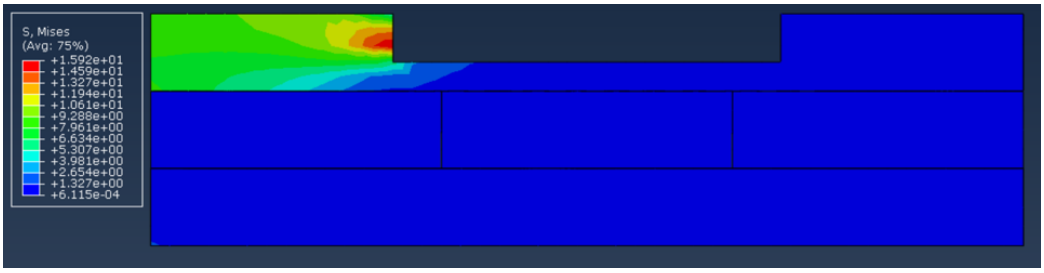

(b) von Mises stresses in concrete top part

Figure 5.3: (a) In the concrete top part of the connection the tension stresses exceeded the maximum tension stresses (b) In the CLT the compression stress have not reached it maximum compression strength

Also, with these shear force tests, the maximum applied force and the slip modules the connection can resist must be compared. In Fig. 5.4 are three different tests. In red is the test conducted in this research with values comparable to the paper of Jiang et al. In grey is the result of the research paper of Jiang et al. In blue is the result of what happens when a concrete strength of C16/20 is used compared to the high-strength concrete used in the paper. The behavior is almost identical for the two models with the same timber and concrete class. The difference in these models can be explained by the fact that some assumptions had to be made because not all timber and concrete class information was available to create the model. It can also be seen that the force displacement of the paper still exceeds that of the lower concrete class. When the slip modules are calculated for these three different tests, it is determined based on the force displacement between 10 and 40 percent of the maximum force. It can be seen in Table 5.1 that the slip modules are almost the same for all of the models. That means that the concrete class does not influence the slip modules much. In the model of Jiang et al., plasticity is not considered. For the model used in this research, plasticity has to be added because of the rotation in the timber. This and the difference that can occur in the maximum shear force are the things that can be concluded following this verification.

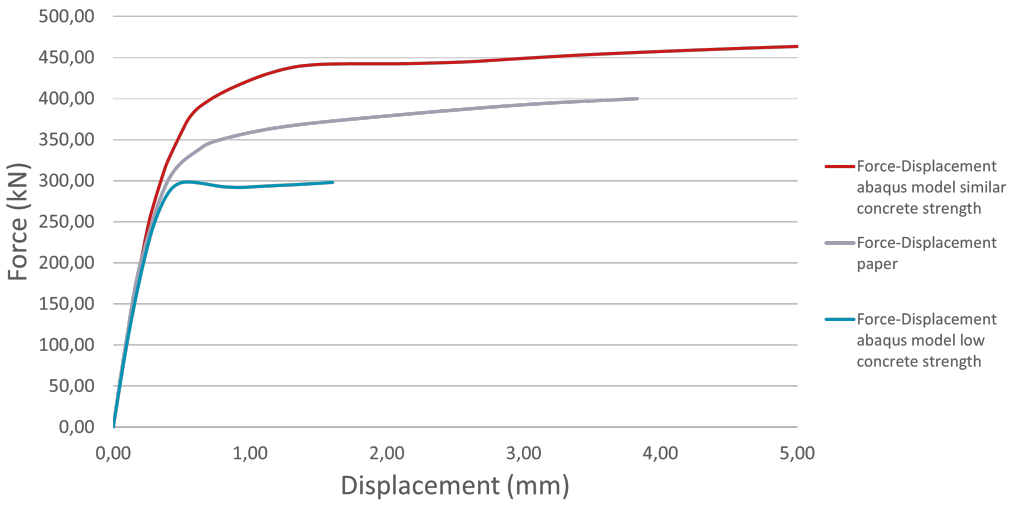

Figure 5.4: Shear force compared between paper [3] and abaqus model

Force-Displacement tests	Max. shear force	Slip modules
Similar concrete strength	466,0 kN	956,8 kN/m
Result paper	400,0 kN	1032,1 kN/m
Concrete strength C16/20	299,8 kN	983,0 kN/m

Table 5.1: Maximum shear force and slip modules results

5.2 Reseached Abaqus model

To elaborate on the model, verified in the last chapter, the different angles in which the connection can be loaded according to the flow of forces have been set up. As mentioned in Chapter 4, there is chosen for a notch depth of 25 and 65 mm. A model is created for both depths in which a top layer of CLT of 40 mm is used with a notch of one of the two depths with a length of 150 mm. The concrete is then placed on top of the CLT, where the CLT is placed under the angles 0, 10, 20, 30, 45, 60, 75, and 90 degrees to estimate the strength and slip modules, which can be seen in Fig 5.5.

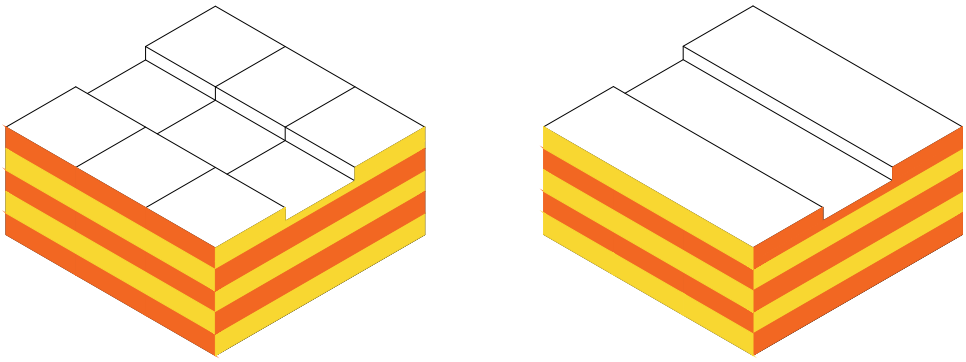

(a) 0 degrees rotate CLT (b) 90 degrees rotate CLT

Figure 5.5: Rotation of the CLT for the different models

In Fig 5.6, the results are considered from the force-displacement diagram of 0, 45, and 90 degrees angles. When the notch depth of 25 mm is considered, the continuous lines, the strength of the timber start to decrease when used in a direction more perpendicular to the main direction. What differs is that during the test from the specimen with an angle of 0 degrees in the concrete corner, the tensile stresses will exceed the maximum tensile force before the maximum stresses are reached in the timber. With the 90-degree rotated CLT specimen, the maximum compressive strength will be reached in the CLT before the maximum tensile stress in the concrete will be reached. The angles between 0 and 90 degrees show a transition from where the concrete tensile strength governs to where the timber compressive strength governs.

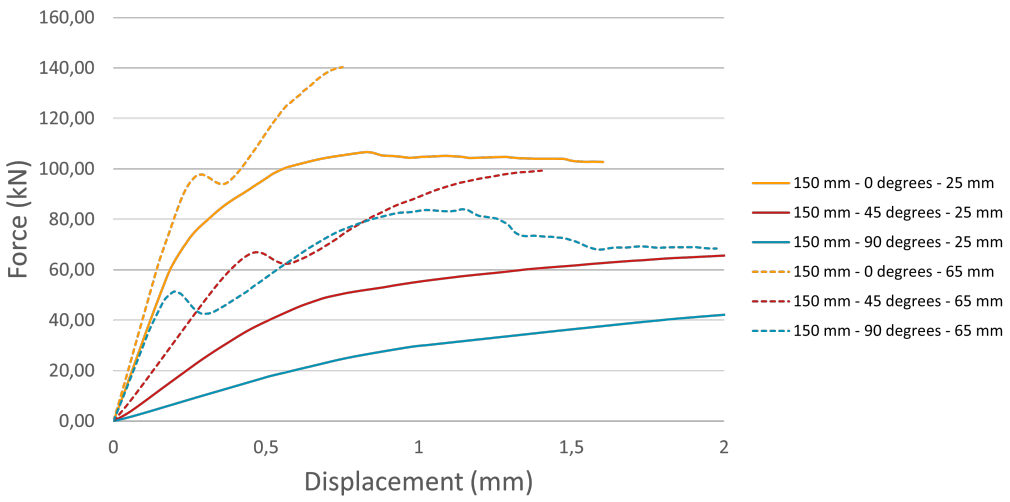

Figure 5.6: Force-Displacement diagram for the angles 0, 45 and 90 degrees

The specimens with a notch depth of 65 mm, shown in Fig 5.5 as dashed lines, behave differently. In the specimen with the CLT rotated at an angle of 0 and 90 degrees, there are two layers of CLT in which the material properties vary. What can be seen is that first, the concrete reaches its maximum tensile strength. After that, the layer of timber perpendicular to the force will reach the maximum compressive strength. Because this will let this layer behave plastically, the forces will concentrate on the other layer of timber. The specimen with the CLT rotated at an angle of 45 degrees will apply force on two layers of timber where there is no layer utilizing the strongest direction. This will cause the timber in these layers to reach the maximum compressive stress earlier than the other two mentioned directions and increase the displacement.

The difference in the maximum applied force on the specimen before the timber fails is due to the difference in stiffness of the layers and the test setup. The difference in stiffness can be seen when the specimen of 0 degrees rotated CLT is loaded. The forces flow through the strongest top layer and directly into it with a small lever between the timber and concrete. With the specimen of 90 degrees, the top layer will be activated and reach its maximum compressive strength and then the second, strongest layer will reach its maximum compressive strength. Moreover, the test specimen exists of three layers. The middle layer has to take all the load instead of where the top and bottom layers can collaborate in the other direction.

If the slip module is considered, it shows that the slip modules decrease until around 45 degrees for both depths. When the angle approaches 90 degrees for a depth of 65 mm, the slip modules increase until the same value

as an angle of 20 degrees. The notch depth of 25 mm will decrease until the contribution to the stiffness is minimal at 90 degrees.

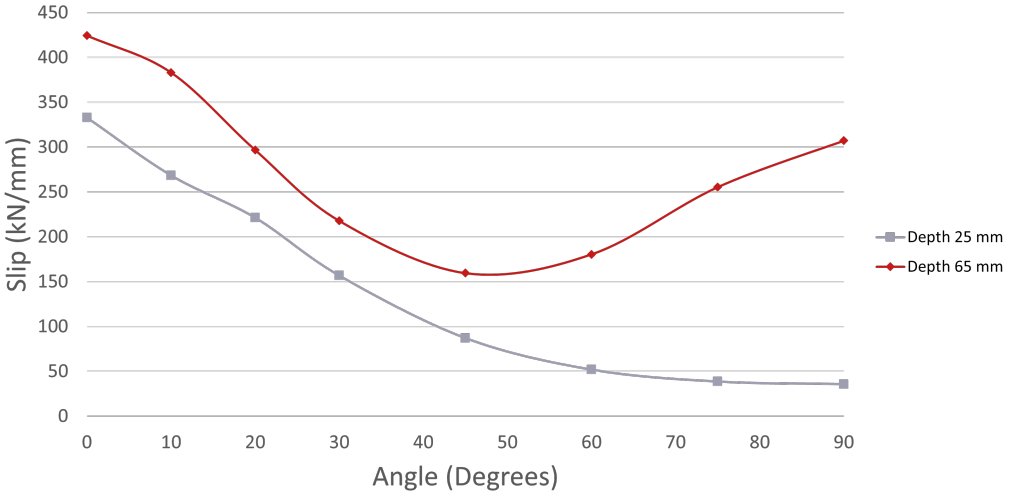

(a) Slip - Angle relation

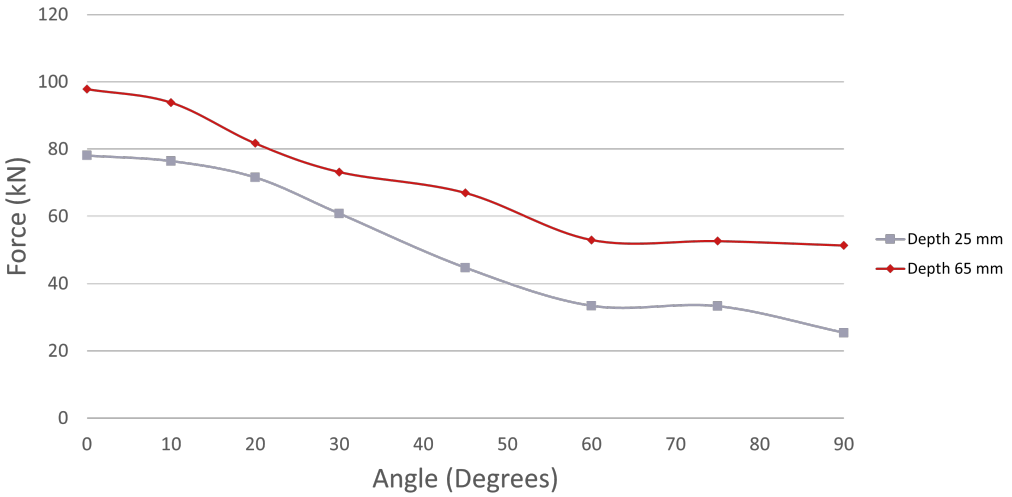

(b) Maximum Elastic Force - Angle relation

Figure 5.7: (a) In this graph the difference in Slip is shown for both notch depths (b) The maximum elastic Force - Angle relation is shown.

What can be concluded from the results discussed in this chapter is that both the maximum elastic force and the slip modules have higher resistance at a notch depth of 65 mm. Until an angle of 45 degrees, it does not matter if a notch depth of 25 or 65 mm is used, the first or second layer of the CLT.

From 45 degrees to 90 degrees, it is recommended to use the notch depth of 65 mm until the second layer.

Chapter 6

Numerical calculation of the one-direction supported floor slabs

In this chapter, a one-directional timber concrete composite floor Abaqus model is created. The aim is to make a starting point for numerical research on multiple directional TCC floors. Which also functions as a verification method that, without any lab results, can produce realistic results. Another objective of this chapter is to see the difference in stiffness between the different setups used and what conclusions can be drawn from it.

First, the model is compared to the results of the tests and Abaqus according to Jiang et al.[3], in which the dimensions and values of the paper have been used. After this validation, the findings of the notch depths, Chapter 5, and the best applicable calculation for TCC, discussed in Chapter 3, have been used to check the model to see if they are realistic values, which are used according to the principles stated in Chapter 4. Different numerical tests have been made in this chapter for these one-directional timber concrete composite floor slabs. The differences occur in the height of the applied concrete top layer, the thickness of the CLT floor slab, the direction in which the layers of the CLT span, and notches that do not span the entire width of the floor slab.

6.1 Verification of the model

Three different methods were used to verify the model. The verification is done by using the test and numerical results from the paper by Jiang et al. and using the Combined Gamma method to calculate the bending stiffness of

the floor. In this paper, two different floors were calculated and dimensioned in Fig. 6.1. The material properties were also taken from this paper. Then, it was set up as a four-point bending test.

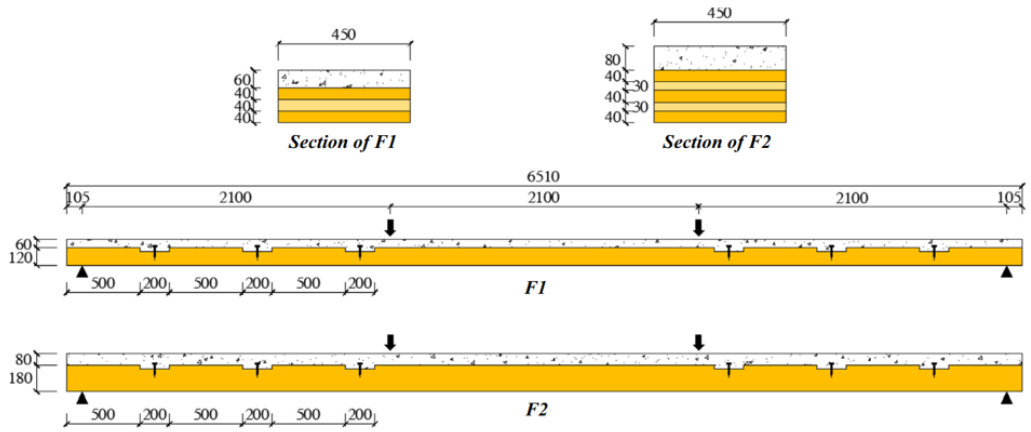

Figure 6.1: Dimensions of the specimens used for verification [3]

First, the four-point bending test is compared with the test results performed in the paper. In Fig. 6.2, these results are compared, and what can be seen is that in the model with the 3-layer CLT, the Load-deflection is first similar to the test data but later only reaches 96.0% of the stiffness of test data. With the 5-layer CLT floor, the results are almost even, and the stiffness is within 98.4% and 102.0% of the stiffness of the test result.

The following comparison is between the results of the Abaqus model from the paper and the one from this study. What emerges from the comparison in Fig. 6.3 of the timber stress distribution is that the gradient of stresses is the same. There is a difference in the stresses of 26.23 N/mm2 and 24.95 N/mm2, but this may be due to the plasticity that was not included in the paper and is included in this study. However, notably, the distribution of the stresses is comparable between the models, also due to the lack of information with which load these stresses were determined.

The second comparison between the Abaqus test results is based on the Combined calculation method discussed in Chapter 3.1.2. The comparison will have no added value for these verification models as the Combined Gamma method results have been used in the same chapter to determine in which range the bending stiffness falls according to applying this calculation method. Nevertheless, the comparison between the Abaqus model and the gamma method has been made in Table 6.1 to compare with the other one-directional floor slab.

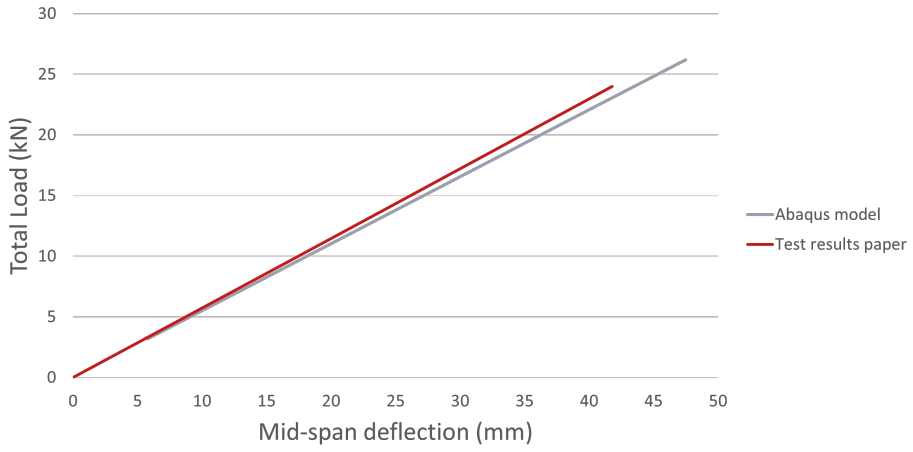

(a) TCC floor slab 3 layers

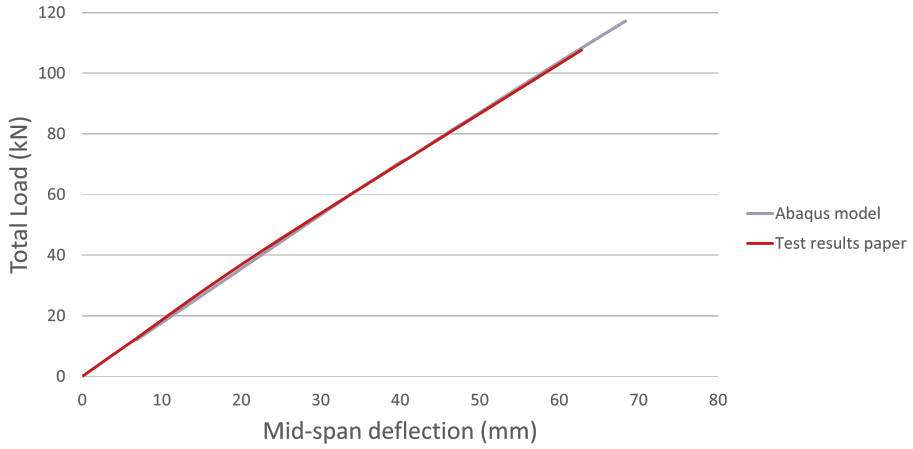

(b) TCC floor slab 5 layers

Figure 6.2: Load-deflection graph between test results of paper [3] and the Abaqus model

CLT layers	**Thickness concrete [mm]**	**$EI_{eff.num}$ [N/mm^2]**	**$EI_{eff.gamma}$ [mm]**	**Change (%)**
3	60	2.446×10^{12}	2.913×10^{12}	119.1
5	80	7.886×10^{12}	8.079×10^{12}	102.5

Table 6.1: Comparison between the bending stiffness of the numerical model and the gamma calculation method for the verification models

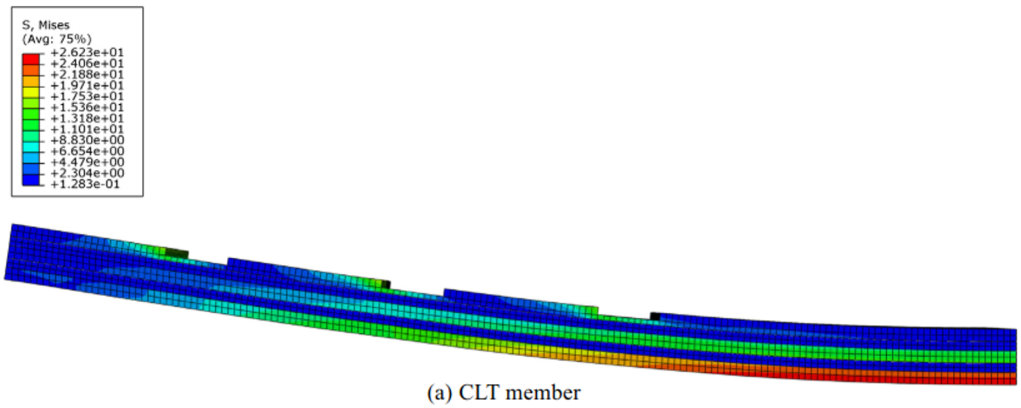

(a) Timber stresses - Abaqus model Jiang et al.

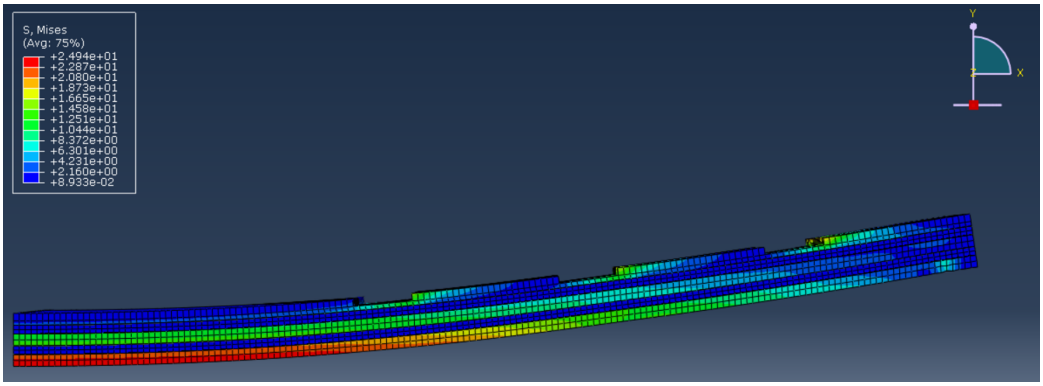

(b) Timber stresses - Abaqus model

Figure 6.3: Comparison in timber stress distribution between the paper and the established model at maximum load

6.2 Different models

This paragraph discusses the numerical results of the different TCC floor slabs. The principles stated in Chapter 4.1 are used to set up these models for these tests. A floor slab of 6.3 meters long is used with 3 notches on each side with a length of 150 mm, described for every floor variant. Multiple variants of CLT are used for every variant to check if the floors can properly be checked with the gamma method.

6.2.1 Standard TCC Floors

Four different floors are used to check the model, as shown in Fig. 6.4. For the CLT, 5-layer and 3-layer timber with a layer thickness of 40 mm were used. These two CLT configurations used a 60 mm and 80mm concrete top layer.

Looking at the stresses that occur in these numerical tests, it is found that both the maximum concrete and timber stresses are not reached. The maximum concrete tensile stress is 2.82 N/mm^2 at the corner of the beginning of the notch for the specimen with 3 layers of CLT and 80 mm of concrete. The maximum timber stress is at a maximum of 5.93 N/mm^2 in the specimen with the same specimen. However, the maximum stress is not in the notch but due to bending in the middle of the plate at the bottom layer of the CLT. The stress that occurs at the notch in the timber is 3.48 N/mm^2.

Another point from the study is to see if the model is appropriately set up and meets the values set earlier in this study to verify this. These were compared using the Combined Gamma Method with the results of section 3.1.3. In that chapter, it is stated that the results are between 99.1% and 121.7%. When that is compared with the results compiled in Table 6.3, it is found that their results are at the lower limit of this calculation. It can be determined from this that it is comparable to the experimental results.

CLT layers	**Thickness concrete [mm]**	**$EI_{eff.num}$ [N/mm^2]**	**Deformation [mm]**
3	60	2.725×10^{12}	21.83
3	80	3.674×10^{12}	17.70
5	60	7.363×10^{12}	8.64
5	80	8.932×10^{12}	7.74

Table 6.2: Calculation of the bending stiffness according to the numerical calculations with a standard setup

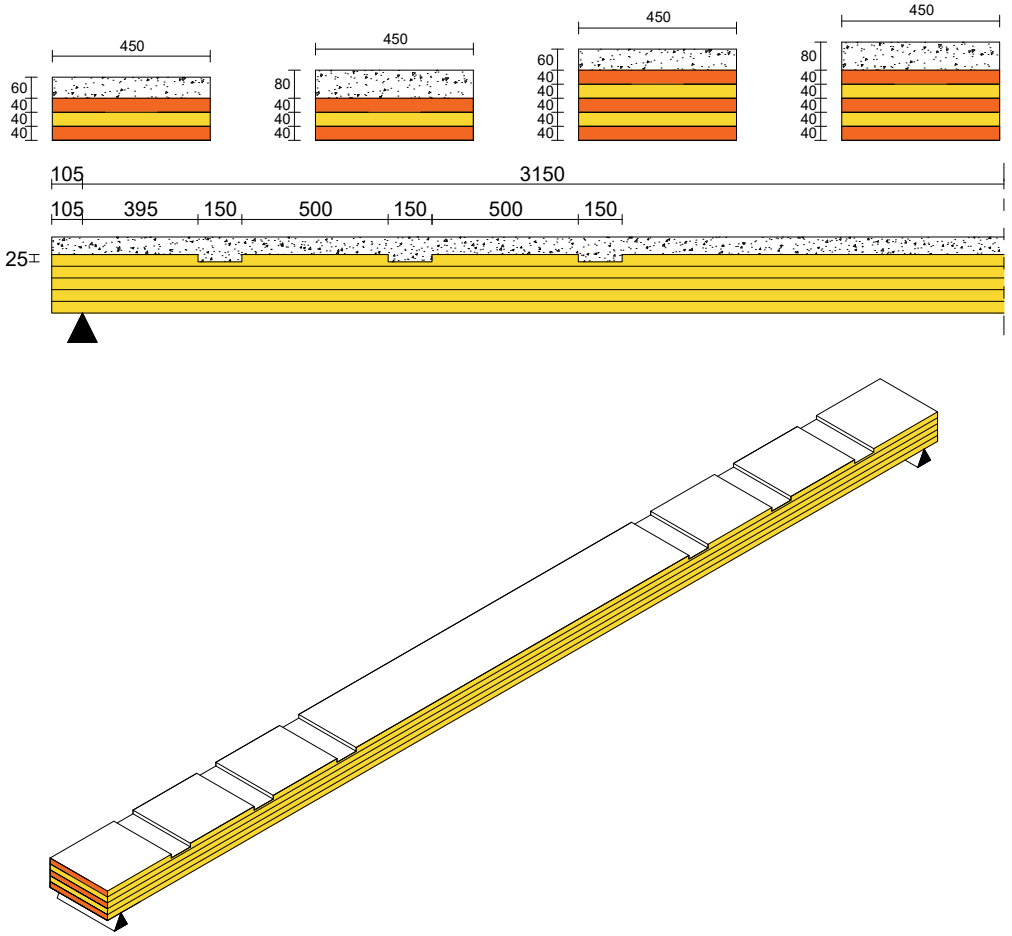

Figure 6.4: The setup for the numerical test for the standard TCC floors. At the top are all the different used cross sections; below that, a side view of the dimensions of the floor and the notches. At the bottom a 3D view of the floor.

CLT layers	**Thickness concrete [mm]**	**$EI_{eff.num}$ [N/mm^2]**	**$EI_{eff.gamma}$ [mm]**	**Change (%)**
3	60	2.725×10^{12}	2.913×10^{12}	106.9
3	80	3.674×10^{12}	3.938×10^{12}	103.7
5	60	7.363×10^{12}	7.533×10^{12}	102.3
5	80	8.932×10^{12}	9.247×10^{12}	103.5

Table 6.3: Comparison between the bending stiffness of the numerical model and the gamma calculation method

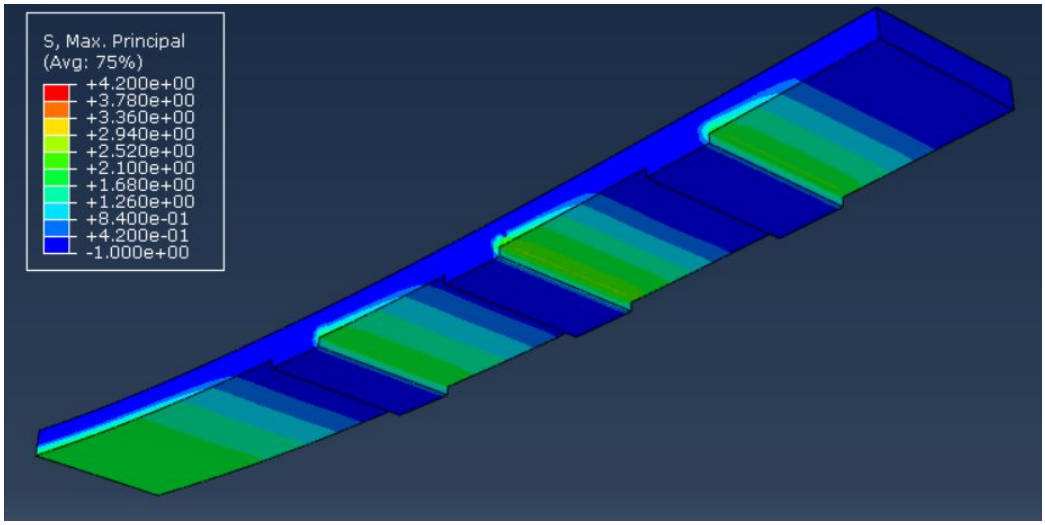

(a) Concrete stresses - TCC floor

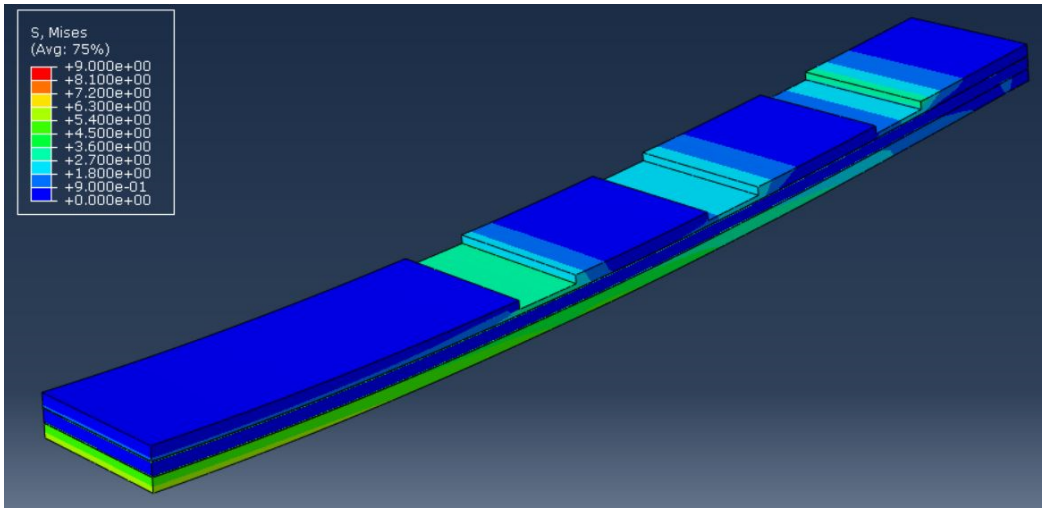

(b) Timber stresses - TCC floor

Figure 6.5: Concrete and timber stress distribution for the TCC floors. Which (a) shows the concrete with a thickness of 80 mm, which shows the governing concrete stress in this type of floor. (b) the governing stress will not happen at the notch but due to bending for the CLT. The governing stresses happen in the 3-layered CLT floor slab with 60 mm of concrete.

6.2.2 TCC Floor in weakest direction

This test is also set up to use the weakest direction of the CLT on a TCC floor, consisting of 3-layer CLT and 5-layer CLT. What emerges from the results of the 3-layer CLT is that the notch that goes up to the first effective layer, the second layer of the CLT, leaves 15 mm timber, and the stresses in this part of the timber exceed the maximum stresses almost immediately. For this reason, these 3-layer floor slabs are not considered in this paragraph.

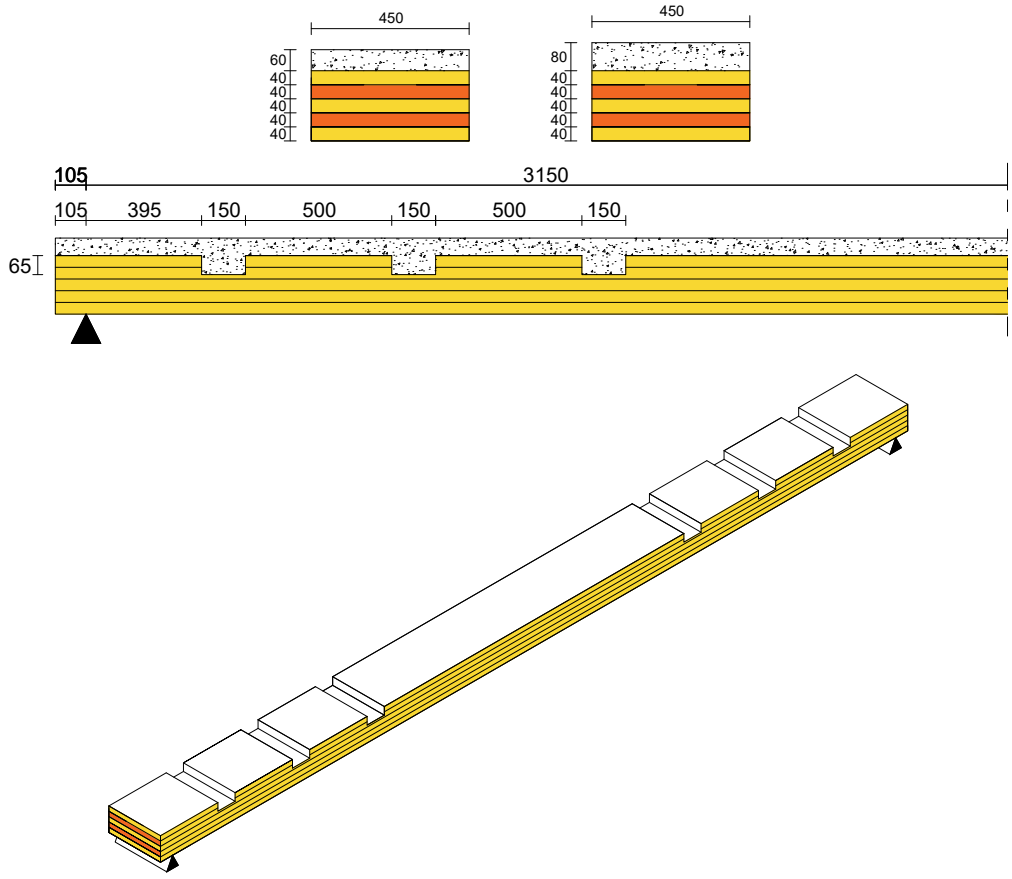

Figure 6.6: The setup for the numerical test for the TCC Floor is in the weakest direction. At the top are all the different used cross-sections. Below the cross-section is a side view of the dimensions of half the floor and the notches. At the bottom is a 3D view of the floor.

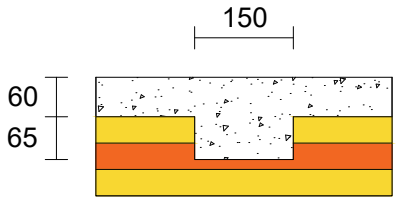

Figure 6.7: TCC floor slab with 3 layers of CLT. With a notch that goes to the first and only effective layer for the stiffness, the thickness will be reduced to only 15 mm

When the stresses are considered for the TCC floors with 5 layers of CLT, it shows that none exceed the maximum material stress. So both the maximum concrete and timber stresses still are not reached. It is found that the maximum concrete stress is 3.20 N/mm2, and the maximum timber stress is a maximum of 4.45 N/mm2. These stresses are significantly higher than the stresses found for the normal situation. None exceed the maximum material stress when considered for all the TCC floors. So, both the maximum concrete and timber stresses still are not reached. It is found that the maximum concrete stress is 3.20 N/mm^2, and the maximum timber stress is a maximum of 4.45 N/mm^2. Both maximum stresses are occurring in the TCC floor slab with the concrete of a thickness of 60 mm.

For verifying this numerical model using the Combined Gamma method, it has been adjusted so that the action of the CLT in these floors works differently in the normal situation, as discussed in section 3.1.2. The results show that, according to Table 6.5, the calculated bending stiffness of these floors for the thickness of 60 and 80 mm in concrete is 103.6% and 104.9%, respectively, higher than the results of the Abaqus model. Even though the Combined Gamma method did not use TCC floors in which the weak direction was used, the action of this floor is realistically modeled.

CLT layers	**Thickness concrete [mm]**	**$EI_{eff.num}$ [N/mm^2]**	**Deformation [mm]**
5	60	4.624×10^{12}	13.75
5	80	5.883×10^{12}	11.75

Table 6.4: Calculation of the bending stiffness according to the numerical calculations with the CLT in the weakest direction

CLT layers	**Thickness concrete [mm]**	$\mathbf{EI_{eff.num}}$ $[\mathbf{N/mm^2}]$	$\mathbf{EI_{eff.gamma}}$ **[mm]**	**Change (%)**
5	60	4.624×10^{12}	4.793×10^{12}	103.6
5	80	5.883×10^{12}	6.172×10^{12}	104.9

Table 6.5: Comparison between the bending stiffness of the numerical model and the gamma calculation method

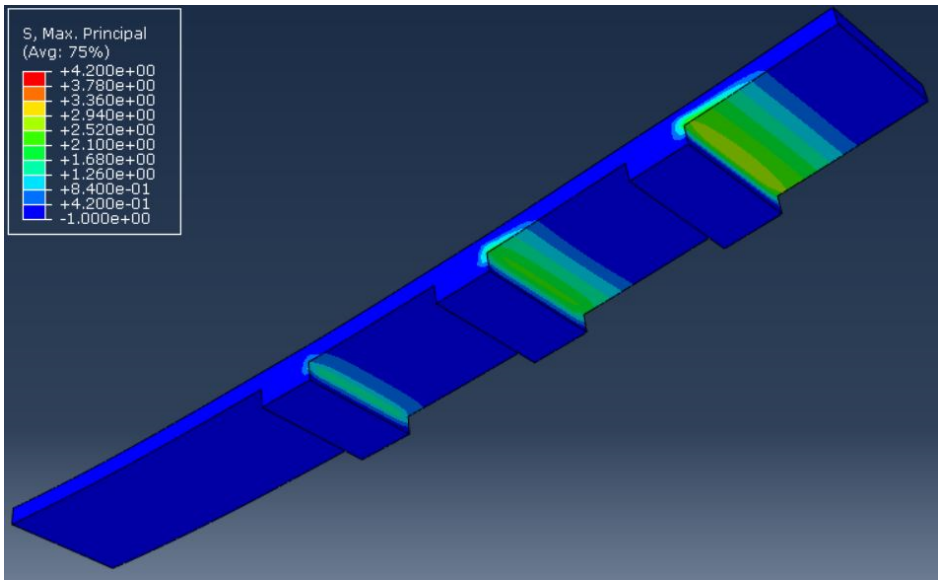

(a) Concrete stresses - TCC floor CLT weak direction

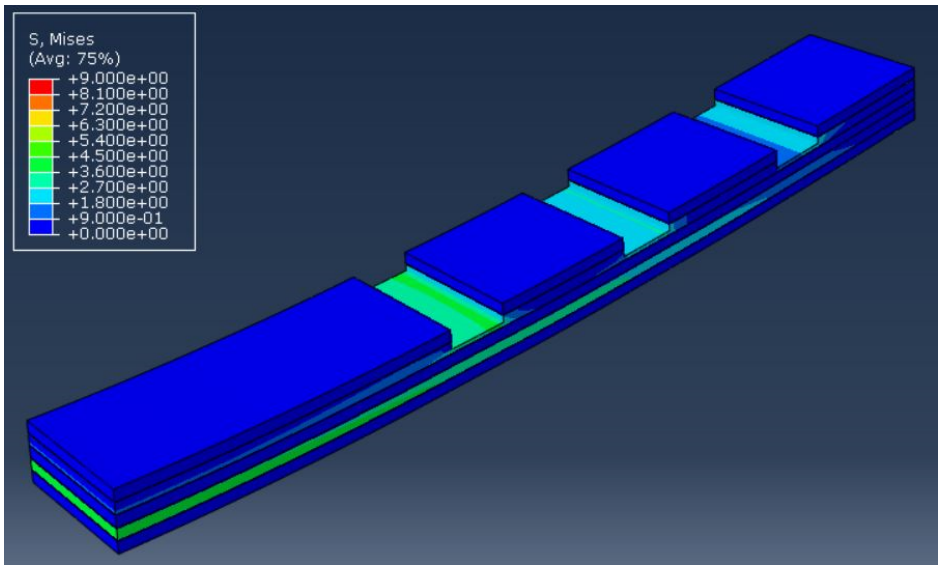

(b) Timber stresses - TCC floor CLT weak direction

Figure 6.8: Concrete and timber stress distribution for the TCC floors in the weakest direction. The maximum stresses for concrete and timber occur in the floor with the concrete slab of 60 mm. (a) shows which governing concrete stresses occur in this type of floor. (b) the governing stress will not happen at the notch but due to bending for the CLT.

6.2.3 Smaller Notch

Since this research is working towards a floor that will not span in one direction but will work in multiple directions, the impact of a narrower notch has also been considered. A model was created using the specifications in section 6.2.1, but where the notch goes over half the width instead of the entire length. This notch will, therefore, be 225 mm. This paragraph will examine the difference in bending stiffness of the two floors and the stresses that occur.

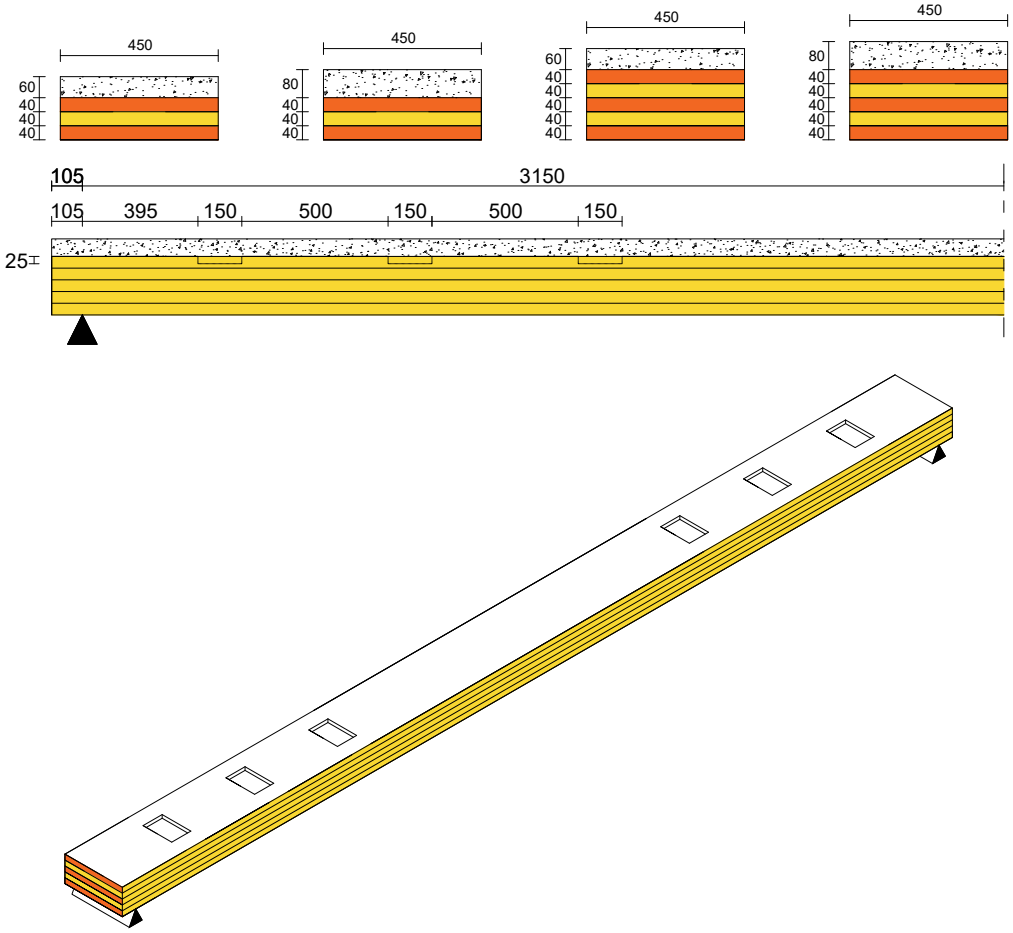

Figure 6.9: The setup for the numerical test for the TCC Floor with smaller notches. At the top are all the different used cross-sections. Below the cross-section is a side view of the dimensions of half the floor and the notches. At the bottom is a 3D view of the floor.

The stress distribution in the TCC floor is shown in Fig. 6.10. In the concrete section, it can be noted that the maximum stress is 4.18 N/mm^2, which happens in the 80 mm concrete slab with 3 layers of CLT. Unlike what happens at the full-length notch, the stress of the notch concentrates here. It is noticeable that the stress focuses around the corners of the notch, which introduces peak stresses. In the stress distribution in the timber, it can also be seen that this concentration occurs around the notch corners, which leads to maximum stress in the wood of 8.52 N/mm^2, which happens in the 60 mm concrete slab with 3 layers of CLT.

When a comparison is made between the peak stress in the notch over its entire length and that over a partial notch. It shows that the tensile strength in the concrete happens in the TCC floor slab with an 80 mm concrete layer and 3 layers of CLT. The entire notch has a stress of 2.82 N/mm^2, and the partial notch has a stress of 4.18 N/mm^2, an increase of 48%. The highest timber stresses in the TCC floor slab will occur in the notch. The entire notch has a stress of 3.48 N/mm^2, and the partial notch has a stress of 8.52 N/mm^2, an increase of 145%.

After comparing the stresses, a comparison was also made between the bending stiffness of the whole notch and the reduced notch. In Table 6.7, it can be seen that the bending stiffness of both floors is relatively close to each other. For the floors with the reduced notch, it is found that the stiffness is reduced to about 96% to 98% of that of the floor with the notch over the entire length.

CLT layers	**Thickness concrete [mm]**	**$EI_{eff.num}$ [N/mm^2]**	**Deformation [mm]**
3	60	2.663×10^{12}	22.34
3	80	3.604×10^{12}	18.04
5	60	7.086×10^{12}	8.97
5	80	8.586×10^{12}	8.05

Table 6.6: Calculation of the bending stiffness according to the numerical calculations with a smaller notch setup

CLT layers	**Thickness concrete [mm]**	$\mathbf{EI_{eff.num.ent}}$ $[\mathbf{N/mm^2}]$	$\mathbf{EI_{eff.num.small}}$ **[mm]**	**Change (%)**
3	60	2.725×10^{12}	2.663×10^{12}	97.7
3	80	3.674×10^{12}	3.604×10^{12}	98.1
5	60	7.363×10^{12}	7.086×10^{12}	96.2
5	80	8.932×10^{12}	8.586×10^{12}	96.1

Table 6.7: Comparison between the bending stiffness of the numerical model of the entire notch and the smaller notch

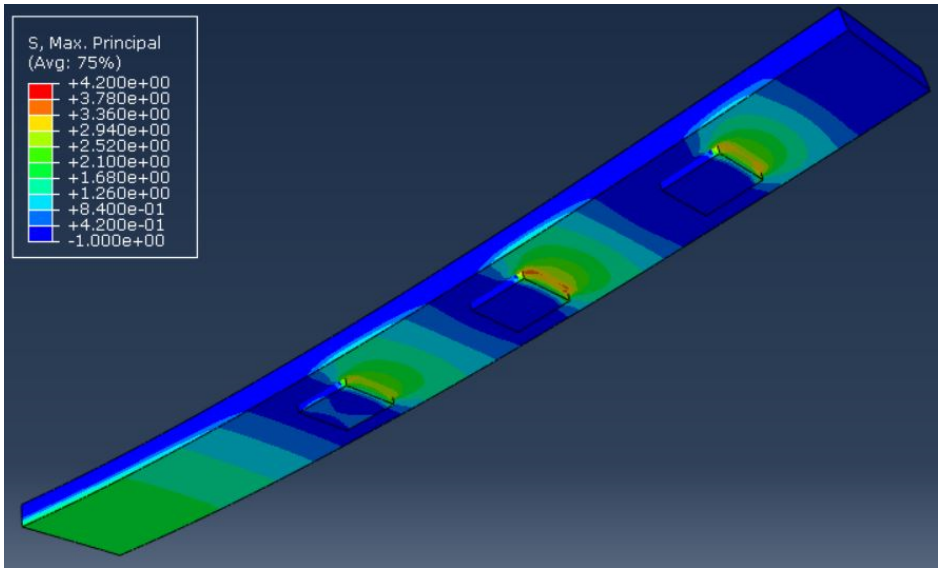

(a) Concrete stresses - TCC floor CLT smaller notch

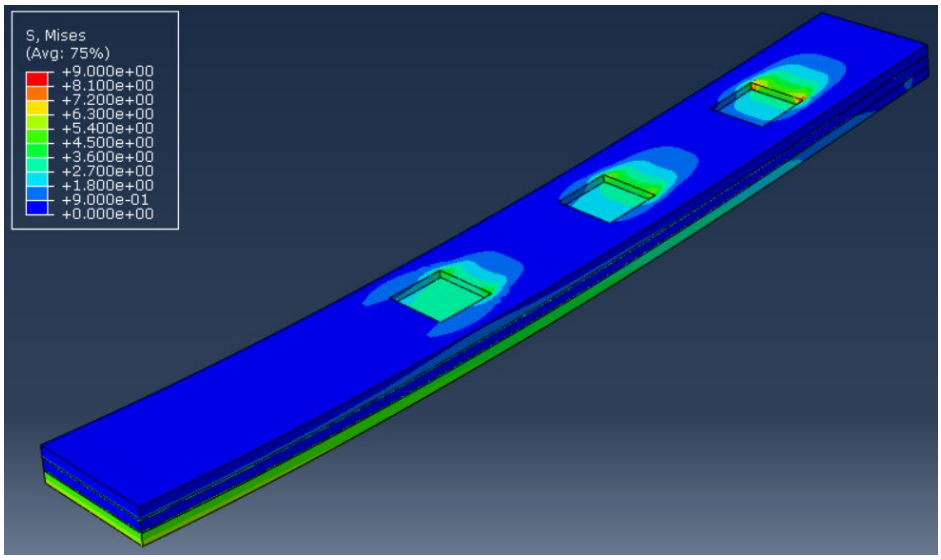

(b) Timber stresses - TCC floor CLT smaller notch

Figure 6.10: Concrete and timber stress distribution for the TCC floors in the weakest direction. (a) shows which governing concrete stresses occur in this type of floor. The maximum stresses for concrete occur in the floor with the concrete slab of 80 mm and 3 layers of CLT. (b) the governing stress will happen at the notch and concentrate in the corners. The maximum stresses for timber occur in the floor with the concrete slab of 60 mm and 3 layers of CLT.

Chapter 7

Numerical calculation point-supported slab

In this chapter, the data from the previous chapters has been used to set up the directional TCC floor. First, the Abaqus model is checked to determine whether the TCC floor setup works the same as for a FEM package. The verification has been done by checking the CLT used in the TCC floor slab. After the verification, the different notch patterns between the concrete and timber are compared to see the influence of each pattern and which pattern should be used for the set dimensions.

7.1 CLT floor slab

The validation of the CLT for the Abaqus model is done to check whether the floor shows comparable results for the CLT when it spans in multiple directions. It is done by creating two Abaqus models with different supports and comparing them with the RFEM calculation. The two dimensions used are a floor of 3500 mm x 3500 and 6000 mm x 3000 mm with a point support and a line support under each edge of the CLT. In Fig. 7.1, the two examples of this setup are shown.

What can be noted from this analysis is that the point-shaped support in terms of deformation and stresses in the Abaqus model is almost identical to the RFEM model. When looking at the line support floor slabs, it can be seen that the deformation and stresses in the Abaqus model differ by at least 20 percent from the RFEM model.

		Abaqus		**RFEM**		**Unity check**	
Dimensions	Support	Deformation	Stress	Deformation	Stress	Deformation	Stress
3500 x 3500 mm	Point	6.23	2.42	6.30	2.72	-1%	-11%
	Line	1.33	0.91	1.70	1.15	-22%	-20%
3000 x 6000 mm	Point	17.10	4.17	17.70	4.30	-3%	-3%
	Line	2.46	1.41	3.10	1.88	-21%	-25%

Table 7.1: Results between Abaqus and RFEM of the CLT floor slab

The point-supported floors are relatively close to the deflections and stress of the RFEM model. The deflection and stresses are within a few percent. For the CLT floor with a fully supported edge, the Abaqus model deviates with a difference of between 20 percent - 25 percent. The difference in the results is likely due to the complexity of the load transfer and the peak moment in the corners of the floor. Based on these results, the Abaqus model with point support for the CLT is adequate to serve as a basis for further TCC floor calculation at multiple supports.

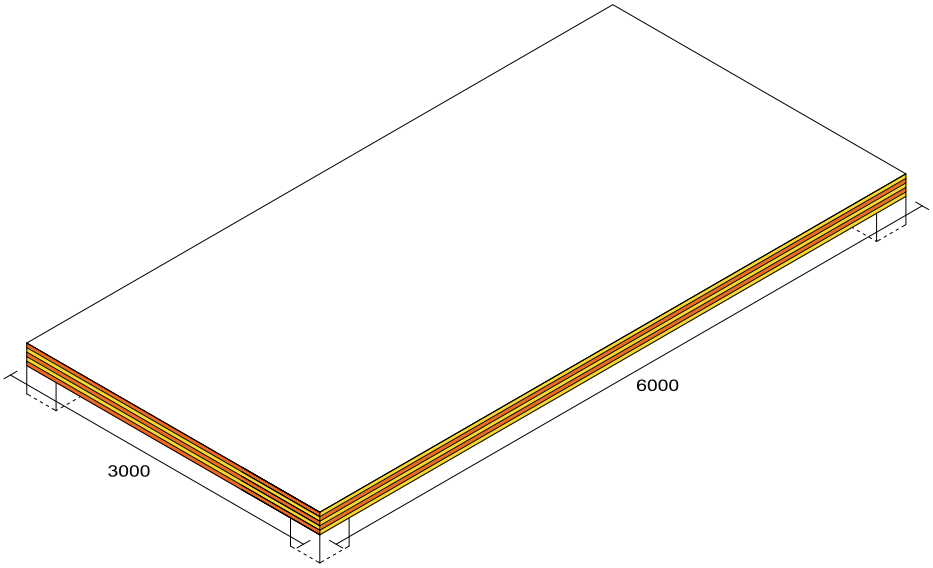

(a) CLT floor slab - 6000 x 3000 mm - point supported

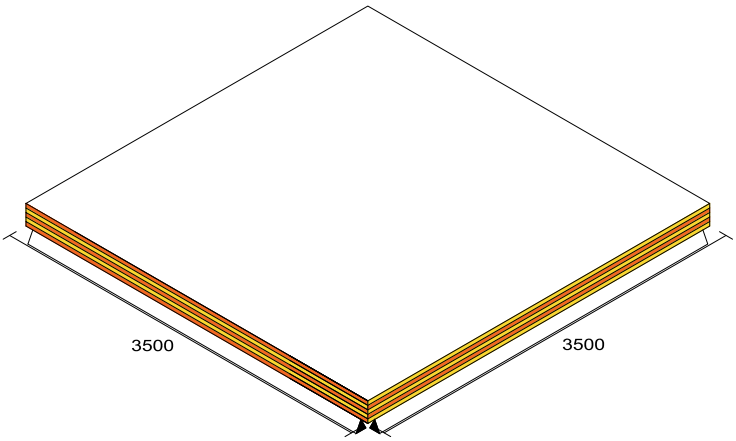

(b) CLT floor slab - 3500 x 3500 mm - line supported

Figure 7.1: CLT floor setups (a) shows the floor slab 3000 x 6000 mm point supported (b) shows the floor slab of 3500 x 3500 mm with a line support

7.2 TCC floor slab

With the information gathered in the last chapters, a model is set up for the TCC floor slab. In Abaqus, a script is created to test these floors with different connect setups while standard material properties and dimensions of the floor stay the same.

While translating the model from a one-directional floor to a multiple-span floor, it was also noticed that the forces become even more concentrated in the notches due to the concentrated load transfer from the point-supported supports. Large distances between notches caused the dimensional notch to be loaded significantly, causing the stresses to increase in the notch. The spacing between notches is kept small, 150 mm, to reduce the maximum stresses in the notch.

7.2.1 Different notch depth

A model is created for this test based on the proposed notch configuration, according to paragraph 5.2. In there, it is stated that the optimized notch depth depended on the angle of the notch relative to how the forces flow through the connection. It is decided to have only 3 angles to keep the shear connection design simple. The angles are 0 degrees, which is in the direction of the main direction of the CLT, 45 degrees, and 90 degrees, perpendicular to the direction of the CLT. Fig. 7.2 shows the setup for this floor. In orange is the notch with a depth of 25 mm, and in blue is the notch with a depth of 65 mm.

The most noticeable thing from the results in Abaqus is that there are peak stresses not at the edge of where the concrete and timber interact to transfer the shear forces between the floors towards the support, but in the part of the notch changes, the depth of 25 mm to 65 mm. It can be seen from the von Mises stresses in Fig. 7.3 that the stresses will concentrate in the notch closest to the support. As a result of the non-equal notch depth, the CLT slab starts to behave differently than expected. The 40 mm extra depth of the deepest notch in the concrete will act as a support at the location of the peak stresses and will rotate the CLT around this point. The rotation causes unpredictable behavior of the floor slab in deformation and where the maximum stresses will occur. Shown in Fig. 7.4 is the deformation, where it can be seen that the concrete stays in place and the CLT deforms around the notch.

Table 7.2 shows the maximum and minimum results for the deformation and the stresses in the TCC floor slab. For the deformation, the strongest direction according to the CLT is spanning in the direction of 6 meters. The

stress S11 and S12 are the stress and shear stress also in the direction of the 6 meters. S33 and S23 are perpendiculair to the strongest direction. What can be noted from the results is that the tension stresses and shear stresses in the concrete in both directions exceeded the maximum allowable stress. The concrete stresses will exceed the maximum allowable tensional forces in S33, in the direction of the 3 meter span, and the shear forces in both directions.

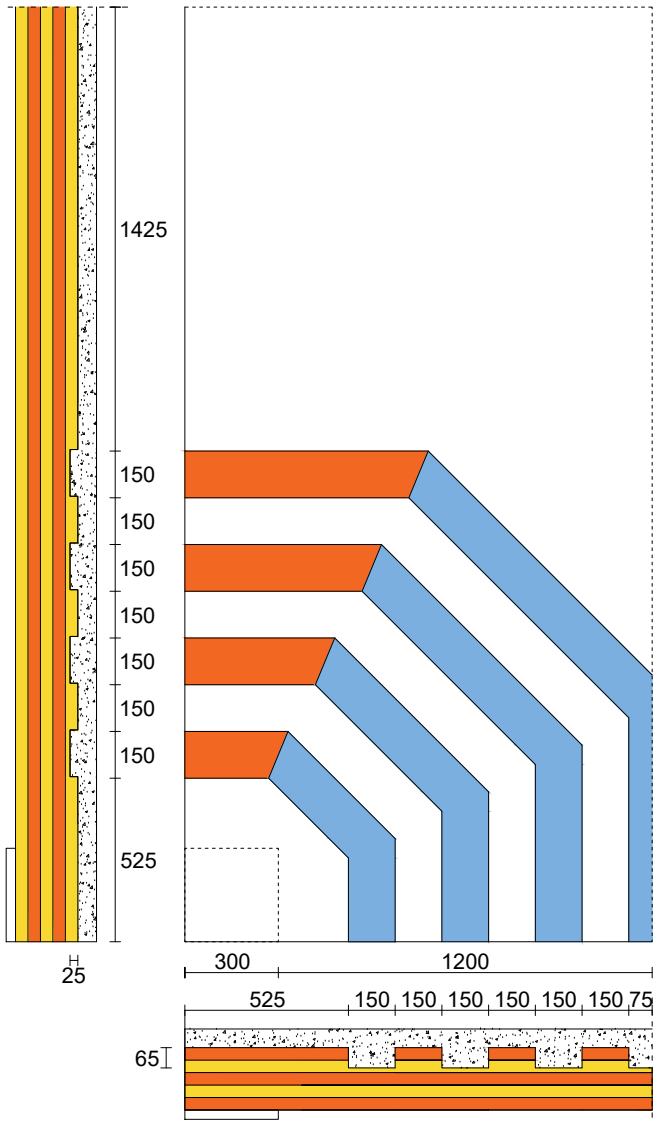

Figure 7.2: Setup of the TCC floor slab with different notch depths. The orange part has a notch depth of 25 mm, and the blue part has a notch depth of 65 mm.

Symbol	Part	Maximum Amount	Maximum Unit	Minimum Amount	Minimum Unit
U_{max}	Overall	7.68	mm		
$U_{strongest\ direction}$	Overall	7.16	mm		
$U_{weakest\ direction}$	Overall	1.32	mm		
S11	Concrete layer	2.34	N/mm^2	-5.77	N/mm^2
	Timber notch layer	4.84	N/mm^2	-6.25	N/mm^2
	Timber overall	4.84	N/mm^2	-6.25	N/mm^2
S33	Concrete layer[1]	3.38	N/mm^2	-3.91	N/mm^2
	Timber notch layer	0.37	N/mm^2	-0.37	N/mm^2
	Timber overall	0.50	N/mm^2	-0.37	N/mm^2
S12	Concrete layer[2]	1.28	N/mm^2	-0.79	N/mm^2
	Timber notch layer	0.77	N/mm^2	-0.86	N/mm^2
	Timber overall	0.83	N/mm^2	-0.86	N/mm^2
S23	Concrete layer[2]	0.82	N/mm^2	-0.44	N/mm^2
	Timber notch layer	0.32	N/mm^2	-0.11	N/mm^2
	Timber overall	0.41	N/mm^2	-0.16	N/mm^2

Table 7.2: Results of the maximum and minimum values obtained from the Numerical model. The materials indicated with [1] will exceed the maximum tension in the concrete, and for the materials with [2], the maximum allowable shear stress is exceeded.

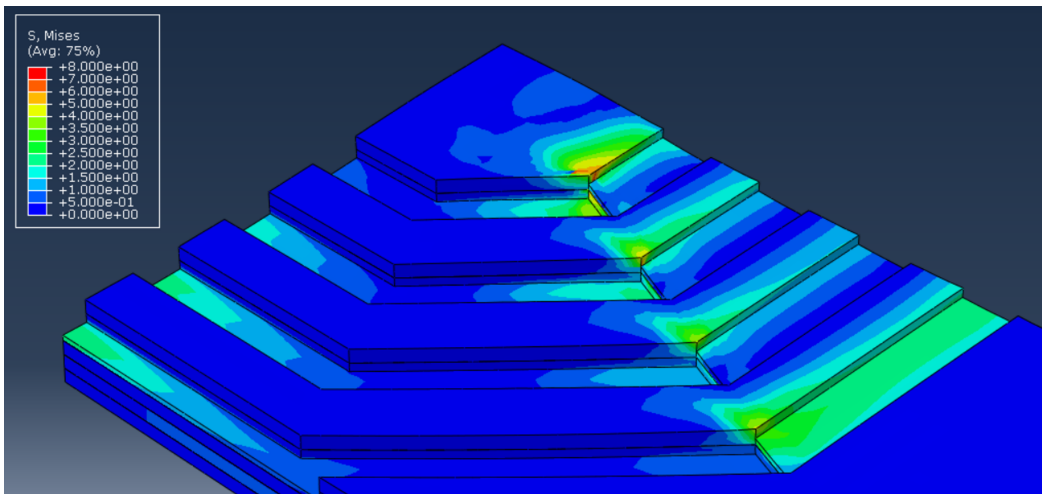

Figure 7.3: Von Mises stresses in the timber part concentrating on the difference in notch depth

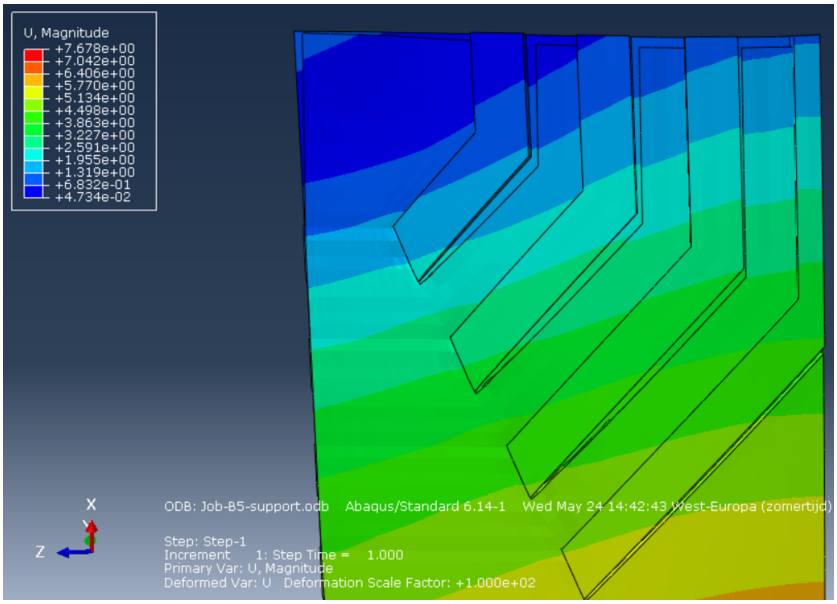

Figure 7.4: Deformation of at the bottom timber and at the top concrete. It shows that notch at the top left corner, the one closest to the support, is causing the timber to rotate around it.

7.2.2 Same notch depth

Based on the design and results of the last model, it was decided to make a model with the exact dimensions of the other floor but with the same notch depth. It was determined to take the notch depth of 65 mm overall because, in Chapter 5, the shear test results showed that this depth will guarantee better results when the notch is perpendicular to the main direction.

The Abaqus results show that the overall behavior is better predictable than the floor slab with different notch depths. It can be seen that the notches will be activated in all directions. The timber stresses in Fig. 7.6 show that the notch in the main direction activates the top layer of the timber, and the rotated notches are activated in the second layer.

As mentioned in the last paragraph, Table 7.3 shows the maximum and minimum results for the deformation and the stresses in the TCC floor slab. The stress S11 and S12 are the stress and shear stress in the direction of the 6 meters. S33 and S23 are perpendicular to the strongest direction. What can be noted from the results is that the tension stresses and shear stresses in the concrete in both directions exceeded the maximum allowable stress. Also, these are comparable with the maximum and minimum results of the model with the different notch depths from the last paragraph. For the

different notch depth, it shows that the stresses will reduce for almost every case except for the stresses and shear stresses in the weakest direction of the timber due to the activation of the other direction. That the other direction will be activated can also be deduced from the fact that the deformation in the weak direction decreases from 1.31 mm to 0.82 mm, meaning that the bending stiffness in that direction is higher.

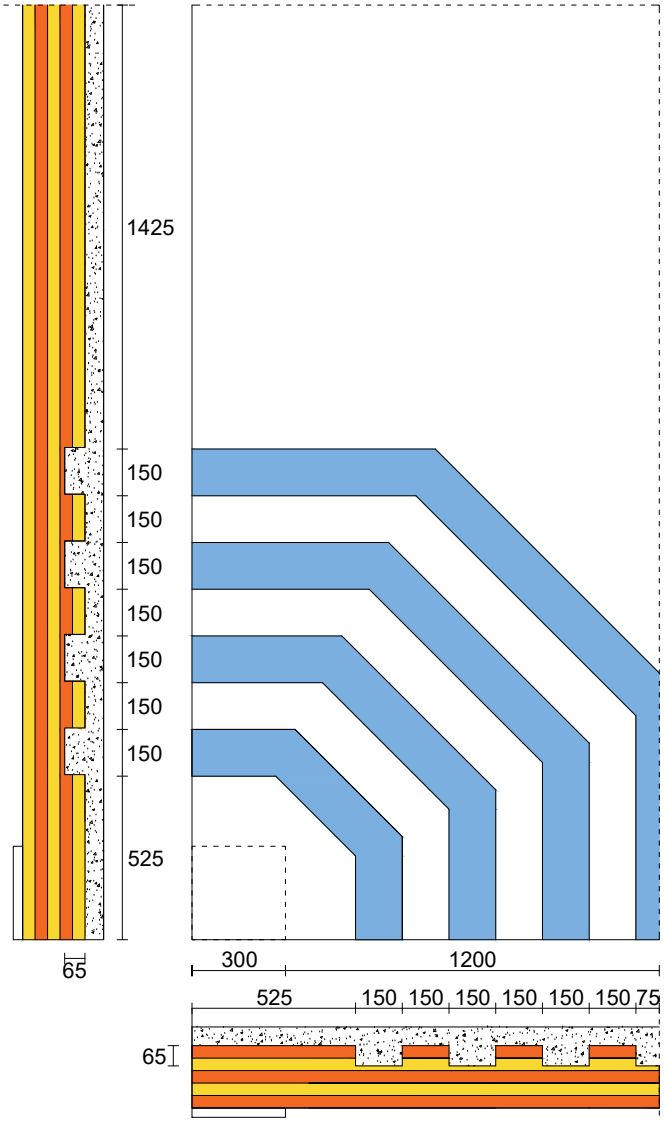

Figure 7.5: Setup of the TCC floor slab with the same notch depth. The blue part are the notches with a depth of 65 mm.

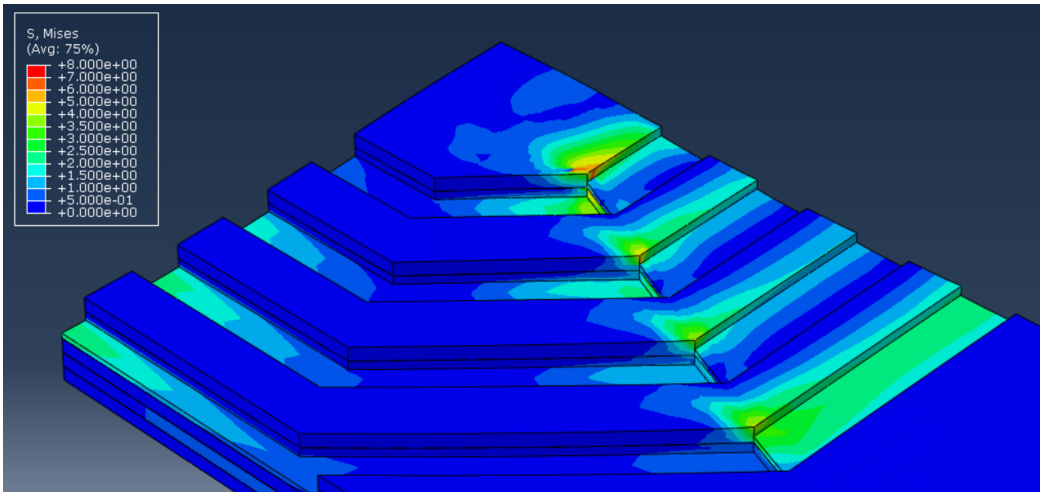

(a) Timber stresses in model with different notch depths

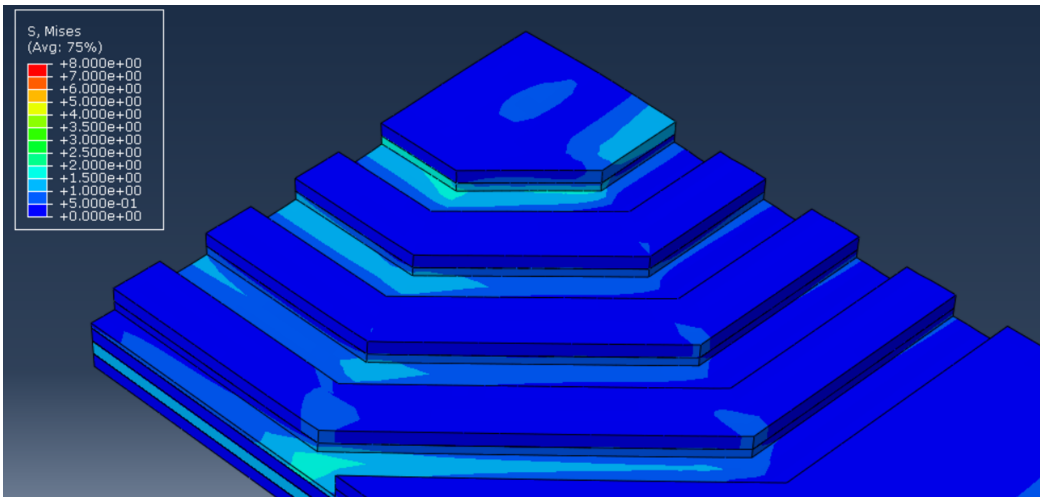

(b) Timber stresses in model with same notch depths

Figure 7.6: Von mises stresses in the timber for both models (a) shows the concentration at the corner where the notch depth changes (b) shows the evenly distributed stresses in the top layer in the main direction and in the second layer in the weakest direction for the notches with the same depth.

		Maximum		Minimum	
Symbol	Part	Amount	Unit	Amount	Unit
U_{max}	Overall	6.54	mm		
$U_{strongest\ direction}$	Overall	6.33	mm		
$U_{weakest\ direction}$	Overall	0.82	mm		
S11	Concrete layer	1.33	N/mm^2	-2.84	N/mm^2
	Timber notch layer	2.02	N/mm^2	-2.10	N/mm^2
	Timber overall	2.59	N/mm^2	-2.10	N/mm^2
S33	Concrete layer	2.11	N/mm^2	-2.12	N/mm^2
	Timber notch layer	0.83	N/mm^2	-0.59	N/mm^2
	Timber overall	0.83	N/mm^2	-0.59	N/mm^2
S12	Concrete layer[2]	0.74	N/mm^2	-0.30	N/mm^2
	Timber notch layer	0.22	N/mm^2	-0.59	N/mm^2
	Timber overall	0.73	N/mm^2	-0.59	N/mm^2
S23	Concrete layer[2]	0.64	N/mm^2	-0.34	N/mm^2
	Timber notch layer	0.67	N/mm^2	-0.07	N/mm^2
	Timber overall	0.67	N/mm^2	-0.15	N/mm^2

Table 7.3: Results of the maximum and minimum values obtained from the Numerical model of the same notch depth. The materials indicated with [2] the maximum allowable shear stress is exceeded.

7.2.3 Line pattern

The notch patterns proposed in the last paragraphs are based on the flow of forces and the optimized angle at which the notches have to be placed. A simple notch pattern was used to check whether the optimization of this connection outweighs its simplicity and manufacturability. This notch pattern consists of straight lines that can more easily be cut on the floor. The straight lines have a notch depth of 25 mm and are only in the top layer of the CLT, as shown in Fig. 7.7.

When the results of this floor slab are considered, it shows that the overall deformation of the floor is the same as the model with the same notch depth. For the deformation, the most significant difference in the bending stiffness of the floor is in the weakest direction. An increase in deformation occurs from 0.82 mm to 2.00 mm. For the stresses, two things can be noticed. The timber stresses in the notches are more concentrated towards the point support, where the stress in the strongest direction is higher than the model with the same notch depth, as shown in Fig. 7.8. The other thing noticeable is

that there is no connection between the materials in the weakest direction the concrete stresses increase significantly. In Fig. 7.9, the stresses in the weakest direction for the model with the same notch depth and the line pattern are shown, showing that concrete stresses increase significantly in the notch. The increase in concrete stresses could lead to applying reinforcement to prevent failure in the concrete. Another difference that should be noticed between the two models is that the line pattern works primarily in one direction because the weakest direction is not activated. This also causes the shear stresses to spread across the edge of the steel support in the strongest direction. With the model of the same notch depth, the shear stresses are distributed around the entire steel support, which causes the concentration of the shear stresses to occur at the corner of the steel support.

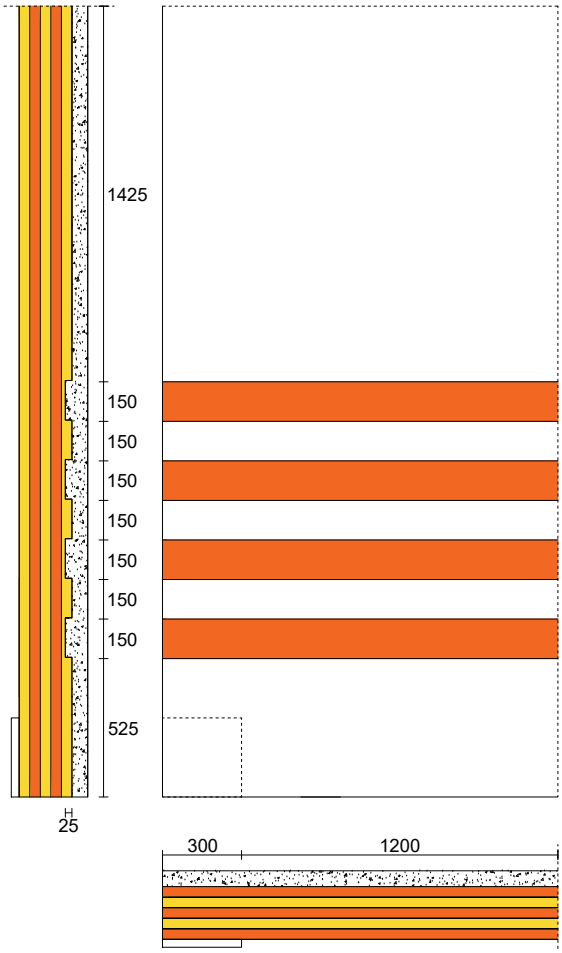

Figure 7.7: Setup of the TCC floor slab with a notch in line pattern. The notches have a depth of 25 mm.

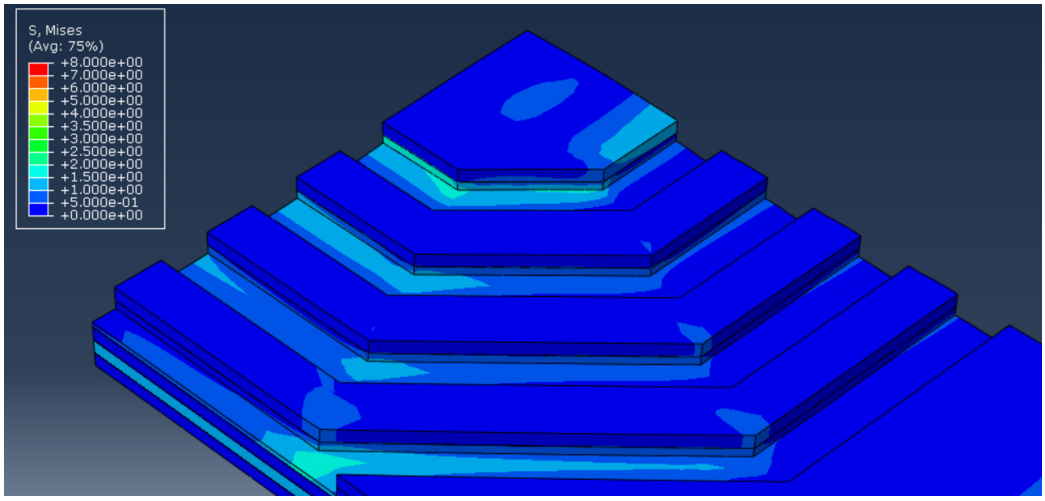

(a) Timber stresses in model with same notch depths

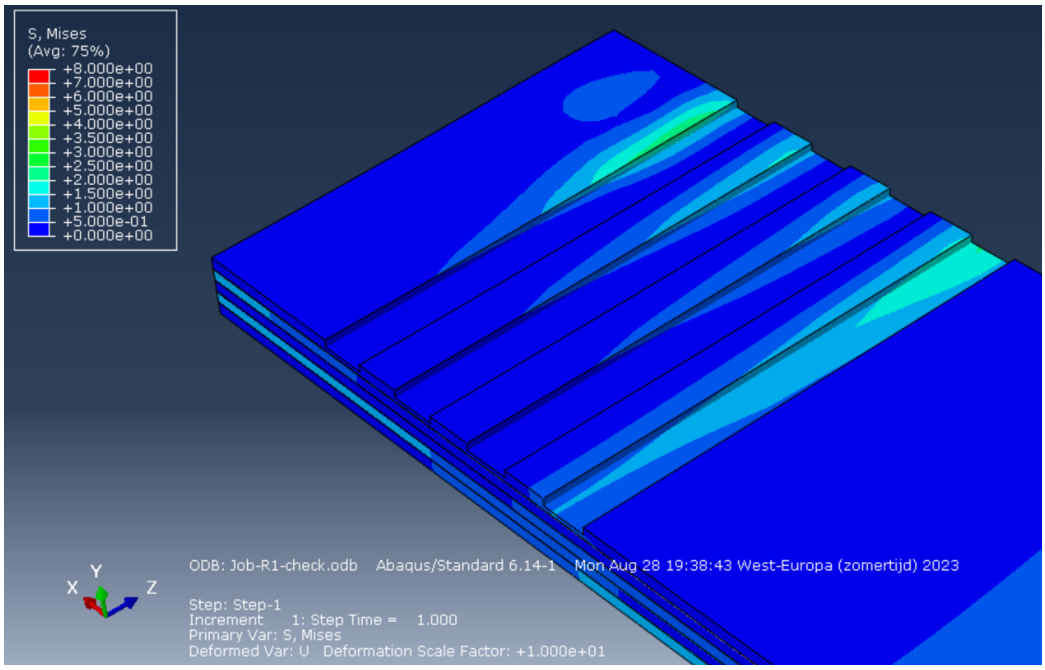

(b) Timber stresses in model with the line pattern

Figure 7.8: Von mises stresses in the timber for both models (a) shows the evenly distributed stresses in the top layer in the main direction and in the second layer in the weakest direction for the notches with the same depth. (b) shows the concentration of the stresses towards the support, which is in the top right corner.

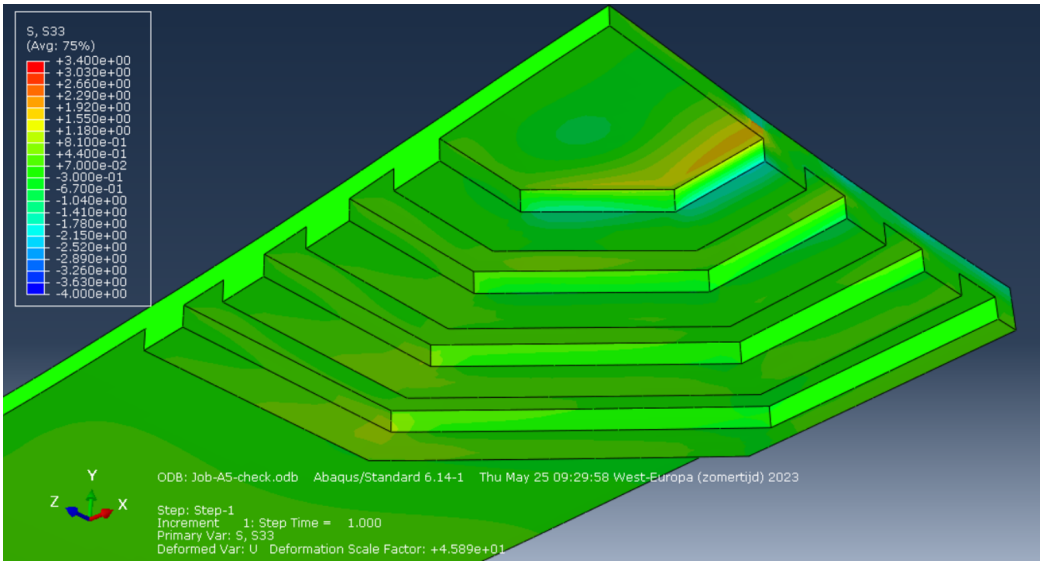

(a) Concrete stresses in S33, weakest direction, in model with same notch depths

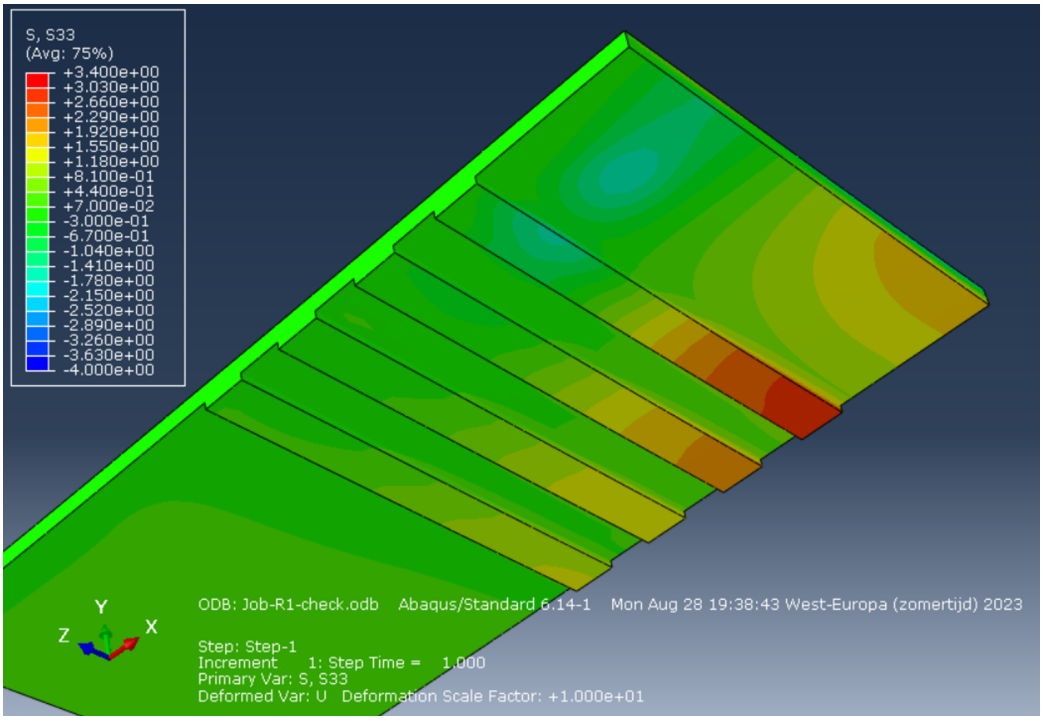

(b) Concrete stresses in S33, weakest direction, in model with the line pattern

Figure 7.9: Concrete stresses in S33, weakest direction, in both models (a) shows the concrete stresses distributed in the model with the same notch depth. (b) shows the concentration of the concrete stresses in the notch

		Maximum		**Minimum**	
Symbol	Part	Amount	Unit	Amount	Unit
U_{max}	Overall	6.48	mm		
$U_{strongest\ direction}$	Overall	6.12	mm		
$U_{weakest\ direction}$	Overall	2.00	mm		
S11	Concrete layer	1.34	N/mm^2	-2.88	N/mm^2
	Timber notch layer	2.25	N/mm^2	-2.12	N/mm^2
	Timber overall	2.57	N/mm^2	-2.12	N/mm^2
S33	Concrete layer	2.83	N/mm^2	-1.99	N/mm^2
	Timber notch layer	0.17	N/mm^2	-0.11	N/mm^2
	Timber overall	0.28	N/mm^2	-0.38	N/mm^2
S12	Concrete layer	0.51	N/mm^2	-0.18	N/mm^2
	Timber notch layer	0.32	N/mm^2	-0.07	N/mm^2
	Timber overall	0.74	N/mm^2	-0.38	N/mm^2
S23	Concrete layer[2]	0.90	N/mm^2	-0.35	N/mm^2
	Timber notch layer	0.14	N/mm^2	-0.01	N/mm^2
	Timber overall	0.51	N/mm^2	-0.15	N/mm^2

Table 7.4: Results of the maximum and minimum values obtained from the Numerical model of the line pattern notch. The materials indicated with [2] the maximum allowable shear stress is exceeded.

7.2.4 One-directional floor slab

An abaqus model of a floor working in one direction was examined to compare the results of a point-supported floor slab with the floor in one direction. This model uses the same notch configuration with a depth of 65 mm as the point-supported floor slabs. What can be observed is that the deformation of the floor is 9.26 mm compared to the 6.48 mm of the point-supported floor with the line pattern. Compared to this model, the stresses in the weakest direction, S33 and S23, are reduced significantly because, in this direction, the floor slab is unused. The shear stresses in the strongest direction, S12, also decrease due to the flow of forces that is not spread anymore through different directions. Compared to the point-supported floor slab, the only thing increasing is compression in the concrete in the middle of the slab and the tension in the bottom of the CLT due to bending.

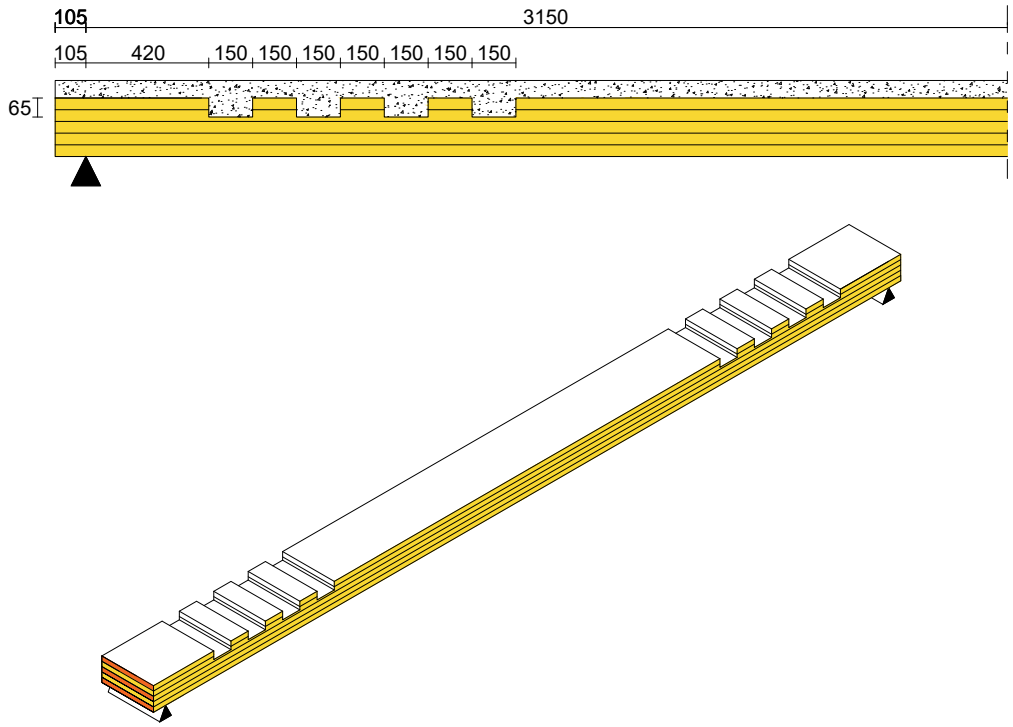

Figure 7.10: The setup for the numerical test of the one-directional floor slab. A side view of the dimensions of the floor and the notches and a 3D view of the floor is shown.

		Maximum		**Minimum**	
Symbol	Part	Amount	Unit	Amount	Unit
U_{max}	Overall	9.26	mm		
S11	Concrete layer[3]	1.66	N/mm^2	-4.18	N/mm^2
	Timber notch layer	0.11	N/mm^2	-1.35	N/mm^2
	Timber overall	3.57	N/mm^2	-1.35	N/mm^2
S33	Concrete layer	0.38	N/mm^2	-0.31	N/mm^2
	Timber notch layer	0.59	N/mm^2	-0.34	N/mm^2
	Timber overall	0.59	N/mm^2	-0.34	N/mm^2
S12	Concrete layer	0.38	N/mm^2	-0.25	N/mm^2
	Timber notch layer	0.10	N/mm^2	-0.04	N/mm^2
	Timber overall	0.43	N/mm^2	-0.45	N/mm^2
S23	Concrete layer	0.09	N/mm^2	-0.09	N/mm^2
	Timber notch layer	0.00	N/mm^2	-0.30	N/mm^2
	Timber overall	0.01	N/mm^2	-0.30	N/mm^2

Table 7.5: Results of the maximum and minimum values obtained from the Numerical model of the one-directional comparison model. The materials indicated with [3] the maximum allowable stress is exceeded.

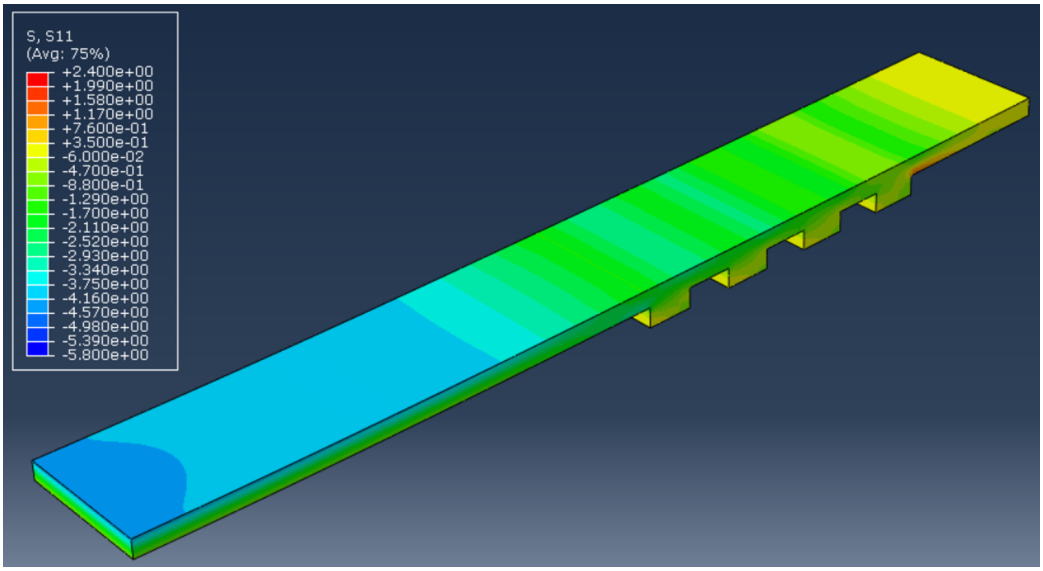

(a) Concrete stresses in S11 in the one-directional model

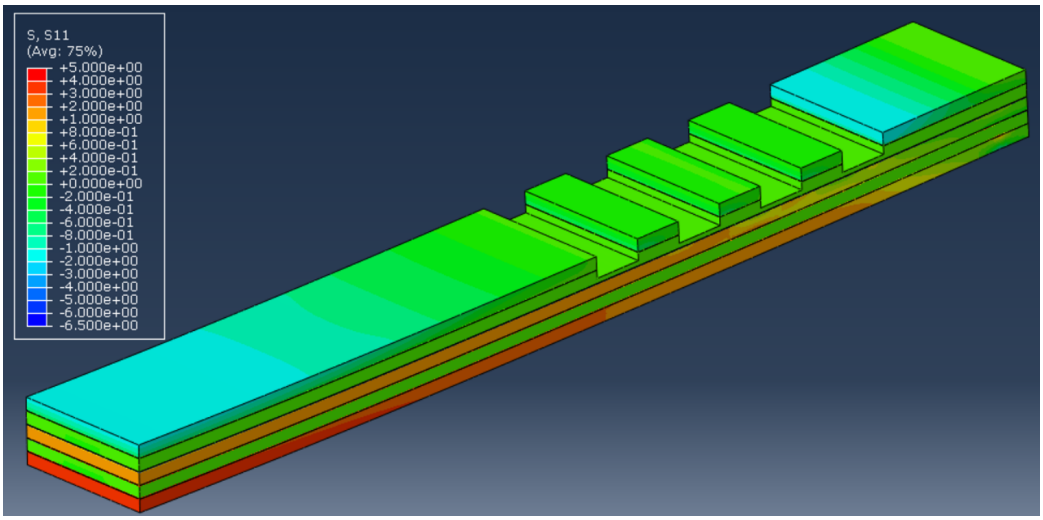

(b) Timber stresses in S11 in the one-directional model

Figure 7.11: Concrete and Timber stresses in S11, main direction. (a) shows the concrete stresses which reach their maximum in the middle (b) shows that the maximum timber stresses are reached in the bottom layer in the middle.

Setup of the connections

The one-directional floor slab shows an increase in deformation. For that reason, the different notch configurations are compared. The standard TCC floor from Paragraph 6.2.1 is used for this, which has similar properties to the one-directional floor slab in this chapter. The only difference is the arrangement of the notches in the timber. In the case of the standard TCC floor slab, these have a distance of 500 mm between them and are spread along the entire floor length as opposed to the other model, where the notch configuration is focused on equally distributed shear forces. Noticeably, the deflection and the stiffness of the floors increase equally on both floors, to the point where the notches stop at the model that focuses on the shear forces. What can be learned from this is that if a notch is created, it does not depend on the center-to-center distance applied. as long as it is spread equally across the floor.

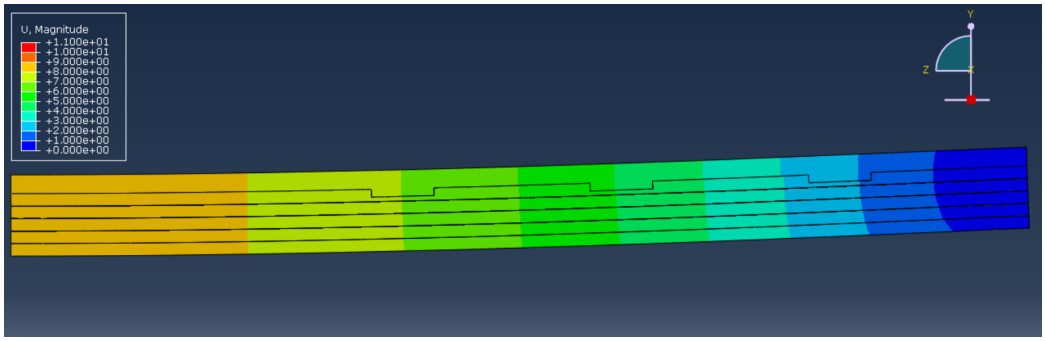

(a) Deformation of the standard TCC floor slab

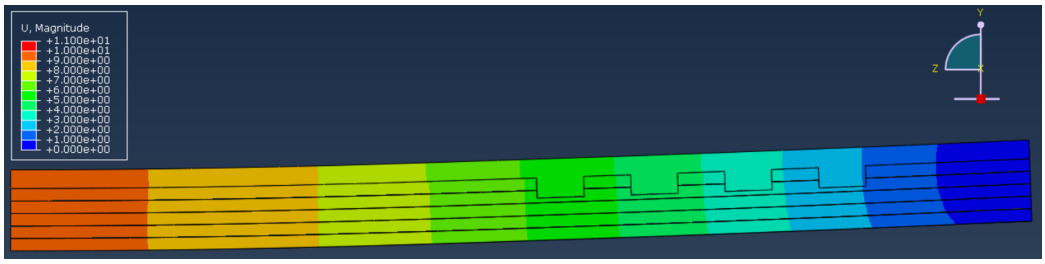

(b) Deformation of the one-directional model

Figure 7.12: Difference in deformation of the one-directional floor slabs. (a) shows the deformation in the standard TCC floor slab (b) shows that the deflection starts to increase after the notches stop towards the center of the floor.

Chapter 8

Conclusion

There are multiple things to consider when designing a point-supported floor compared to a one-directional floor. The notches in the floor should be designed so that the priority is not the stiffness of the floor but the load transfer to the support point. For the one-directional floor, the design focuses on the bending stresses and stiffness that determine the cooperation between the concrete and timber. While with the point-supported floors, the design must be made so that the notch stress does not exceed the maximum stresses.

Also, the length and width ratio of the floor are essential for the stresses that occur in the floor. In this thesis, a floor with a ratio of 6 by 3 meters is applied. These dimensions ensure that the floor works mainly in the strongest direction. The straight line pattern is the most sufficient way to make notches for this ratio. For length-width ratios closer to 1, the straight line pattern will not be sufficient because the stresses in the other direction will increase, in which the notches designed according to the forces flow will distribute the stresses more evenly over the notch and be used more optimally.

To make a comparison between the one-directional floor and the point-supported floor. The one-directional span for a TCC floor is generally more sufficient than the point-supported TCC floor. For the one-directional TCC floor, the shear test that usually needs to be done for this type of floor is only needed in one direction instead of multiple directions, which is needed for the point-supported floor, and the stresses are more predictable in these types of floors which makes them easier to design. Local weakening for the one-directional floor of the CLT floor slab is also not an issue because it is not needed to make the notches in the second layer of the CLT. This does not reduce the choosable option, like for the point supported floor slab, to only CLT with 5 layers.

Chapter 9

Discussion

Multiple steps validate the results obtained from the test with the point-supported TCC floor slab. An analytic calculation model is combined with a FEM model to show that the results are valid, and multiple steps are taken during this thesis to secure this. After the shear tests and the flow of forces, it was expected that the weak direction of the floors would have more influence on the flow of forces, but that was not the case for a floor with the dimensions discussed in this thesis. There are two reasons that this happens. The strongest direction of the TCC floor has so much influence that the weak direction almost becomes irrelevant. The supports are assumed to be stiff steel plates, which do not prevent the floor from bending around a point or edge.

The limitation of this thesis is that the data for most validation points are limited. For example, the analytic calculation method is only based on a small number of tests of the TCC floor slabs, the notch connection in the weakest direction is never tested, and the point-supported floor slab has never been researched. A few validation steps must be researched further to show that these are valid.

This research gives some guidelines for using point-supported floor slabs, but some steps have to be researched further to create an end product that can be used in the built environment. Follow-up research is suggested for three different types of research:

1. Obtaining test results from the shear test in the weakest direction. With this, it can be validated that the assumed results in this thesis are correct.

2. Research the setup of the notches to optimize the combination of contributing to the bending stiffness and the reduction of shear stress in the notch due to the concentrated force towards the point support.

This research helps to provide guidelines on how to design the notches for these types of floors.

3. Research the influence of the dimensions of the TCC floor slab and what happens when the ratio length and width change.

Chapter 10

Recommendations

As a structural engineer, it is recommended to know which changes are happening between the point-supported TCC floor slabs and the one-directional span floor slab by comparing the results. The focus changes from the stresses that occur in the concrete and timber to the shear stresses that are occurring in both materials. The design for the bending stiffness is changing. The one-directional floor slab mainly focuses on spreading the notches evenly over the entire floor slab. In contrast, the point-supported floor slab needs to be designed for the notches to spread the shear stress evenly over the notches, placing the notches more toward the support. Moreover, the floor's dimensions significantly influence the notch pattern overall design.

Based on Paragraph 3.1.3, it is recommended to consider the different results from the Gamma method between the ductile and brittle behavior of the floor slabs. It is stated that the Gamma method overestimates the bending stiffness for TCC floor slabs with notches and adhesives. The connection that uses screws is underestimating the tested bending stiffness by the same Gamma method. When designing these types of floors, it is wise to realize how significant the deviation can be when using the gamma method for the different connections.

Bibliography

[1] Xiaoyu Zhang, Xiamin Hu, Hongwei Gong, Jing Zhang, Zhicheng Lv, and Wan Hong. Experimental study on the impact sound insulation of cross laminated timber and timber-concrete composite floors. *Applied Acoustics*, 161:107173, 2020.

[2] Marius Leonardus Robertus van der Linden and HJ Blass. Timber-concrete composite floor systems. In *International Wood Engineering Conference, New Orleans, USA*, 1996.

[3] Yuchen Jiang and Roberto Crocetti. CLT-concrete composite floors with notched shear connectors. *Constr. Build. Mater.*, 195:127–139, January 2019.

[4] Serge Lamothe, Luca Sorelli, Pierre Blanchet, and Philippe Galimard. Lightweight and slender timber-concrete composite floors made of clt-hpc and clt-uhpc with ductile notch connectors. *Engineering Structures*, 243:112409, 2021.

[5] Yingwei Bao, Weidong Lu, Kong Yue, Hao Zhou, Binhui Lu, and Zhentao Chen. Structural performance of cross-laminated timber-concrete composite floors with inclined self-tapping screws bearing unidirectional tension-shear loads. *Journal of Building Engineering*, page 104653, 2022.

[6] Khai Quang Mai, Aron Park, Khoa Tan Nguyen, and Kihak Lee. Full-scale static and dynamic experiments of hybrid clt–concrete composite floor. *Construction and Building Materials*, 170:55–65, 2018.

[7] Ján Kanócz, Viktória Bajzecerová, and Š Šteller. Timber-concrete composite elements with various composite connections. part 3: Adhesive connection. *Wood research*, 60(6):939–952, 2015.

[8] Md Shahnewaz, Robert Jackson, and Thomas Tannert. Cross-laminated timber concrete composite systems for long-span floors. In *Structures Congress 2022*, pages 356–363.

[9] Stefan Loebus and Stefan Winter. *Zweiachsige Tragwirkung bei Holz-Beton-Verbundkonstruktionen-Entwicklung von Bemessungsverfahren und Konstruktionsdetails für zweiachsige Lastabtragung bei der Holz-Beton-Verbundbauweise*. Fraunhofer IRB Verlag, 2017.

[10] Nen-En Cen. - *Design of timber structures - Part 1-1: General -Common rules and rules for buildings*. European Committe for Standarization, Brussels, Belgium, 1995.

[11] ISO 6891 (1983). *Timber structures - Joints made with mechanical fasteners - General principles for the determination of strength and deformation characteristics.* ISO 6891, 1983.

[12] Julien Gamerro. Development of novel standardized structural timber elements using wood-wood connections. Technical report, EPFL, 2020.

[13] Alfredo Manuel Pereira Geraldes Dias. Mechanical behaviour of timber-concrete joints. 2005.

[14] M Wallner-Novak, J Koppelhuber, and K Pock. *Cross-laminated timber structural design–Basic design and engineering principles according to Eurocode*. 2014.

[15] Milad Hafezolghorani, Farzad Hejazi, Ramin Vaghei, Mohd Saleh Bin Jaafar, and Keyhan Karimzade. Simplified damage plasticity model for concrete. *Structural Engineering International*, 27(1):68–78, 2017.

List of Figures

List of Tables

Acknowledgements

Allereerst wil ik mijn begeleider Arjan Habraken bedanken voor de tijd, moeite en feedback tijdens de afstudeerbegeleidingen en wil ik Faas Moonen en Anton van der Esch bedanken voor het beoordelen van deze Thesis.

Mijn ouders en de rest van de familie voor de moeite die ze ieder weekend namen om te halen en brengen om mij op en neer te laten reizen naar Eindhoven. En voor hun onvoorwaardelijk steun tijdens mijn studententijd en natuurlijk de tijd daarvoor al.

Mijn vrienden van “ValkenFissa” die er altijd voor me zijn en waarop ik meer dan een decennium al op kan rekenen.

En als laatste, maar zeker niet als minste, wil ik de mensen van Vloer 5 en KOers bedanken voor hun gezelligheid, motivatie en mogelijkheid om te discussiëren. Zonder hen was het studentenleven toch een stukje lastiger en een stuk saaier geweest.

Appendix A

Results of comparison Gamma method with test results

							EI,eff				***EI,eff***		***%***		
	Research number	Name in paper	Source	Type connection	CLT Layers	**Tests**	Calculated paper	40% Fmax	40%-10% Fmax	Seperated calculation method	Combined calculation method	Seperated calculation method	Combined calculation method	Amount of specimen
1	A1	F1	CLT-concre	Notch	3	***2,55E+12***	2,72E+12	2,52E+12	2,39E+12	3,02E+12	2,91E+12	126,3%	121,7%	1
2	A2	A2 - TC4.5	TIMBER – (	Adhesive	3	***1,11E+12***	1,38E+12	1,09E+12	1,34E+12	1,47E+12	1,44E+12	109,7%	107,2%	3
3	A3	A3 - TC6.0	TIMBER – (	Adhesive	3	***3,30E+12***	3,43E+12	2,91E+12	3,30E+12	3,72E+12	3,50E+12	112,8%	106,0%	3
4	A4	A4 - TN1-20-10-200	Structural	Screws	3	***1,84E+12***		2,85E+12	3,12E+12	2,12E+12	1,98E+12	67,9%	63,3%	3
5	A5	A5 - TN1-20-12-200	Structural	Screws	3	***1,89E+12***		2,98E+12	3,28E+12	2,10E+12	1,94E+12	64,1%	59,1%	3
6	A6	A6 - TN1-20-12-300	Structural	Screws	3	***1,67E+12***		2,79E+12	3,20E+12	2,01E+12	1,86E+12	62,7%	58,1%	3
7	B1	F2	CLT-concre	Notch	5	***7,74E+12***	7,90E+12	8,16E+12	8,15E+12	8,71E+12	8,08E+12	106,9%	99,1%	1
8	B2	B2 - FN1-19-12-300	Structural	Screws	5	***5,44E+12***		1,04E+13	1,19E+13	5,96E+12	5,24E+12	50,2%	44,1%	3
9	B3	B3 - FN1-20-12-300	Structural	Screws	5	***5,60E+12***		9,19E+12	1,01E+13	6,05E+12	5,39E+12	59,7%	53,2%	3
10	B4	B4 - SFS-45-s150	Full-scale s	Screws	5	***1,64E+13***	1,26E+13	1,65E+13	1,71E+13	1,16E+13	1,09E+13	67,9%	63,7%	1
11	B5	B5 - SFS-45-s300	Full-scale s	Screws	5	***1,49E+13***	1,09E+13	1,50E+13	1,65E+13	1,10E+13	1,04E+13	66,8%	62,8%	1
12	B6	B6 - SFS-90-s150	Full-scale s	Screws	5	***1,38E+13***	6,10E+12	1,42E+13	1,36E+13	1,14E+13	1,07E+13	83,6%	78,5%	1
13	B7	B7 - CLT-UHPFRC	Lightweigh	Notch (triang	5	-		1,06E+13	1,27E+13	1,39E+13	1,33E+13	110,1%	104,9%	2
14	B8	B8 - CLT-HPC-12	Lightweigh	Notch (triang	5	-		6,46E+12	8,57E+12	1,27E+13	1,21E+13	148,1%	141,5%	2
15	B9	B9 - CLT-HPC-34	Lightweigh	Notch (triang	5	-		9,79E+12	1,28E+13	1,27E+13	1,21E+13	98,9%	94,5%	2
16	C1	C1 - TCC 1	Cross-Lami	Screws	7	-		6,55E+13	7,82E+13	1,22E+14	9,83E+13	156,1%	125,7%	2
17	C2	C2 - TCC 2	Cross-Lami	Steel plate	7	-		7,83E+13	1,09E+14	1,05E+14	8,77E+13	96,4%	80,5%	2
18	C3	C3 - TCC 3	Cross-Lami	Steel mesh	7	-		8,42E+13	1,10E+14	1,35E+14	1,06E+14	123,0%	96,4%	2
19	C4	C4 - TCC 1 9,6	Cross-Lami	Screws	7	-		1,22E+14	1,90E+14	1,48E+14	1,37E+14	77,7%	71,9%	2
20	C5	C5 - TCC 2 9,6	Cross-Lami	Steel plate	7	-		1,42E+14	1,63E+14	1,40E+14	1,30E+14	85,9%	79,9%	2
21	C6	C6 - TCC 3 9,6	Cross-Lami	Steel mesh	7	-		1,47E+14	1,81E+14	1,53E+14	1,41E+14	84,3%	77,8%	2

A.1 Calculation A1

A.1.1 Mechanical properties

Ec	32530,4	N/mm2	
Etimber	11000	N/mm2	
Gr	60	N/mm2	Shear modulus paralell to the grain
h	40	mm	
Kser / K0.4	865	kN/mm	
seff	700	mm	
fck	47,1	N/mm2	
fcd	31,40	N/mm2	
fctm	3,91	N/mm2	
fctk.0,05	2,74	N/mm2	
fctd	1,83	N/mm2	

			Area		Iy	
h.con	60	mm	27000	mm2	8100000	mm4
h.1	40	mm	18000	mm2	2400000	mm4
h.between	40	mm	18000	mm2	2400000	mm4
h.2	40	mm	18000	mm2	2400000	mm4
width	450	mm				
length	6300	mm				

A.1.2 Seperated calculation method

ac	31,2	mm	118,8	mm
a1	58,8	mm	118,8	mm

γcon	0,850
γ1	1,000

EI.con	9,90E+11	Nmm2
EI.1	2,03E+12	Nmm2
EI(eff)	***3,02E+12***	***Nmm2***

Layers	Thickness	z	centre of gravity	Direction	E	G	EI	EAz	EIy Som	Ieff som	Eieff red		
1	40	40,0	18000,00	Parallel	11000	688	2,64E+10	3,17E+11	3,43E+11	3,12E+07	3,32E+11	y1	0,965
2	40	0,0	600,00	Perpendicular	367	60	8,80E+08	6,60E-18	8,80E+08	2,40E+06			
3	40	-40,0	18000,00	Parallel	11000	688	2,64E+10	3,17E+11	3,43E+11	3,12E+07	3,32E+11	y2	0,965
Total height	120,0	mm							EIeff	Ieff	***EIeff***		
Zs	60,0	mm							6,87E+11	6,48E+07	***6,64E+11***		

V

28969,4	27000,0	0,0	0,0	0,0	54000,0
-27000,0	-28969,4	0,0	0,0	0,0	-54000,0
0,0	0,0	1,0	0,0	0,0	0,0
0,0	0,0	0,0	1,0	0,0	0,0
0,0	0,0	0,0	0,0	1,0	0,0

S

C1,2	675
C2,3	0
C3,4	0
C4,5	0

D1	49,2
D2	49,2
D3	0,0
D4	0,0
D5	0,0

2,6E-04	2,4E-04	0,0E+00	0,0E+00	0,0E+00	0,965
-2,4E-04	-2,6E-04	0,0E+00	0,0E+00	0,0E+00	0,965
0,0E+00	0,0E+00	1,0E+00	0,0E+00	0,0E+00	0,000
0,0E+00	0,0E+00	0,0E+00	1,0E+00	0,0E+00	0,000
0,0E+00	0,0E+00	0,0E+00	0,0E+00	1,0E+00	0,000

a1	40,0
a2	-40,0
a3	0,0
a4	0,0
a5	0,0

A.1.3 Combined calculation method

Lagen	Hoogte	z	centre of gravity	Direction	E	G	EI	EAz	EIy Som	Ieff som	Eieff red		
1	60	28,3	79847,2	Parallel	32530	688	2,63E+11	7,03E+11	9,66E+11	2,97E+07	8,97E+11	y1	0,902
3	40	-21,7	18000,0	Parallel	11000	688	2,64E+10	9,33E+10	1,20E+11	1,09E+07	1,12E+11	y2	0,920
4	40	-61,7	600,0	Perpendicular	367	60	8,80E+08	2,51E+10	2,60E+10	7,10E+07			
5	40	-101,7	18000,0	Parallel	11000	688	2,64E+10	2,05E+12	2,07E+12	1,89E+08	1,90E+12	y3	0,916
Total height	180,0	mm							EIeff	Ieff	***EIeff***		
Zs	121,7	mm							3,19E+12	3,00E+08	***2,91E+12***		

V					S
41133,5	26830,5	0,0	0,0	0,0	61785,7
-34955,3	-42555,4	68655,9	0,0	0,0	-7785,7
0,0	14655,9	-73663,9	0,0	0,0	-54000,0
0,0	0,0	0,0	1,0	0,0	0,0
0,0	0,0	0,0	0,0	1,0	0,0
1,2E-04	1,1E-04	1,0E-04	0,0E+00	0,0E+00	0,902
-1,4E-04	-1,6E-04	-1,5E-04	0,0E+00	0,0E+00	0,920
-2,8E-05	-3,3E-05	-4,4E-05	0,0E+00	0,0E+00	0,916
0,0E+00	0,0E+00	0,0E+00	1,0E+00	0,0E+00	0,000
0,0E+00	0,0E+00	0,0E+00	0,0E+00	1,0E+00	0,000

C1,2	1235,7
C2,3	675,0
C3,4	0,0
C4,5	0,0
D1	218,4
D2	49,2
D3	49,2
D4	0,0
D5	0,0
a1	28,3
a2	-21,7
a3	-101,7
a4	0,0
a5	0,0

A.2 Calculation A2

A.2.1 Mechanical properties

Ec	20800,0	N/mm2				
Etimber	11600	N/mm2				
Gr	72	N/mm2	Shear modulus paralell to the grain			
h	20	mm				
Kser / K0.4	10000	kN/mm				
seff	1	mm				
fck	19,3	N/mm2				
fcd	12,87	N/mm2				
fctm	2,16	N/mm2				
fctk.0,05	1,51	N/mm2				
fctd	1,01	N/mm2				
			Area		Iy	
h.con	50	mm	30000	mm2	6250000	mm4
h.1	30	mm	18000	mm2	1350000	mm4
h.between	20	mm	12000	mm2	400000	mm4
h.2	30	mm	18000	mm2	1350000	mm4
width	600	mm				
length	4400	mm				

A.2.2 Seperated calculation method

ac	26,1	mm	78,9	mm
a1	38,9	mm	78,9	mm

γcon	1,000
γ1	1,000

EI.con	5,54E+11	Nmm2
EI.1	9,19E+11	Nmm2

EI(eff)	***1,47E+12***	***Nmm2***

Layers	Thickness	z	centre of gravity	Direction	E	G	EI	EAz	EIy Som	Ieff som	Eieff red		
1	30	25,0	18000,00	Parallel	11600	725	1,57E+10	1,31E+11	1,46E+11	1,26E+07	1,43E+11	y1	0,976
2	20	0,0	400,00	Perpendicular	387	72	1,55E+08	4,64E-18	1,55E+08	4,00E+05			
3	30	-25,0	18000,00	Parallel	11600	725	1,57E+10	1,31E+11	1,46E+11	1,26E+07	1,43E+11	y2	0,976
Total height	80,0	mm							EIeff	Ieff	***EIeff***		
Zs	40,0	mm							2,92E+11	2,56E+07	***2,86E+11***		

V

56661,1	54000,0	0,0	0,0	0,0	108000,0
-54000,0	-56661,1	0,0	0,0	0,0	-108000,0
0,0	0,0	1,0	0,0	0,0	0,0
0,0	0,0	0,0	1,0	0,0	0,0
0,0	0,0	0,0	0,0	1,0	0,0

S

C1,2	2160
C2,3	0
C3,4	0
C4,5	0

1,9E-04	1,8E-04	0,0E+00	0,0E+00	0,0E+00	0,976
-1,8E-04	-1,9E-04	0,0E+00	0,0E+00	0,0E+00	0,976
0,0E+00	0,0E+00	1,0E+00	0,0E+00	0,0E+00	0,000
0,0E+00	0,0E+00	0,0E+00	1,0E+00	0,0E+00	0,000
0,0E+00	0,0E+00	0,0E+00	0,0E+00	1,0E+00	0,000

D1	106,4
D2	106,4
D3	0,0
D4	0,0
D5	0,0

a1	25,0
a2	-25,0
a3	0,0
a4	0,0
a5	0,0

A.2.3 Combined calculation method

Layers	Thickness	z	centre of gravity	Direction	E	G	EI	EAz	EIy Som	Ieff som	Eieff red		
1	50	26,2	53793,1	Parallel	20800	725	1,30E+11	4,29E+11	5,59E+11	2,69E+07	5,47E+11	y1	0,970
3	30	-13,8	18000,0	Parallel	11600	725	1,57E+10	3,96E+10	5,52E+10	4,76E+06	5,52E+10	y2	1,000
4	20	-38,8	400,0	Perpendicular	387	72	1,55E+08	6,97E+09	7,13E+09	1,84E+07			
5	30	-63,8	18000,0	Parallel	11600	725	1,57E+10	8,49E+11	8,65E+11	7,45E+07	8,35E+11	y3	0,965
Total height	130,0	mm							EIeff	Ieff	***EIeff***		
Zs	78,8	mm							1,49E+12	1,25E+08	***1,44E+12***		

V

2,62E+08	1,38E+08	0,00E+00	0,00E+00	0,00E+00	4,00E+08
-2,62E+08	-1,38E+08	1,38E+05	0,00E+00	0,00E+00	-4,00E+08
0,00E+00	2,97E+04	-1,45E+05	0,00E+00	0,00E+00	-1,08E+05
0,00E+00	0,00E+00	0,00E+00	1,00E+00	0,00E+00	0,00E+00
0,00E+00	0,00E+00	0,00E+00	0,00E+00	1,00E+00	0,00E+00

S

7,2E-05	7,2E-05	6,9E-05	0,0E+00	0,0E+00	0,970
-1,4E-04	-1,4E-04	-1,3E-04	0,0E+00	0,0E+00	1,057
-2,8E-05	-2,8E-05	-3,4E-05	0,0E+00	0,0E+00	0,965
0,0E+00	0,0E+00	0,0E+00	1,0E+00	0,0E+00	0,000
0,0E+00	0,0E+00	0,0E+00	0,0E+00	1,0E+00	0,000

C1,2	1,00E+07
C2,3	2,16E+03
C3,4	0,00E+00
C4,5	0,00E+00

D1	318,1
D2	106,4
D3	106,4
D4	0,0
D5	0,0

a1	26,2
a2	-13,8
a3	-63,8
a4	0,0
a5	0,0

A.3 Calculation A3

A.3.1 Mechanical properties

Ec	20800,0	N/mm2				
Etimber	11600	N/mm2				
Gr	72	N/mm2	Shear modulus paralell to the grain			
h	40	mm				
Kser / K0.4	10000	kN/mm				
seff	1	mm				
fck	19,3	N/mm2				
fcd	12,87	N/mm2				
fctm	2,16	N/mm2				
fctk.0,05	1,51	N/mm2				
fctd	1,01	N/mm2				
			Area		Iy	
h.con	60	mm	36000	mm2	10800000	mm4
h.1	40	mm	24000	mm2	3200000	mm4
h.between	40	mm	24000	mm2	3200000	mm4
h.2	40	mm	24000	mm2	3200000	mm4
width	600	mm				
length	4400	mm				

A.3.2 Seperated calculation method

ac	38,4	mm	111,6	mm
a1	51,6	mm	111,6	mm
γcon	1,000			
γ1	1,000			
EI.con	1,33E+12	Nmm2		
EI.1	2,39E+12	Nmm2		
EI(eff)	***3,72E+12***	***Nmm2***		

Layers	Thickness	z	centre of gravity	Direction	E	G	EI	EAz	EIy Som	Ieff som	Eieff red		
1	40	40,0	24000,00	Parallel	11600	725	3,71E+10	4,45E+11	4,83E+11	4,16E+07	4,55E+11	y1	0,938
2	40	0,0	800,00	Perpendicular	387	72	1,24E+09	9,28E-18	1,24E+09	3,20E+06			
3	40	-40,0	24000,00	Parallel	11600	725	3,71E+10	4,45E+11	4,83E+11	4,16E+07	4,55E+11	y2	0,938
Total height	120,0	mm							EIeff	Ieff	EIeff		
Zs	60,0	mm							9,66E+11	8,64E+07	9,10E+11		

V

					S
48877,1	43200,0	0,0	0,0	0,0	86400,0
-43200,0	-48877,1	0,0	0,0	0,0	-86400,0
0,0	0,0	1,0	0,0	0,0	0,0
0,0	0,0	0,0	1,0	0,0	0,0
0,0	0,0	0,0	0,0	1,0	0,0

9,4E-05	8,3E-05	0,0E+00	0,0E+00	0,0E+00	0,938
-8,3E-05	-9,4E-05	0,0E+00	0,0E+00	0,0E+00	0,938
0,0E+00	0,0E+00	1,0E+00	0,0E+00	0,0E+00	0,000
0,0E+00	0,0E+00	0,0E+00	1,0E+00	0,0E+00	0,000
0,0E+00	0,0E+00	0,0E+00	0,0E+00	1,0E+00	0,000

C1,2	1080
C2,3	0
C3,4	0
C4,5	0

D1	141,9
D2	141,9
D3	0,0
D4	0,0
D5	0,0

a1	40,0
a2	-40,0
a3	0,0
a4	0,0
a5	0,0

A.3.3 Combined calculation method

Layers	Thickness	z	centre of gravity	Direction	E	G	EI	EAz	EIy Som	Ieff som	Eieff red		
1	60	38,7	64551,7	Parallel	20800	725	2,25E+11	1,12E+12	1,35E+12	6,48E+07	1,27E+12	y1	0,931
3	40	-11,3	24000,0	Parallel	11600	725	3,71E+10	3,53E+10	7,24E+10	6,24E+06	7,24E+10	y2	1,000
4	40	-51,3	800,0	Perpendicular	387	72	1,24E+09	2,44E+10	2,56E+10	6,62E+07			
5	40	-91,3	24000,0	Parallel	11600	725	3,71E+10	2,32E+12	2,36E+12	2,03E+08	2,15E+12	y3	0,910
Total height	180,0								EIeff	Ieff	EIeff		
Zs	111,3								3,80E+12	3,40E+08	3,49E+12		

V

3,87E+08	1,13E+08	0,00E+00	0,00E+00	0,00E+00	5,00E+08
-3,87E+08	-1,13E+08	9,86E+04	0,00E+00	0,00E+00	-5,00E+08
0,00E+00	1,22E+04	-1,12E+05	0,00E+00	0,00E+00	-8,64E+04
0,00E+00	0,00E+00	0,00E+00	1,00E+00	0,00E+00	0,00E+00
0,00E+00	0,00E+00	0,00E+00	0,00E+00	1,00E+00	0,00E+00

S

C1,2	1,00E+07
C2,3	1,08E+03
C3,4	0,00E+00
C4,5	0,00E+00

4,0E-05	4,0E-05	3,5E-05	0,0E+00	0,0E+00	0,931
-1,4E-04	-1,4E-04	-1,2E-04	0,0E+00	0,0E+00	1,239
-1,5E-05	-1,5E-05	-2,2E-05	0,0E+00	0,0E+00	0,910
0,0E+00	0,0E+00	0,0E+00	1,0E+00	0,0E+00	0,000
0,0E+00	0,0E+00	0,0E+00	0,0E+00	1,0E+00	0,000

D1	381,7
D2	141,9
D3	141,9
D4	0,0
D5	0,0

a1	38,7
a2	-11,3
a3	-91,3
a4	0,0
a5	0,0

A.4 Calculation A4

A.4.1 Mechanical properties

Ec	31000,0	N/mm2	
Etimber	10102	N/mm2	
Gr	60	N/mm2	Shear modulus paralell to the grain
h	35	mm	
Kser / K0.4	211,3	kN/mm	
seff	200	mm	
fck	29,5	N/mm2	
fcd	19,67	N/mm2	
fctm	2,86	N/mm2	
fctk.0,05	2,00	N/mm2	
fctd	1,34	N/mm2	

			Area		Iy	
h.con	70	mm	28000	mm2	11433333,33	mm4
h.1	35	mm	14000	mm2	1429166,667	mm4
h.between	35	mm	14000	mm2	1429166,667	mm4
h.2	35	mm	14000	mm2	1429166,667	mm4
width	400	mm				
length	3600	mm				

A.4.2 Seperated calculation method

ac	30,3	mm	109,7	mm
a1	57,2	mm	109,7	mm

γcon	0,615
γ1	1,000

EI.con	8,45E+11	Nmm2
EI.1	1,28E+12	Nmm2
EI(eff)	***2,12E+12***	***Nmm2***

Layers	Thickness	z	centre of gravity	Direction	E	G	EI	EAz	EIy Som	Ieff som	Eieff red		
1	35	35,0	14000,00	Parallel	10102	631	1,44E+10	1,73E+11	1,88E+11	1,86E+07	1,75E+11	y1	0,927
2	35	0,0	466,67	Perpendicular	337	60	4,81E+08	2,38E-22	4,81E+08	1,43E+06			
3	35	-35,0	14000,00	Parallel	10102	631	1,44E+10	1,73E+11	1,88E+11	1,86E+07	1,75E+11	y2	0,927
Total height	105,0	mm							EIeff	Ieff	EIeff		
Zs	52,5	mm							3,76E+11	3,86E+07	3,50E+11		

V

					S		
27769,6	24000,0	0,0	0,0	0,0	48000,0	C1,2	685,7143
-24000,0	-27769,6	0,0	0,0	0,0	-48000,0	C2,3	0
0,0	0,0	1,0	0,0	0,0	0,0	C3,4	0
0,0	0,0	0,0	1,0	0,0	0,0	C4,5	0
0,0	0,0	0,0	0,0	1,0	0,0		
						D1	107,7
						D2	107,7
1,4E-04	1,2E-04	0,0E+00	0,0E+00	0,0E+00	0,927	D3	0,0
-1,2E-04	-1,4E-04	0,0E+00	0,0E+00	0,0E+00	0,927	D4	0,0
0,0E+00	0,0E+00	1,0E+00	0,0E+00	0,0E+00	0,000	D5	0,0
0,0E+00	0,0E+00	0,0E+00	1,0E+00	0,0E+00	0,000		
0,0E+00	0,0E+00	0,0E+00	0,0E+00	1,0E+00	0,000	a1	35,0
						a2	-35,0
						a3	0,0
						a4	0,0
						a5	0,0

A.4.3 Combined calculation method

Layers	Thickness	z	centre of gravity	Direction	E	G	EI	EAz	EIy Som	Ieff som	Eieff red		
1	70	21,8	85923,6	Parallel	31000	631	3,54E+11	4,12E+11	7,66E+11	2,47E+07	6,81E+11	y1	0,793
3	35	-30,7	14000,0	Parallel	10102	631	1,44E+10	1,34E+11	1,48E+11	1,46E+07	1,21E+11	y2	0,795
4	35	-65,7	466,7	Perpendicular	337	60	4,81E+08	2,04E+10	2,08E+10	6,19E+07			
5	35	-100,7	14000,0	Parallel	10102	631	1,44E+10	1,43E+12	1,45E+12	1,43E+08	1,18E+12	y3	0,810
Total height	175,0	mm							EIeff	Ieff	EIeff		
Zs	118,2	mm							2,38E+12	2,45E+08	1,98E+12		

V

37398,8	32461,1	0,0	0,0	0,0
-23005,2	-56839,0	69068,7	0,0	0,0
0,0	21068,7	-79917,1	0,0	0,0
0,0	0,0	0,0	1,0	0,0
0,0	0,0	0,0	0,0	1,0

S

55466,3	
-7466,3	
-48000,0	
0,0	
0,0	

C1,2	1056,5
C2,3	685,7
C3,4	0,0
C4,5	0,0

D1	661,0
D2	107,7
D3	107,7
D4	0,0
D5	0,0

5,5E-05	4,7E-05	4,0E-05	0,0E+00	0,0E+00	0,793
-3,3E-05	-5,4E-05	-4,6E-05	0,0E+00	0,0E+00	0,795
-8,7E-06	-1,4E-05	-2,5E-05	0,0E+00	0,0E+00	0,810
0,0E+00	0,0E+00	0,0E+00	1,0E+00	0,0E+00	0,000
0,0E+00	0,0E+00	0,0E+00	0,0E+00	1,0E+00	0,000

a1	21,8
a2	-30,7
a3	-100,7
a4	0,0
a5	0,0

A.5 Calculation A5

A.5.1 Mechanical properties

Ec	31000,0	N/mm2	
Etimber	10102	N/mm2	
Gr	60	N/mm2	Shear modulus paralell to the grain
h	35	mm	
Kser / K0.4	232,54	kN/mm	
seff	200	mm	
fck	29,5	N/mm2	
fcd	19,67	N/mm2	
fctm	2,86	N/mm2	
fctk.0,05	2,00	N/mm2	
fctd	1,34	N/mm2	

			Area		Iy	
h.con	70	mm	28000	mm2	11433333,33	mm4
h.1	35	mm	14000	mm2	1429166,667	mm4
h.between	35	mm	14000	mm2	1429166,667	mm4
h.2	35	mm	14000	mm2	1429166,667	mm4
width	400	mm				
length	3300	mm				

A.5.2 Seperated calculation method

ac	30,9	mm	109,1	mm
a1	56,6	mm	109,1	mm

γcon	0,596
γ1	1,000

EI.con	8,49E+11	Nmm2
EI.1	1,25E+12	Nmm2
EI(eff)	***2,10E+12***	***Nmm2***

Layers	Thickness	z	centre of gravity	Direction	E	G	EI	EAz	EIy Som	Ieff som	Eieff red		
1	35	35,0	14000,00	Parallel	10102	631	1,44E+10	1,73E+11	1,88E+11	1,86E+07	1,73E+11	y1	0,915
2	35	0,0	466,67	Perpendicular	337	60	4,81E+08	2,38E-22	4,81E+08	1,43E+06			
3	35	-35,0	14000,00	Parallel	10102	631	1,44E+10	1,73E+11	1,88E+11	1,86E+07	1,73E+11	y2	0,915
Total height	105,0	mm							EIeff	Ieff	EIeff		
Zs	52,5	mm							3,76E+11	3,86E+07	3,46E+11		

V

28486,2	24000,0	0,0	0,0	0,0	
-24000,0	-28486,2	0,0	0,0	0,0	
0,0	0,0	1,0	0,0	0,0	
0,0	0,0	0,0	1,0	0,0	
0,0	0,0	0,0	0,0	1,0	

S

48000,0	
-48000,0	
0,0	
0,0	
0,0	

C1,2	685,7143
C2,3	0
C3,4	0
C4,5	0

D1	128,2
D2	128,2
D3	0,0
D4	0,0
D5	0,0

1,2E-04	1,0E-04	0,0E+00	0,0E+00	0,0E+00	0,915
-1,0E-04	-1,2E-04	0,0E+00	0,0E+00	0,0E+00	0,915
0,0E+00	0,0E+00	1,0E+00	0,0E+00	0,0E+00	0,000
0,0E+00	0,0E+00	0,0E+00	1,0E+00	0,0E+00	0,000
0,0E+00	0,0E+00	0,0E+00	0,0E+00	1,0E+00	0,000

a1	35,0
a2	-35,0
a3	0,0
a4	0,0
a5	0,0

A.5.3 Combined calculation method

Layers	Thickness	z	centre of gravity	Direction	E	G	EI	EAz	EIy Som	Ieff som	Eieff red		
1	70	21,8	85923,6	Parallel	31000	631	3,54E+11	4,12E+11	7,66E+11	2,47E+07	6,73E+11	y1	0,775
3	35	-30,7	14000,0	Parallel	10102	631	1,44E+10	1,34E+11	1,48E+11	1,46E+07	1,20E+11	y2	0,788
4	35	-65,7	466,7	Perpendicular	337	60	4,81E+08	2,04E+10	2,08E+10	6,19E+07			
5	35	-100,7	14000,0	Parallel	10102	631	1,44E+10	1,43E+12	1,45E+12	1,43E+08	1,15E+12	y3	0,788
Total height	175,0	mm							EIeff	Ieff	EIeff		
Zs	118,2	mm							2,38E+12	2,45E+08	1,94E+12		

V

42447,2	35724,1	0,0	0,0	0,0
-25317,6	-60731,0	69068,7	0,0	0,0
0,0	21068,7	-81979,2	0,0	0,0
0,0	0,0	0,0	1,0	0,0
0,0	0,0	0,0	0,0	1,0

S

61041,8	
-13041,8	
-48000,0	
0,0	
0,0	

C1,2	1162,7
C2,3	685,7
C3,4	0,0
C4,5	0,0

D1	786,7
D2	128,2
D3	128,2
D4	0,0
D5	0,0

4,7E-05	3,9E-05	3,3E-05	0,0E+00	0,0E+00	0,775
-2,8E-05	-4,6E-05	-3,9E-05	0,0E+00	0,0E+00	0,788
-7,1E-06	-1,2E-05	-2,2E-05	0,0E+00	0,0E+00	0,788
0,0E+00	0,0E+00	0,0E+00	1,0E+00	0,0E+00	0,000
0,0E+00	0,0E+00	0,0E+00	0,0E+00	1,0E+00	0,000

a1	21,8
a2	-30,7
a3	-100,7
a4	0,0
a5	0,0

A.6 Calculation A6

A.6.1 Mechanical properties

Ec	31000,0	N/mm2	
Etimber	10102	N/mm2	
Gr	60	N/mm2	Shear modulus paralell to the grain
h	35	mm	
Kser / K0.4	232,54	kN/mm	
seff	300	mm	
fck	29,5	N/mm2	
fcd	19,67	N/mm2	
fctm	2,86	N/mm2	
fctk.0,05	***2,00***	***N/mm2***	
fctd	1,34	N/mm2	

			Area		Iy	
h.con	70	mm	28000	mm2	11433333,33	mm4
h.1	35	mm	14000	mm2	1429166,667	mm4
h.between	35	mm	14000	mm2	1429166,667	mm4
h.2	35	mm	14000	mm2	1429166,667	mm4
width	400	mm				
length	3300	mm				

A.6.2 Seperated calculation method

ac	34,7	mm	105,3	mm
a1	52,8	mm	105,3	mm

γcon	0,496
γ1	1,000

EI.con	8,73E+11	Nmm2
EI.1	1,13E+12	Nmm2
EI(eff)	***2,01E+12***	***Nmm2***

Layers	Thickness	z	centre of gravity	Direction	E	G	EI	EAz	EIy Som	Ieff som	Eieff red		
1	35	35,0	14000,00	Parallel	10102	631	1,44E+10	1,73E+11	1,88E+11	1,86E+07	1,73E+11	y1	0,915
2	35	0,0	466,67	Perpendicular	337	60	4,81E+08	2,38E-22	4,81E+08	1,43E+06			
3	35	-35,0	14000,00	Parallel	10102	631	1,44E+10	1,73E+11	1,88E+11	1,86E+07	1,73E+11	y2	0,915
Total height	105,0	mm							EIeff	Ieff	EIeff		
Zs	52,5	mm							3,76E+11	3,86E+07	3,46E+11		

V

					S		
28486,2	24000,0	0,0	0,0	0,0	48000,0	C1,2	685,7143
-24000,0	-28486,2	0,0	0,0	0,0	-48000,0	C2,3	0
0,0	0,0	1,0	0,0	0,0	0,0	C3,4	0
0,0	0,0	0,0	1,0	0,0	0,0	C4,5	0
0,0	0,0	0,0	0,0	1,0	0,0		
						D1	128,2
						D2	128,2
1,2E-04	1,0E-04	0,0E+00	0,0E+00	0,0E+00	0,915	D3	0,0
-1,0E-04	-1,2E-04	0,0E+00	0,0E+00	0,0E+00	0,915	D4	0,0
0,0E+00	0,0E+00	1,0E+00	0,0E+00	0,0E+00	0,000	D5	0,0
0,0E+00	0,0E+00	0,0E+00	1,0E+00	0,0E+00	0,000		
0,0E+00	0,0E+00	0,0E+00	0,0E+00	1,0E+00	0,000	a1	35,0
						a2	-35,0
						a3	0,0
						a4	0,0
						a5	0,0

A.6.3 Combined calculation method

Layers	Thickness	z	centre of gravity	Direction	E	G	EI	EAz	EIy Som	Ieff som	Eieff red		
1	70	21,8	85923,6	Parallel	31000	631	3,54E+11	4,12E+11	7,66E+11	2,47E+07	6,53E+11	y1	0,726
3	35	-30,7	14000,0	Parallel	10102	631	1,44E+10	1,34E+11	1,48E+11	1,46E+07	1,04E+11	y2	0,672
4	35	-65,7	466,7	Perpendicular	337	60	4,81E+08	2,04E+10	2,08E+10	6,19E+07			
5	35	-100,7	14000,0	Parallel	10102	631	1,44E+10	1,43E+12	1,45E+12	1,43E+08	1,10E+12	y3	0,758
Total height	175,0	mm							EIeff	Ieff	***EIeff***		
Zs	118,2	mm							2,38E+12	2,45E+08	***1,86E+12***		

V					S		
34008,0	23816,1	0,0	0,0	0,0	40694,5	C1,2	775,1
-16878,4	-48823,0	69068,7	0,0	0,0	7305,5	C2,3	685,7
0,0	21068,7	-81979,2	0,0	0,0	-48000,0	C3,4	0,0
0,0	0,0	0,0	1,0	0,0	0,0	C4,5	0,0
0,0	0,0	0,0	0,0	1,0	0,0		
						D1	786,7
						D2	128,2
4,7E-05	3,6E-05	3,1E-05	0,0E+00	0,0E+00	0,726	D3	128,2
-2,6E-05	-5,2E-05	-4,4E-05	0,0E+00	0,0E+00	0,672	D4	0,0
-6,6E-06	-1,3E-05	-2,3E-05	0,0E+00	0,0E+00	0,758	D5	0,0
0,0E+00	0,0E+00	0,0E+00	1,0E+00	0,0E+00	0,000		
0,0E+00	0,0E+00	0,0E+00	0,0E+00	1,0E+00	0,000	a1	21,8
						a2	-30,7
						a3	-100,7
						a4	0,0
						a5	0,0

A.7 Calculation B1

A.7.1 Mechanical properties

Ec	32530,4	N/mm^2	
Etimber	11000	N/mm^2	
Gr	60	N/mm^2	Shear modulus parallel to the grain
h	30	mm	
Kser / K0.4	865	kN/mm	
seff	700	mm	
fck	47,1	N/mm^2	
fcd	31,40	N/mm^2	
fctm	3,91	N/mm^2	
fctk.0,05	2,74	N/mm^2	
fctd	1,83	N/mm^2	

			Area mm^2	Iy mm^4
h.con	80	mm	36000	19200000
h.1	40	mm	18000	2400000
h.between	30	mm	13500	1012500
h.2	40	mm	18000	2400000
h.between	30	mm	13500	1012500
h.3	40	mm	18000	2400000
width	450	mm		
length	6300	mm		

A.7.2 Seperated calculation method

ac	50,1	mm	169,9	mm
a1	79,9	mm	169,9	mm

γcon	0,809
γ1	1,000

EI.con	3,00E+12	Nmm2
EI.1	5,71E+12	Nmm2
EI(eff)	***8,71E+12***	***Nmm2***

Layers	Thickness	z	centre of gravity	Direction	E	G	EI	EAz	EIy Som	Ieff som	Eieff red		
1	40	70,0	18000,00	Parallel	11000	688	2,64E+10	9,70E+11	9,97E+11	9,06E+07	9,46E+11	y1	0,948
2	30	35,0	450,00	Perpendicular	367	60	3,71E+08	6,06E+09	6,44E+09	1,76E+07			
3	40	0,0	18000,00	Parallel	11000	688	2,64E+10	1,98E-16	2,64E+10	2,40E+06	2,64E+10	y2	0,688
4	30	-35,0	450,00	Perpendicular	367	60	3,71E+08	6,06E+09	6,44E+09	1,76E+07			
5	40	-70,0	18000,00	Parallel	11000	688	2,64E+10	9,70E+11	9,97E+11	9,06E+07	9,46E+11	y3	0,948
Total height	180,0	mm							EIeff	Ieff	***EIeff***		
Zs	90,0	mm							2,03E+12	2,19E+08	***1,92E+12***		

V					S		
66446,5	0,0	0,0	0,0	0,0	63000,0	C1,2	900
-63000,0	0,0	63000,0	0,0	0,0	0,0	C2,3	900
0,0	0,0	-66446,5	0,0	0,0	-63000,0	C3,4	0
0,0	0,0	0,0	1,0	0,0	0,0	C4,5	0
0,0	0,0	0,0	0,0	1,0	0,0		
						D1	49,2
						D2	49,2
1,1E-04	9,5E-05	9,0E-05	0,0E+00	0,0E+00	0,948	D3	49,2
6,6E+09	7,0E+09	6,6E+09	0,0E+00	0,0E+00	0,688	D4	0,0
-9,0E-05	-9,5E-05	-1,1E-04	0,0E+00	0,0E+00	0,948	D5	0,0
0,0E+00	0,0E+00	0,0E+00	1,0E+00	0,0E+00	0,000		
0,0E+00	0,0E+00	0,0E+00	0,0E+00	1,0E+00	0,000	a1	70,0
						a2	0,0
						a3	-70,0
						a4	0,0
						a5	0,0

A.7.3 Combined calculation method

Layers	Thickness	z	centre of gravity	Direction	E	G	EI	EAz	EIy Som	Ieff som	Eieff red		
1	80	44,2	106463,1	Parallel	32530		6,25E+11	2,29E+12	2,92E+12	8,96E+07	2,56E+12	y1	0,846
3	40	-15,8	18000,0	Parallel	11000	688	2,64E+10	4,92E+10	7,56E+10	6,88E+06	6,94E+10	y2	0,874
4	30	-50,8	450,0	Perpendicular	367	60	3,71E+08	1,28E+10	1,31E+10	3,58E+07			
5	40	-85,8	18000,0	Parallel	11000	688	2,64E+10	1,46E+12	1,48E+12	1,35E+08	1,26E+12	y3	0,844
6	30	-120,8	450,0	Perpendicular	367	60	3,71E+08	7,22E+10	***7,26E+10***	1,98E+08			
7	40	-155,8	18000,0	Parallel	11000	688	2,64E+10	4,80E+12	***4,83E+12***	4,39E+08	4,19E+12	y4	0,867
Total height	260,0	mm							EIeff	Ieff	***EIeff***		
Zs	175,8	mm							9,39E+12	9,04E+08	***8,08E+12***		

V					S		
67535,1	19487,9	0,0	0,0	0,0	74142,9	C1,2	1235,7
-54654,9	-34457,9	77193,5	0,0	0,0	-11142,9	C2,3	900,0
0,0	14193,5	-158610,0	140193,5	0,0	0,0	C3,4	900,0
0,0	0,0	77193,5	-147863,0	0,0	-63000,0	C4,5	0,0
0,0	0,0	0,0	0,0	1,0	0,0		
						D1	291,2
						D2	49,2
5,5E-05	4,9E-05	4,4E-05	4,2E-05	0,0E+00	0,846	D3	49,2
-1,4E-04	-1,7E-04	-1,5E-04	-1,5E-04	0,0E+00	0,874	D4	49,2
-2,3E-05	-2,8E-05	-3,7E-05	-3,5E-05	0,0E+00	0,844	D5	0,0
-1,2E-05	-1,5E-05	-1,9E-05	-2,5E-05	0,0E+00	0,867		
0,0E+00	0,0E+00	0,0E+00	0,0E+00	1,0E+00	0,000	a1	44,2
						a2	-15,8
						a3	-85,8
						a4	-155,8
						a5	0,0

A.8 Calculation B2

A.8.1 Mechanical properties

Ec	31000,0	N/mm^2	
Etimber	10102	N/mm^2	
Gr	60	N/mm^2	Shear modulus parallel to the grain
h	35	mm	
Kser / K0.4	255,18	kN/mm	
seff	300	mm	
fck	29,5	N/mm^2	
fcd	19,67	N/mm^2	
fctm	2,86	N/mm^2	
fctk.0,05	2,00	N/mm^2	
fctd	1,34	N/mm^2	

			Area mm^2	Iy mm^4
h.con	80	mm	32000	17066666,67
h.1	35	mm	14000	1429166,667
h.between	35	mm	14000	1429166,667
h.2	35	mm	14000	1429166,667
h.between	35	mm	14000	1429166,667
h.3	35	mm	14000	1429166,667
width	400	mm		
length	4500	mm		

A.8.2 Seperated calculation method

ac	51,2	mm	163,8	mm
a1	76,3	mm	163,8	mm

γcon	0,638	
γ1	1,000	

EI.con	2,19E+12	Nmm2
EI.1	3,77E+12	Nmm2

EI(eff)	***5,96E+12***	***Nmm2***

Layers	Thickness	z	centre of gravity	Direction	E	G	EI	EAz	EIy Som	Ieff som	Eieff red		
1	35	70,0	14000,00	Parallel	10102	631	1,44E+10	6,93E+11	7,07E+11	7,00E+07	6,44E+11	y1	0,909
2	35	35,0	466,67	Perpendicular	337	60	4,81E+08	5,77E+09	6,26E+09	1,86E+07			
3	35	0,0	14000,00	Parallel	10102	631	1,44E+10	1,41E-16	1,44E+10	1,43E+06	1,44E+10	y2	0,688
4	35	-35,0	466,67	Perpendicular	337	60	4,81E+08	5,77E+09	6,26E+09	1,86E+07			
5	35	-70,0	14000,00	Parallel	10102	631	1,44E+10	6,93E+11	7,07E+11	7,00E+07	6,44E+11	y3	0,909
Total height	175,0	mm							EIeff	Ieff	***EIeff***		
Zs	87,5	mm							1,44E+12	1,79E+08	***1,30E+12***		

V

52825,1	0,0	0,0	0,0	0,0
-48000,0	0,0	48000,0	0,0	0,0
0,0	0,0	-52825,1	0,0	0,0
0,0	0,0	0,0	1,0	0,0
0,0	0,0	0,0	0,0	1,0

S

48000,0	
0,0	
-48000,0	
0,0	
0,0	

C1,2	685,7143
C2,3	685,7143
C3,4	0
C4,5	0

D1	68,9
D2	68,9
D3	68,9
D4	0,0
D5	0,0

8,0E-05	6,7E-05	6,1E-05	0,0E+00	0,0E+00	0,909
4,7E+09	5,1E+09	4,7E+09	0,0E+00	0,0E+00	0,688
-6,1E-05	-6,7E-05	-8,0E-05	0,0E+00	0,0E+00	0,909
0,0E+00	0,0E+00	0,0E+00	1,0E+00	0,0E+00	0,000
0,0E+00	0,0E+00	0,0E+00	0,0E+00	1,0E+00	0,000

a1	70,0
a2	0,0
a3	-70,0
a4	0,0
a5	0,0

A.8.3 Combined calculation method

Layers	Thickness	z	centre of gravity	Direction	E	G	EI	EAz	EIy Som	Ieff som	Eieff red		
1	80	38,8	98198,4	Parallel	31000	631	5,29E+11	1,49E+12	2,02E+12	6,52E+07	1,62E+12	y1	0,732
3	35	-18,7	14000,0	Parallel	10102	631	1,44E+10	4,95E+10	6,40E+10	6,33E+06	4,87E+10	y2	0,693
4	35	-53,7	466,7	Perpendicular	337	60	4,81E+08	1,36E+10	1,41E+10	4,18E+07			
5	35	-88,7	14000,0	Parallel	10102	631	1,44E+10	1,11E+12	1,13E+12	1,12E+08	8,20E+11	y3	0,724
6	35	-123,7	466,7	Perpendicular	337	60	***4,81E+08***	7,22E+10	7,26E+10	2,16E+08			
7	35	-158,7	14000,0	Parallel	10102	631	***1,44E+10***	3,56E+12	3,58E+12	3,54E+08	2,75E+12	y4	0,769
Total height	255,0	mm							EIeff	Ieff	***EIeff***		
Zs	176,2	mm							6,88E+12	7,95E+08	***5,24E+12***		

V					S		
51744,6	15917,7	0,0	0,0	0,0	48909,5	C1,2	850,6
-32991,8	-30039,8	60832,1	0,0	0,0	-909,5	C2,3	685,7
0,0	12832,1	-127779,3	108832,1	0,0	0,0	C3,4	685,7
0,0	0,0	60832,1	-119772,3	0,0	-48000,0	C4,5	0,0
0,0	0,0	0,0	0,0	1,0	0,0		
						D1	483,5
						D2	68,9
4,1E-05	3,4E-05	2,8E-05	2,6E-05	0,0E+00	0,732	D3	68,9
-7,0E-05	-1,1E-04	-9,2E-05	-8,4E-05	0,0E+00	0,693	D4	68,9
-1,2E-05	-1,9E-05	-3,0E-05	-2,7E-05	0,0E+00	0,724	D5	0,0
-6,3E-06	-9,9E-06	-1,5E-05	-2,2E-05	0,0E+00	0,769		
0,0E+00	0,0E+00	0,0E+00	0,0E+00	1,0E+00	0,000	a1	38,8
						a2	-18,7
						a3	-88,7
						a4	-158,7
						a5	0,0

A.9 Calculation B3

A.9.1 Mechanical properties

Ec	31000,0	N/mm^2	
Etimber	10102	N/mm^2	
Gr	60	N/mm^2	Shear modulus parallel to the grain
h	35	mm	
Kser / K0.4	255,18	kN/mm	
seff	300	mm	
fck	29,5	N/mm^2	
fcd	19,67	N/mm^2	
fctm	2,86	N/mm^2	
fctk.0,05	2,00	N/mm^2	
fctd	1,34	N/mm^2	

			Area mm^2	Iy mm^4
h.con	80	mm	32000	17066666,67
h.1	35	mm	14000	1429166,667
h.between	35	mm	14000	1429166,667
h.2	35	mm	14000	1429166,667
h.between	35	mm	14000	1429166,667
h.3	35	mm	14000	1429166,667
width	400	mm		
length	4800	mm		

A.9.2 Seperated calculation method

ac	49,8	mm	165,2	mm
a1	77,7	mm	165,2	mm

γcon	0,667	
γ1	1,000	

EI.con	2,17E+12	Nmm2
EI.1	3,88E+12	Nmm2

EI(eff) 6,05E+12 Nmm2

Layers	Thickness	z	centre of gravity	Direction	E	G	EI	EAz	EIy Som	Ieff som	Eieff red		
1	35	70,0	14000,00	Parallel	10102	631	1,44E+10	6,93E+11	7,07E+11	7,00E+07	6,51E+11	y1	0,919
2	35	35,0	466,67	Perpendicular	337	60	4,81E+08	5,77E+09	6,26E+09	1,86E+07			
3	35	0,0	14000,00	Parallel	10102	631	1,44E+10	1,41E-16	1,44E+10	1,43E+06	1,44E+10	y2	0,656
4	35	-35,0	466,67	Perpendicular	337	60	4,81E+08	5,77E+09	6,26E+09	1,86E+07			
5	35	-70,0	14000,00	Parallel	10102	631	1,44E+10	6,93E+11	7,07E+11	7,00E+07	6,51E+11	y3	0,919
Total height	175,0	mm							EIeff	Ieff	***EIeff***		
Zs	87,5	mm							1,44E+12	1,79E+08	***1,32E+12***		

V					S		
52240,8	0,0	0,0	0,0	0,0	48000,0	C1,2	685,71
-48000,0	0,0	48000,0	0,0	0,0	0,0	C2,3	685,71
0,0	0,0	-52240,8	0,0	0,0	-48000,0	C3,4	0
0,0	0,0	0,0	1,0	0,0	0,0	C4,5	0
0,0	0,0	0,0	0,0	1,0	0,0		
						D1	60,6
						D2	60,6
8,9E-05	7,6E-05	7,0E-05	0,0E+00	0,0E+00	0,919	D3	60,6
5,3E+09	5,8E+09	5,3E+09	0,0E+00	0,0E+00	0,656	D4	0,0
-7,0E-05	-7,6E-05	-8,9E-05	0,0E+00	0,0E+00	0,919	D5	0,0
0,0E+00	0,0E+00	0,0E+00	1,0E+00	0,0E+00	0,000		
0,0E+00	0,0E+00	0,0E+00	0,0E+00	1,0E+00	0,000	a1	70,0
						a2	0,0
						a3	-70,0
						a4	0,0
						a5	0,0

A.9.3 Combined calculation method

Layers	Thickness	z	centre of gravity	Direction	E	G	EI	EAz	EIy Som	Ieff som	Eieff red		
1	80	38,8	98198,4	Parallel	31000	631	5,29E+11	1,49E+12	2,02E+12	6,52E+07	1,66E+12	y1	0,756
3	35	-18,7	14000,0	Parallel	10102	631	1,44E+10	4,95E+10	6,40E+10	6,33E+06	5,03E+10	y2	0,724
4	35	-53,7	466,7	Perpendicular	337	60	4,81E+08	1,36E+10	1,41E+10	4,18E+07			
5	35	-88,7	14000,0	Parallel	10102	631	1,44E+10	1,11E+12	1,13E+12	1,12E+08	8,50E+11	y3	0,750
6	35	-123,7	466,7	Perpendicular	***337***	60	4,81E+08	7,22E+10	7,26E+10	2,16E+08			
7	35	-158,7	14000,0	Parallel	***10102***	631	1,44E+10	3,56E+12	3,58E+12	3,54E+08	2,83E+12	y4	0,791
Total height	255,0	mm							EIeff	Ieff	EIeff		
Zs	176,2	mm							6,88E+12	7,95E+08	5,39E+12		

V

49473,7	15917,7	0,0	0,0	0,0
-32991,8	-29883,6	60832,1	0,0	0,0
0,0	12832,1	-127038,8	108832,1	0,0
0,0	0,0	60832,1	-118447,5	0,0
0,0	0,0	0,0	0,0	1,0

S

48909,5	C1,2
-909,5	C2,3
0,0	C3,4
-48000,0	C4,5
0,0	

850,6	
685,7	
685,7	
0,0	

D1	424,9
D2	60,6
D3	60,6
D4	60,6
D5	0,0

4,6E-05	3,9E-05	3,3E-05	3,0E-05	0,0E+00	0,756
-8,0E-05	-1,2E-04	-1,0E-04	-9,5E-05	0,0E+00	0,724
-1,4E-05	-2,2E-05	-3,3E-05	-3,0E-05	0,0E+00	0,750
-7,4E-06	-1,1E-05	-1,7E-05	-2,4E-05	0,0E+00	0,791
0,0E+00	0,0E+00	0,0E+00	0,0E+00	1,0E+00	0,000

a1	38,8
a2	-18,7
a3	-88,7
a4	-158,7
a5	0,0

A.10 Calculation B4

A.10.1 Mechanical properties

Ec	14920,0	N/mm^2	
Etimber	12000	N/mm^2	
Gr	60	N/mm^2	Shear modulus parallel to the grain
h	30	mm	
Kser / K0.4	320	kN/mm	
seff	150	mm	
fck	27,29	N/mm^2	
fcd	18,19	N/mm^2	
fctm	2,72	N/mm^2	
fctk.0,05	1,90	N/mm^2	
fctd	1,27	N/mm^2	

			Area mm^2	Iy mm^4
h.con	100	mm	90000	75000000
h.1	30	mm	27000	2025000
h.between	30	mm	27000	2025000
h.2	30	mm	27000	2025000
h.between	30	mm	27000	2025000
h.3	30	mm	27000	2025000
width	900	mm		
length	5800	mm		

A.10.2 Seperated calculation method

ac	57,7	mm	142,3	mm
a1	67,3	mm	142,3	mm

γcon	0,844	
γ1	1,000	

EI.con	4,89E+12	Nmm2
EI.1	6,69E+12	Nmm2

EI(eff)	***1,16E+13***	***Nmm2***

Layers	Thickness	z	centre of gravity	Direction	E	G	EI	EAz	EIy Som	Ieff som	Eieff red		
1	30	60,0	27000,00	Parallel	12000	750	2,43E+10	1,17E+12	1,19E+12	9,92E+07	1,13E+12	y1	0,950
2	30	30,0	900,00	Perpendicular	400	60	8,10E+08	9,72E+09	1,05E+10	2,63E+07			
3	30	0,0	27000,00	Parallel	12000	750	2,43E+10	3,24E-16	2,43E+10	2,03E+06	2,43E+10	y2	0,688
4	30	-30,0	900,00	Perpendicular	400	60	8,10E+08	9,72E+09	1,05E+10	2,63E+07			
5	30	-60,0	27000,00	Parallel	12000	750	2,43E+10	1,17E+12	1,19E+12	9,92E+07	1,13E+12	y3	0,950
Total height	150,0	mm							EIeff	Ieff	***EIeff***		
Zs	75,0	mm							2,43E+12	2,53E+08	***2,29E+12***		

V					S		
113703,5	0,0	0,0	0,0	0,0	108000,0	C1,2	1800
-108000,0	0,0	108000,0	0,0	0,0	0,0	C2,3	1800
0,0	0,0	-113703,5	0,0	0,0	-108000,0	C3,4	0
0,0	0,0	0,0	1,0	0,0	0,0	C4,5	0
0,0	0,0	0,0	0,0	1,0	0,0		
						D1	95,1
						D2	95,1
6,3E-05	5,7E-05	5,5E-05	0,0E+00	0,0E+00	0,950	D3	95,1
3,4E+09	3,6E+09	3,4E+09	0,0E+00	0,0E+00	0,688	D4	0,0
-5,5E-05	-5,7E-05	-6,3E-05	0,0E+00	0,0E+00	0,950	D5	0,0
0,0E+00	0,0E+00	0,0E+00	1,0E+00	0,0E+00	0,000		
0,0E+00	0,0E+00	0,0E+00	0,0E+00	1,0E+00	0,000	a1	60,0
						a2	0,0
						a3	-60,0
						a4	0,0
						a5	0,0

A.10.3 Combined calculation method

Layers	Thickness	z	centre of gravity	Direction	E	G	EI	EAz	EIy Som	Ieff som	Eieff red		
1	100	53,2	111900,0	Parallel	14920	750	1,12E+12	3,79E+12	4,91E+12	3,29E+08	4,37E+12	y1	0,856
3	30	-11,8	27000,0	Parallel	12000	750	2,43E+10	4,54E+10	6,97E+10	5,81E+06	6,69E+10	y2	0,939
4	30	-41,8	900,0	Perpendicular	400	60	8,10E+08	1,89E+10	1,97E+10	4,93E+07			
5	30	-71,8	27000,0	Parallel	12000	750	2,43E+10	1,67E+12	1,70E+12	1,41E+08	1,46E+12	y3	0,860
6	30	-101,8	900,0	Perpendicular	400	60	8,10E+08	1,12E+11	1,13E+11	2,82E+08			
7	30	-131,8	27000,0	Parallel	12000	750	2,43E+10	5,63E+12	5,66E+12	4,71E+08	4,96E+12	y4	0,877
Total height	250,0	mm							EIeff	Ieff	EIeff		
Zs	146,8	mm							1,25E+13	1,28E+09	1,09E+13		

V

134347,8	25261,4	0,0	0,0	0,0
-113405,2	-47701,4	129314,3	0,0	0,0
0,0	21314,3	-265457,8	237314,3	0,0
0,0	0,0	129314,3	-249846,9	0,0
0,0	0,0	0,0	0,0	1,0

S

138666,7
-30666,7
0,0
-108000,0
0,0

C1,2	2133,3
C2,3	1800,0
C3,4	1800,0
C4,5	0,0

D1	394,0
D2	95,1
D3	95,1
D4	95,1
D5	0,0

3,0E-05	2,7E-05	2,4E-05	2,3E-05	0,0E+00	0,856
-1,2E-04	-1,4E-04	-1,3E-04	-1,2E-04	0,0E+00	0,939
-1,8E-05	-2,1E-05	-2,6E-05	-2,5E-05	0,0E+00	0,860
-9,3E-06	-1,1E-05	-1,4E-05	-1,7E-05	0,0E+00	0,877
0,0E+00	0,0E+00	0,0E+00	0,0E+00	1,0E+00	0,000

a1	53,2
a2	-11,8
a3	-71,8
a4	-131,8
a5	0,0

A.11 Calculation B5

A.11.1 Mechanical properties

Ec	14920,0	N/mm^2	
Etimber	12000	N/mm^2	
Gr	60	N/mm^2	Shear modulus parallel to the grain
h	30	mm	
Kser / K0.4	320	kN/mm	
seff	300	mm	
fck	27,29	N/mm^2	
fcd	18,19	N/mm^2	
fctm	2,72	N/mm^2	
fctk.0,05	1,90	N/mm^2	
fctd	1,27	N/mm^2	

			Area mm^2	Iy mm^4
h.con	100	mm	90000	75000000
h.1	30	mm	27000	2025000
h.between	30	mm	27000	2025000
h.2	30	mm	27000	2025000
h.between	30	mm	27000	2025000
h.3	30	mm	27000	2025000
width	900	mm		
length	5800	mm		

A.11.2 Seperated calculation method

ac	62,2	mm	137,8	mm
a1	62,8	mm	137,8	mm

γcon	0,730	
γ1	1,000	

EI.con	4,92E+12	Nmm2
EI.1	6,12E+12	Nmm2

EI(eff)	***1,10E+13***	***Nmm2***

Layers	Thickness	z	centre of gravity	Direction	E	G	EI	EAz	EIy Som	Ieff som	Eieff red		
1	30	60,0	27000,00	Parallel	12000	750	2,43E+10	1,17E+12	1,19E+12	9,92E+07	1,13E+12	y1	0,950
2	30	30,0	900,00	Perpendicular	400	60	8,10E+08	9,72E+09	1,05E+10	2,63E+07			
3	30	0,0	27000,00	Parallel	12000	750	2,43E+10	3,24E-16	2,43E+10	2,03E+06	2,43E+10	y2	0,688
4	30	-30,0	900,00	Perpendicular	400	60	8,10E+08	9,72E+09	1,05E+10	2,63E+07			
5	30	-60,0	27000,00	Parallel	12000	750	2,43E+10	1,17E+12	1,19E+12	9,92E+07	1,13E+12	y3	0,950
Total height	150,0	mm							EIeff	Ieff	***EIeff***		
Zs	75,0	mm							2,43E+12	2,53E+08	***2,29E+12***		

V					S		
113703,5	0,0	0,0	0,0	0,0	108000,0	C1,2	1800
-108000,0	0,0	108000,0	0,0	0,0	0,0	C2,3	1800
0,0	0,0	-113703,5	0,0	0,0	-108000,0	C3,4	0
0,0	0,0	0,0	1,0	0,0	0,0	C4,5	0
0,0	0,0	0,0	0,0	1,0	0,0		
						D1	95,1
						D2	95,1
6,3E-05	5,7E-05	5,5E-05	0,0E+00	0,0E+00	0,950	D3	95,1
3,4E+09	3,6E+09	3,4E+09	0,0E+00	0,0E+00	0,688	D4	0,0
-5,5E-05	-5,7E-05	-6,3E-05	0,0E+00	0,0E+00	0,950	D5	0,0
0,0E+00	0,0E+00	0,0E+00	1,0E+00	0,0E+00	0,000		
0,0E+00	0,0E+00	0,0E+00	0,0E+00	1,0E+00	0,000	a1	60,0
						a2	0,0
						a3	-60,0
						a4	0,0
						a5	0,0

A.11.3 Combined calculation method

Layers	Thickness	z	centre of gravity	Direction	E	G	EI	EAz	EIy Som	Ieff som	Eieff red		
1	100	53,2	111900,0	Parallel	14920	750	1,12E+12	3,79E+12	4,91E+12	3,29E+08	4,16E+12	y1	0,801
3	30	-11,8	27000,0	Parallel	12000	750	2,43E+10	4,54E+10	6,97E+10	5,81E+06	5,01E+10	y2	0,568
4	30	-41,8	900,0	Perpendicular	400	60	8,10E+08	1,89E+10	1,97E+10	4,93E+07			
5	30	-71,8	27000,0	Parallel	12000	750	2,43E+10	1,67E+12	1,70E+12	1,41E+08	1,37E+12	y3	0,804
6	30	-101,8	900,0	Perpendicular	400	60	8,10E+08	1,12E+11	1,13E+11	2,82E+08			
7	30	-131,8	27000,0	Parallel	12000	750	2,43E+10	5,63E+12	5,66E+12	4,71E+08	4,80E+12	y4	0,848
Total height	250,0	mm							EIeff	Ieff	EIeff		
Zs	146,8	mm							1,25E+13	1,28E+09	1,04E+13		

V					S		
77645,2	12630,7	0,0	0,0	0,0	69333,3	C1,2	1066,7
-56702,6	-35070,7	129314,3	0,0	0,0	38666,7	C2,3	1800,0
0,0	21314,3	-265457,8	237314,3	0,0	0,0	C3,4	1800,0
0,0	0,0	129314,3	-249846,9	0,0	-108000,0	C4,5	0,0
0,0	0,0	0,0	0,0	1,0	0,0		
						D1	394,0
						D2	95,1
3,1E-05	2,5E-05	2,3E-05	2,1E-05	0,0E+00	0,801	D3	95,1
-1,1E-04	-1,5E-04	-1,4E-04	-1,3E-04	0,0E+00	0,568	D4	95,1
-1,7E-05	-2,3E-05	-2,8E-05	-2,6E-05	0,0E+00	0,804	D5	0,0
-8,7E-06	-1,2E-05	-1,4E-05	-1,8E-05	0,0E+00	0,848		
0,0E+00	0,0E+00	0,0E+00	0,0E+00	1,0E+00	0,000	a1	53,2
						a2	-11,8
						a3	-71,8
						a4	-131,8
						a5	0,0

A.12 Calculation B6

A.12.1 Mechanical properties

Ec	14920,0	N/mm^2	
Etimber	12000	N/mm^2	
Gr	60	N/mm^2	Shear modulus parallel to the grain
h	30	mm	
Kser / K0.4	240	kN/mm	
seff	150	mm	
fck	27,29	N/mm^2	
fcd	18,19	N/mm^2	
fctm	2,72	N/mm^2	
fctk.0,05	1,90	N/mm^2	
fctd	1,27	N/mm^2	

			Area mm^2	Iy mm^4
h.con	100	mm	90000	75000000
h.1	30	mm	27000	2025000
h.between	30	mm	27000	2025000
h.2	30	mm	27000	2025000
h.between	30	mm	27000	2025000
h.3	30	mm	27000	2025000
width	900	mm		
length	5800	mm		

A.12.2 Seperated calculation method

ac	59,3	mm	140,7	mm
a1	65,7	mm	140,7	mm

γcon	0,802	
γ1	1,000	

EI.con	4,91E+12	Nmm2
EI.1	6,49E+12	Nmm2

EI(eff) 1,14E+13 Nmm2

Layers	Thickness	z	centre of gravity	Direction	E	G	EI	EAz	EIy Som	Ieff som	Eieff red		
1	30	60,0	27000,00	Parallel	12000	750	2,43E+10	1,17E+12	1,19E+12	9,92E+07	1,13E+12	y1	0,950
2	30	30,0	900,00	Perpendicular	400	60	8,10E+08	9,72E+09	1,05E+10	2,63E+07			
3	30	0,0	27000,00	Parallel	12000	750	2,43E+10	3,24E-16	2,43E+10	2,03E+06	2,43E+10	y2	0,688
4	30	-30,0	900,00	Perpendicular	400	60	8,10E+08	9,72E+09	1,05E+10	2,63E+07			
5	30	-60,0	27000,00	Parallel	12000	750	2,43E+10	1,17E+12	1,19E+12	9,92E+07	1,13E+12	y3	0,950
Total height	150,0	mm							EIeff	Ieff	***EIeff***		
Zs	75,0	mm							2,43E+12	2,53E+08	***2,29E+12***		

V					S		
113703,5	0,0	0,0	0,0	0,0	108000,0	C1,2	1800
-108000,0	0,0	108000,0	0,0	0,0	0,0	C2,3	1800
0,0	0,0	-113703,5	0,0	0,0	-108000,0	C3,4	0
0,0	0,0	0,0	1,0	0,0	0,0	C4,5	0
0,0	0,0	0,0	0,0	1,0	0,0		
						D1	95,1
						D2	95,1
6,3E-05	5,7E-05	5,5E-05	0,0E+00	0,0E+00	0,950	D3	95,1
3,4E+09	3,6E+09	3,4E+09	0,0E+00	0,0E+00	0,688	D4	0,0
-5,5E-05	-5,7E-05	-6,3E-05	0,0E+00	0,0E+00	0,950	D5	0,0
0,0E+00	0,0E+00	0,0E+00	1,0E+00	0,0E+00	0,000		
0,0E+00	0,0E+00	0,0E+00	0,0E+00	1,0E+00	0,000	a1	60,0
						a2	0,0
						a3	-60,0
						a4	0,0
						a5	0,0

A.12.3 Combined calculation method

Layers	Thickness	z	centre of gravity	Direction	E	G	EI	EAz	EIy Som	Ieff som	Eieff red		
1	100	53,2	111900,0	Parallel	14920	750	1,12E+12	3,79E+12	4,91E+12	3,29E+08	4,29E+12	y1	0,836
3	30	-11,8	27000,0	Parallel	12000	750	2,43E+10	4,54E+10	6,97E+10	5,81E+06	6,11E+10	y2	0,810
4	30	-41,8	900,0	Perpendicular	400	60	8,10E+08	1,89E+10	1,97E+10	4,93E+07			
5	30	-71,8	27000,0	Parallel	12000	750	2,43E+10	1,67E+12	1,70E+12	1,41E+08	1,43E+12	y3	0,840
6	30	-101,8	900,0	Perpendicular	400	60	8,10E+08	1,12E+11	1,13E+11	2,82E+08			
7	30	-131,8	27000,0	Parallel	12000	750	2,43E+10	5,63E+12	5,66E+12	4,71E+08	4,91E+12	y4	0,867
Total height	250,0	mm							EIeff	Ieff	***EIeff***		
Zs	146,8	mm							1,25E+13	1,28E+09	***1,07E+13***		

V

105996,5	18946,1	0,0	0,0	0,0
-85053,9	-41386,0	129314,3	0,0	0,0
0,0	21314,3	-265457,8	237314,3	0,0
0,0	0,0	129314,3	-249846,9	0,0
0,0	0,0	0,0	0,0	1,0

3,0E-05	2,6E-05	2,4E-05	2,2E-05	0,0E+00	0,836
-1,2E-04	-1,5E-04	-1,3E-04	-1,3E-04	0,0E+00	0,810
-1,7E-05	-2,2E-05	-2,7E-05	-2,5E-05	0,0E+00	0,840
-9,0E-06	-1,1E-05	-1,4E-05	-1,7E-05	0,0E+00	0,867
0,0E+00	0,0E+00	0,0E+00	0,0E+00	1,0E+00	0,000

S

104000,0	
4000,0	
0,0	
-108000,0	
0,0	

C1,2	1600,0
C2,3	1800,0
C3,4	1800,0
C4,5	0,0

D1	394,0
D2	95,1
D3	95,1
D4	95,1
D5	0,0

a1	53,2
a2	-11,8
a3	-71,8
a4	-131,8
a5	0,0

A.13 Calculation B7

A.13.1 Mechanical properties

Ec	41200,0	N/mm^2	
Etimber	11700	N/mm^2	
Gr	60	N/mm^2	Shear modulus parallel to the grain
h	35	mm	
Kser / K0.4	398	kN/mm	
seff	850	mm	
fck	119,6	N/mm^2	
fcd	79,73	N/mm^2	
fctm	7,28	N/mm^2	
fctk.0,05	5,10	N/mm^2	
fctd	3,40	N/mm^2	

			Area mm^2	Iy mm^4
h.con	70	mm	63000	25725000
h.1	35	mm	31500	3215625
h.between	35	mm	31500	3215625
h.2	35	mm	31500	3215625
h.between	35	mm	31500	3215625
h.3	35	mm	31500	3215625
width	900	mm		
length	8000	mm		

A.13.2 Seperated calculation method

ac	54,1	mm	155,9	mm
a1	68,4	mm	155,9	mm
γcon	0,539			
γ1	1,000			
EI.con	5,15E+12	Nmm2		
EI.1	8,77E+12	Nmm2		
EI(eff)	***1,39E+13***	***Nmm2***		

Layers	Thickness	z	centre of gravity	Direction	E	G	EI	EAz	EIy Som	Ieff som	Eieff red		
1	35	70,0	31500,00	Parallel	11700	731	3,76E+10	1,81E+12	1,84E+12	1,58E+08	1,78E+12	y1	0,964
2	35	35,0	1050,00	Perpendicular	390	60	1,25E+09	1,50E+10	1,63E+10	4,18E+07			
3	35	0,0	31500,00	Parallel	11700	731	3,76E+10	3,69E-16	3,76E+10	3,22E+06	3,76E+10	y2	0,500
4	35	-35,0	1050,00	Perpendicular	390	60	1,25E+09	1,50E+10	1,63E+10	4,18E+07			
5	35	-70,0	31500,00	Parallel	11700	731	3,76E+10	1,81E+12	1,84E+12	1,58E+08	1,78E+12	y3	0,964
Total height	175,0	mm							EIeff	Ieff	***EIeff***		
Zs	87,5	mm							3,76E+12	4,02E+08	***3,60E+12***		

V

111978,5	0,0	0,0	0,0	0,0
-108000,0	0,0	108000,0	0,0	0,0
0,0	0,0	-111978,5	0,0	0,0
0,0	0,0	0,0	1,0	0,0
0,0	0,0	0,0	0,0	1,0

S

108000,0	C1,2 1542,857
0,0	C2,3 1542,857
-108000,0	C3,4 0
0,0	C4,5 0
0,0	

	D1 56,8
	D2 56,8
0,964	D3 56,8
0,500	D4 0,0
0,964	D5 0,0
0,000	
0,000	a1 70,0
	a2 0,0
	a3 -70,0
	a4 0,0
	a5 0,0

8,9E-05	8,3E-05	8,0E-05	0,0E+00	0,0E+00
5,8E+09	6,0E+09	5,8E+09	0,0E+00	0,0E+00
-8,0E-05	-8,3E-05	-8,9E-05	0,0E+00	0,0E+00
0,0E+00	0,0E+00	0,0E+00	1,0E+00	0,0E+00
0,0E+00	0,0E+00	0,0E+00	0,0E+00	1,0E+00

A.13.3 Combined calculation method

Layers	Thickness	z	centre of gravity	Direction	E	G	EI	EAz	EIy Som	Ieff som	Eieff red		
1	70	37,2	221846,2	Parallel	41200	731	1,06E+12	3,58E+12	4,64E+12	1,13E+08	3,73E+12	y1	0,744
3	35	-15,3	31500,0	Parallel	11700	731	3,76E+10	8,67E+10	1,24E+11	1,06E+07	4,46E+10	y2	0,080
4	35	-50,3	1050,0	Perpendicular	390	60	1,25E+09	3,11E+10	3,24E+10	8,30E+07			
5	35	-85,3	31500,0	Parallel	11700	731	3,76E+10	2,68E+12	2,72E+12	2,33E+08	2,05E+12	y3	0,751
6	35	-120,3	1050,0	Perpendicular	390	60	1,25E+09	1,78E+11	1,79E+11	4,59E+08			
7	35	-155,3	31500,0	Parallel	11700	731	3,76E+10	8,89E+12	8,93E+12	7,63E+08	7,44E+12	y4	0,833
Total height	245,0	mm							EIeff	Ieff	EIeff		
Zs	172,8	mm							1,66E+13	1,66E+09	1,33E+13		

V

32273,9	7182,7	0,0	0,0	0,0
-17399,7	-31721,7	131667,2	0,0	0,0
0,0	23667,2	-268184,8	239667,2	0,0
0,0	0,0	131667,2	-248496,0	0,0
0,0	0,0	0,0	0,0	1,0

S

24582,4	
83417,6	
0,0	
-108000,0	
0,0	

C1,2	468,2
C2,3	1542,9
C3,4	1542,9
C4,5	0,0

D1	400,3
D2	56,8
D3	56,8
D4	56,8
D5	0,0

5,2E-05	3,9E-05	3,6E-05	3,5E-05	0,0E+00	0,744
-9,3E-05	-1,7E-04	-1,6E-04	-1,6E-04	0,0E+00	0,080
-1,6E-05	-2,9E-05	-3,4E-05	-3,3E-05	0,0E+00	0,751
-8,3E-06	-1,5E-05	-1,8E-05	-2,1E-05	0,0E+00	0,833
0,0E+00	0,0E+00	0,0E+00	0,0E+00	1,0E+00	0,000

a1	37,2
a2	-15,3
a3	-85,3
a4	-155,3
a5	0,0

A.14 Calculation B8 & B9

These floors have the same properties and thickness. The difference is in the preparation of the TCC floor slab

A.14.1 Mechanical properties

Ec	30100,0	N/mm^2	
Etimber	11700	N/mm^2	
Gr	60	N/mm^2	Shear modulus parallel to the grain
h	35	mm	
Kser / K0.4	351	kN/mm	
seff	850	mm	
fck	63,6	N/mm^2	
fcd	42,40	N/mm^2	
fctm	4,78	N/mm^2	
fctk.0,05	3,35	N/mm^2	
fctd	2,23	N/mm^2	

			Area mm^2	Iy mm^4
h.con	70	mm	63000	25725000
h.1	35	mm	31500	3215625
h.between	35	mm	31500	3215625
h.2	35	mm	31500	3215625
h.between	35	mm	31500	3215625
h.3	35	mm	31500	3215625
width	900	mm		
length	8000	mm		

A.14.2 Seperated calculation method

ac	61,1	mm	148,9	mm
a1	61,4	mm	148,9	mm

γcon	0,585
γ1	1,000

EI.con	4,92E+12	Nmm2
EI.1	7,76E+12	Nmm2

EI(eff) 1,27E+13 Nmm2

Layers	Thickness	z	centre of gravity	Direction	E	G	EI	EAz	EIy Som	Ieff som	Eieff red		
1	35	70,0	31500,00	Parallel	11700	731	3,76E+10	1,81E+12	1,84E+12	1,58E+08	1,78E+12	y1	0,964
2	35	35,0	1050,00	Perpendicular	390	60	1,25E+09	1,50E+10	1,63E+10	4,18E+07			
3	35	0,0	31500,00	Parallel	11700	731	3,76E+10	3,69E-16	3,76E+10	3,22E+06	3,76E+10	y2	0,500
4	35	-35,0	1050,00	Perpendicular	390	60	1,25E+09	1,50E+10	1,63E+10	4,18E+07			
5	35	-70,0	31500,00	Parallel	11700	731	3,76E+10	1,81E+12	1,84E+12	1,58E+08	1,78E+12	y3	0,964
Total height	175,0	mm							EIeff	Ieff	***EIeff***		
Zs	87,5	mm							3,76E+12	4,02E+08	***3,60E+12***		

V					S		
111978,5	0,0	0,0	0,0	0,0	108000,0	C1,2	1542,857
-108000,0	0,0	108000,0	0,0	0,0	0,0	C2,3	1542,857
0,0	0,0	-111978,5	0,0	0,0	-108000,0	C3,4	0
0,0	0,0	0,0	1,0	0,0	0,0	C4,5	0
0,0	0,0	0,0	0,0	1,0	0,0		
						D1	56,8
						D2	56,8
8,9E-05	8,3E-05	8,0E-05	0,0E+00	0,0E+00	0,964	D3	56,8
5,8E+09	6,0E+09	5,8E+09	0,0E+00	0,0E+00	0,500	D4	0,0
-8,0E-05	-8,3E-05	-8,9E-05	0,0E+00	0,0E+00	0,964	D5	0,0
0,0E+00	0,0E+00	0,0E+00	1,0E+00	0,0E+00	0,000		
0,0E+00	0,0E+00	0,0E+00	0,0E+00	1,0E+00	0,000	a1	70,0
						a2	0,0
						a3	-70,0
						a4	0,0
						a5	0,0

A.14.3 Combined calculation method

Layers	Thickness	z	centre of gravity	Direction	E	G	EI	EAz	EIy Som	Ieff som	Eieff red		
1	70	45,7	162076,9	Parallel	30100	731	7,74E+11	3,97E+12	4,74E+12	1,58E+08	3,73E+12	y1	0,744
3	35	-6,8	31500,0	Parallel	11700	731	3,76E+10	1,68E+10	5,44E+10	4,65E+06	3,76E+10	y2	0,000
4	35	-41,8	1050,0	Perpendicular	390	60	1,25E+09	2,14E+10	2,27E+10	5,81E+07			
5	35	-76,8	31500,0	Parallel	11700	731	3,76E+10	2,17E+12	2,21E+12	1,89E+08	1,67E+12	y3	0,752
6	35	-111,8	1050,0	Perpendicular	390	60	1,25E+09	1,53E+11	1,55E+11	3,97E+08			
7	35	-146,8	31500,0	Parallel	11700	731	3,76E+10	7,94E+12	7,97E+12	6,82E+08	6,70E+12	y4	0,839
Total height	245,0	mm							EIeff	Ieff	***EIeff***		
Zs	164,3	mm							1,52E+13	1,49E+09	***1,21E+13***		

V					S		
32268,2	2788,9	0,0	0,0	0,0	21679,4	C1,2	412,9
-18890,5	-13592,8	118420,1	0,0	0,0	86320,6	C2,3	1542,9
0,0	10420,1	-241202,4	226420,1	0,0	0,0	C3,4	1542,9
0,0	0,0	118420,1	-234760,8	0,0	-108000,0	C4,5	0,0
0,0	0,0	0,0	0,0	1,0	0,0		
						D1	292,4
						D2	56,8
5,4E-05	3,9E-05	3,6E-05	3,5E-05	0,0E+00	0,744	D3	56,8
-2,6E-04	-4,5E-04	-4,2E-04	-4,0E-04	0,0E+00	-0,837	D4	56,8
-2,1E-05	-3,7E-05	-4,2E-05	-4,0E-05	0,0E+00	0,752	D5	0,0
-1,1E-05	-1,8E-05	-2,1E-05	-2,5E-05	0,0E+00	0,839		
0,0E+00	0,0E+00	0,0E+00	0,0E+00	1,0E+00	0,000	a1	45,7
						a2	-6,8
						a3	-76,8
						a4	-146,8
						a5	0,0

A.15 Calculation C1

A.15.1 Mechanical properties

Ec	28042,2	N/mm^2	
Etimber	12410,6	N/mm^2	
Gr	60	N/mm^2	Shear modulus parallel to the grain
h	35	mm	
Kser / K0.4	498	kN/mm	
seff	150	mm	
fck	27,29	N/mm^2	
fcd	18,19	N/mm^2	
fctm	2,72	N/mm^2	
fctk.0,05	1,90	N/mm^2	
fctd	1,27	N/mm^2	

			Area mm^2	Iy mm^4
h.con	150	mm	360000	675000000
h.1	35	mm	84000	8575000
h.between	35	mm	84000	8575000
h.2	35	mm	84000	8575000
h.between	35	mm	84000	8575000
h.3	35	mm	84000	8575000
h.between	35	mm	84000	8575000
h.4	35	mm	84000	8575000
width	2400	mm		
length	4600	mm		

A.15.2 Seperated calculation method

ac	98,7	mm	221,2	mm
a1	98,8	mm	221,2	mm

γcon	0,414
γ1	1,000

EI.con	5,96E+13	Nmm2
EI.1	6,24E+13	Nmm2

EI(eff) 1,22E+14 Nmm2

Layers	Thickness	z	centre of gravity	Direction	E	G	EI	EAz	EIy Som	Ieff som	Eieff red		
1	35	105,0	84000,00	Parallel	12411	776	1,06E+11	1,15E+13	1,16E+13	9,35E+08	9,71E+12	y1	0,836
2	35	70,0	2800,00	Perpendicular	414	60	3,55E+09	1,70E+11	1,74E+11	4,20E+08			
3	35	35,0	84000,00	Parallel	12411	776	1,06E+11	1,28E+12	1,38E+12	1,11E+08	1,13E+12	y2	0,804
4	35	0,0	2800,00	Perpendicular	414	60	3,55E+09	3,47E-17	3,55E+09	8,58E+06			
5	35	-35,0	84000,00	Parallel	12411	776	1,06E+11	1,28E+12	1,38E+12	1,11E+08	1,13E+12	y3	0,804
6	35	-70,0	2800,00	Perpendicular	414	60	3,55E+09	1,70E+11	***1,74E+11***	4,20E+08			
7	35	-105,0	84000,00	Parallel	12411	776	1,06E+11	1,15E+13	***1,16E+13***	9,35E+08	9,71E+12	y4	0,836
Total height	245,0	mm							EIeff	Ieff	***EIeff***		
Zs	122,5	mm							2,63E+13	2,94E+09	***2,17E+13***		

V					S		
483055,7	-144000,0	0,0	0,0	0,0	288000,0	C1,2	4114,286
-432000,0	305018,6	144000,0	0,0	0,0	0,0	C2,3	4114,286
0,0	-144000,0	-305018,6	432000,0	0,0	0,0	C3,4	4114,286
0,0	0,0	144000,0	-483055,7	0,0	-288000,0	C4,5	0
0,0	0,0	0,0	0,0	1,0	0,0		
						D1	486,2
						D2	486,2
6,6E-06	5,1E-06	4,2E-06	3,7E-06	0,0E+00	0,836	D3	486,2
1,5E-05	1,7E-05	1,4E-05	1,2E-05	0,0E+00	0,804	D4	486,2
-1,2E-05	-1,4E-05	-1,7E-05	-1,5E-05	0,0E+00	0,804	D5	0,0
-3,7E-06	-4,2E-06	-5,1E-06	-6,6E-06	0,0E+00	0,836		
0,0E+00	0,0E+00	0,0E+00	0,0E+00	1,0E+00	0,000	a1	105,0
						a2	35,0
						a3	-35,0
						a4	-105,0
						a5	0,0

A.15.3 Combined calculation method

Layers	Thickness	z	centre of gravity	Direction	E	G	EI	EAz	EIy Som	Ieff som	Eieff red		
1	150	58,7	813436,2	Parallel	28042	776	1,89E+13	3,48E+13	5,38E+13	1,92E+09	3,77E+13	y1	0,539
2	35	-33,8	84000,0	Parallel	12411	776	1,06E+11	1,19E+12	1,29E+12	1,04E+08	6,66E+11	y2	0,471
3	35	-68,8	2800,0	Perpendicular	414	60	3,55E+09	1,64E+11	1,68E+11	4,06E+08			
4	35	-103,8	84000,0	Parallel	12411	776	1,06E+11	1,12E+13	1,13E+13	9,13E+08	5,68E+12	y3	0,497
5	35	-138,8	2800,0	Perpendicular	414	60	3,55E+09	6,69E+11	6,73E+11	1,63E+09			
6	35	-173,8	84000,0	Parallel	12411	776	1,06E+11	3,15E+13	3,16E+13	2,54E+09	1,70E+13	y4	0,537
7	35	-208,8	2800,0	Perpendicular	414	60	3,55E+09	1,51E+12	***1,52E+12***	3,67E+09			
8	35	-243,8	84000,0	Parallel	12411	776	1,06E+11	6,19E+13	***6,20E+13***	5,00E+09	3,72E+13	y5	0,599
Total height	395,0	mm							EIeff	Ieff	EIeff		
Zs	261,3	mm							1,62E+14	1,62E+10	9,83E+13		

V

471657,9	112061,1	0,0	0,0	0,0
-195038,9	-267344,4	426870,9	0,0	0,0
0,0	138870,9	-904191,3	714870,9	0,0
0,0	0,0	426870,9	########	1002870,9
0,0	0,0	0,0	714870,9	-1121394,7

S

307100,0
-19100,0
0,0
0,0
-288000,0

C1,2	3320,0
C2,3	4114,3
C3,4	4114,3
C4,5	4114,3

D1	4708,7
D2	486,2
D3	486,2
D4	486,2
D5	486,2

3,0E-06	2,1E-06	1,6E-06	1,3E-06	1,2E-06	0,539
-3,6E-06	-8,8E-06	-6,7E-06	-5,5E-06	-4,9E-06	0,471
-9,0E-07	-2,2E-06	-3,5E-06	-2,8E-06	-2,5E-06	0,497
-4,4E-07	-1,1E-06	-1,7E-06	-2,5E-06	-2,3E-06	0,537
-2,8E-07	-6,8E-07	-1,1E-06	-1,6E-06	-2,3E-06	0,599

a1	58,7
a2	-33,8
a3	-103,8
a4	-173,8
a5	-243,8

A.16 Calculation C2

A.16.1 Mechanical properties

Ec	28042,2	N/mm^2	
Etimber	12410,56	N/mm^2	
Gr	60	N/mm^2	Shear modulus parallel to the grain
h	35	mm	
Kser / K0.4	3708	kN/mm	
seff	575	mm	
fck	27,29	N/mm^2	
fcd	18,19	N/mm^2	
fctm	2,72	N/mm^2	
fctk.0,05	1,90	N/mm^2	
fctd	1,27	N/mm^2	

			Area mm^2	Iy mm^4
h.con	150	mm	360000	675000000
h.1	35	mm	84000	8575000
h.between	35	mm	84000	8575000
h.2	35	mm	84000	8575000
h.between	35	mm	84000	8575000
h.3	35	mm	84000	8575000
h.between	35	mm	84000	8575000
h.4	35	mm	84000	8575000
width	2400	mm		
length	4600	mm		

A.16.2 Seperated calculation method

ac	119,3	mm	200,7	mm
a1	78,2	mm	200,7	mm

γcon	0,271	
γ1	1,000	

EI.con	5,78E+13	Nmm2
EI.1	4,72E+13	Nmm2

EI(eff) 1,05E+14 Nmm2

Layers	Thickness	z	centre of gravity	Direction	E	G	EI	EAz	EIy Som	Ieff som	Eieff red		
1	35	105,0	84000,00	Parallel	12411	776	1,06E+11	1,15E+13	1,16E+13	9,35E+08	9,71E+12	y1	0,836
2	35	70,0	2800,00	Perpendicular	414	60	3,55E+09	1,70E+11	1,74E+11	4,20E+08			
3	35	35,0	84000,00	Parallel	12411	776	1,06E+11	1,28E+12	1,38E+12	1,11E+08	1,13E+12	y2	0,804
4	35	0,0	2800,00	Perpendicular	414	60	3,55E+09	3,47E-17	3,55E+09	8,58E+06			
5	35	-35,0	84000,00	Parallel	12411	776	1,06E+11	1,28E+12	1,38E+12	1,11E+08	1,13E+12	y3	0,804
6	35	-70,0	2800,00	Perpendicular	414	60	***3,55E+09***	1,70E+11	1,74E+11	4,20E+08			
7	35	-105,0	84000,00	Parallel	12411	776	***1,06E+11***	1,15E+13	1,16E+13	9,35E+08	9,71E+12	y4	0,836
Total height	245,0	mm							EIeff	Ieff	***EIeff***		
Zs	122,5	mm							2,63E+13	2,94E+09	***2,17E+13***		

V					S		
483055,7	-144000,0	0,0	0,0	0,0	288000,0	C1,2	4114,286
-432000,0	305018,6	144000,0	0,0	0,0	0,0	C2,3	4114,286
0,0	-144000,0	-305018,6	432000,0	0,0	0,0	C3,4	4114,286
0,0	0,0	144000,0	-483055,7	0,0	-288000,0	C4,5	0
0,0	0,0	0,0	0,0	1,0	0,0		
						D1	486,2
						D2	486,2
6,6E-06	5,1E-06	4,2E-06	3,7E-06	0,0E+00	0,836	D3	486,2
1,5E-05	1,7E-05	1,4E-05	1,2E-05	0,0E+00	0,804	D4	486,2
-1,2E-05	-1,4E-05	-1,7E-05	-1,5E-05	0,0E+00	0,804	D5	0,0
-3,7E-06	-4,2E-06	-5,1E-06	-6,6E-06	0,0E+00	0,836		
0,0E+00	0,0E+00	0,0E+00	0,0E+00	1,0E+00	0,000	a1	105,0
						a2	35,0
						a3	-35,0
						a4	-105,0
						a5	0,0

A.16.3 Combined calculation method

Layers	Thickness	z	centre of gravity	Direction	E	G	EI	EAz	EIy Som	Ieff som	Eieff red		
1	150	58,7	813436,2	Parallel	28042	776	1,89E+13	3,48E+13	5,38E+13	1,92E+09	3,43E+13	y1	0,440
2	35	-33,8	84000,0	Parallel	12411	776	1,06E+11	1,19E+12	1,29E+12	1,04E+08	1,06E+11	y2	0,000
3	35	-68,8	2800,0	Perpendicular	414	60	3,55E+09	1,64E+11	1,68E+11	4,06E+08			
4	35	-103,8	84000,0	Parallel	12411	776	1,06E+11	1,12E+13	1,13E+13	9,13E+08	4,10E+12	y3	0,356
5	35	-138,8	2800,0	Perpendicular	414	60	3,55E+09	6,69E+11	6,73E+11	1,63E+09			
6	35	-173,8	84000,0	Parallel	12411	776	1,06E+11	3,15E+13	3,16E+13	2,54E+09	1,48E+13	y4	0,468
7	35	-208,8	2800,0	Perpendicular	414	60	***3,55E+09***	1,51E+12	1,52E+12	3,67E+09			
8	35	-243,8	84000,0	Parallel	12411	776	***1,06E+11***	6,19E+13	6,20E+13	5,00E+09	3,45E+13	y5	0,555
Total height	395,0	mm							EIeff	Ieff	EIeff		
Zs	261,3	mm							1,62E+14	1,62E+10	8,78E+13		

V

379229,9	58955,8	0,0	0,0	0,0	161566,7
-102610,8	-214239,1	426870,9	0,0	0,0	126433,3
0,0	138870,9	-904191,3	714870,9	0,0	0,0
0,0	0,0	426870,9	########	1002870,9	0,0
0,0	0,0	0,0	714870,9	-1121394,7	-288000,0

3,1E-06	1,7E-06	1,3E-06	1,1E-06	9,5E-07	0,440
-3,0E-06	-1,1E-05	-8,4E-06	-6,9E-06	-6,1E-06	-0,092
-7,4E-07	-2,7E-06	-3,9E-06	-3,2E-06	-2,8E-06	0,356
-3,6E-07	-1,3E-06	-1,9E-06	-2,7E-06	-2,4E-06	0,468
-2,3E-07	-8,5E-07	-1,2E-06	-1,7E-06	-2,4E-06	0,555

S

C1,2	1746,7
C2,3	4114,3
C3,4	4114,3
C4,5	4114,3
D1	4708,7
D2	486,2
D3	486,2
D4	486,2
D5	486,2
a1	58,7
a2	-33,8
a3	-103,8
a4	-173,8
a5	-243,8

A.17 Calculation C3

A.17.1 Mechanical properties

Ec	28042,2	N/mm^2	
Etimber	12410,56	N/mm^2	
Gr	60	N/mm^2	Shear modulus parallel to the grain
h	35	mm	
Kser / K0.4	3708	kN/mm	
seff	575	mm	
fck	27,29	N/mm^2	
fcd	18,19	N/mm^2	
fctm	2,72	N/mm^2	
fctk.0,05	1,90	N/mm^2	
fctd	1,27	N/mm^2	

			Area mm^2	Iy mm^4
h.con	150	mm	360000	675000000
h.1	35	mm	84000	8575000
h.between	35	mm	84000	8575000
h.2	35	mm	84000	8575000
h.between	35	mm	84000	8575000
h.3	35	mm	84000	8575000
h.between	35	mm	84000	8575000
h.4	35	mm	84000	8575000
width	2400	mm		
length	4600	mm		

A.17.2 Seperated calculation method

ac	82,3	mm	237,7	mm
a1	115,2	mm	237,7	mm

γcon	0,578	
γ1	1,000	

EI.con	5,85E+13	Nmm2
EI.1	1,23E+14	Nmm2

EI(eff) 1,81E+14 Nmm2

Layers	Thickness	z	centre of gravity	Direction	E	G	EI	EAz	EIy Som	Ieff som	Eieff red		
1	35	105,0	84000,00	Parallel	12411	776	1,06E+11	1,15E+13	1,16E+13	9,35E+08	9,71E+12	y1	0,836
2	35	70,0	2800,00	Perpendicular	414	60	3,55E+09	1,70E+11	1,74E+11	4,20E+08			
3	35	35,0	84000,00	Parallel	12411	776	1,06E+11	1,28E+12	1,38E+12	1,11E+08	1,13E+12	y2	0,804
4	35	0,0	2800,00	Perpendicular	414	60	3,55E+09	3,47E-17	3,55E+09	8,58E+06			
5	35	-35,0	84000,00	Parallel	12411	776	1,06E+11	1,28E+12	1,38E+12	1,11E+08	1,13E+12	y3	0,804
6	35	-70,0	2800,00	Perpendicular	***414***	60	3,55E+09	1,70E+11	1,74E+11	4,20E+08			
7	35	-105,0	84000,00	Parallel	***12411***	776	1,06E+11	1,15E+13	1,16E+13	9,35E+08	9,71E+12	y4	0,836
Total height	245,0	mm							EIeff	Ieff	***EIeff***		
Zs	122,5	mm							2,63E+13	2,94E+09	***2,17E+13***		

V

483055,7	-144000,0	0,0	0,0	0,0
-432000,0	305018,6	144000,0	0,0	0,0
0,0	-144000,0	-305018,6	432000,0	0,0
0,0	0,0	144000,0	-483055,7	0,0
0,0	0,0	0,0	0,0	1,0

6,6E-06	5,1E-06	4,2E-06	3,7E-06	0,0E+00	0,836
1,5E-05	1,7E-05	1,4E-05	1,2E-05	0,0E+00	0,804
-1,2E-05	-1,4E-05	-1,7E-05	-1,5E-05	0,0E+00	0,804
-3,7E-06	-4,2E-06	-5,1E-06	-6,6E-06	0,0E+00	0,836
0,0E+00	0,0E+00	0,0E+00	0,0E+00	1,0E+00	0,000

S

288000,0	
0,0	
0,0	
-288000,0	
0,0	

C1,2	4114,286
C2,3	4114,286
C3,4	4114,286
C4,5	0

D1	486,2
D2	486,2
D3	486,2
D4	486,2
D5	0,0

a1	105,0
a2	35,0
a3	-35,0
a4	-105,0
a5	0,0

A.17.3 Combined calculation method

Layers	Thickness	z	centre of gravity	Direction	E	G	EI	EAz	EIy Som	Ieff som	Eieff red		
1	150	58,7	813436,2	Parallel	28042	776	1,89E+13	3,48E+13	5,38E+13	1,92E+09	4,03E+13	y1	0,613
2	35	-33,8	84000,0	Parallel	12411	776	1,06E+11	1,19E+12	1,29E+12	1,04E+08	1,17E+12	y2	0,894
3	35	-68,8	2800,0	Perpendicular	414	60	3,55E+09	1,64E+11	1,68E+11	4,06E+08			
4	35	-103,8	84000,0	Parallel	12411	776	1,06E+11	1,12E+13	1,13E+13	9,13E+08	6,87E+12	y3	0,602
5	35	-138,8	2800,0	Perpendicular	414	60	3,55E+09	6,69E+11	6,73E+11	1,63E+09			
6	35	-173,8	84000,0	Parallel	12411	776	1,06E+11	3,15E+13	3,16E+13	2,54E+09	1,86E+13	y4	0,588
7	35	-208,8	2800,0	Perpendicular	***414***	60	3,55E+09	1,51E+12	1,52E+12	3,67E+09			
8	35	-243,8	84000,0	Parallel	***12411***	776	1,06E+11	6,19E+13	6,20E+13	5,00E+09	3,92E+13	y5	0,632
Total height	395,0	mm							EIeff	Ieff	EIeff		
Zs	261,3	mm							1,62E+14	1,62E+10	1,06E+14		

V					S		
655458,3	217665,1	0,0	0,0	0,0	596504,3	C1,2	6448,7
-378839,3	-372948,4	426870,9	0,0	0,0	-308504,3	C2,3	4114,3
0,0	138870,9	-904191,3	714870,9	0,0	0,0	C3,4	4114,3
0,0	0,0	426870,9	########	1002870,9	0,0	C4,5	4114,3
0,0	0,0	0,0	714870,9	-1121394,7	-288000,0		
						D1	4708,7
						D2	486,2
2,9E-06	2,4E-06	1,8E-06	1,5E-06	1,3E-06	0,613	D3	486,2
-4,1E-06	-7,1E-06	-5,5E-06	-4,5E-06	-4,0E-06	0,894	D4	486,2
-1,0E-06	-1,8E-06	-3,2E-06	-2,6E-06	-2,3E-06	0,602	D5	486,2
-5,0E-07	-8,7E-07	-1,5E-06	-2,4E-06	-2,2E-06	0,588		
-3,2E-07	-5,5E-07	-9,9E-07	-1,5E-06	-2,3E-06	0,632	a1	58,7
						a2	-33,8
						a3	-103,8
						a4	-173,8
						a5	-243,8

A.18 Calculation C4

A.18.1 Mechanical properties

Ec	28042,2	N/mm^2	
Etimber	12410,56	N/mm^2	
Gr	60	N/mm^2	Shear modulus parallel to the grain
h	35	mm	
Kser / K0.4	498	kN/mm	
seff	150	mm	
fck	27,29	N/mm^2	
fcd	18,19	N/mm^2	
fctm	2,72	N/mm^2	
fctk.0,05	1,90	N/mm^2	
fctd	1,27	N/mm^2	

			Area mm^2	Iy mm^4
h.con	150	mm	360000	675000000
h.1	35	mm	84000	8575000
h.between	35	mm	84000	8575000
h.2	35	mm	84000	8575000
h.between	35	mm	84000	8575000
h.3	35	mm	84000	8575000
h.between	35	mm	84000	8575000
h.4	35	mm	84000	8575000
width	2400	mm		
length	9200	mm		

A.18.2 Seperated calculation method

ac	70,9	mm	220,2	mm
a1	126,6	mm	193,4	mm

γcon	0,738	
γ1	1,000	

EI.con	5,63E+13	Nmm2
EI.1	9,16E+13	Nmm2

EI(eff) 1,48E+14 Nmm2

Layers	Thickness	z	centre of gravity	Direction	E	G	EI	EAz	EIy Som	Ieff som	Eieff red		
1	35	105,0	84000,00	Parallel	12411	776	1,06E+11	1,15E+13	1,16E+13	9,35E+08	**1,11E+13**	**y1**	**0,953**
2	35	70,0	2800,00	Perpendicular	414	60	3,55E+09	1,70E+11	1,74E+11	4,20E+08			
3	35	35,0	84000,00	Parallel	12411	776	1,06E+11	1,28E+12	1,38E+12	1,11E+08	**1,31E+12**	**y2**	**0,944**
4	35	0,0	2800,00	Perpendicular	414	60	3,55E+09	3,47E-17	3,55E+09	8,58E+06			
5	35	-35,0	84000,00	Parallel	12411	776	1,06E+11	1,28E+12	1,38E+12	1,11E+08	**1,31E+12**	**y3**	**0,944**
6	35	-70,0	2800,00	Perpendicular	414	60	3,55E+09	1,70E+11	1,74E+11	4,20E+08			
7	35	-105,0	84000,00	Parallel	12411	776	1,06E+11	1,15E+13	1,16E+13	9,35E+08	**1,11E+13**	**y4**	**0,953**
Total height	245,0	mm							**EIeff**	**Ieff**	***EIeff***		
Zs	122,5	mm							**2,63E+13**	**2,94E+09**	***2,47E+13***		

A.18.3 Combined calculation method

Layers	Thickness	z	centre of gravity	Direction	E	G	EI	EAz	EIy Som	Ieff som	Eieff red		
1	150	58,7	813436,2	Parallel	28042	776	1,89E+13	3,48E+13	5,38E+13	1,92E+09	4,74E+13	y1	0,816
2	35	-33,8	84000,0	Parallel	12411	776	1,06E+11	1,19E+12	1,29E+12	1,04E+08	1,08E+12	y2	0,816
3	35	-68,8	2800,0	Perpendicular	414	60	3,55E+09	1,64E+11	1,68E+11	4,06E+08			
4	35	-103,8	84000,0	Parallel	12411	776	1,06E+11	1,12E+13	1,13E+13	9,13E+08	9,26E+12	y3	0,816
5	35	-138,8	2800,0	Perpendicular	414	60	3,55E+09	6,69E+11	6,73E+11	1,63E+09			
6	35	-173,8	84000,0	Parallel	12411	776	1,06E+11	3,15E+13	3,16E+13	2,54E+09	2,62E+13	y4	0,830
7	35	-208,8	2800,0	Perpendicular	414	60	3,55E+09	1,51E+12	1,52E+12	3,67E+09			
8	35	-243,8	84000,0	Parallel	12411	776	1,06E+11	6,19E+13	6,20E+13	5,00E+09	5,30E+13	y5	0,854
Total height	395,0	mm							EIeff	Ieff	***EIeff***		
Zs	261,3	mm							1,62E+14	1,62E+10	***1,37E+14***		

V

264193,6	112061,1	0,0	0,0	0,0	307100,0
-195038,9	-255035,1	426870,9	0,0	0,0	-19100,0
0,0	138870,9	-866354,2	714870,9	0,0	0,0
0,0	0,0	426870,9	########	1002870,9	0,0
0,0	0,0	0,0	714870,9	-1032501,8	-288000,0

S

C1,2	3320,0
C2,3	4114,3
C3,4	4114,3
C4,5	4114,3

D1	1177,2
D2	121,6
D3	121,6
D4	121,6
D5	121,6

1,1E-05	9,6E-06	8,8E-06	8,3E-06	8,1E-06	0,816
-1,7E-05	-2,3E-05	-2,1E-05	-2,0E-05	-1,9E-05	0,816
-5,0E-06	-6,8E-06	-8,4E-06	-7,9E-06	-7,7E-06	0,816
-2,8E-06	-3,8E-06	-4,7E-06	-5,8E-06	-5,6E-06	0,830
-2,0E-06	-2,6E-06	-3,3E-06	-4,0E-06	-4,9E-06	0,854

a1	58,7
a2	-33,8
a3	-103,8
a4	-173,8
a5	-243,8

A.19 Calculation C5

A.19.1 Mechanical properties

Ec	28042,2	N/mm^2	
Etimber	12410,56	N/mm^2	
Gr	60	N/mm^2	Shear modulus parallel to the grain
h	35	mm	
Kser / K0.4	524	kN/mm	
seff	300	mm	
fck	27,29	N/mm^2	
fcd	18,19	N/mm^2	
fctm	2,72	N/mm^2	
fctk.0,05	1,90	N/mm^2	
fctd	1,27	N/mm^2	

			Area mm^2	Iy mm^4
h.con	150	mm	360000	675000000
h.1	35	mm	84000	8575000
h.between	35	mm	84000	8575000
h.2	35	mm	84000	8575000
h.between	35	mm	84000	8575000
h.3	35	mm	84000	8575000
h.between	35	mm	84000	8575000
h.4	35	mm	84000	8575000
width	2400	mm		
length	9200	mm		

A.19.2 Seperated calculation method

ac	80,7	mm	239,3	mm
a1	116,8	mm	239,3	mm

γcon	0,597	
γ1	1,000	

EI.con	5,82E+13	Nmm2
EI.1	8,16E+13	Nmm2

EI(eff) 1,40E+14 Nmm2

Layers	Thickness	z	centre of gravity	Direction	E	G	EI	EAz	EIy Som	Ieff som	Eieff red		
1	35	105,0	84000,00	Parallel	12411	776	1,06E+11	1,15E+13	1,16E+13	9,35E+08	**1,11E+13**	**y1**	**0,953**
2	35	70,0	2800,00	Perpendicular	414	60	3,55E+09	1,70E+11	1,74E+11	4,20E+08			
3	35	35,0	84000,00	Parallel	12411	776	1,06E+11	1,28E+12	1,38E+12	1,11E+08	**1,31E+12**	**y2**	**0,944**
4	35	0,0	2800,00	Perpendicular	414	60	3,55E+09	3,47E-17	3,55E+09	8,58E+06			
5	35	-35,0	84000,00	Parallel	12411	776	1,06E+11	1,28E+12	1,38E+12	1,11E+08	**1,31E+12**	**y3**	**0,944**
6	35	-70,0	2800,00	Perpendicular	414	60	3,55E+09	1,70E+11	1,74E+11	4,20E+08			
7	35	-105,0	84000,00	Parallel	12411	776	1,06E+11	1,15E+13	1,16E+13	9,35E+08	**1,11E+13**	**y4**	**0,953**
Total height	245,0	mm							EIeff	Ieff	**EIeff**		
Zs	122,5	mm							**2,63E+13**	**2,94E+09**	**2,47E+13**		

V

483055,7	-144000,0	0,0	0,0	0,0
-432000,0	305018,6	144000,0	0,0	0,0
0,0	-144000,0	-305018,6	432000,0	0,0
0,0	0,0	144000,0	-483055,7	0,0
0,0	0,0	0,0	0,0	1,0

6,6E-06	5,1E-06	4,2E-06	3,7E-06	0,0E+00	0,836
1,5E-05	1,7E-05	1,4E-05	1,2E-05	0,0E+00	0,804
-1,2E-05	-1,4E-05	-1,7E-05	-1,5E-05	0,0E+00	0,804
-3,7E-06	-4,2E-06	-5,1E-06	-6,6E-06	0,0E+00	0,836
0,0E+00	0,0E+00	0,0E+00	0,0E+00	1,0E+00	0,000

S

288000,0	C1,2 4114,286
0,0	C2,3 4114,286
0,0	C3,4 4114,286
-288000,0	C4,5 0
0,0	

D1	486,2
D2	486,2
D3	486,2
D4	486,2
D5	0,0

a1	105,0
a2	35,0
a3	-35,0
a4	-105,0
a5	0,0

A.19.3 Combined calculation method

Layers	Thickness	z	centre of gravity	Direction	E	G	EI	EAz	EIy Som	Ieff som	Eieff red		
1	150	58,7	813436,2	Parallel	28042	776	1,89E+13	3,48E+13	5,38E+13	1,92E+09	4,53E+13	y1	0,756
2	35	-33,8	84000,0	Parallel	12411	776	1,06E+11	1,19E+12	1,29E+12	1,04E+08	7,44E+11	y2	0,537
3	35	-68,8	2800,0	Perpendicular	414	60	3,55E+09	1,64E+11	1,68E+11	4,06E+08			
4	35	-103,8	84000,0	Parallel	12411	776	1,06E+11	1,12E+13	1,13E+13	9,13E+08	8,32E+12	y3	0,732
5	35	-138,8	2800,0	Perpendicular	414	60	3,55E+09	6,69E+11	6,73E+11	1,63E+09			
6	35	-173,8	84000,0	Parallel	12411	776	1,06E+11	3,15E+13	3,16E+13	2,54E+09	2,47E+13	y4	0,783
7	35	-208,8	2800,0	Perpendicular	414	60	3,55E+09	1,51E+12	1,52E+12	3,67E+09			
8	35	-243,8	84000,0	Parallel	12411	776	1,06E+11	6,19E+13	6,20E+13	5,00E+09	5,10E+13	y5	0,821
Total height	395,0	mm							*EIeff*	Ieff	***EIeff***		
Zs	261,3	mm							*1,62E+14*	1,62E+10	***1,30E+14***		

V

171765,6	58955,8	0,0	0,0	0,0	
-102610,8	-201929,9	426870,9	0,0	0,0	
0,0	138870,9	-866354,2	714870,9	0,0	
0,0	0,0	426870,9	########	1002870,9	
0,0	0,0	0,0	714870,9	-1032501,8	
1,1E-05	8,9E-06	8,2E-06	7,7E-06	7,5E-06	
-1,5E-05	-2,6E-05	-2,4E-05	-2,3E-05	-2,2E-05	
-4,6E-06	-7,8E-06	-9,3E-06	-8,8E-06	-8,5E-06	
-2,6E-06	-4,4E-06	-5,3E-06	-6,3E-06	-6,1E-06	
-1,8E-06	-3,0E-06	-3,6E-06	-4,4E-06	-5,2E-06	

S

161566,7	
126433,3	
0,0	
0,0	
-288000,0	
0,756	
0,537	
0,732	
0,783	
0,821	

C1,2	1746,7
C2,3	4114,3
C3,4	4114,3
C4,5	4114,3
D1	1177,2
D2	121,6
D3	121,6
D4	121,6
D5	121,6
a1	58,7
a2	-33,8
a3	-103,8
a4	-173,8
a5	-243,8

A.20 Calculation C6

A.20.1 Mechanical properties

Ec	28042,2	N/mm^2	
Etimber	12410,56	N/mm^2	
Gr	60	N/mm^2	Shear modulus parallel to the grain
h	35	mm	
Kser / K0.4	3708	kN/mm	
seff	575	mm	
fck	27,29	N/mm^2	
fcd	18,19	N/mm^2	
fctm	2,72	N/mm^2	
fctk.0,05	1,90	N/mm^2	
fctd	1,27	N/mm^2	

			Area mm^2	Iy mm^4
h.con	150	mm	360000	675000000
h.1	35	mm	84000	8575000
h.between	35	mm	84000	8575000
h.2	35	mm	84000	8575000
h.between	35	mm	84000	8575000
h.3	35	mm	84000	8575000
h.between	35	mm	84000	8575000
h.4	35	mm	84000	8575000
width	2400	mm		
length	9200	mm		

A.20.2 Seperated calculation method

ac	64,8	mm	255,2	mm
a1	132,7	mm	255,2	mm

γcon	0,846	
γ1	1,000	

EI.con	5,48E+13	Nmm2
EI.1	1,53E+14	Nmm2

EI(eff) 2,08E+14 Nmm2

Layers	Thickness	z	centre of gravity	Direction	E	G	EI	EAz	EIy Som	Ieff som	Eieff red		
1	35	105,0	84000,00	Parallel	12411	776	1,06E+11	1,15E+13	1,16E+13	9,35E+08	**1,11E+13**	**y1**	**0,953**
2	35	70,0	2800,00	Perpendicular	414	60	3,55E+09	1,70E+11	1,74E+11	4,20E+08			
3	35	35,0	84000,00	Parallel	12411	776	1,06E+11	1,28E+12	1,38E+12	1,11E+08	**1,31E+12**	**y2**	**0,944**
4	35	0,0	2800,00	Perpendicular	414	60	3,55E+09	3,47E-17	3,55E+09	8,58E+06			
5	35	-35,0	84000,00	Parallel	12411	776	1,06E+11	1,28E+12	1,38E+12	1,11E+08	**1,31E+12**	**y3**	**0,944**
6	35	-70,0	2800,00	Perpendicular	414	60	3,55E+09	1,70E+11	1,74E+11	4,20E+08			
7	35	-105,0	84000,00	Parallel	12411	776	1,06E+11	1,15E+13	1,16E+13	9,35E+08	**1,11E+13**	**y4**	**0,953**
Total height	245,0	mm							*EIeff*	*Ieff*	***EIeff***		
Zs	122,5	mm							**2,63E+13**	**2,94E+09**	***2,47E+13***		

V					S		
483055,7	-144000,0	0,0	0,0	0,0	288000,0	C1,2	4114,286
-432000,0	305018,6	144000,0	0,0	0,0	0,0	C2,3	4114,286
0,0	-144000,0	-305018,6	432000,0	0,0	0,0	C3,4	4114,286
0,0	0,0	144000,0	-483055,7	0,0	-288000,0	C4,5	0
0,0	0,0	0,0	0,0	1,0	0,0		
						D1	486,2
						D2	486,2
6,6E-06	5,1E-06	4,2E-06	3,7E-06	0,0E+00	0,836	D3	486,2
1,5E-05	1,7E-05	1,4E-05	1,2E-05	0,0E+00	0,804	D4	486,2
-1,2E-05	-1,4E-05	-1,7E-05	-1,5E-05	0,0E+00	0,804	D5	0,0
-3,7E-06	-4,2E-06	-5,1E-06	-6,6E-06	0,0E+00	0,836		
0,0E+00	0,0E+00	0,0E+00	0,0E+00	1,0E+00	0,000	a1	105,0
						a2	35,0
						a3	-35,0
						a4	-105,0
						a5	0,0

A.20.3 Combined calculation method

Layers	Thickness	z	centre of gravity	Direction	E	G	EI	EAz	EIy Som	Ieff som	Eieff red		
1	150	58,7	813436,2	Parallel	28042	776	1,89E+13	3,48E+13	5,38E+13	1,92E+09	4,86E+13	y1	0,853
2	35	-33,8	84000,0	Parallel	12411	776	1,06E+11	1,19E+12	1,29E+12	1,04E+08	1,28E+12	y2	0,985
3	35	-68,8	2800,0	Perpendicular	414	60	3,55E+09	1,64E+11	1,68E+11	4,06E+08			
4	35	-103,8	84000,0	Parallel	12411	776	1,06E+11	1,12E+13	1,13E+13	9,13E+08	9,83E+12	y3	0,866
5	35	-138,8	2800,0	Perpendicular	414	60	3,55E+09	6,69E+11	6,73E+11	1,63E+09			
6	35	-173,8	84000,0	Parallel	12411	776	1,06E+11	3,15E+13	3,16E+13	2,54E+09	2,71E+13	y4	0,859
7	35	-208,8	2800,0	Perpendicular	414	60	3,55E+09	1,51E+12	1,52E+12	3,67E+09			
8	35	-243,8	84000,0	Parallel	12411	776	1,06E+11	6,19E+13	6,20E+13	5,00E+09	5,42E+13	y5	0,873
Total height	395,0	mm							EIeff	Ieff	***EIeff***		
Zs	261,3	mm							1,62E+14	1,62E+10	***1,41E+14***		

V

447994,0	217665,1	0,0	0,0	0,0	
-378839,3	-360639,1	426870,9	0,0	0,0	
0,0	138870,9	-866354,2	714870,9	0,0	
0,0	0,0	426870,9	########	1002870,9	
0,0	0,0	0,0	714870,9	-1032501,8	

S

596504,3	
-308504,3	
0,0	
0,0	
-288000,0	

C1,2	6448,7
C2,3	4114,3
C3,4	4114,3
C4,5	4114,3

D1	1177,2
D2	121,6
D3	121,6
D4	121,6
D5	121,6

1,1E-05	1,0E-05	9,2E-06	8,7E-06	8,5E-06	0,853
-1,7E-05	-2,1E-05	-1,9E-05	-1,8E-05	-1,7E-05	0,985
-5,2E-06	-6,2E-06	-7,9E-06	-7,4E-06	-7,2E-06	0,866
-2,9E-06	-3,5E-06	-4,4E-06	-5,5E-06	-5,4E-06	0,859
-2,0E-06	-2,4E-06	-3,1E-06	-3,8E-06	-4,7E-06	0,873

a1	58,7
a2	-33,8
a3	-103,8
a4	-173,8
a5	-243,8

Appendix B

Numerical results of the shear tests

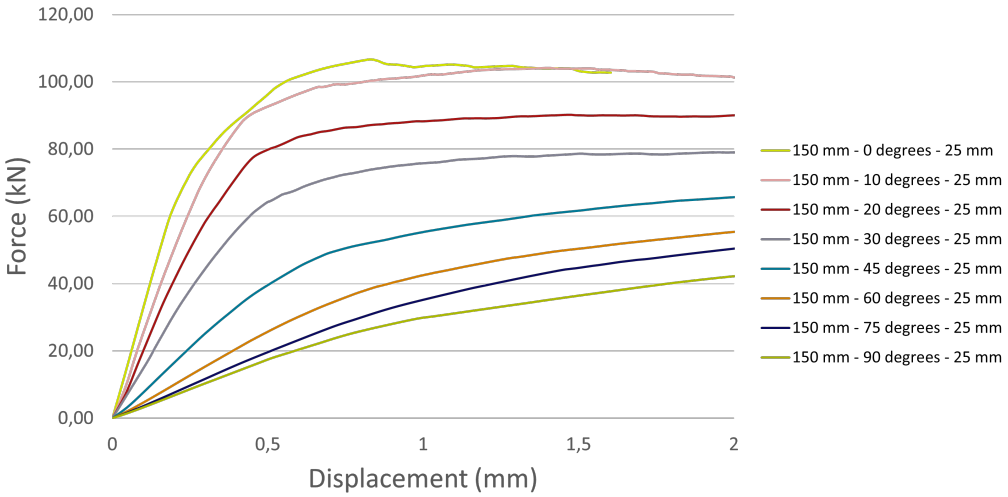

(a) Force Displacement diagram of the notch depth of 25 mm

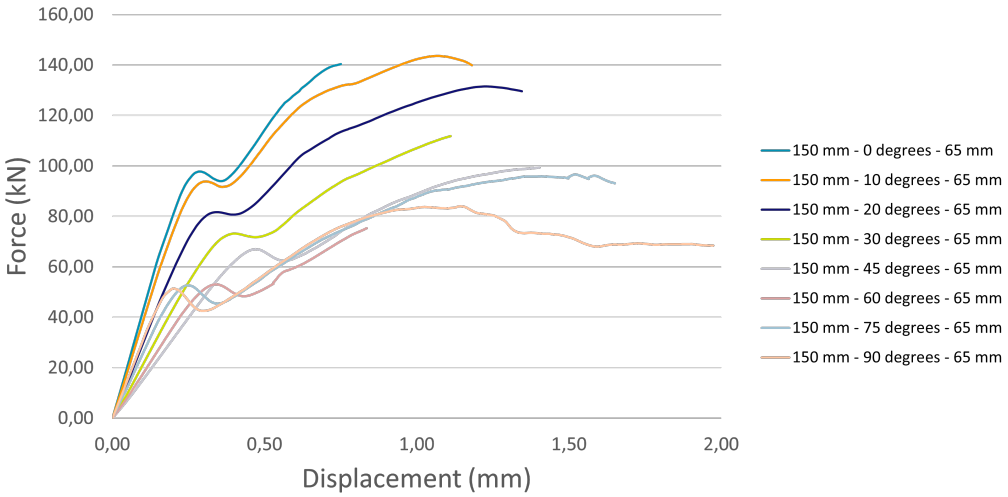

(b) Force Displacement diagram of the notch depth of 65 mm

Figure B.1: Force Displacement of the notch shear tests. (a) shows the different angles of a notch depth of 25 mm. (b) shows the different angles for a notch depth of 65 mm.

Appendix C

Results of comparison Gamma method with the numerical model

Specimen	CLT Layers	Strength	TCC	Deformation	q load	length	Calculated Stiffness	Opmerking	Seperated gamma method	%	Combined gamma method	%
1	5	Parallel	0	19,23	2,29	6300	2,445E+12	Without concrete	2,41E+12	98,5%	2,41E+12	98,5%
1b	5	Parallel	0	63,91	2,29	6300	7,357E+11	Other direction	6,71E+11	91,3%	6,71E+11	91,3%
2	5	Parallel	60	8,64	3,10	6300	7,363E+12	With 60mm concrete	7,94E+12	107,8%	7,237E+12	98,3%
3	5	Parallel	60	8,97	3,10	6300	7,086E+12	Smaller notch	7,56E+12	106,7%	6,892E+12	97,3%
4	5	Perpendicular	60	13,75	3,10	6300	4,624E+12	Other direction	4,92E+12	106,3%	4,793E+12	103,6%
5	5	Parallel	80	7,74	3,37	6300	8,932E+12	With 80mm concrete	9,72E+12	108,8%	8,837E+12	98,9%
6	5	Parallel	80	8,05	3,37	6300	8,586E+12	Smaller notch	9,26E+12	107,8%	8,501E+12	99,0%
7	5	Perpendicular	80	11,75	3,37	6300	5,883E+12	Other direction	6,45E+12	109,7%	6,172E+12	104,9%
									Seperated gamma method	%	Combined gamma method	%
8	3	Parallel	0	65,64	2,09	6300	6,531E+11	Without concrete	6,61E+11	101,2%	6,61E+11	101,2%
9	3	Parallel	60	21,83	2,90	6300	2,725E+12	With 60mm concrete	2,92E+12	107,0%	2,813E+12	103,2%
10	3	Parallel	60	22,34	2,90	6300	2,663E+12	Smaller notch	2,78E+12	104,3%	2,679E+12	100,6%
12	3	Parallel	80	17,70	3,17	6300	3,674E+12	With 80mm concrete	4,08E+12	111,1%	3,938E+12	107,2%
13	3	Parallel	80	18,04	3,17	6300	3,604E+12	Smaller notch	3,89E+12	107,9%	3,750E+12	104,1%

Appendix D

Abaqus results for the point supported TCC floor slabs

D.1 Different notch depth

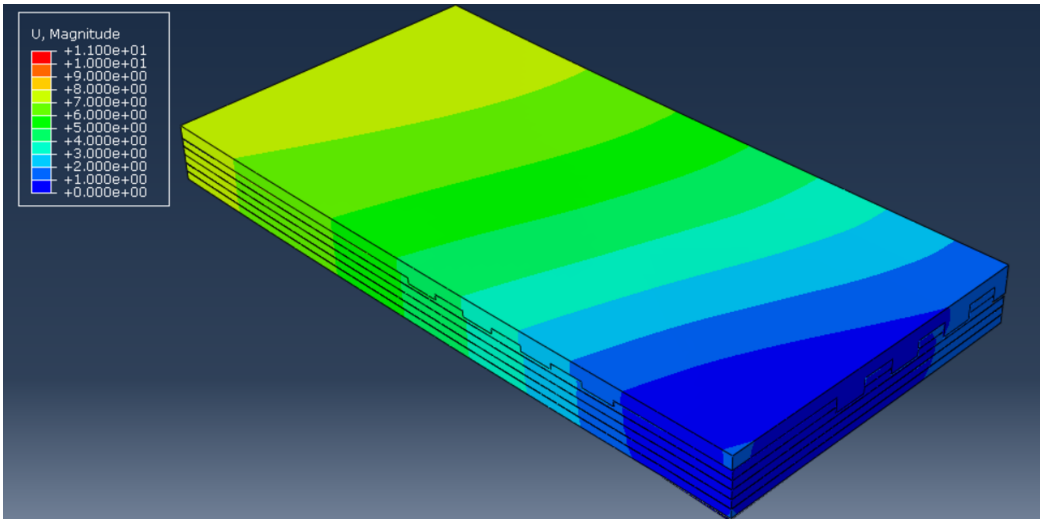

Figure D.1: Deformation of the TCC floor slab with different notch depths

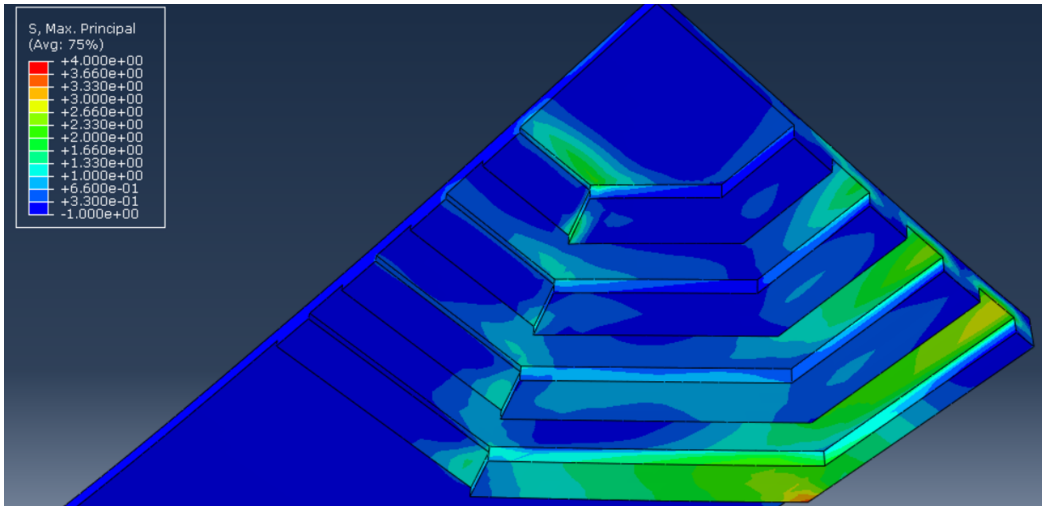

(a) Principal stresses in the concrete slab

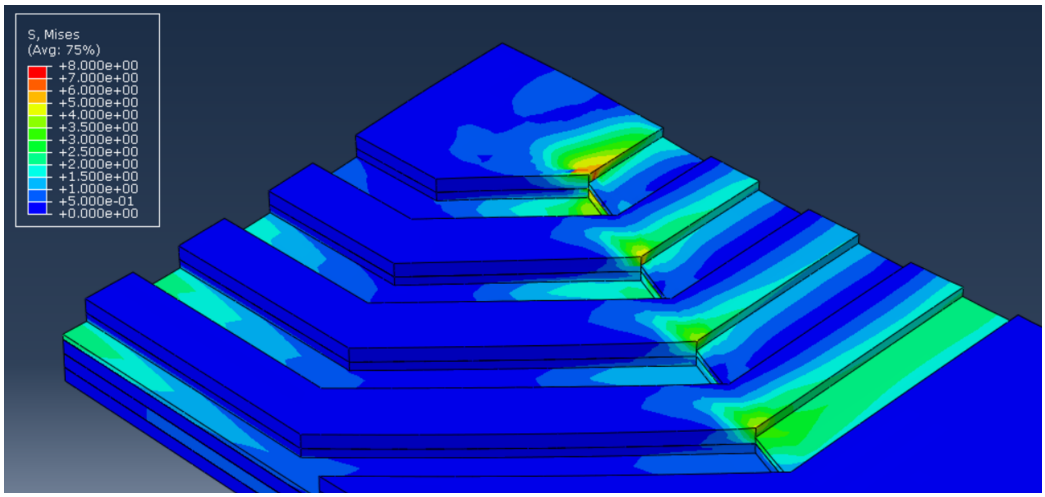

(b) Von Mises stresses in the CLT

Figure D.2: Principal and von Mises stresses in the concrete and CLT slab

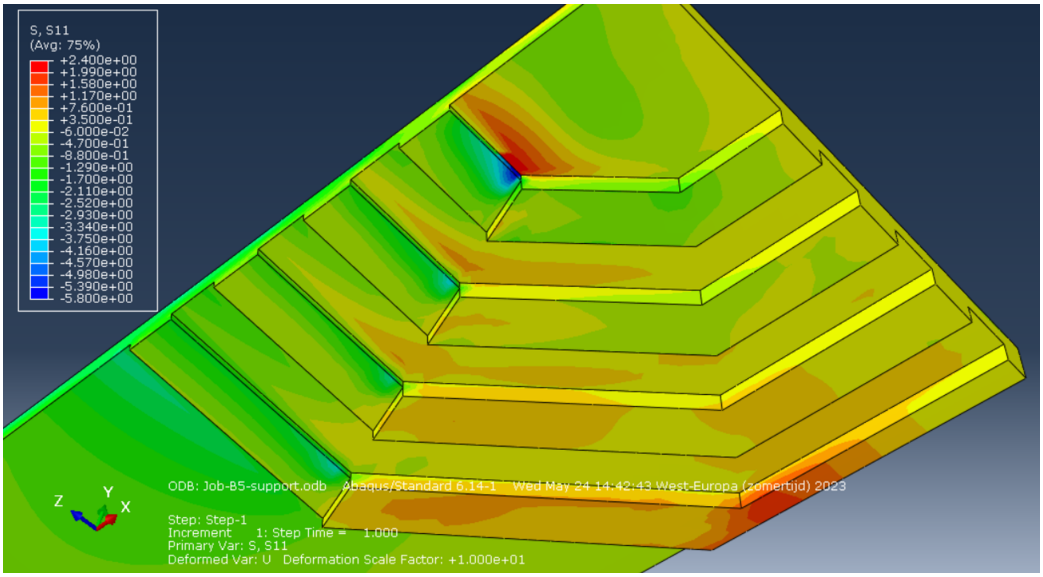

(a) S11 stresses, main direction of the material, in the concrete slab

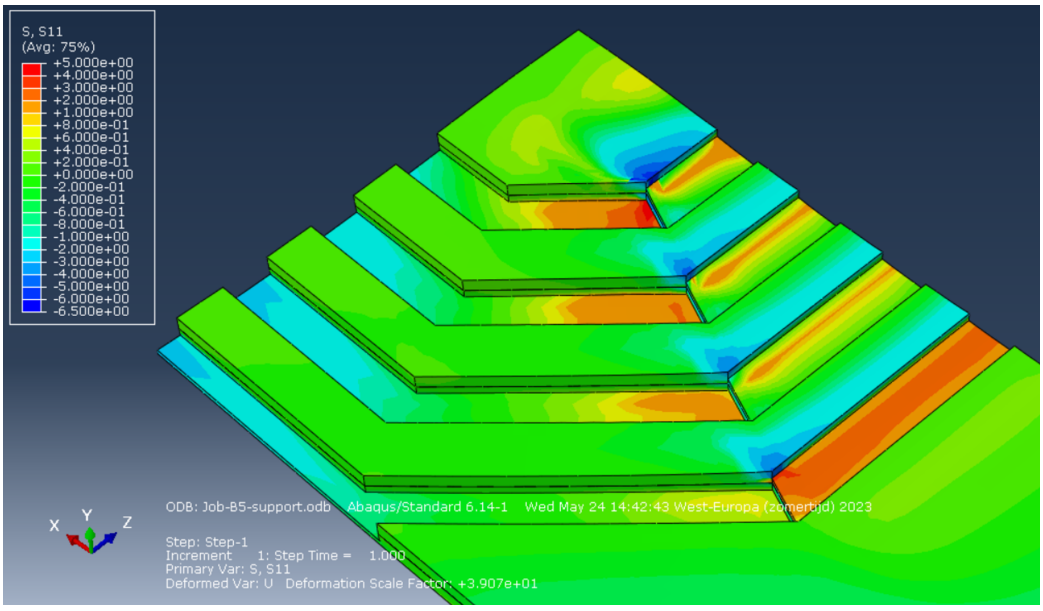

(b) S11 stresses, main direction of the material, in the CLT

Figure D.3: S11 stresses in the concrete and CLT slab

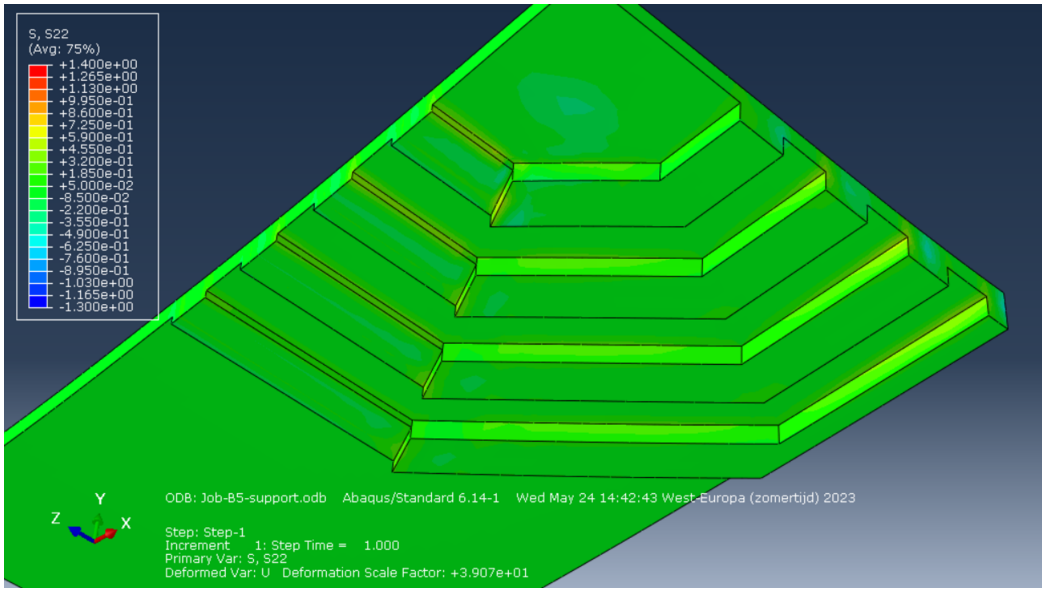

(a) S22 stresses in the concrete slab

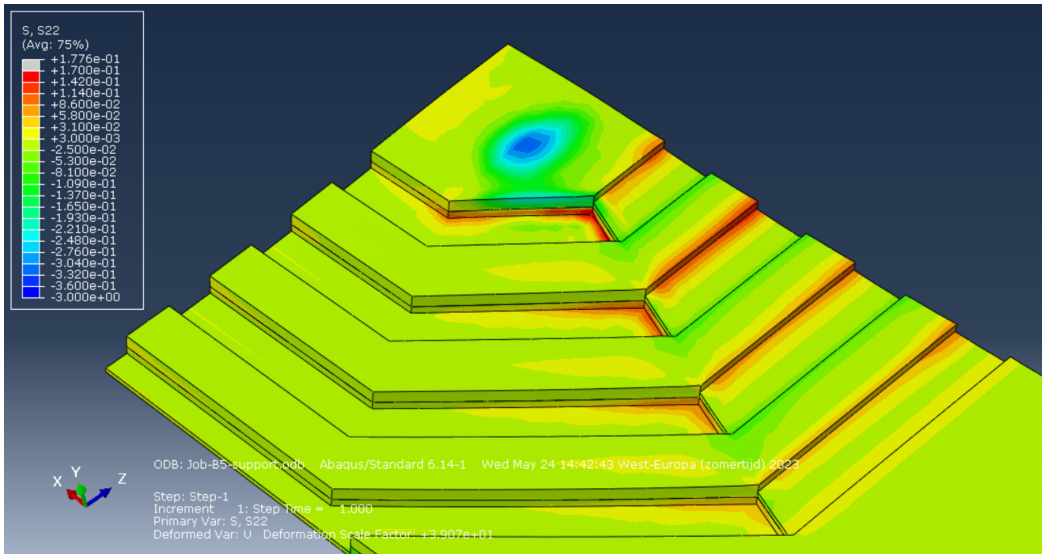

(b) S22 stresses in the CLT

Figure D.4: S22 stresses in the concrete and CLT slab

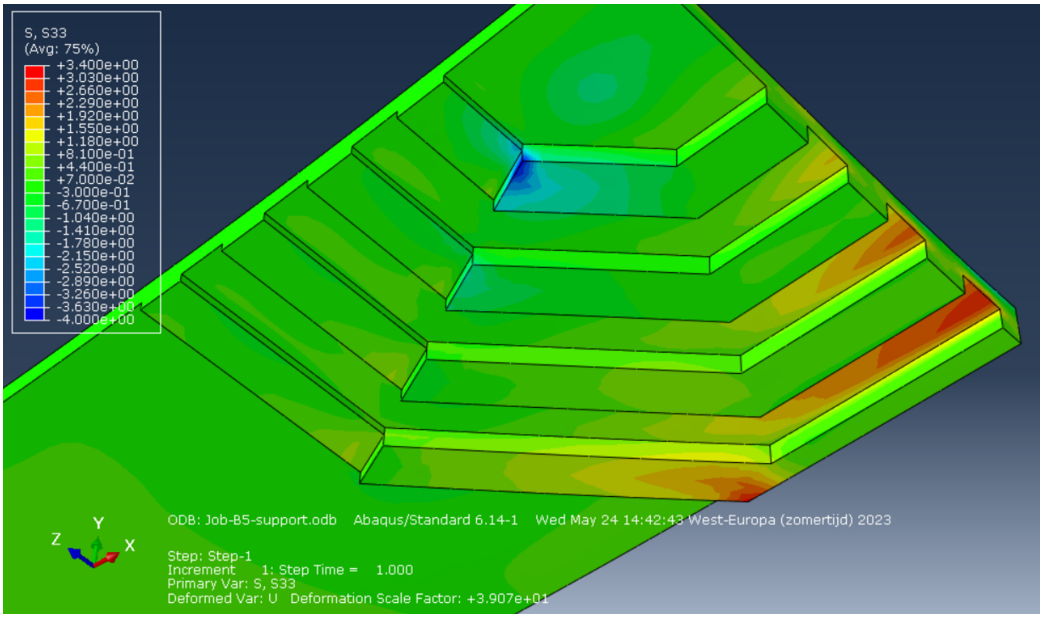

(a) S33 stresses, weakest direction of the material, in the concrete slab

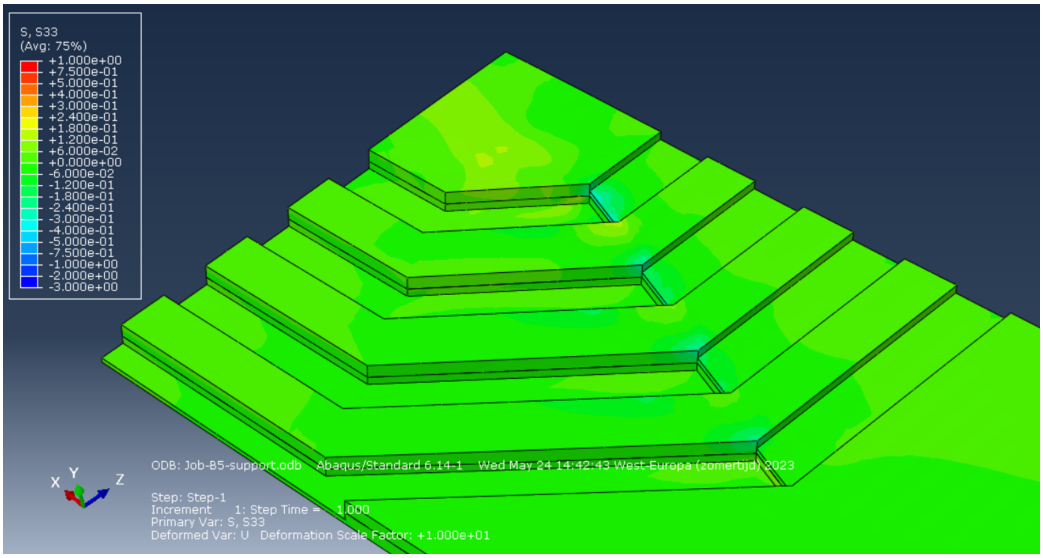

(b) S33 stresses, weakest direction of the material, in the CLT

Figure D.5: S33 stresses in the concrete and CLT slab

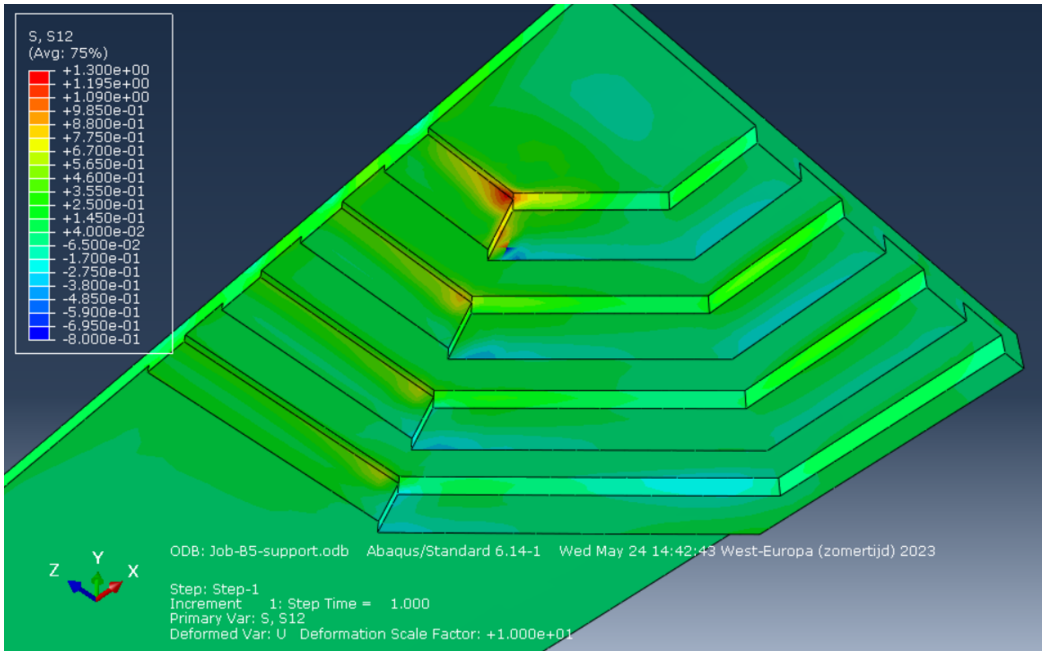

(a) S12 shear stresses, main direction of the material, in the concrete slab

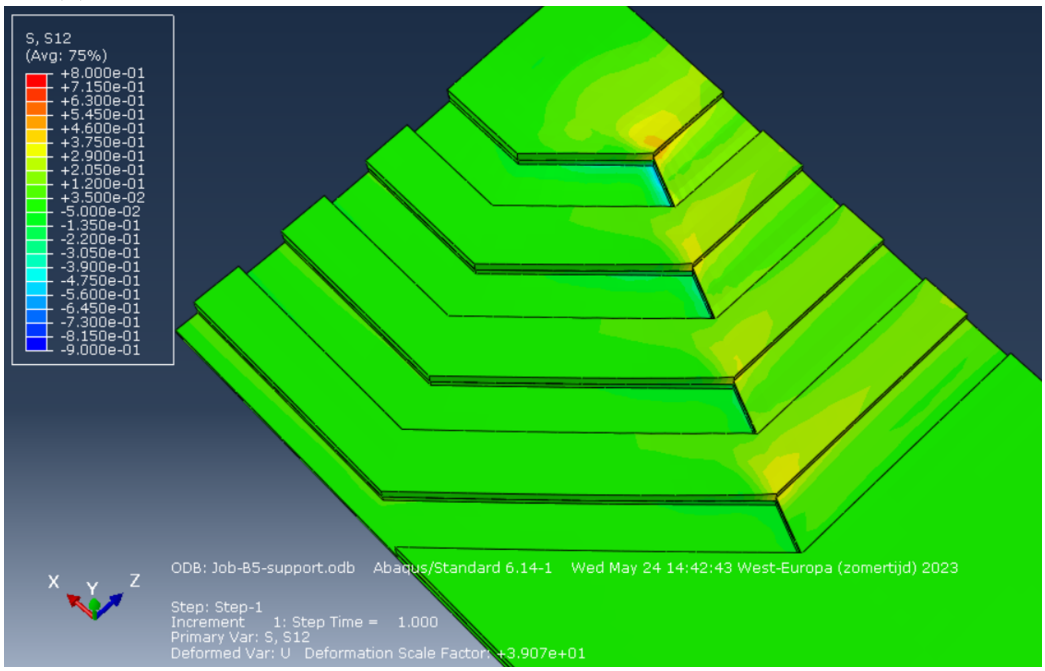

(b) S12 shear stresses, main direction of the material, in the CLT

Figure D.6: S12 shear stresses in the concrete and CLT

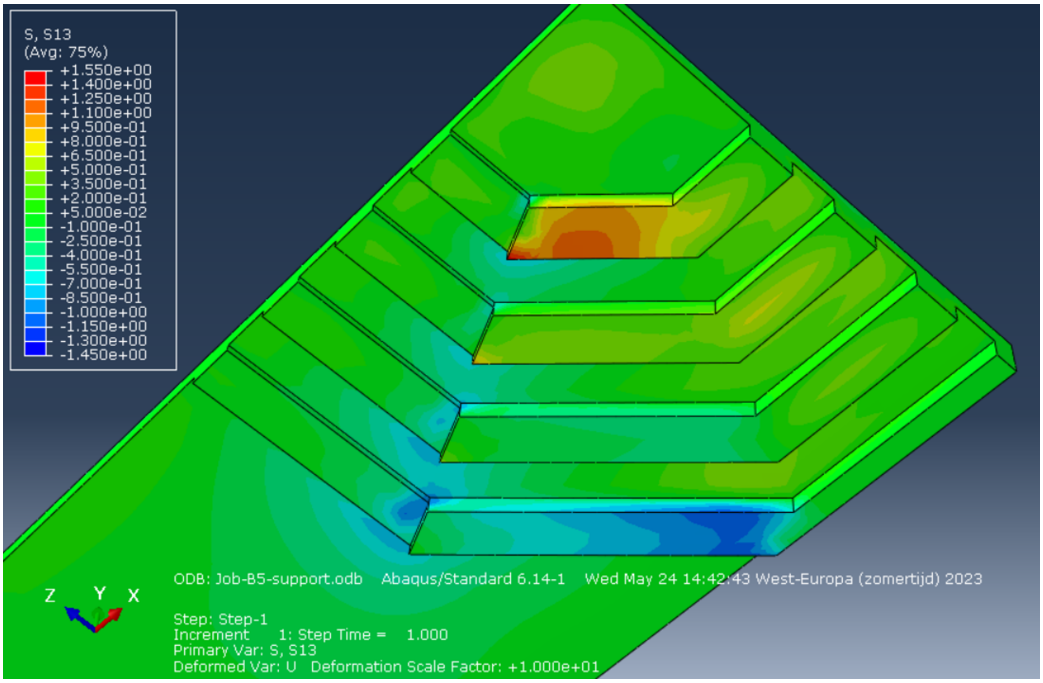

(a) S13 stresses in the concrete slab

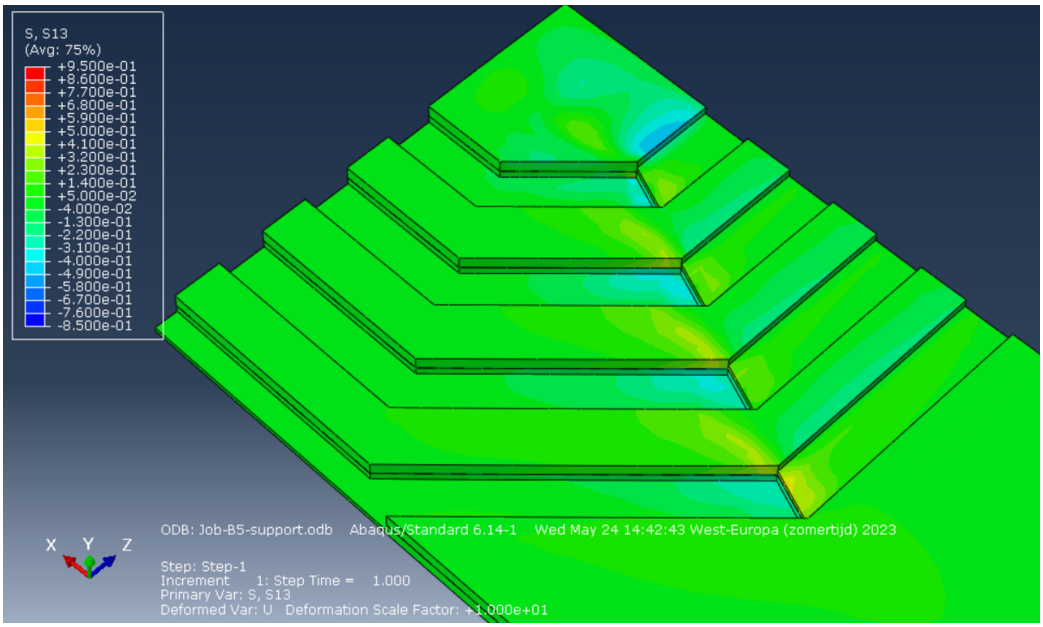

(b) S13 stresses in the CLT

Figure D.7: S13 shear stresses in the concrete and CLT

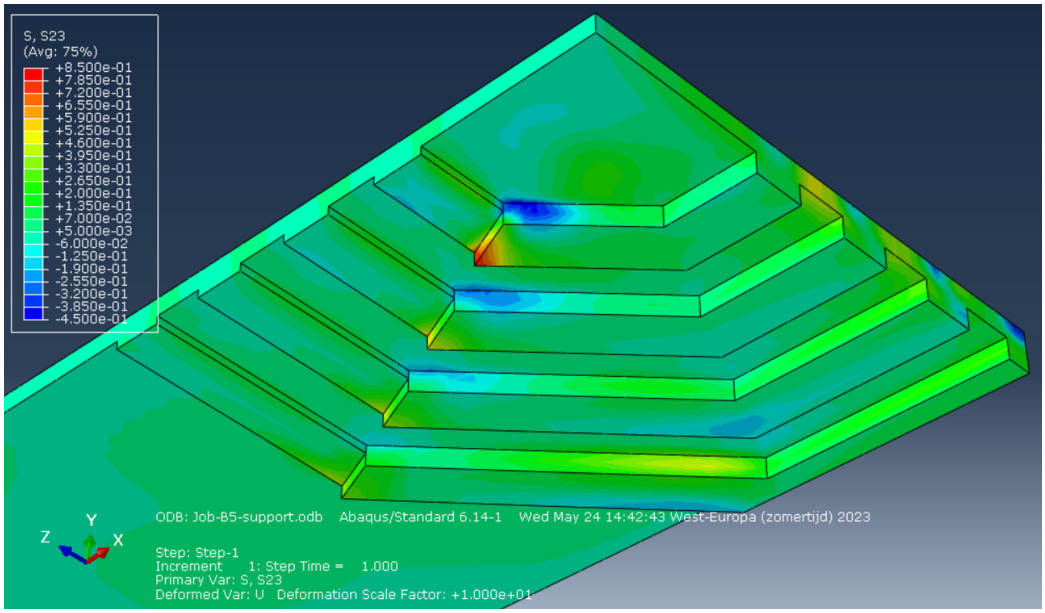

(a) S23 stresses in the concrete slab

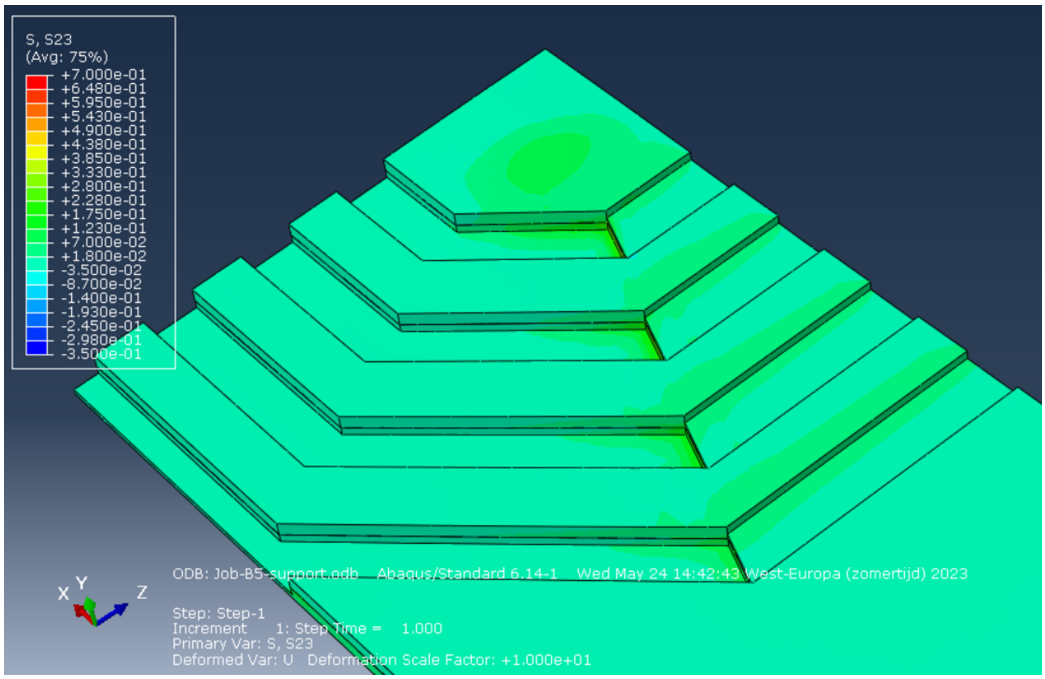

(b) S23 stresses in the CLT

Figure D.8: S13 shear stresses in the concrete and CLT

D.2 Same notch depth

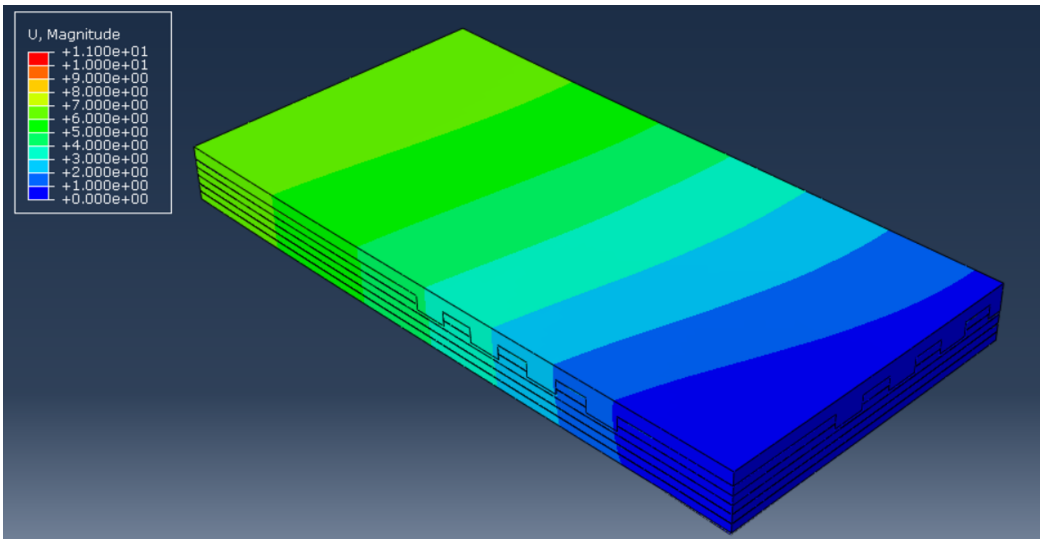

Figure D.9: Deformation of the TCC floor slab with same notch depths

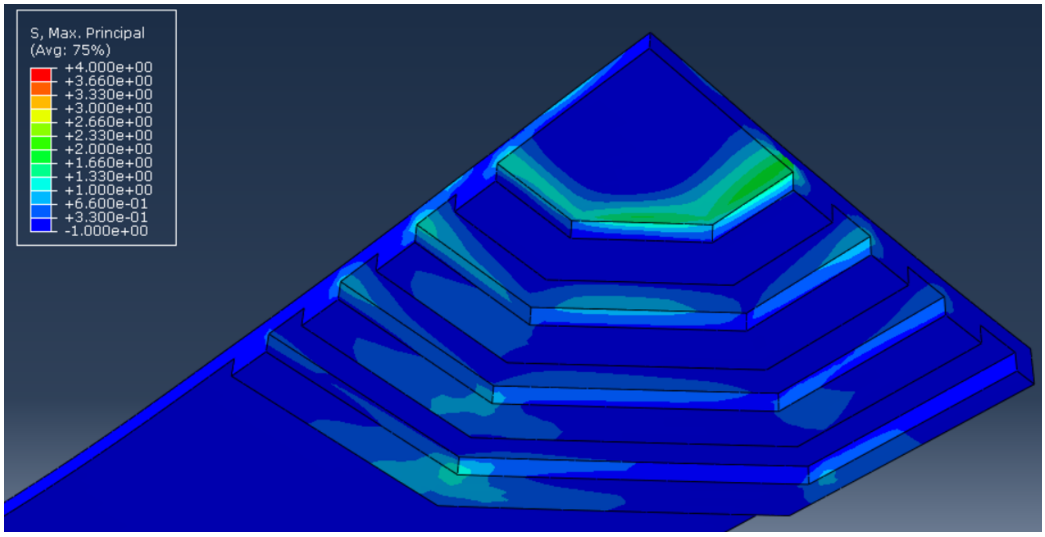

(a) Principal stresses in the concrete slab

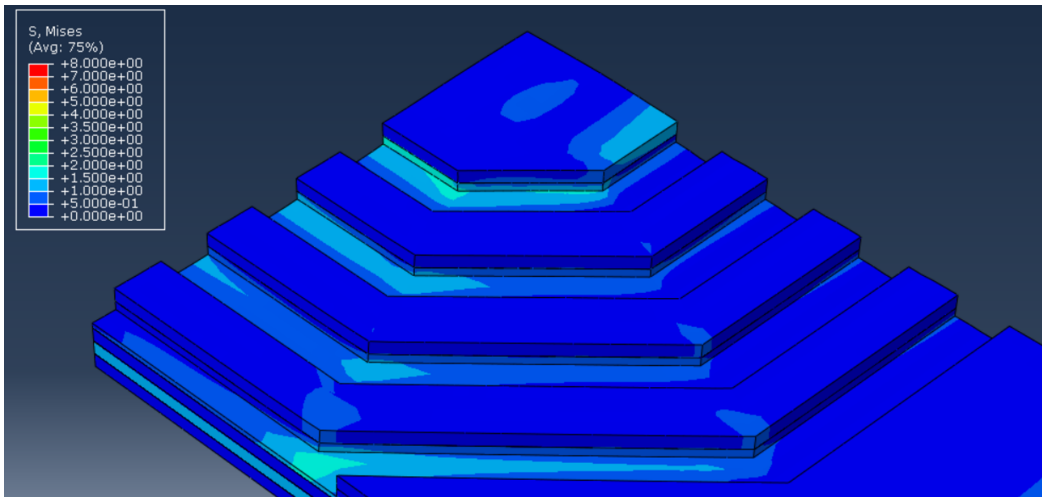

(b) Von Mises stresses in the CLT

Figure D.10: Principal and von Mises stresses in the concrete and CLT slab

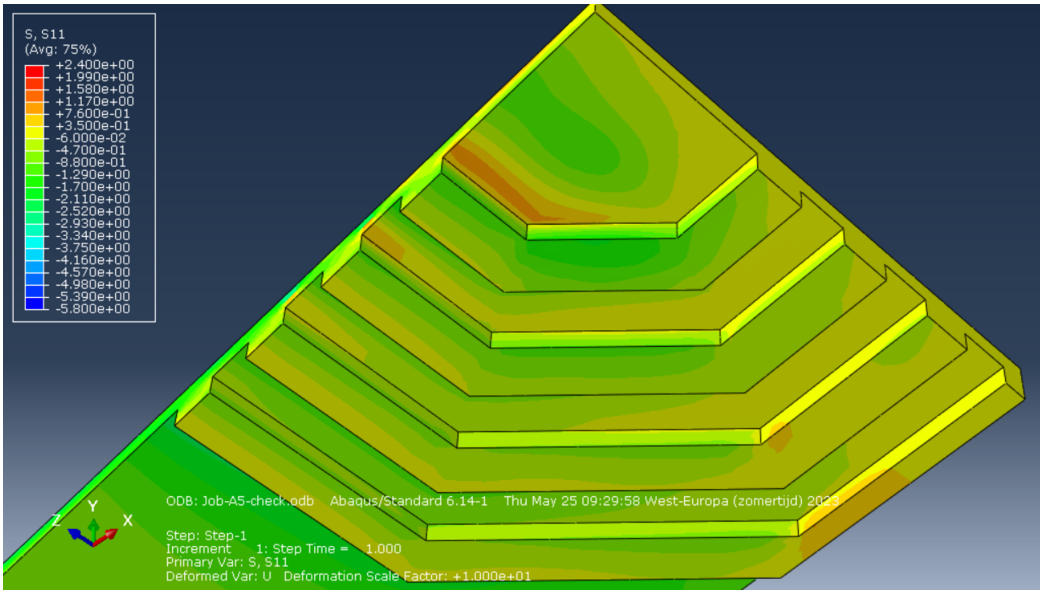

(a) S11 stresses, main direction of the material, in the concrete slab

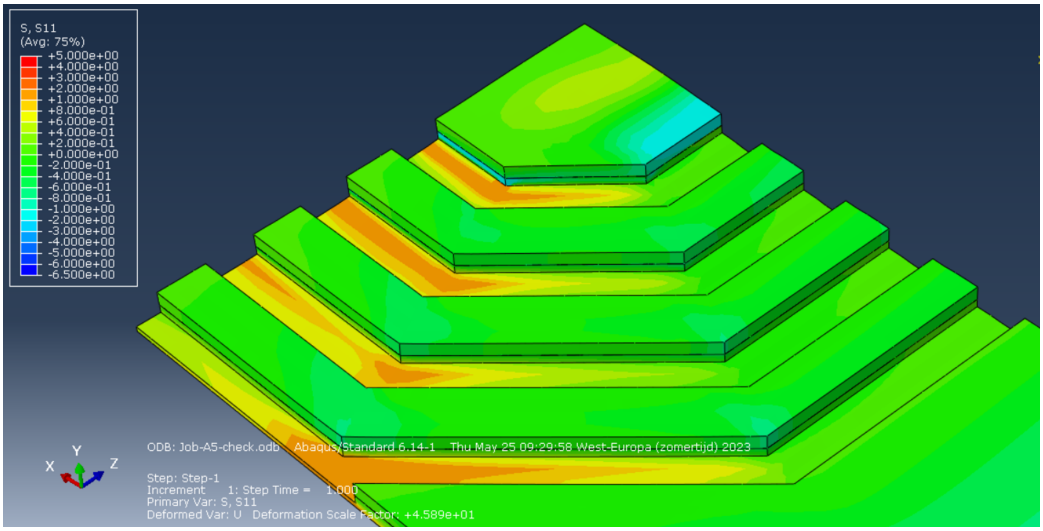

(b) S11 stresses, main direction of the material, in the CLT

Figure D.11: S11 stresses in the concrete and CLT slab

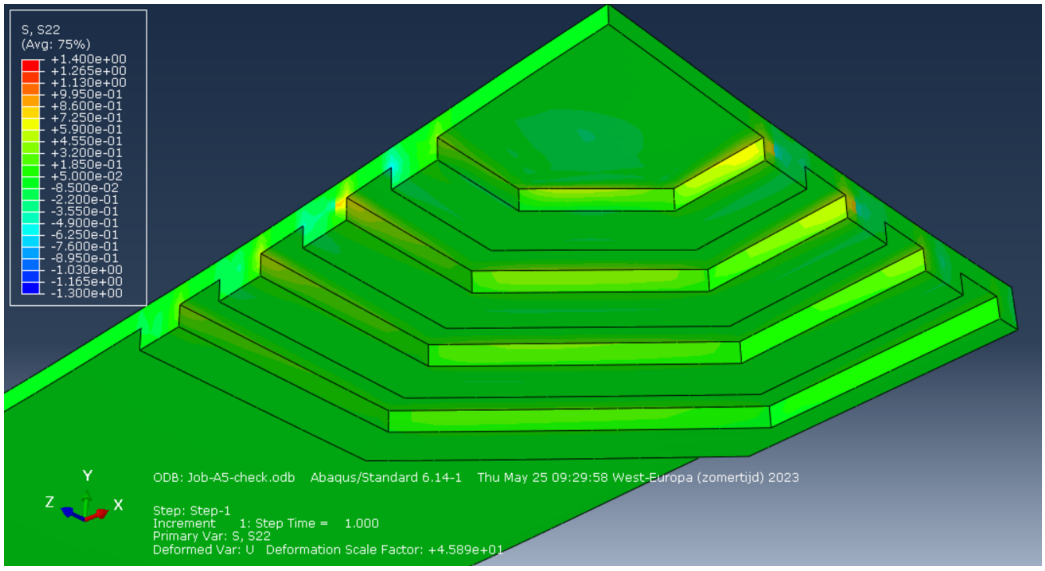

(a) S22 stresses in the concrete slab

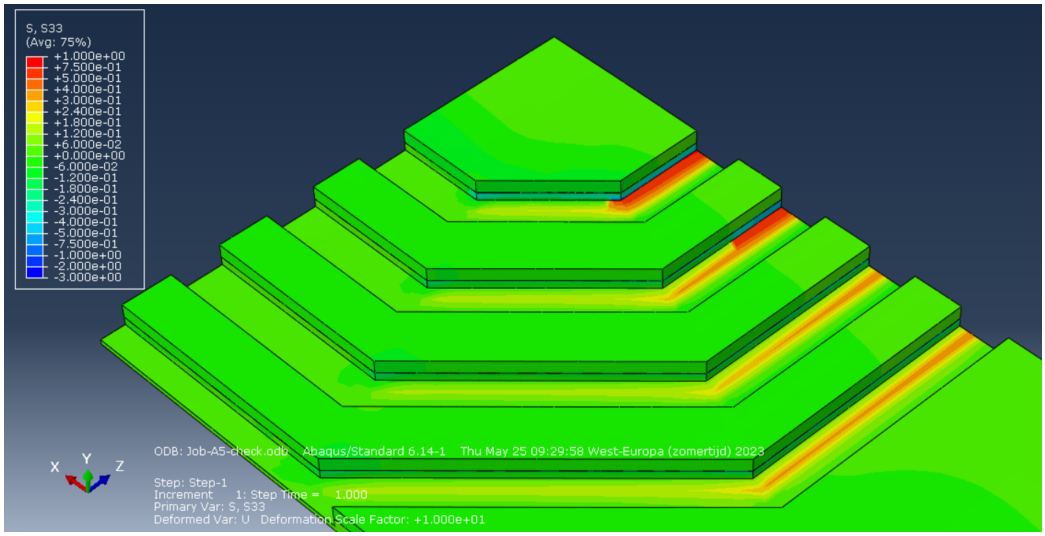

(b) S22 stresses in the CLT

Figure D.12: S22 stresses in the concrete and CLT slab

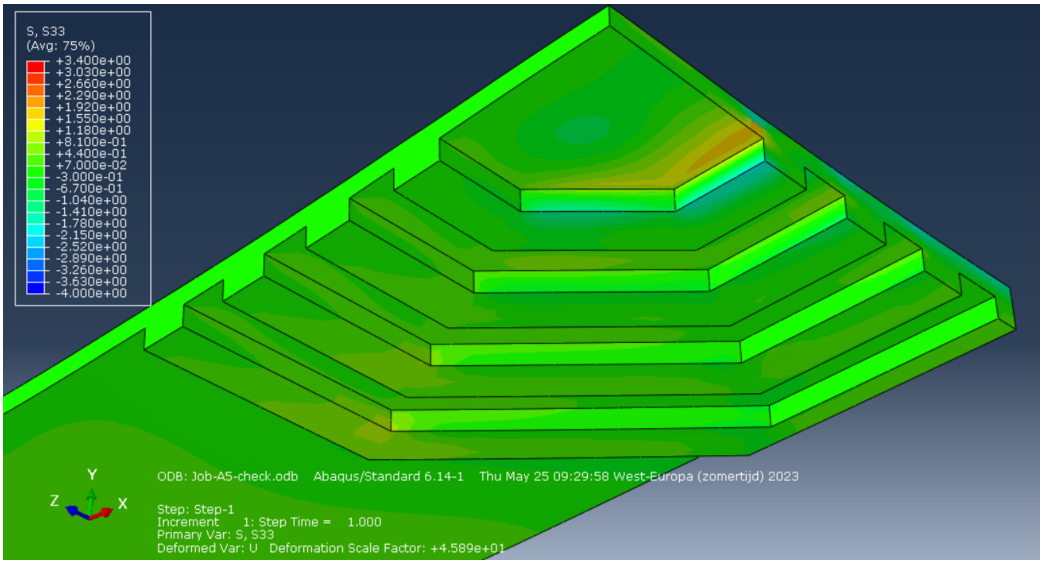

(a) S33 stresses, weakest direction of the material, in the concrete slab

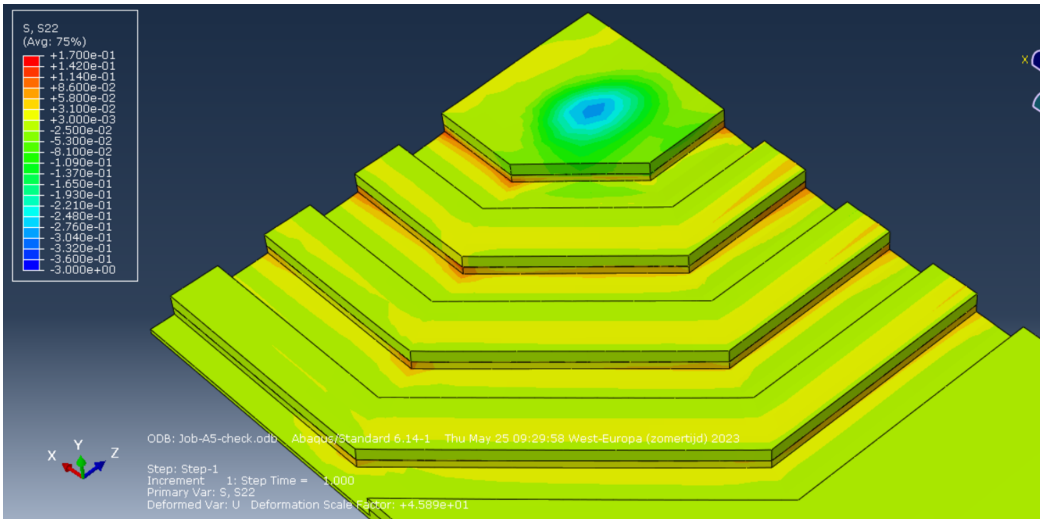

(b) S33 stresses, weakest direction of the material, in the CLT

Figure D.13: S33 stresses in the concrete and CLT slab

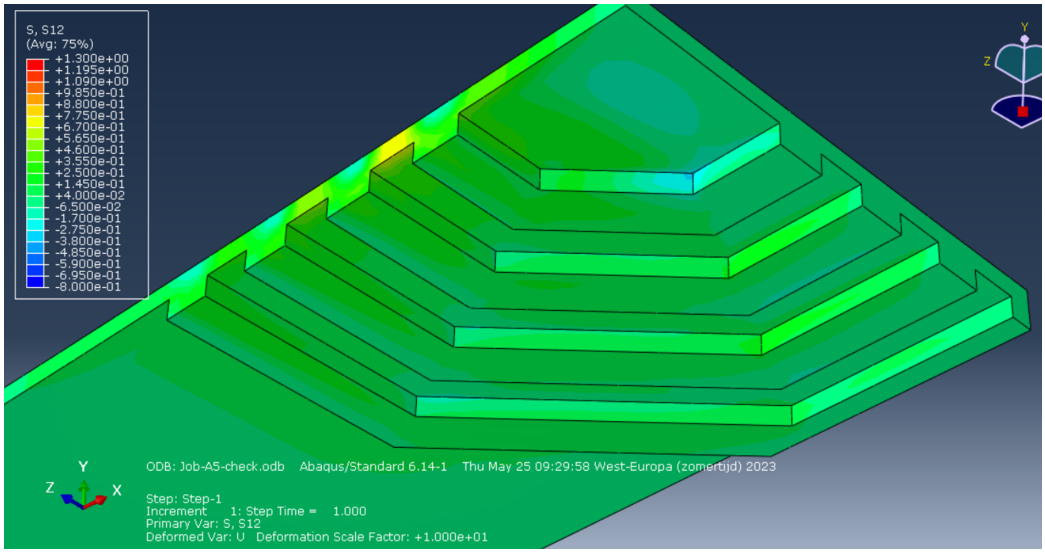

(a) S12 shear stresses, main direction of the material, in the concrete slab

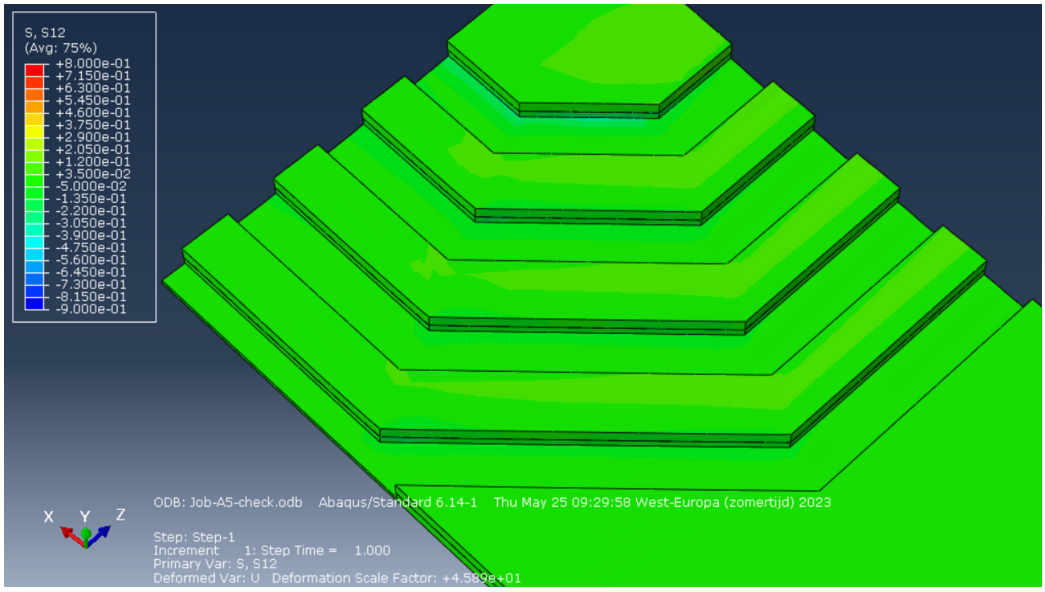

(b) S12 shear stresses, main direction of the material, in the CLT

Figure D.14: S12 shear stresses in the concrete and CLT

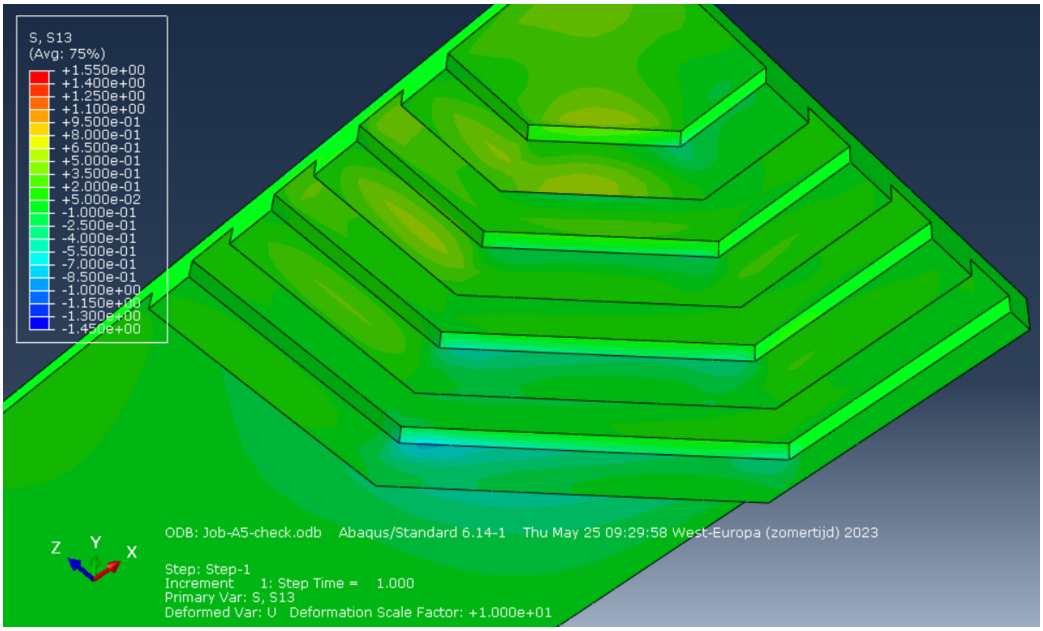

(a) S13 stresses in the concrete slab

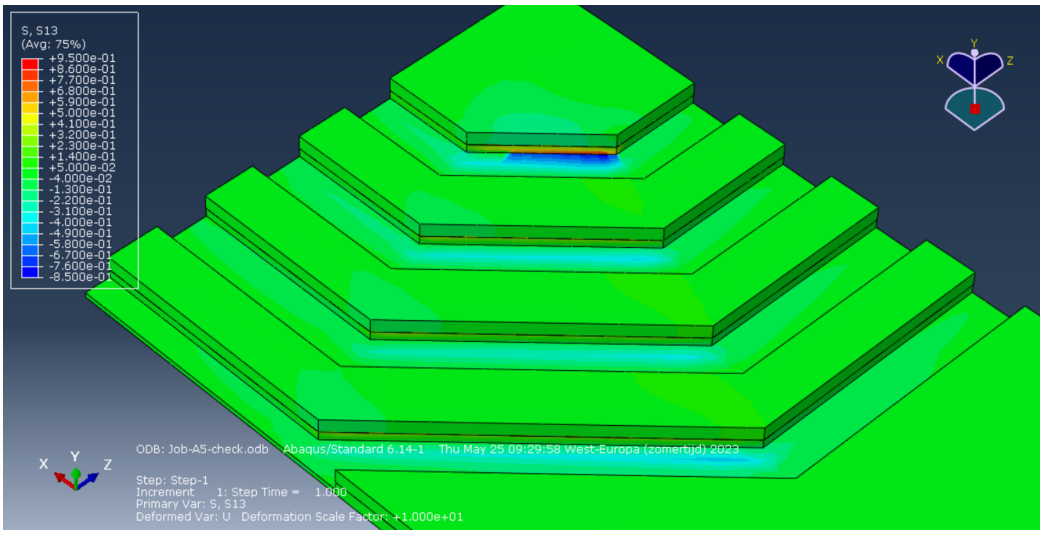

(b) S13 stresses in the CLT

Figure D.15: S13 shear stresses in the concrete and CLT

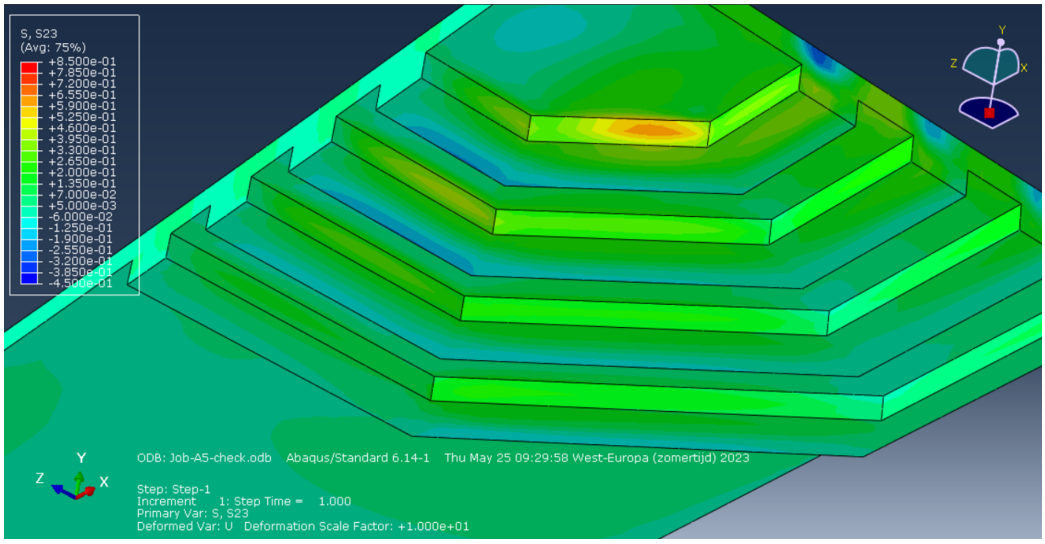

(a) S23 stresses in the concrete slab

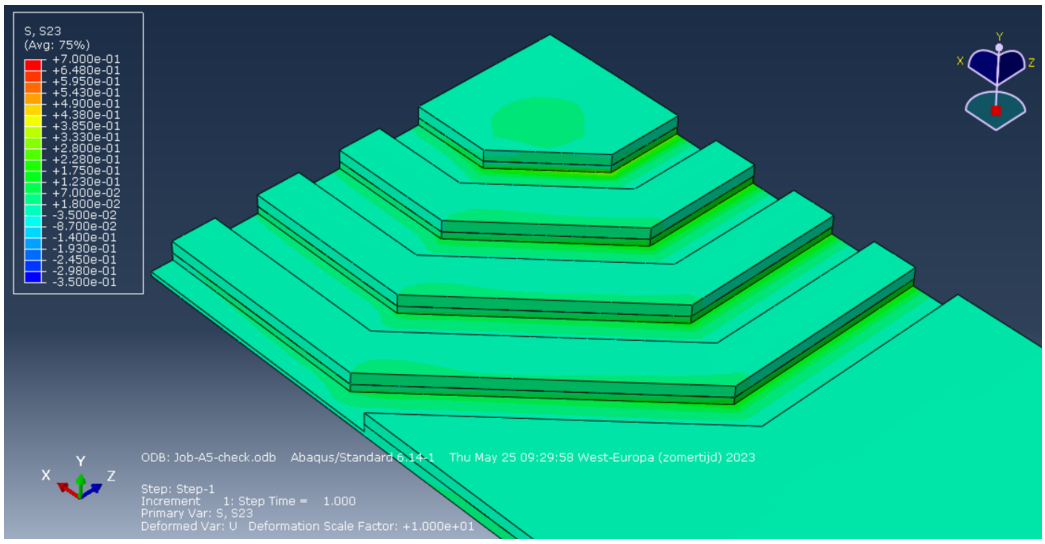

(b) S23 stresses in the CLT

Figure D.16: S23 shear stresses in the concrete and CLT

D.3 Line pattern

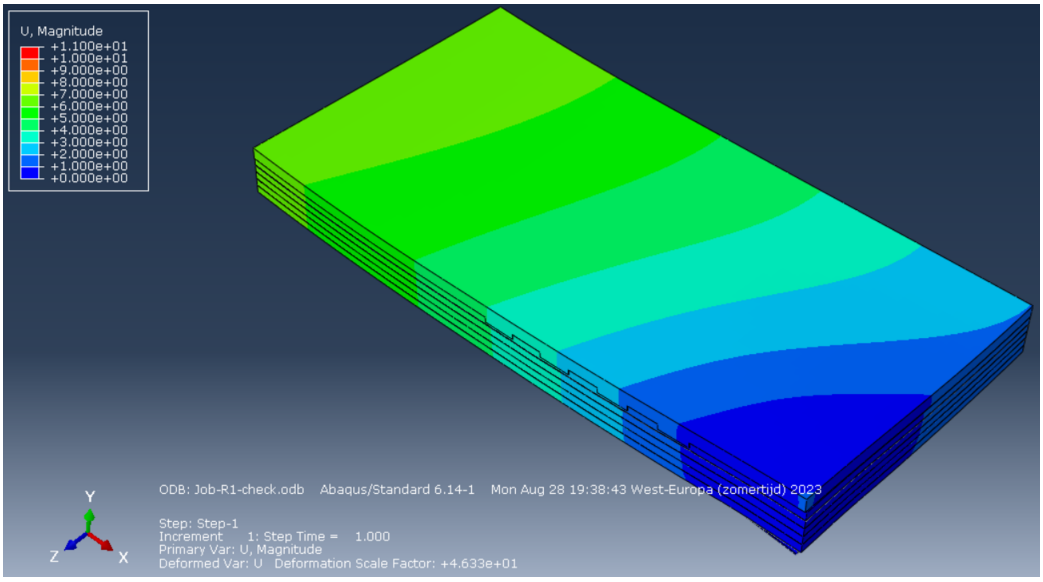

Figure D.17: Deformation of the TCC floor slab with line pattern notches

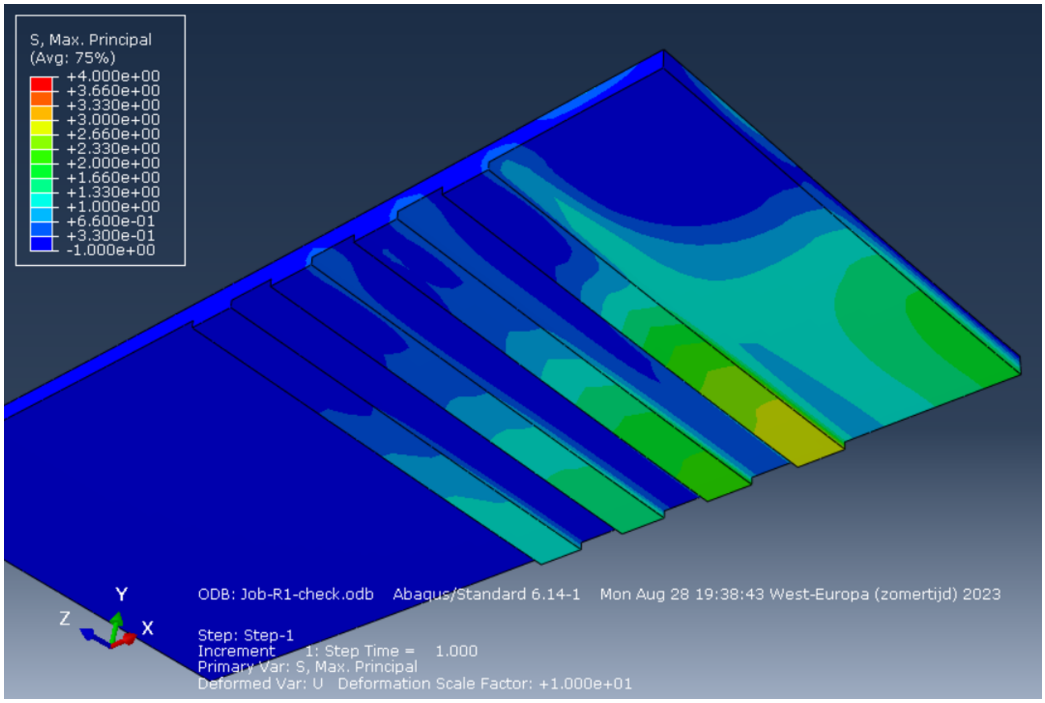

(a) Principal stresses in the concrete slab

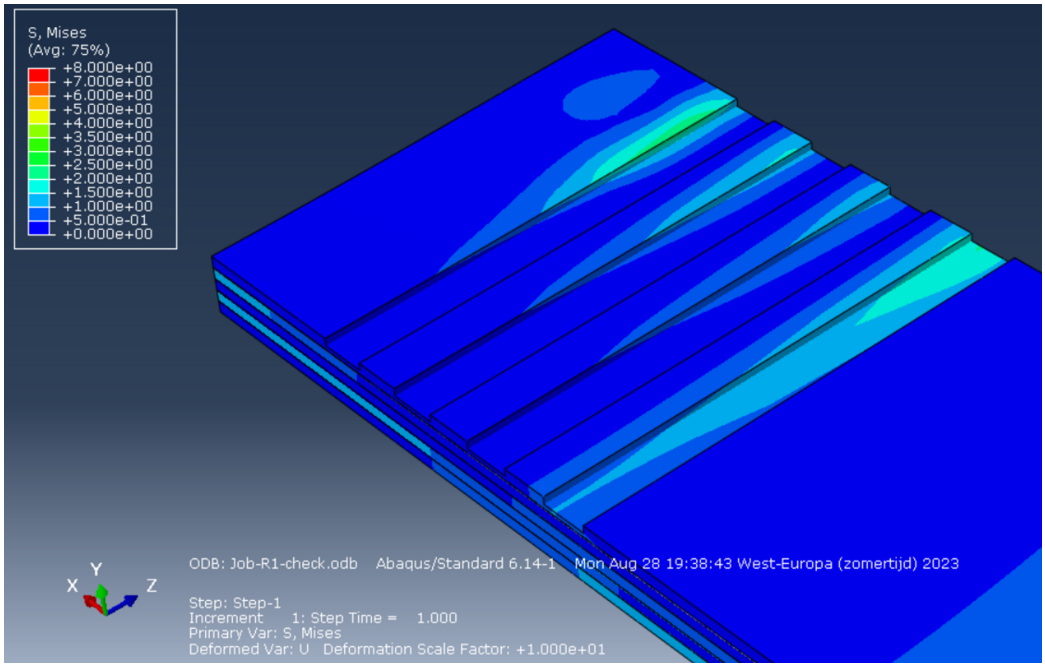

(b) Von Mises stresses in the CLT

Figure D.18: Principal and von Mises stresses in the concrete and CLT slab

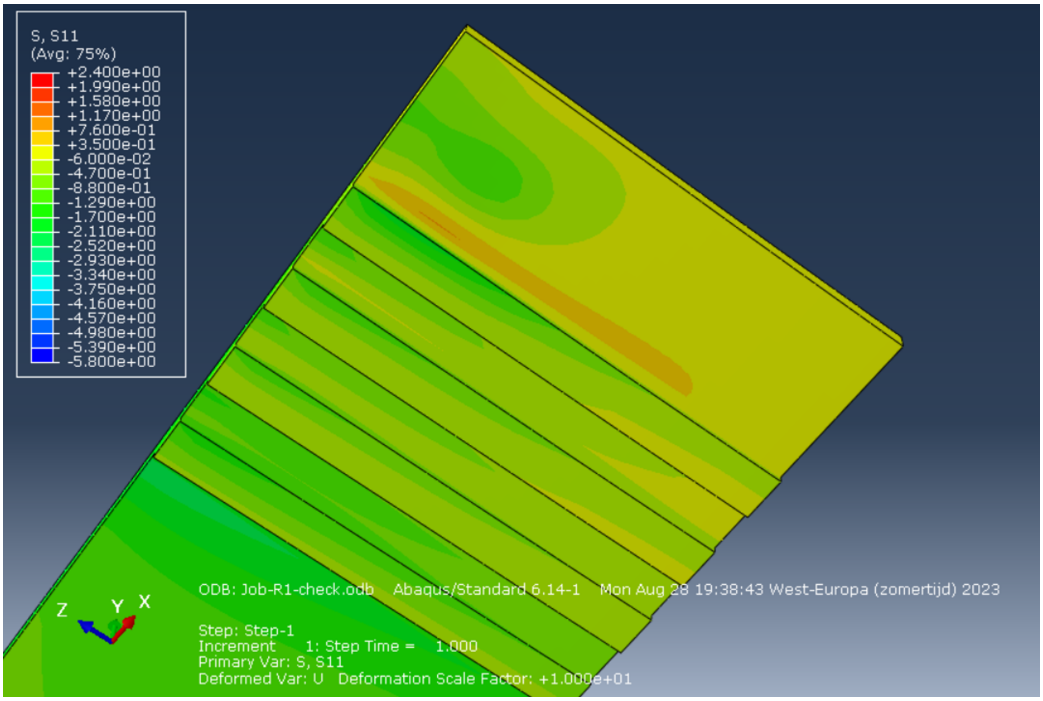

(a) S11 stresses, main direction of the material, in the concrete slab

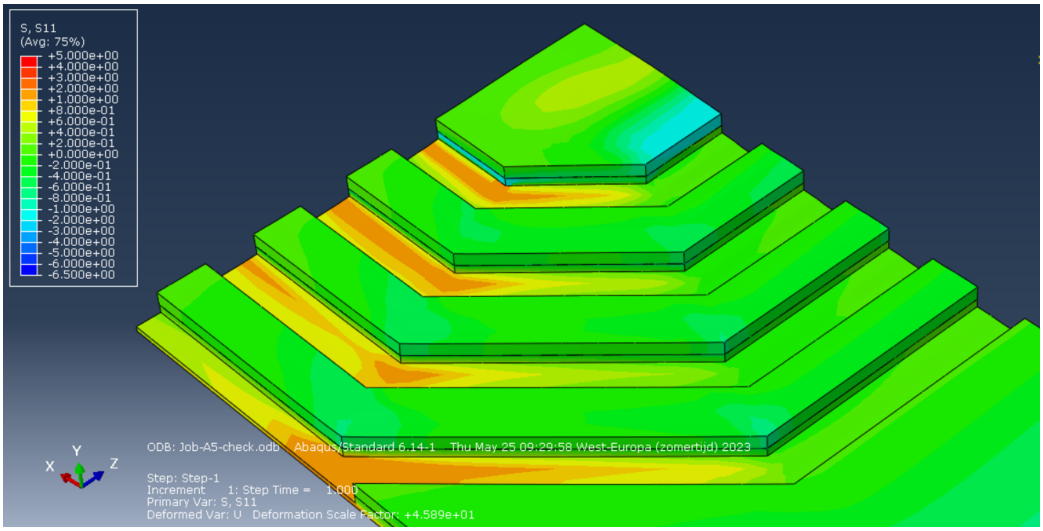

(b) S11 stresses, main direction of the material, in the CLT

Figure D.19: S11 stresses in the concrete and CLT slab

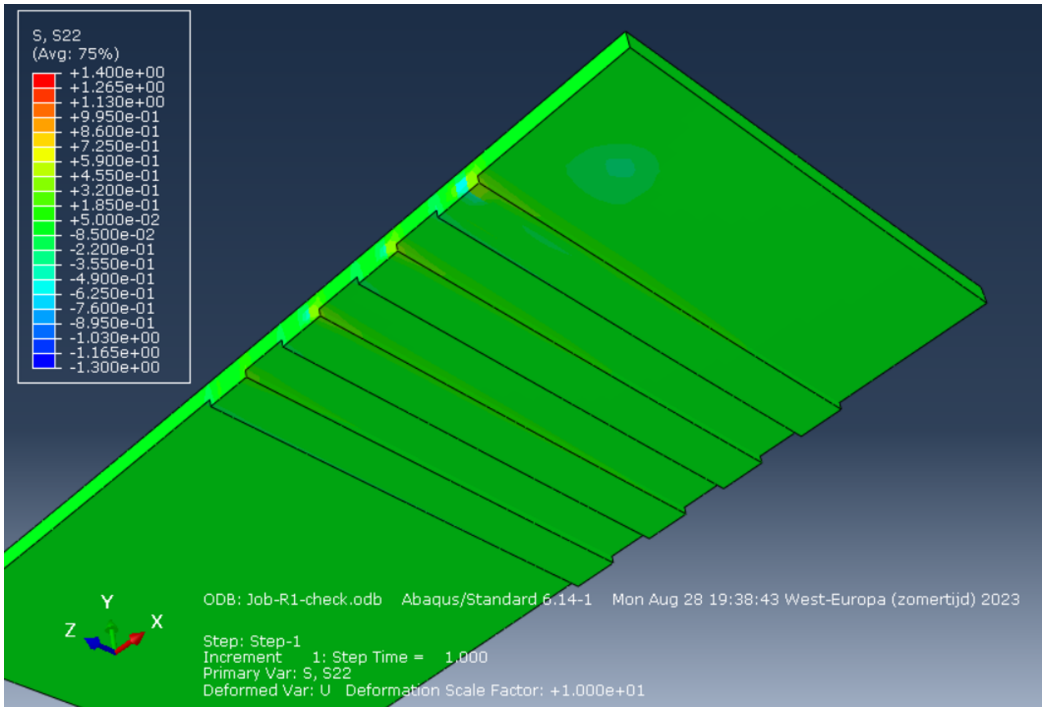

(a) S22 stresses in the concrete slab

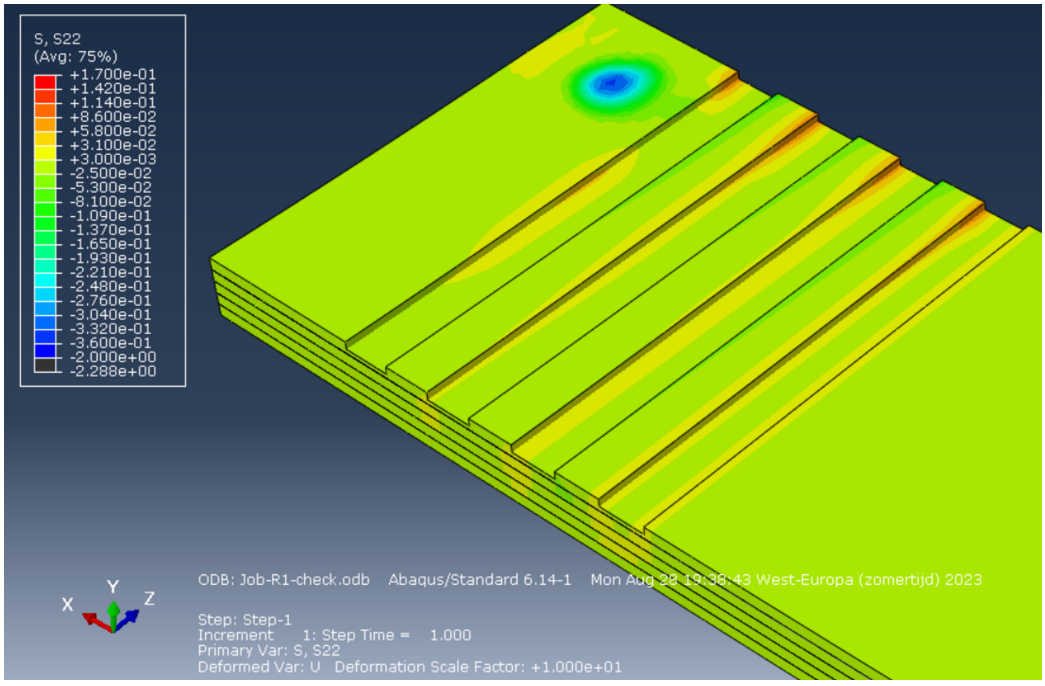

(b) S22 stresses in the CLT

Figure D.20: S22 stresses in the concrete and CLT slab

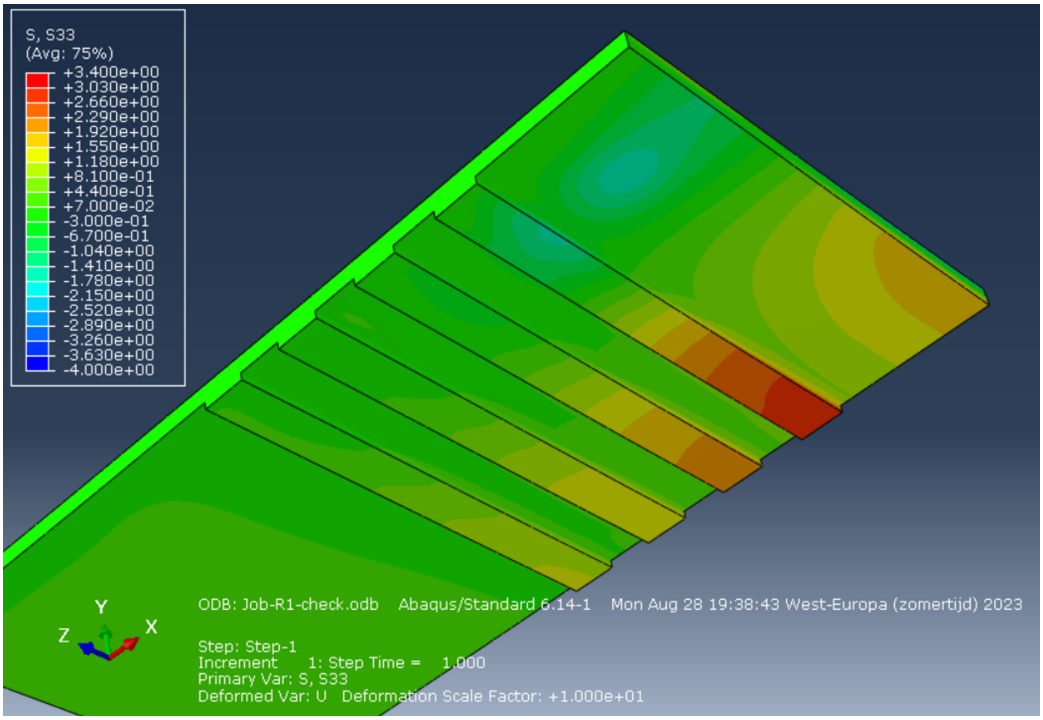

(a) S33 stresses, weakest direction of the material, in the concrete slab

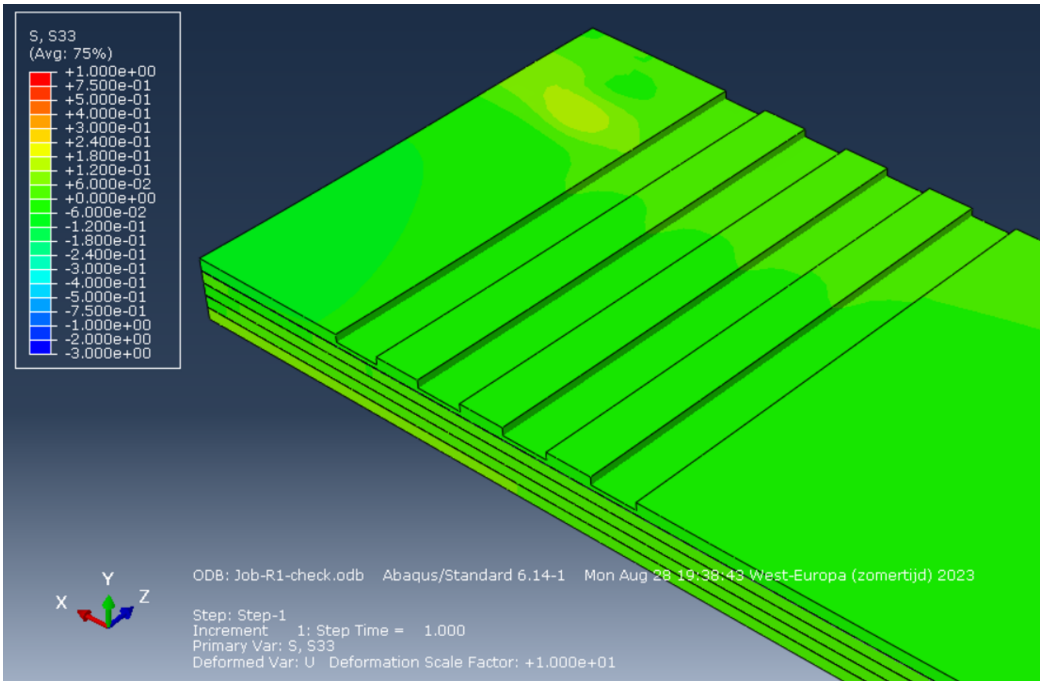

(b) S33 stresses, weakest direction of the material, in the CLT

Figure D.21: S33 stresses in the concrete and CLT slab

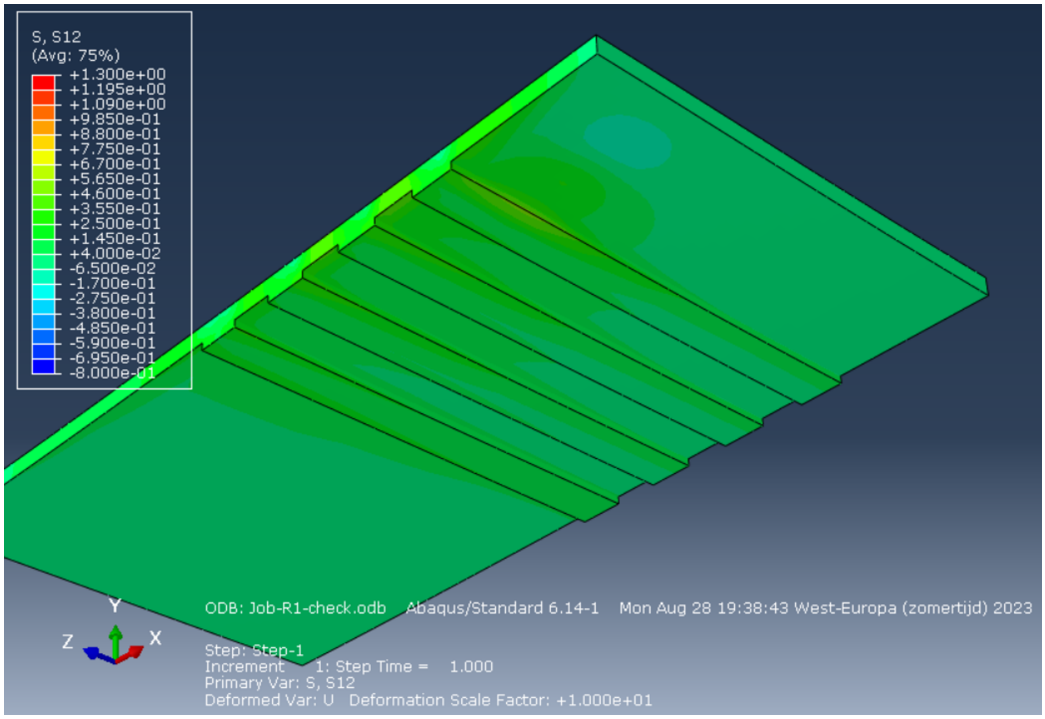

(a) S12 shear stresses, main direction of the material, in the concrete slab

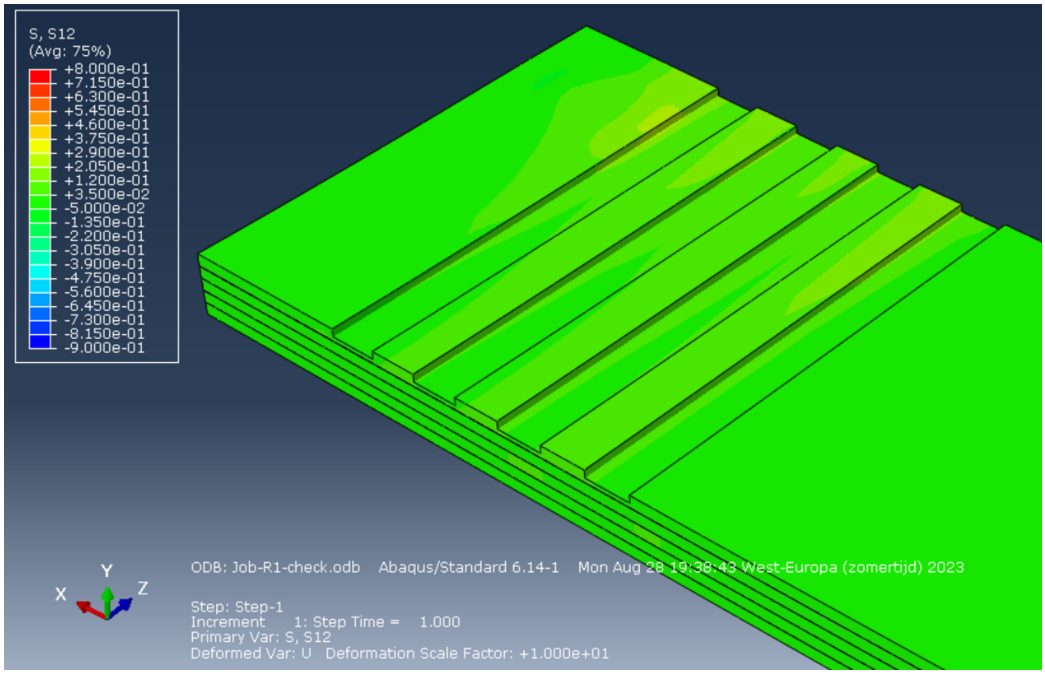

(b) S12 shear stresses, main direction of the material, in the CLT

Figure D.22: S12 shear stresses in the concrete and CLT

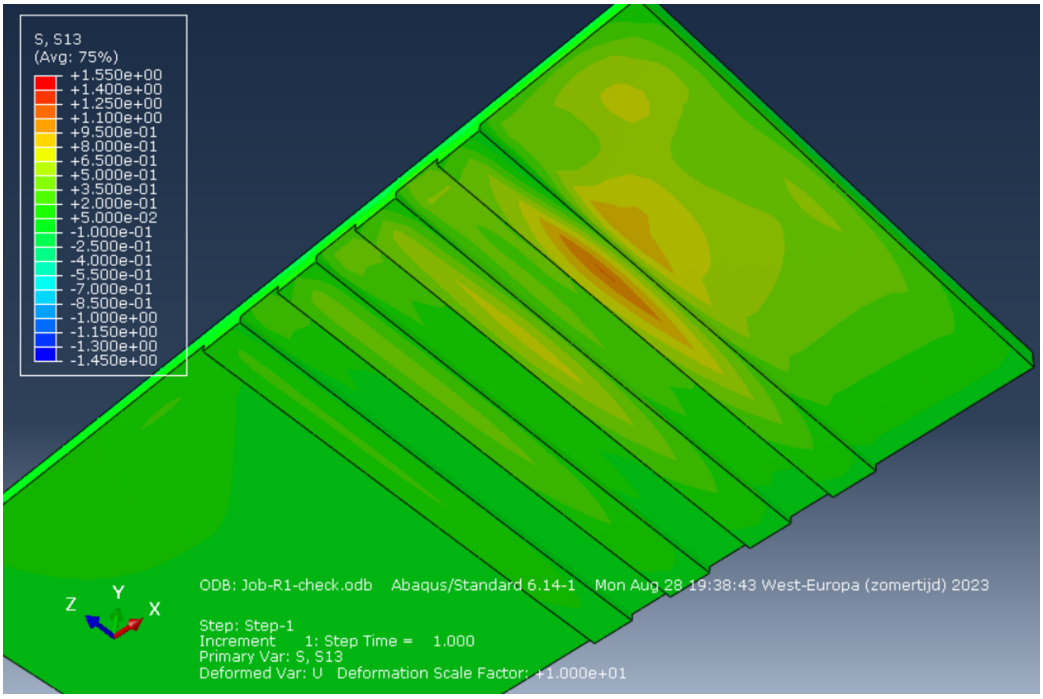

(a) S13 stresses in the concrete slab

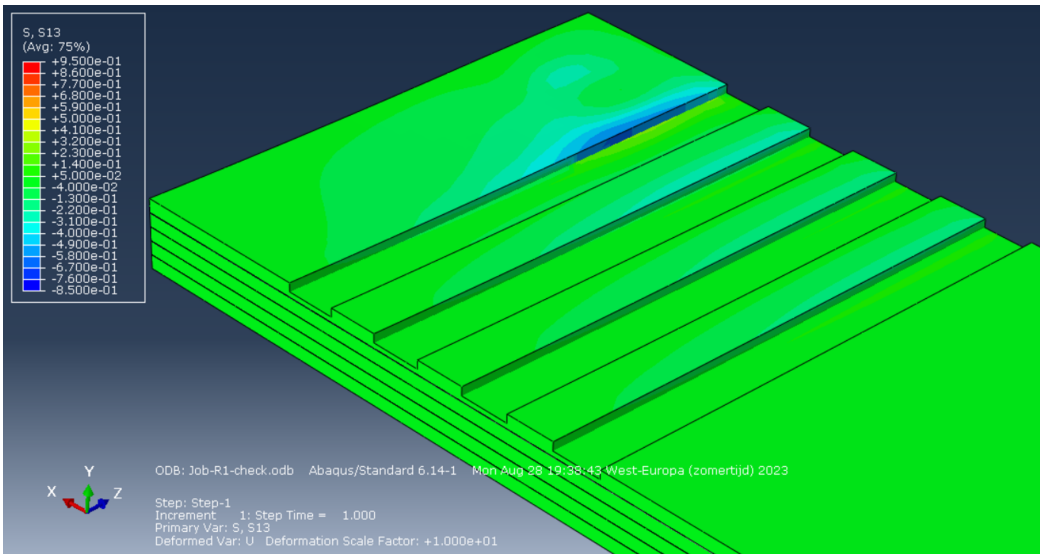

(b) S13 stresses in the CLT

Figure D.23: S13 shear stresses in the concrete and CLT

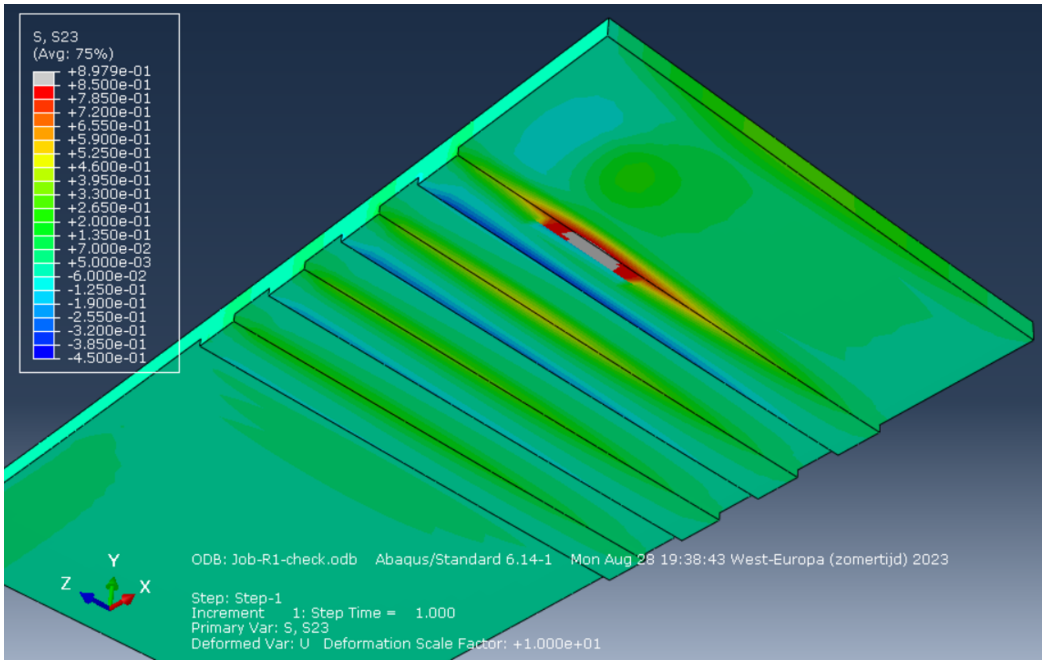

(a) S23 stresses in the concrete slab

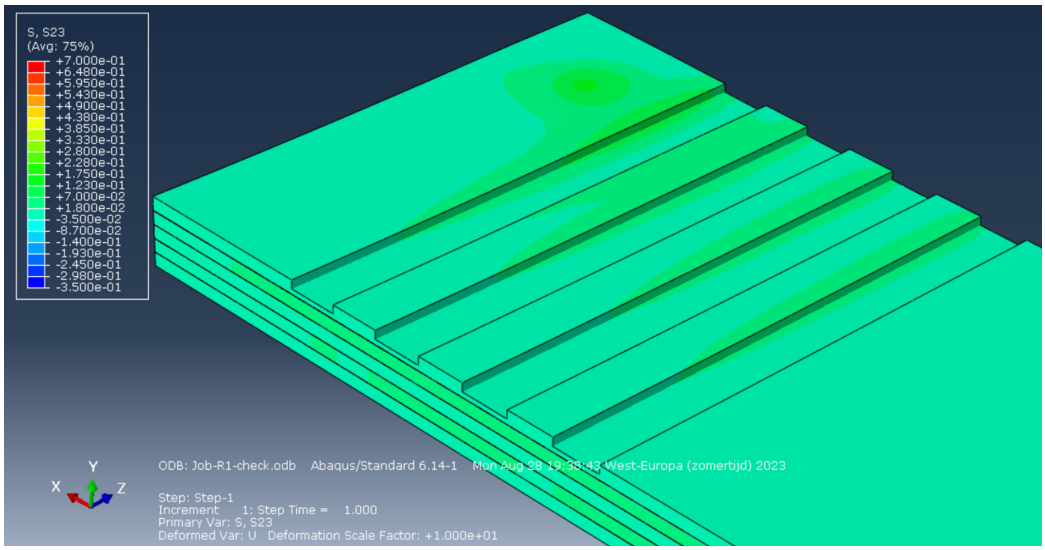

(b) S23 stresses in the CLT

Figure D.24: S23 shear stresses in the concrete and CLT

D.4 One-directional floor slab

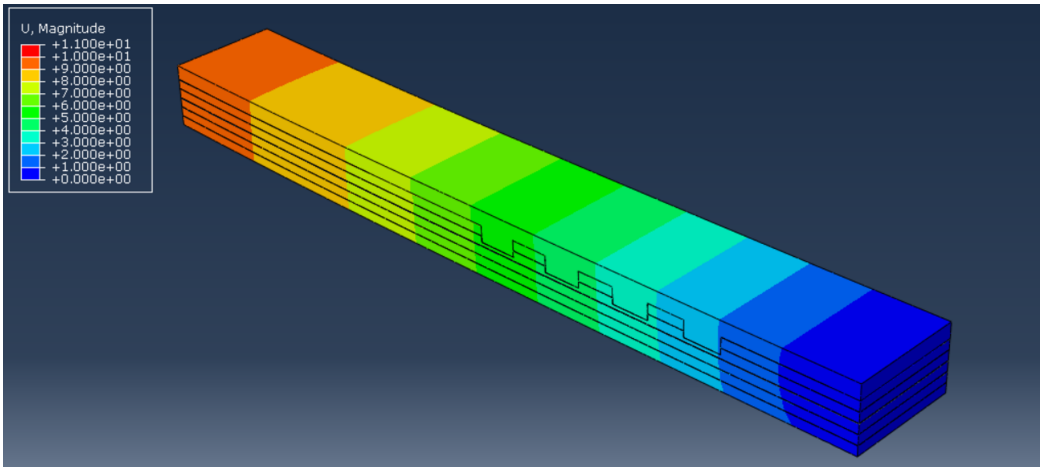

Figure D.25: Deformation of the one-directional TCC floor slab

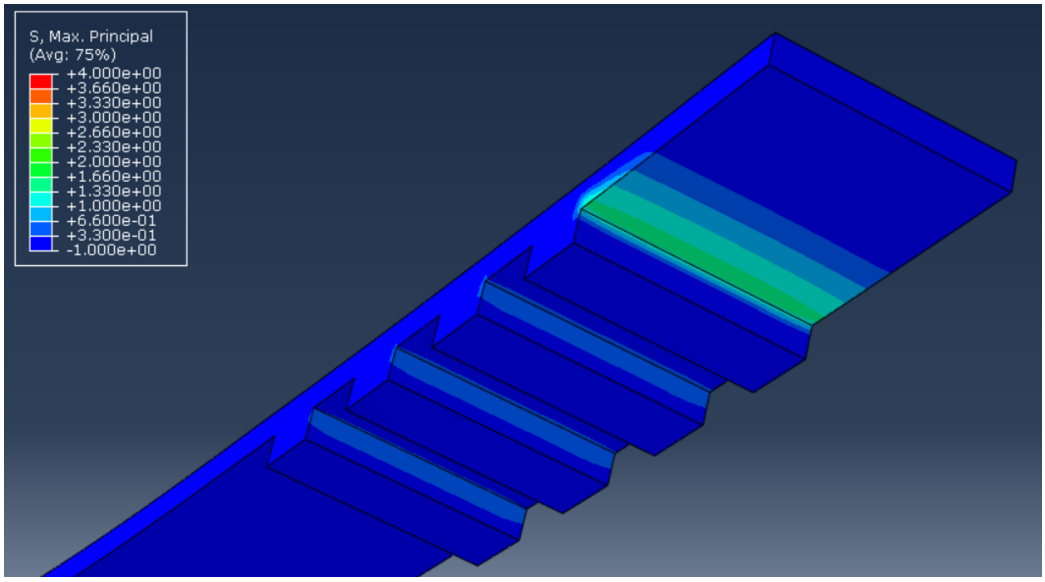

(a) Principal stresses in the concrete slab

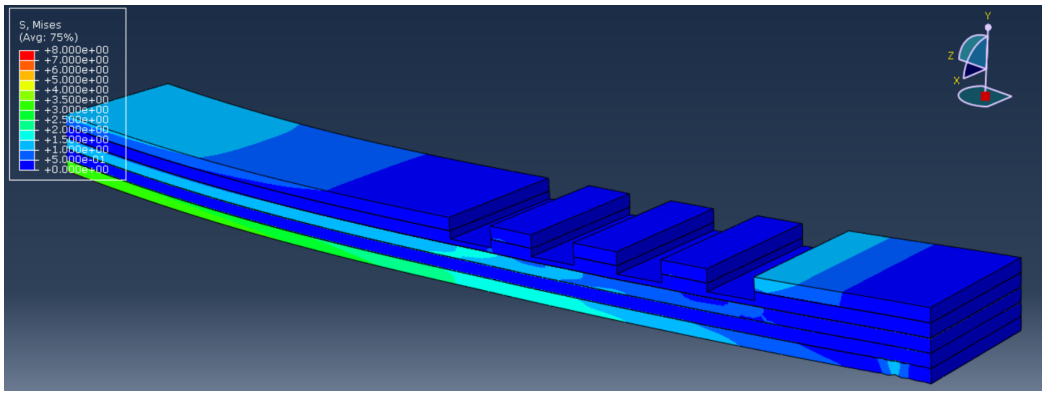

(b) Von Mises stresses in the CLT

Figure D.26: Principal and von Mises stresses in the concrete and CLT slab

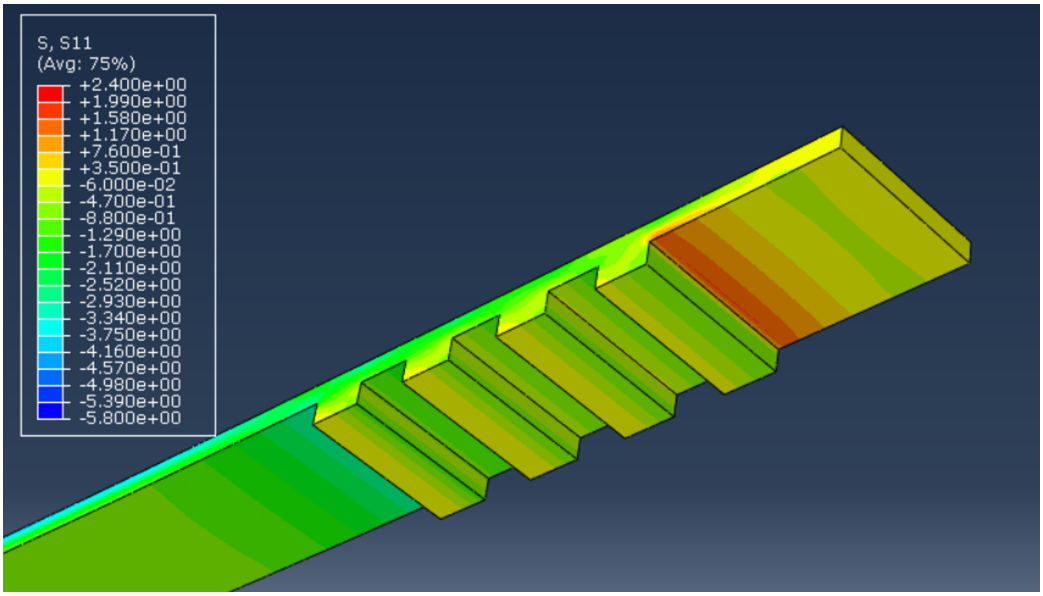

(a) S11 stresses, main direction of the material, in the concrete slab

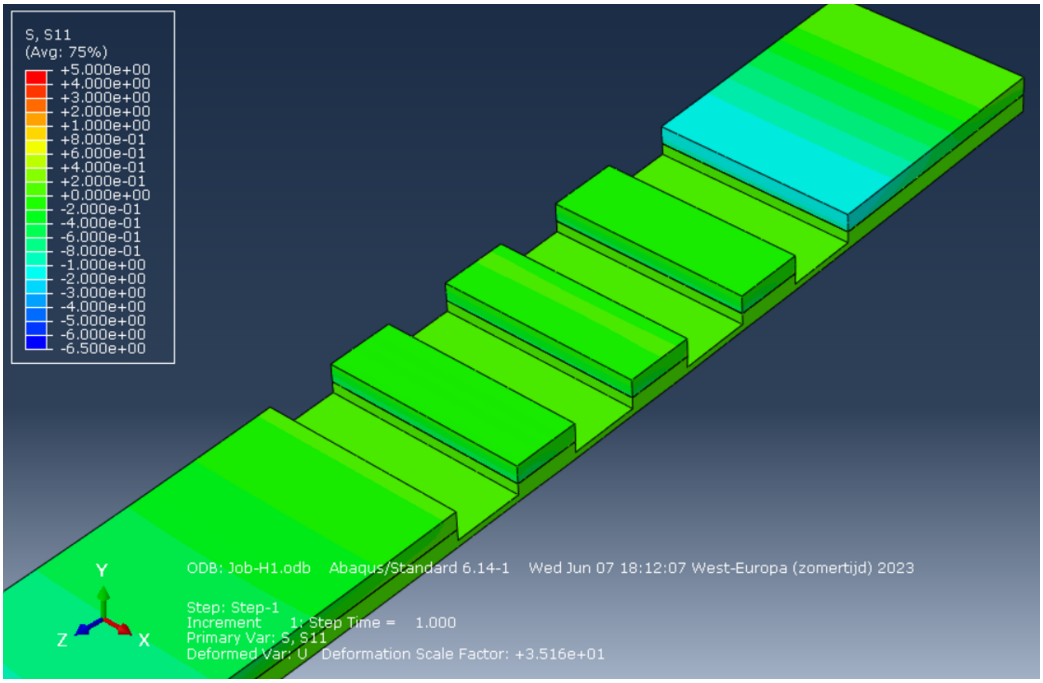

(b) S11 stresses, main direction of the material, in the CLT

Figure D.27: S11 stresses in the concrete and CLT slab

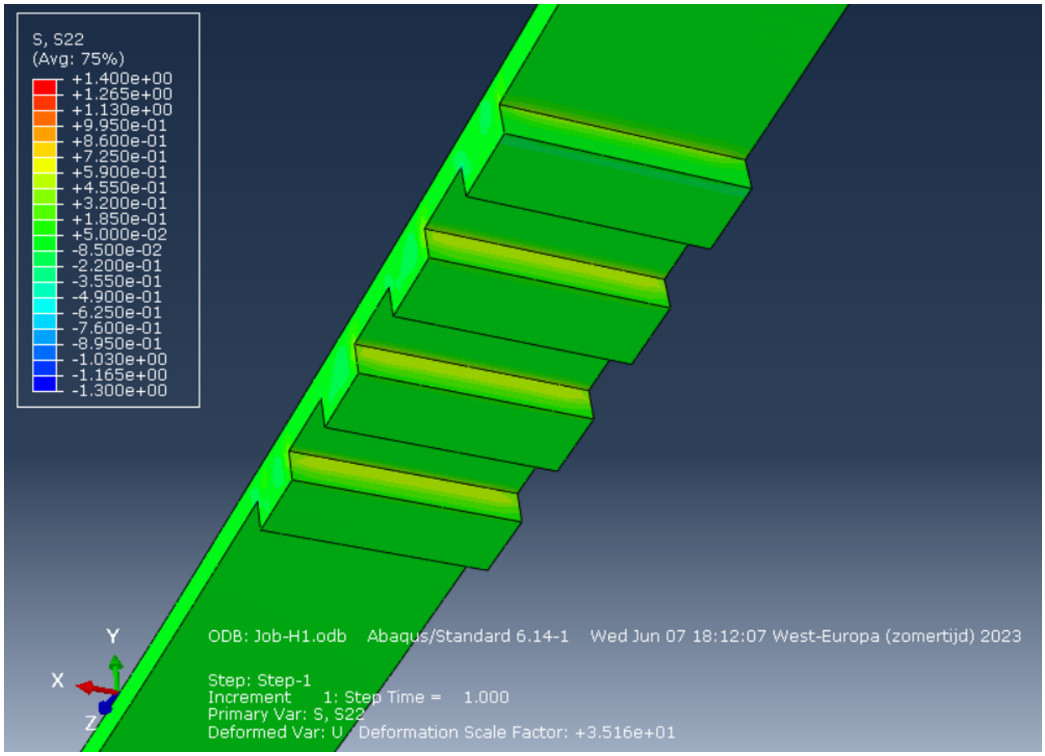

(a) S22 stresses in the concrete slab

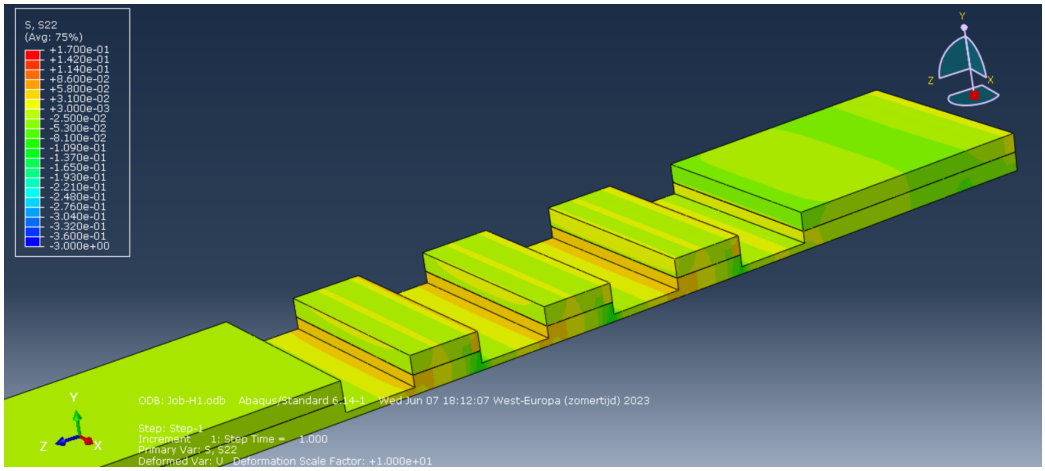

(b) S22 stresses in the CLT

Figure D.28: S22 stresses in the concrete and CLT slab

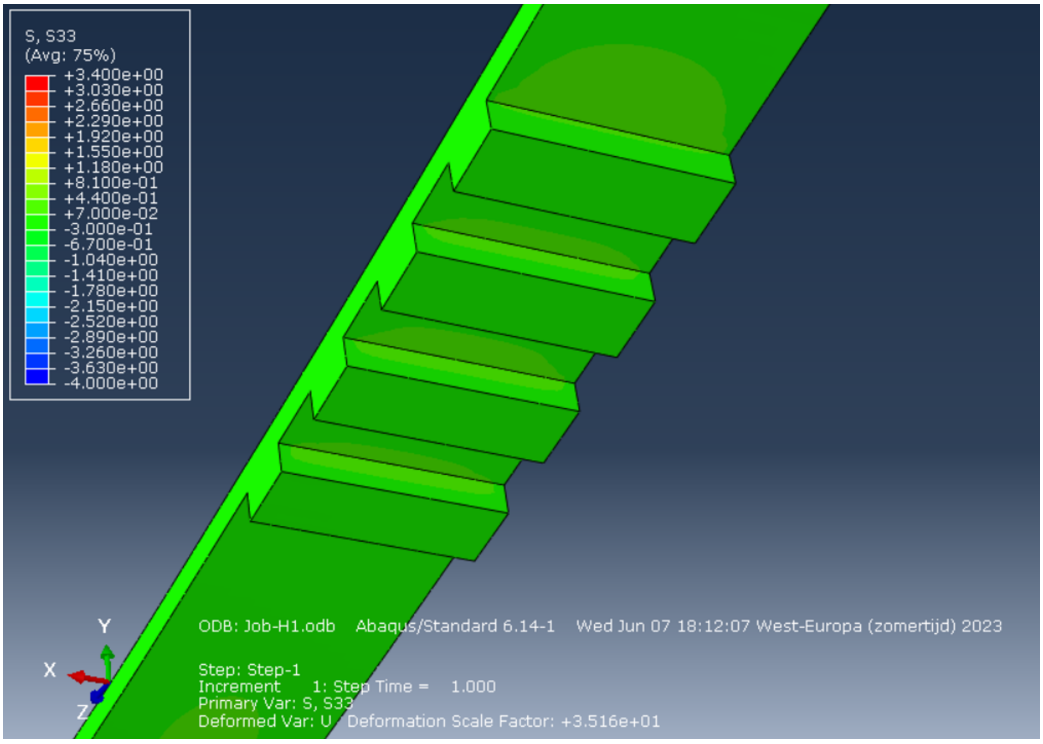

(a) S33 stresses, weakest direction of the material, in the concrete slab

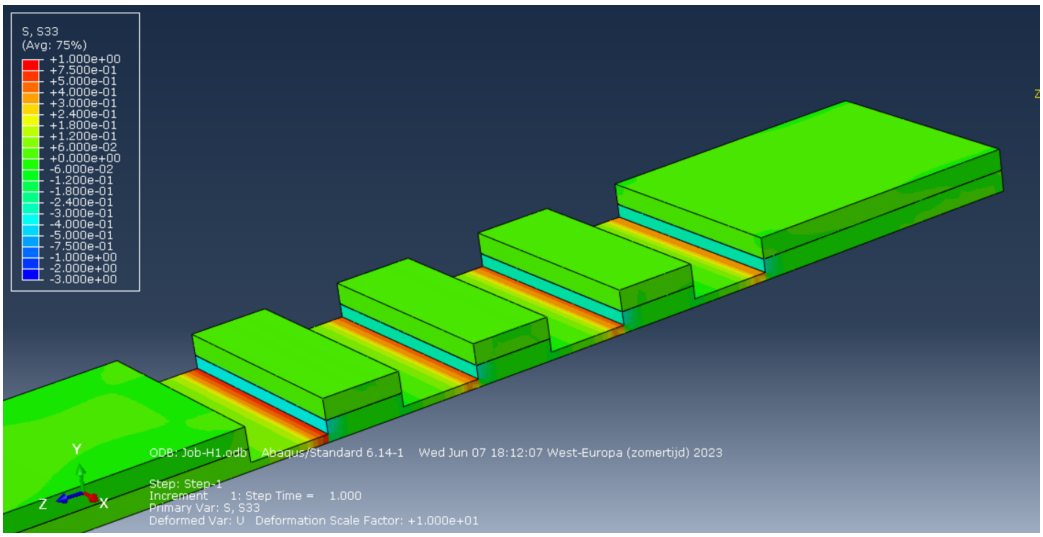

(b) S33 stresses, weakest direction of the material, in the CLT

Figure D.29: S33 stresses in the concrete and CLT slab

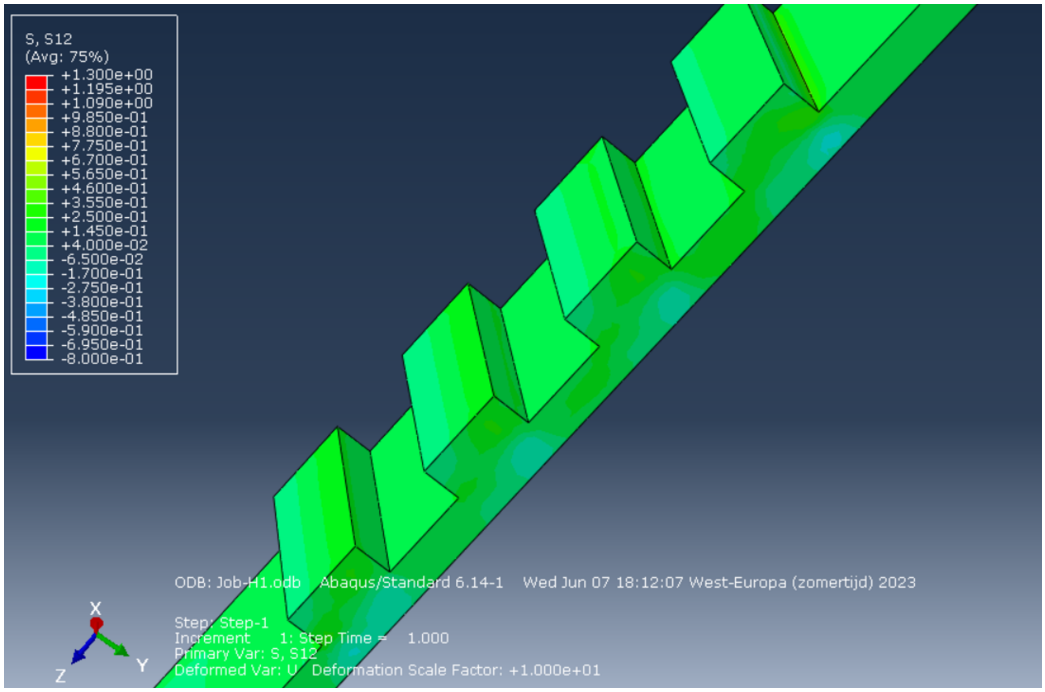

(a) S12 shear stresses, main direction of the material, in the concrete slab

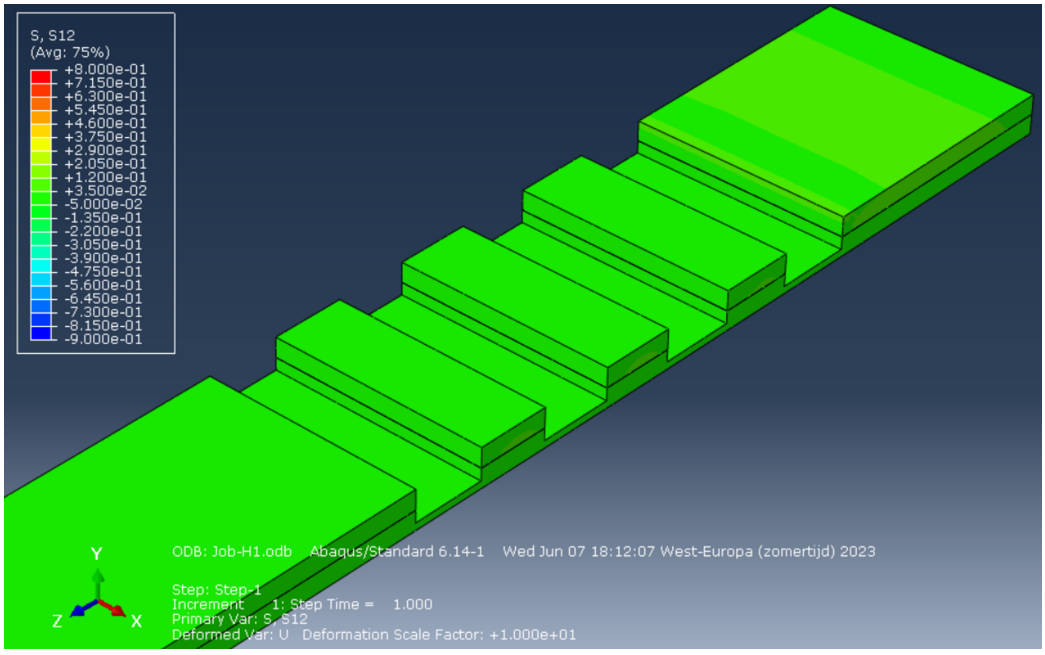

(b) S12 shear stresses, main direction of the material, in the CLT

Figure D.30: S12 shear stresses in the concrete and CLT

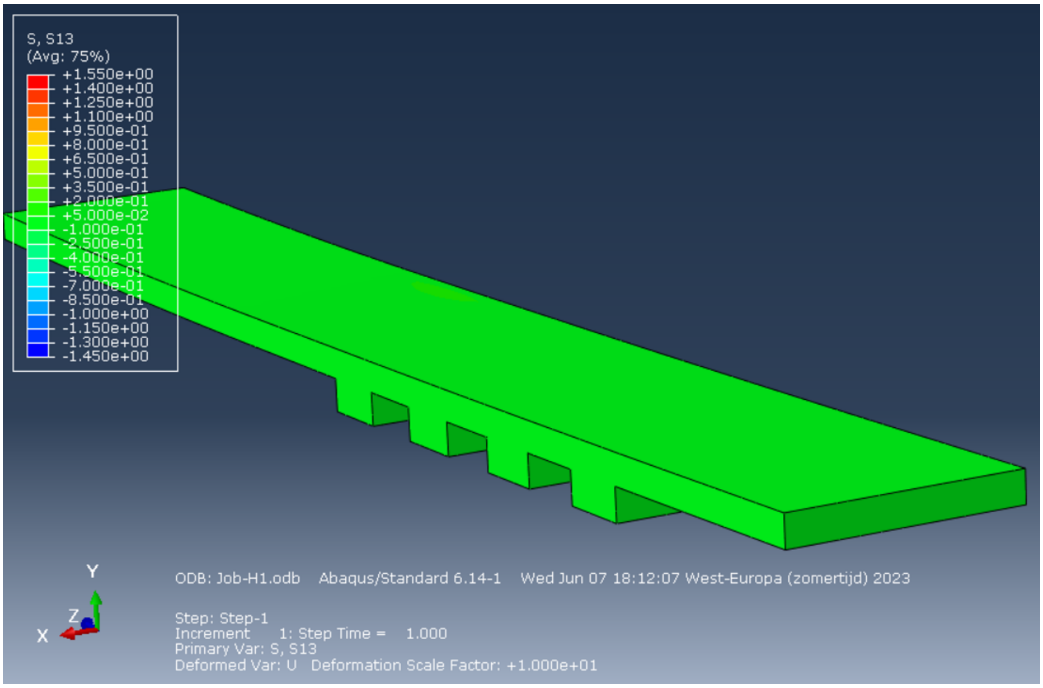

(a) S13 stresses in the concrete slab

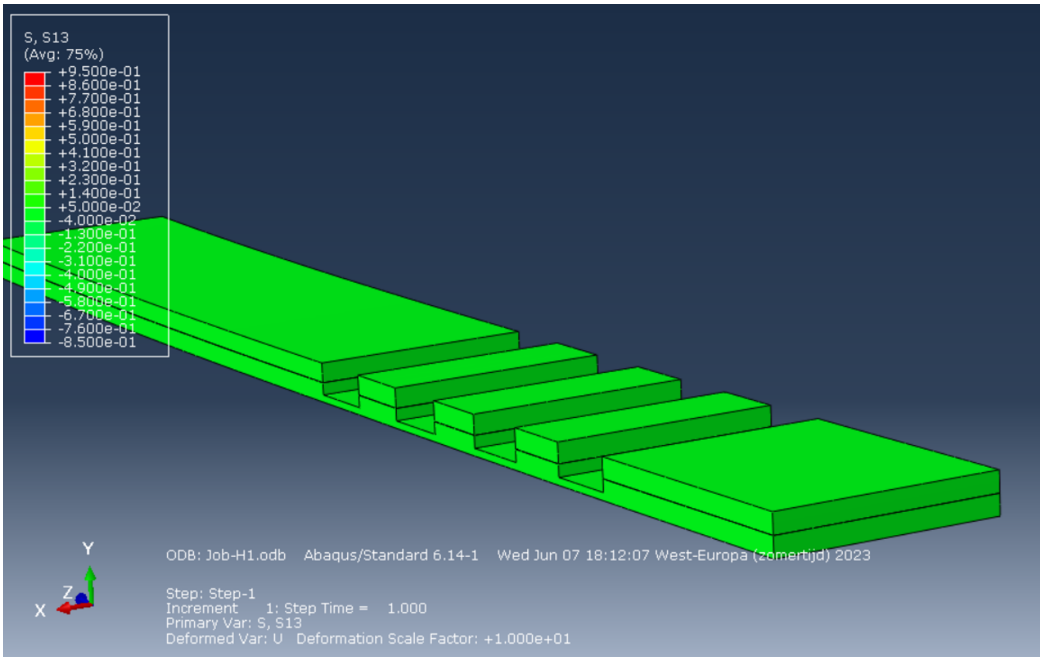

(b) S13 stresses in the CLT

Figure D.31: S13 shear stresses in the concrete and CLT

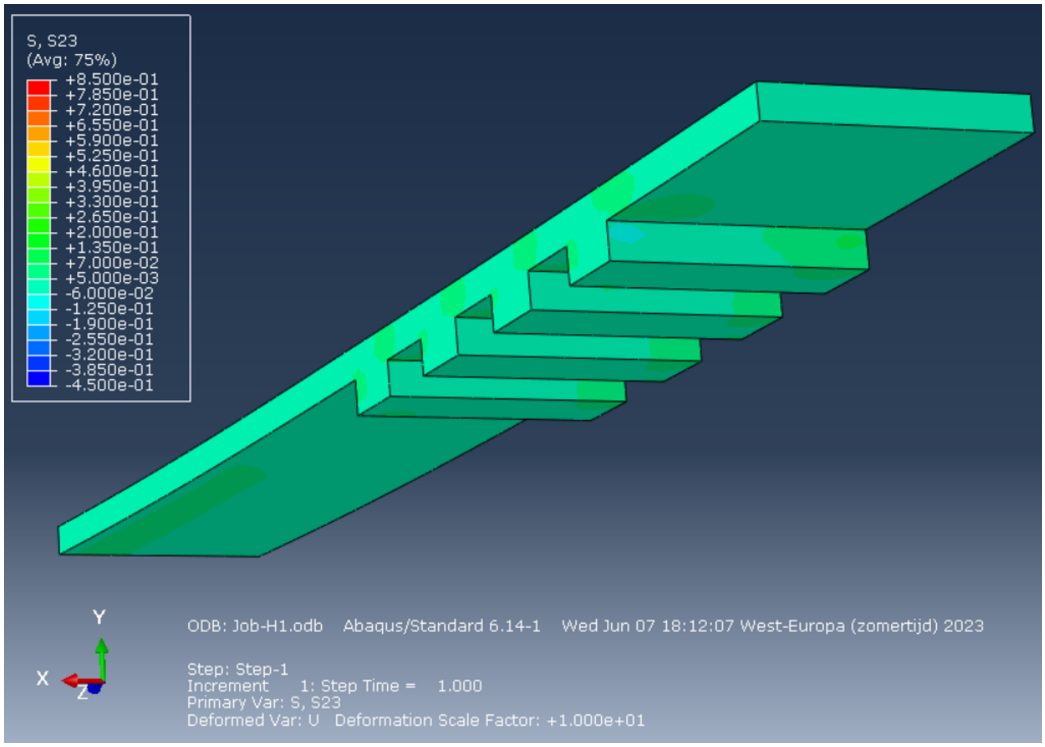

(a) S23 stresses in the concrete slab

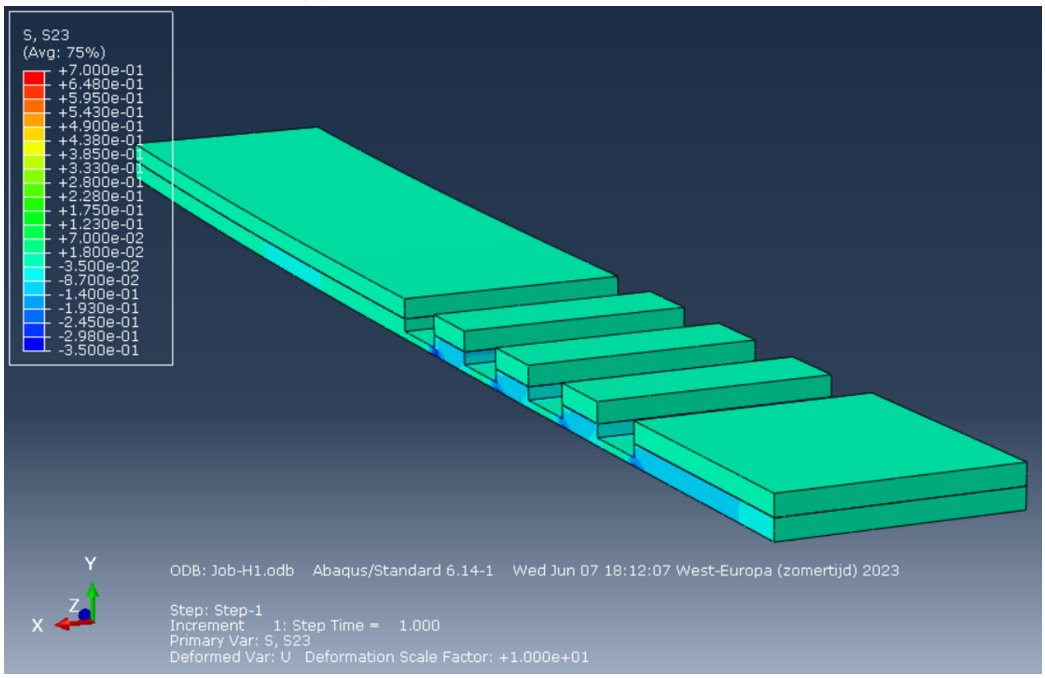

(b) S23 stresses in the CLT

Figure D.32: S23 shear stresses in the concrete and CLT

Appendix E

Numerical results of the shear tests

```
#floor specimen clear script
# -*- coding: mbcs -*-
from part import *
from material import *
from section import *
from assembly import *
from step import *
from interaction import *
from load import *
from mesh import *
from optimization import *
from job import *
from sketch import *
from visualization import *
from connectorBehavior import *

#profielen
mdb.models['Model-1'].ConstrainedSketch(name='__profile__', sheetSize=200.0)
mdb.models['Model-1'].sketches['__profile__'].rectangle(point1=(0.0, 0.0),
    point2=(3000.0, 60.0))
mdb.models['Model-1'].Part(dimensionality=THREE_D, name='Part-Concrete-Top',
    type=DEFORMABLE_BODY)
mdb.models['Model-1'].parts['Part-Concrete-Top'].BaseSolidExtrude(depth=450.0,
    sketch=mdb.models['Model-1'].sketches['__profile__'])
del mdb.models['Model-1'].sketches['__profile__']
mdb.models['Model-1'].ConstrainedSketch(name='__profile__', sheetSize=200.0)
mdb.models['Model-1'].sketches['__profile__'].rectangle(point1=(0.0, 0.0),
    point2=(450.0, 40.0))
mdb.models['Model-1'].Part(dimensionality=THREE_D, name='Part-Top-CLT', type=
    DEFORMABLE_BODY)
mdb.models['Model-1'].parts['Part-Top-CLT'].BaseSolidExtrude(depth=3000.0,
    sketch=mdb.models['Model-1'].sketches['__profile__'])
del mdb.models['Model-1'].sketches['__profile__']
mdb.models['Model-1'].Part(name='Part-Middle-CLT', objectToCopy=
    mdb.models['Model-1'].parts['Part-Top-CLT'])
mdb.models['Model-1'].Part(name='Part-Bottom-CLT', objectToCopy=
    mdb.models['Model-1'].parts['Part-Top-CLT'])
mdb.models['Model-1'].ConstrainedSketch(name='__profile__', sheetSize=200.0)
mdb.models['Model-1'].sketches['__profile__'].rectangle(point1=(0.0, 0.0),
    point2=(450.0, 40.0))
mdb.models['Model-1'].Part(dimensionality=THREE_D, name='Part-Trans-1', type=
    DEFORMABLE_BODY)
```

```
mdb.models['Model-1'].parts['Part-Trans-1'].BaseSolidExtrude(depth=3000.0,
    sketch=mdb.models['Model-1'].sketches['__profile__'])
del mdb.models['Model-1'].sketches['__profile__']
mdb.models['Model-1'].Part(name='Part-Trans-2', objectToCopy=
    mdb.models['Model-1'].parts['Part-Trans-1'])

#Inkepping
mdb.models['Model-1'].ConstrainedSketch(gridSpacing=151.67, name='__profile__',
    sheetSize=6067.12, transform=
    mdb.models['Model-1'].parts['Part-Concrete-Top'].MakeSketchTransform(
    sketchPlane=mdb.models['Model-1'].parts['Part-Concrete-Top'].faces[3],
    sketchPlaneSide=SIDE1,
    sketchUpEdge=mdb.models['Model-1'].parts['Part-Concrete-Top'].edges[8],
    sketchOrientation=RIGHT, origin=(1500.0, 0.0, 225.0)))
mdb.models['Model-1'].parts['Part-Concrete-Top'].projectReferencesOntoSketch(
    filter=COPLANAR_EDGES, sketch=
    mdb.models['Model-1'].sketches['__profile__'])
mdb.models['Model-1'].sketches['__profile__'].rectangle(point1=(975.0, 225.0),
    point2=(825.0, -225.0))
mdb.models['Model-1'].sketches['__profile__'].rectangle(point1=(675.0, 225.0),
    point2=(525.0, -225.0))
mdb.models['Model-1'].sketches['__profile__'].rectangle(point1=(375.0, 225.0),
    point2=(225.0, -225.0))
mdb.models['Model-1'].sketches['__profile__'].rectangle(point1=(75.0, 225.0),
    point2=(-75.0, -225.0))
mdb.models['Model-1'].parts['Part-Concrete-Top'].SolidExtrude(depth=65.0,
    flipExtrudeDirection=OFF, sketch=
    mdb.models['Model-1'].sketches['__profile__'], sketchOrientation=RIGHT,
    sketchPlane=mdb.models['Model-1'].parts['Part-Concrete-Top'].faces[3],
    sketchPlaneSide=SIDE1, sketchUpEdge=
    mdb.models['Model-1'].parts['Part-Concrete-Top'].edges[8])
del mdb.models['Model-1'].sketches['__profile__']


#Materials
mdb.models['Model-1'].Material(name='Material-Timber')
mdb.models['Model-1'].materials['Material-Timber'].Elastic(table=((11000.0,
    370.0, 370.0, 0.0, 0.0, 0.0, 690.0, 690.0, 69.0), ), type=
    ENGINEERING_CONSTANTS)
mdb.models['Model-1'].materials['Material-Timber'].Plastic(table=((15.0, 0.0),
    (30.0, 0.0005)))
mdb.models['Model-1'].Material(name='Material-Concrete')
```

```
mdb.models['Model-1'].materials['Material-Concrete'].Density(table=((
    2.4e-09, ), ))
mdb.models['Model-1'].materials['Material-Concrete'].Elastic(table=((32530.4,
    0.2), ))
mdb.models['Model-1'].materials['Material-Concrete'].ConcreteDamagedPlasticity(
    table=((31.0, 0.1, 1.16, 0.67, 0.0001), ))
mdb.models['Model-1'].materials['Material-Concrete'].concreteDamagedPlasticity.ConcreteCompressionHardening(
    table=((20.4, 0.0), (25.6, 2.6666e-05), (30.0, 8e-05), (33.6, 0.00016), (
    36.4, 0.000266667), (38.4, 0.0004), (39.6, 0.00056), (40.0, 0.000746667), (
    39.6, 0.00096), (38.4, 0.0012), (36.4, 0.001466667), (33.6, 0.00176), (
    30.0, 0.00208), (25.6, 0.002426667), (20.4, 0.0028), (14.4, 0.0032), (7.6,
    0.003626667)))
mdb.models['Model-1'].materials['Material-Concrete'].concreteDamagedPlasticity.ConcreteTensionStiffening(
    table=((4.0, 0.0), (0.04, 0.00133333)))
mdb.models['Model-1'].materials['Material-Concrete'].concreteDamagedPlasticity.ConcreteCompressionDamage(
    table=((0.0, 0.0), (0.0, 2.6666e-05), (0.0, 8e-05), (0.0, 0.00016), (0.0,
    0.000266667), (0.0, 0.0004), (0.0, 0.00056), (0.0, 0.000746667), (0.01,
    0.00096), (0.04, 0.0012), (0.09, 0.001466667), (0.16, 0.00176), (0.25,
    0.00208), (0.36, 0.002426667), (0.49, 0.0028), (0.64, 0.0032), (0.81,
    0.003626667)))
mdb.models['Model-1'].materials['Material-Concrete'].concreteDamagedPlasticity.ConcreteTensionDamage(
    table=((0.0, 0.0), (0.99, 0.001333333)))

#mdb.models['Model-1'].Material(name='Material-Concrete')
#mdb.models['Model-1'].materials['Material-Concrete'].Density(table=((
    #-2.47612361169829, ), ))
#mdb.models['Model-1'].materials['Material-Concrete'].elastic.setValues(table=((
    #32530.4, 0.2), ))
#mdb.models['Model-1'].materials['Material-Concrete'].concreteDamagedPlasticity.concreteCompressionHardening.setValues(
    #table=((20.4, 0.0), (25.6, 2.6666e-05), (30.0, 8e-05), (33.6, 0.00016), (
    #36.4, 0.000266667), (38.4, 0.0004), (39.6, 0.00056), (40.0, 0.000746667), (
    #39.6, 0.00096), (38.4, 0.0012), (36.4, 0.001466667), (33.6, 0.00176), (
    #30.0, 0.00208), (25.6, 0.002426667), (20.4, 0.0028), (14.4, 0.0032), (7.6,
    #0.003626667)))
#mdb.models['Model-1'].materials['Material-Concrete'].concreteDamagedPlasticity.concreteTensionStiffening.setValues(
    #table=((4.0, 0.0), (0.04, 0.001333333)))
#mdb.models['Model-1'].materials['Material-Concrete'].concreteDamagedPlasticity.concreteCompressionDamage.setValues(
    #table=((0.0, 0.0), (0.0, 2.6666e-05), (0.0, 8e-05), (0.0, 0.00016), (0.0,
    #0.000266667), (0.0, 0.0004), (0.0, 0.00056), (0.0, 0.000746667), (0.01,
    #0.00096), (0.04, 0.0012), (0.09, 0.001466667), (0.16, 0.00176), (0.25,
    #0.00208), (0.36, 0.002426667), (0.49, 0.0028), (0.64, 0.0032), (0.81,
    #0.003626667)))
```

```
#mdb.models['Model-1'].materials['Material-Concrete'].concreteDamagedPlasticity.concreteTensionDamage.setValues(
    #table=((0.0, 0.0), (0.99, 0.001333333)))

#Assembly
mdb.models['Model-1'].rootAssembly.DatumCsysByDefault(CARTESIAN)
mdb.models['Model-1'].rootAssembly.Instance(dependent=ON, name=
    'Part-Bottom-CLT-1', part=mdb.models['Model-1'].parts['Part-Bottom-CLT'])
mdb.models['Model-1'].rootAssembly.Instance(dependent=ON, name='Part-Trans-2-1'
    , part=mdb.models['Model-1'].parts['Part-Trans-2'])
mdb.models['Model-1'].rootAssembly.instances['Part-Trans-2-1'].translate(
    vector=(495.0, 0.0, 0.0))
mdb.models['Model-1'].rootAssembly.translate(instanceList=('Part-Trans-2-1', ),
    vector=(-495.0, 40.0, 0.0))
mdb.models['Model-1'].rootAssembly.Instance(dependent=ON, name=
    'Part-Middle-CLT-1', part=mdb.models['Model-1'].parts['Part-Middle-CLT'])
mdb.models['Model-1'].rootAssembly.instances['Part-Middle-CLT-1'].translate(
    vector=(495.0, 0.0, 0.0))
mdb.models['Model-1'].rootAssembly.translate(instanceList=('Part-Middle-CLT-1',
    ), vector=(-495.0, 70.0, 0.0))
mdb.models['Model-1'].rootAssembly.Instance(dependent=ON, name='Part-Trans-1-1'
    , part=mdb.models['Model-1'].parts['Part-Trans-1'])
mdb.models['Model-1'].rootAssembly.instances['Part-Trans-1-1'].translate(
    vector=(495.0, 0.0, 0.0))
mdb.models['Model-1'].rootAssembly.translate(instanceList=('Part-Trans-1-1', ),
    vector=(-495.0, 110.0, 0.0))
mdb.models['Model-1'].rootAssembly.Instance(dependent=ON, name='Part-Top-CLT-1'
    , part=mdb.models['Model-1'].parts['Part-Top-CLT'])
mdb.models['Model-1'].rootAssembly.instances['Part-Top-CLT-1'].translate(
    vector=(495.0, 0.0, 0.0))
mdb.models['Model-1'].rootAssembly.translate(instanceList=('Part-Top-CLT-1', ),
    vector=(-495.0, 140.0, 0.0))
mdb.models['Model-1'].rootAssembly.Instance(dependent=ON, name=
    'Part-Concrete-Top-1', part=
    mdb.models['Model-1'].parts['Part-Concrete-Top'])
mdb.models['Model-1'].rootAssembly.instances['Part-Concrete-Top-1'].translate(
    vector=(775.5, 0.0, 0.0))
mdb.models['Model-1'].rootAssembly.rotate(angle=90.0, axisDirection=(0.0, 80.0,
    0.0), axisPoint=(4030.5, 0.0, 450.0), instanceList=('Part-Concrete-Top-1',
    ))
mdb.models['Model-1'].rootAssembly.translate(instanceList=(
    'Part-Concrete-Top-1', ), vector=(-3580.5, 180.0, -450.0))
```

```
#Cut in top CLT
mdb.models['Model-1'].rootAssembly.InstanceFromBooleanCut(cuttingInstances=(
    mdb.models['Model-1'].rootAssembly.instances['Part-Concrete-Top-1'], ),
    instanceToBeCut=
    mdb.models['Model-1'].rootAssembly.instances['Part-Top-CLT-1'], name=
    'Part-Top-CLT-cut', originalInstances=DELETE)

#adding Concrete to top
mdb.models['Model-1'].rootAssembly.Instance(dependent=ON, name=
    'Part-Concrete-Top-1', part=
    mdb.models['Model-1'].parts['Part-Concrete-Top'])
mdb.models['Model-1'].rootAssembly.instances['Part-Concrete-Top-1'].translate(
    vector=(775.5, 0.0, 0.0))
mdb.models['Model-1'].rootAssembly.rotate(angle=90.0, axisDirection=(0.0, 80.0,
    0.0), axisPoint=(4030.5, 0.0, 450.0), instanceList=('Part-Concrete-Top-1',
    ))
mdb.models['Model-1'].rootAssembly.translate(instanceList=(
    'Part-Concrete-Top-1', ), vector=(-3580.5, 180.0, -450.0))

#adding material and orientation of layers
mdb.models['Model-1'].HomogeneousSolidSection(material='Material-Concrete',
    name='Section-Concrete', thickness=None)
mdb.models['Model-1'].parts['Part-Concrete-Top'].Set(cells=
    mdb.models['Model-1'].parts['Part-Concrete-Top'].cells.getSequenceFromMask(
    ('[#1 ]', ), ), name='Set-1')
mdb.models['Model-1'].parts['Part-Concrete-Top'].SectionAssignment(offset=0.0,
    offsetField='', offsetType=MIDDLE_SURFACE, region=
    mdb.models['Model-1'].parts['Part-Concrete-Top'].sets['Set-1'],
    sectionName='Section-Concrete', thicknessAssignment=FROM_SECTION)
mdb.models['Model-1'].parts['Part-Concrete-Top'].MaterialOrientation(
    additionalRotationType=ROTATION_NONE, axis=AXIS_1, fieldName='', localCsys=
    None, orientationType=GLOBAL, region=Region(
    cells=mdb.models['Model-1'].parts['Part-Concrete-Top'].cells.getSequenceFromMask(
    mask=('[#1 ]', ), )), stackDirection=STACK_3)
mdb.models['Model-1'].HomogeneousSolidSection(material='Material-Timber', name=
    'Section-Timber', thickness=None)
mdb.models['Model-1'].parts['Part-Bottom-CLT'].Set(cells=
    mdb.models['Model-1'].parts['Part-Bottom-CLT'].cells.getSequenceFromMask((
    '[#1 ]', ), ), name='Set-1')
mdb.models['Model-1'].parts['Part-Bottom-CLT'].SectionAssignment(offset=0.0,
    offsetField='', offsetType=MIDDLE_SURFACE, region=
```

```
    mdb.models['Model-1'].parts['Part-Bottom-CLT'].sets['Set-1'], sectionName=
    'Section-Timber', thicknessAssignment=FROM_SECTION)
mdb.models['Model-1'].parts['Part-Bottom-CLT'].MaterialOrientation(
    additionalRotationField='', additionalRotationType=ROTATION_ANGLE, angle=
    90.0, axis=AXIS_2, fieldName='', localCsys=None, orientationType=SYSTEM,
    region=Region(
    cells=mdb.models['Model-1'].parts['Part-Bottom-CLT'].cells.getSequenceFromMask(
    mask=('[#1 ]', ), )), stackDirection=STACK_3)
mdb.models['Model-1'].parts['Part-Middle-CLT'].Set(cells=
    mdb.models['Model-1'].parts['Part-Middle-CLT'].cells.getSequenceFromMask((
    '[#1 ]', ), ), name='Set-1')
mdb.models['Model-1'].parts['Part-Middle-CLT'].SectionAssignment(offset=0.0,
    offsetField='', offsetType=MIDDLE_SURFACE, region=
    mdb.models['Model-1'].parts['Part-Middle-CLT'].sets['Set-1'], sectionName=
    'Section-Timber', thicknessAssignment=FROM_SECTION)
mdb.models['Model-1'].parts['Part-Middle-CLT'].MaterialOrientation(
    additionalRotationField='', additionalRotationType=ROTATION_ANGLE, angle=
    90.0, axis=AXIS_2, fieldName='', localCsys=None, orientationType=SYSTEM,
    region=Region(
    cells=mdb.models['Model-1'].parts['Part-Middle-CLT'].cells.getSequenceFromMask(
    mask=('[#1 ]', ), )), stackDirection=STACK_3)
mdb.models['Model-1'].parts['Part-Top-CLT'].Set(cells=
    mdb.models['Model-1'].parts['Part-Top-CLT'].cells.getSequenceFromMask((
    '[#1 ]', ), ), name='Set-1')
mdb.models['Model-1'].parts['Part-Top-CLT'].SectionAssignment(offset=0.0,
    offsetField='', offsetType=MIDDLE_SURFACE, region=
    mdb.models['Model-1'].parts['Part-Top-CLT'].sets['Set-1'], sectionName=
    'Section-Timber', thicknessAssignment=FROM_SECTION)
mdb.models['Model-1'].parts['Part-Top-CLT'].MaterialOrientation(
    additionalRotationField='', additionalRotationType=ROTATION_ANGLE, angle=
    90.0, axis=AXIS_2, fieldName='', localCsys=None, orientationType=SYSTEM,
    region=Region(
    cells=mdb.models['Model-1'].parts['Part-Top-CLT'].cells.getSequenceFromMask(
    mask=('[#1 ]', ), )), stackDirection=STACK_3)
mdb.models['Model-1'].parts['Part-Top-CLT-cut'].Set(cells=
    mdb.models['Model-1'].parts['Part-Top-CLT-cut'].cells.getSequenceFromMask((
    '[#1 ]', ), ), name='Set-1')
mdb.models['Model-1'].parts['Part-Top-CLT-cut'].SectionAssignment(offset=0.0,
    offsetField='', offsetType=MIDDLE_SURFACE, region=
    mdb.models['Model-1'].parts['Part-Top-CLT-cut'].sets['Set-1'], sectionName=
    'Section-Timber', thicknessAssignment=FROM_SECTION)
mdb.models['Model-1'].parts['Part-Top-CLT-cut'].MaterialOrientation(
```

```
    additionalRotationField='', additionalRotationType=ROTATION_ANGLE, angle=
    90.0, axis=AXIS_2, fieldName='', localCsys=None, orientationType=SYSTEM,
    region=Region(
    cells=mdb.models['Model-1'].parts['Part-Top-CLT-cut'].cells.getSequenceFromMask(
    mask=('[#1 ]', ), ), ), stackDirection=STACK_3)
mdb.models['Model-1'].parts['Part-Trans-1'].Set(cells=
    mdb.models['Model-1'].parts['Part-Trans-1'].cells.getSequenceFromMask((
    '[#1 ]', ), ), name='Set-1')
mdb.models['Model-1'].parts['Part-Trans-1'].SectionAssignment(offset=0.0,
    offsetField='', offsetType=MIDDLE_SURFACE, region=
    mdb.models['Model-1'].parts['Part-Trans-1'].sets['Set-1'], sectionName=
    'Section-Timber', thicknessAssignment=FROM_SECTION)
mdb.models['Model-1'].parts['Part-Trans-1'].MaterialOrientation(
    additionalRotationType=ROTATION_NONE, axis=AXIS_1, fieldName='', localCsys=
    None, orientationType=GLOBAL, region=Region(
    cells=mdb.models['Model-1'].parts['Part-Trans-1'].cells.getSequenceFromMask(
    mask=('[#1 ]', ), ), ), stackDirection=STACK_3)
mdb.models['Model-1'].parts['Part-Trans-2'].Set(cells=
    mdb.models['Model-1'].parts['Part-Trans-2'].cells.getSequenceFromMask((
    '[#1 ]', ), ), name='Set-1')
mdb.models['Model-1'].parts['Part-Trans-2'].SectionAssignment(offset=0.0,
    offsetField='', offsetType=MIDDLE_SURFACE, region=
    mdb.models['Model-1'].parts['Part-Trans-2'].sets['Set-1'], sectionName=
    'Section-Timber', thicknessAssignment=FROM_SECTION)
mdb.models['Model-1'].parts['Part-Trans-2'].MaterialOrientation(
    additionalRotationType=ROTATION_NONE, axis=AXIS_1, fieldName='', localCsys=
    None, orientationType=GLOBAL, region=Region(
    cells=mdb.models['Model-1'].parts['Part-Trans-2'].cells.getSequenceFromMask(
    mask=('[#1 ]', ), ), ), stackDirection=STACK_3)

#Interaction
mdb.models['Model-1'].ContactProperty('IntProp-CLT-Concrete')
mdb.models['Model-1'].interactionProperties['IntProp-CLT-Concrete'].NormalBehavior(
    allowSeparation=ON, constraintEnforcementMethod=DEFAULT,
    pressureOverclosure=HARD)
mdb.models['Model-1'].interactionProperties['IntProp-CLT-Concrete'].normalBehavior.setValues(
    allowSeparation=ON, constraintEnforcementMethod=DEFAULT,
    pressureOverclosure=HARD)
mdb.models['Model-1'].interactionProperties['IntProp-CLT-Concrete'].TangentialBehavior(
    dependencies=0, directionality=ISOTROPIC, elasticSlipStiffness=None,
    formulation=PENALTY, fraction=0.005, maximumElasticSlip=FRACTION,
    pressureDependency=OFF, shearStressLimit=None, slipRateDependency=OFF,
```

```
    table=((0.57, ), ), temperatureDependency=OFF)
mdb.models['Model-1'].ContactProperty('IntProp-Cohesive')
mdb.models['Model-1'].interactionProperties['IntProp-Cohesive'].CohesiveBehavior(
    )
mdb.models['Model-1'].ContactProperty('IntProp-General')
mdb.models['Model-1'].interactionProperties['IntProp-General'].TangentialBehavior(
    dependencies=0, directionality=ISOTROPIC, elasticSlipStiffness=None,
    formulation=PENALTY, fraction=0.005, maximumElasticSlip=FRACTION,
    pressureDependency=OFF, shearStressLimit=None, slipRateDependency=OFF,
    table=((0.005, ), ), temperatureDependency=OFF)
mdb.models['Model-1'].interactionProperties['IntProp-General'].NormalBehavior(
    allowSeparation=ON, constraintEnforcementMethod=DEFAULT,
    pressureOverclosure=HARD)
mdb.models['Model-1'].rootAssembly.regenerate()

#Creating step
mdb.models['Model-1'].StaticStep(initialInc=1.00, maxNumInc=10000, name=
    'Step-1', previous='Initial')
del mdb.models['Model-1'].historyOutputRequests['H-Output-1']

#creating surfaces
mdb.models['Model-1'].rootAssembly.Surface(name='Surf-Concrete-bottom',
    side1Faces=
    mdb.models['Model-1'].rootAssembly.instances['Part-Concrete-Top-1'].faces.getSequenceFromMask(
    ('[#1ffff ]', ), ))
mdb.models['Model-1'].rootAssembly.Surface(name='Surf-Top-CLT-1', side1Faces=
    mdb.models['Model-1'].rootAssembly.instances['Part-Top-CLT-cut-1'].faces.getSequenceFromMask(
    mask=('[#284f24c9 ]', ), )+\
    mdb.models['Model-1'].rootAssembly.instances['Part-Trans2-2-1'].faces.getSequenceFromMask(
    mask=('[#fff ]', ), ))
mdb.models['Model-1'].rootAssembly.Surface(name='Surf-Top-CLT-2', side1Faces=
    mdb.models['Model-1'].rootAssembly.instances['Part-Top-CLT-cut-1'].faces.getSequenceFromMask(
    ('[#2108102 ]', ), ))
mdb.models['Model-1'].rootAssembly.Surface(name='Surf-Trans1-1', side1Faces=
    mdb.models['Model-1'].rootAssembly.instances['Part-Trans2-2-1'].faces.getSequenceFromMask(
    ('[#5e000 ]', ), ))
mdb.models['Model-1'].rootAssembly.Surface(name='Surf-Trans1-2', side1Faces=
    mdb.models['Model-1'].rootAssembly.instances['Part-Trans2-2-1'].faces.getSequenceFromMask(
    ('[#80000 ]', ), ))
mdb.models['Model-1'].rootAssembly.Surface(name='Surf-Middle-1', side1Faces=
    mdb.models['Model-1'].rootAssembly.instances['Part-Middle-CLT-1'].faces.getSequenceFromMask(
    ('[#2 ]', ), ))
```

```
mdb.models['Model-1'].rootAssembly.Surface(name='Surf-Middle-2', side1Faces=
    mdb.models['Model-1'].rootAssembly.instances['Part-Middle-CLT-1'].faces.getSequenceFromMask(
    ('[#8 ]', ), ))
mdb.models['Model-1'].rootAssembly.Surface(name='Surf-Trans2-1', side1Faces=
    mdb.models['Model-1'].rootAssembly.instances['Part-Trans-2-1'].faces.getSequenceFromMask(
    ('[#2 ]', ), ))
mdb.models['Model-1'].rootAssembly.Surface(name='Surf-trans2-2', side1Faces=
    mdb.models['Model-1'].rootAssembly.instances['Part-Trans-2-1'].faces.getSequenceFromMask(
    ('[#8 ]', ), ))
mdb.models['Model-1'].rootAssembly.Surface(name='Surf-Bottom-1', side1Faces=
    mdb.models['Model-1'].rootAssembly.instances['Part-Bottom-CLT-1'].faces.getSequenceFromMask(
    ('[#2 ]', ), ))

#Interaction
mdb.models['Model-1'].SurfaceToSurfaceContactStd(adjustMethod=NONE,
    clearanceRegion=None, createStepName='Step-1', datumAxis=None,
    initialClearance=OMIT, interactionProperty='IntProp-CLT-Concrete', master=
    mdb.models['Model-1'].rootAssembly.surfaces['Surf-Concrete-bottom'], name=
    'Int-1', slave=
    mdb.models['Model-1'].rootAssembly.surfaces['Surf-Top-CLT-1'], sliding=
    FINITE, thickness=ON)
mdb.models['Model-1'].SurfaceToSurfaceContactStd(adjustMethod=NONE,
    clearanceRegion=None, createStepName='Step-1', datumAxis=None,
    initialClearance=OMIT, interactionProperty='IntProp-Cohesive', master=
    mdb.models['Model-1'].rootAssembly.surfaces['Surf-Top-CLT-2'], name='Int-2'
    , slave=mdb.models['Model-1'].rootAssembly.surfaces['Surf-Trans1-1'],
    sliding=FINITE, thickness=ON)
mdb.models['Model-1'].SurfaceToSurfaceContactStd(adjustMethod=NONE,
    clearanceRegion=None, createStepName='Step-1', datumAxis=None,
    initialClearance=OMIT, interactionProperty='IntProp-Cohesive', master=
    mdb.models['Model-1'].rootAssembly.surfaces['Surf-Trans1-2'], name='Int-3',
    slave=mdb.models['Model-1'].rootAssembly.surfaces['Surf-Middle-1'],
    sliding=FINITE, thickness=ON)
mdb.models['Model-1'].SurfaceToSurfaceContactStd(adjustMethod=NONE,
    clearanceRegion=None, createStepName='Step-1', datumAxis=None,
    initialClearance=OMIT, interactionProperty='IntProp-Cohesive', master=
    mdb.models['Model-1'].rootAssembly.surfaces['Surf-Middle-2'], name='Int-4',
    slave=mdb.models['Model-1'].rootAssembly.surfaces['Surf-Trans2-1'],
    sliding=FINITE, thickness=ON)
mdb.models['Model-1'].SurfaceToSurfaceContactStd(adjustMethod=NONE,
    clearanceRegion=None, createStepName='Step-1', datumAxis=None,
    initialClearance=OMIT, interactionProperty='IntProp-Cohesive', master=
```

```
    mdb.models['Model-1'].rootAssembly.surfaces['Surf-trans2-2'], name='Int-5',
    slave=mdb.models['Model-1'].rootAssembly.surfaces['Surf-Bottom-1'],
    sliding=FINITE, thickness=ON)

#create sets
mdb.models['Model-1'].rootAssembly.Set(faces=
    mdb.models['Model-1'].rootAssembly.instances['Part-Concrete-Top-1'].faces.getSequenceFromMask(
    mask=('[#20000 ]', ), )+\
    mdb.models['Model-1'].rootAssembly.instances['Part-Top-CLT-cut-1'].faces.getSequenceFromMask(
    mask=('[#1000000 ]', ), )+\
    mdb.models['Model-1'].rootAssembly.instances['Part-Trans2-2-1'].faces.getSequenceFromMask(
    mask=('[#100000 ]', ), )+\
    mdb.models['Model-1'].rootAssembly.instances['Part-Middle-CLT-1'].faces.getSequenceFromMask(
    mask=('[#10 ]', ), )+\
    mdb.models['Model-1'].rootAssembly.instances['Part-Trans-2-1'].faces.getSequenceFromMask(
    mask=('[#10 ]', ), )+\
    mdb.models['Model-1'].rootAssembly.instances['Part-Bottom-CLT-1'].faces.getSequenceFromMask(
    mask=('[#10 ]', ), ), name='Set-Symmetry')
mdb.models['Model-1'].rootAssembly.makeIndependent(instances=(
    mdb.models['Model-1'].rootAssembly.instances['Part-Bottom-CLT-1'],
    mdb.models['Model-1'].rootAssembly.instances['Part-Trans-2-1'],
    mdb.models['Model-1'].rootAssembly.instances['Part-Middle-CLT-1'],
    mdb.models['Model-1'].rootAssembly.instances['Part-Concrete-Top-1'],
    mdb.models['Model-1'].rootAssembly.instances['Part-Top-CLT-cut-1'],
    mdb.models['Model-1'].rootAssembly.instances['Part-Trans2-2-1']))


#create boundary conditions
mdb.models['Model-1'].XsymmBC(createStepName='Initial', localCsys=None, name=
    'BC-1', region=mdb.models['Model-1'].rootAssembly.sets['Set-Symmetry'])
mdb.models['Model-1'].boundaryConditions['BC-1'].setValues(typeName=YSYMM)
mdb.models['Model-1'].boundaryConditions['BC-1'].setValues(typeName=ZSYMM)
mdb.models['Model-1'].rootAssembly.Set(edges=
    mdb.models['Model-1'].rootAssembly.instances['Part-Bottom-CLT-1'].edges.getSequenceFromMask(
    ('[#1 ]', ), ), name='Set-2')
mdb.models['Model-1'].DisplacementBC(amplitude=UNSET, createStepName='Initial',
    distributionType=UNIFORM, fieldName='', localCsys=None, name='BC-2',
    region=mdb.models['Model-1'].rootAssembly.sets['Set-2'], u1=SET, u2=SET,
    u3=UNSET, ur1=UNSET, ur2=UNSET, ur3=UNSET)
mdb.models['Model-1'].rootAssembly.Set(edges=
    mdb.models['Model-1'].rootAssembly.instances['Part-Concrete-Top-1'].edges.getSequenceFromMask(
    ('[#1 ]', ), ), name='Set-Displacement')
```

```
mdb.models['Model-1'].DisplacementBC(amplitude=UNSET, createStepName='Initial',
    distributionType=UNIFORM, fieldName='', localCsys=None, name=
    'BC-Displacement', region=
    mdb.models['Model-1'].rootAssembly.sets['Set-Displacement'], u1=UNSET, u2=
    SET, u3=UNSET, ur1=UNSET, ur2=UNSET, ur3=UNSET)
del mdb.models['Model-1'].boundaryConditions['BC-Displacement']
mdb.models['Model-1'].DisplacementBC(amplitude=UNSET, createStepName='Step-1',
    distributionType=UNIFORM, fieldName='', fixed=OFF, localCsys=None, name=
    'BC-Displacement', region=
    mdb.models['Model-1'].rootAssembly.sets['Set-Displacement'], u1=UNSET, u2=
    -60.0, u3=UNSET, ur1=UNSET, ur2=UNSET, ur3=UNSET)

#create history output
mdb.models['Model-1'].HistoryOutputRequest(createStepName='Step-1', name=
    'H-Output-Force', rebar=EXCLUDE, region=
    mdb.models['Model-1'].rootAssembly.sets['Set-2'], sectionPoints=DEFAULT,
    variables=('RF2', ))
mdb.models['Model-1'].rootAssembly.Set(name='Set-Displacement-points',
    vertices=
    mdb.models['Model-1'].rootAssembly.instances['Part-Bottom-CLT-1'].vertices.getSequenceFromMask(
    ('[#c ]', ), ))
mdb.models['Model-1'].HistoryOutputRequest(createStepName='Step-1', name=
    'H-Output-Displacement', rebar=EXCLUDE, region=
    mdb.models['Model-1'].rootAssembly.sets['Set-Displacement-points'],
    sectionPoints=DEFAULT, variables=('U2', ))

#Dividing top clt and concrete for mesh


#Mesh & seed of the model


#adjusting the finite sliding to small sliding for CLT


#new
mdb.models['Model-1'].rootAssembly.translate(instanceList=('Part-Bottom-CLT-1',
    'Part-Trans-2-1', 'Part-Middle-CLT-1', 'Part-Trans-1-1'), vector=(0.0,
    -10.0, 0.0))
mdb.models['Model-1'].rootAssembly.translate(instanceList=('Part-Bottom-CLT-1',
    'Part-Trans-2-1'), vector=(0.0, -10.0, 0.0))
mdb.models['Model-1'].rootAssembly.InstanceFromBooleanCut(cuttingInstances=(
```

```
    mdb.models['Model-1'].rootAssembly.instances['Part-Concrete-Top-1'], ),
    instanceToBeCut=
    mdb.models['Model-1'].rootAssembly.instances['Part-Trans-1-1'], name=
    'Part-Trans2-cut', originalInstances=DELETE)
mdb.models['Model-1'].rootAssembly.Instance(dependent=ON, name=
    'Part-Concrete-Top-1', part=
    mdb.models['Model-1'].parts['Part-Concrete-Top'])
mdb.models['Model-1'].rootAssembly.instances['Part-Concrete-Top-1'].translate(
    vector=(775.5, 0.0, 0.0))
mdb.models['Model-1'].rootAssembly.rotate(angle=90.0, axisDirection=(0.0, 80.0,
    0.0), axisPoint=(4030.5, 0.0, 450.0), instanceList=('Part-Concrete-Top-1',
    ))
mdb.models['Model-1'].rootAssembly.translate(instanceList=(
    'Part-Concrete-Top-1', ), vector=(-3580.5, 180.0, -450.0))
mdb.models['Model-1'].rootAssembly.Set(faces=
    mdb.models['Model-1'].rootAssembly.instances['Part-Trans-2-1'].faces.getSequenceFromMask(
    mask=('[#10 ]', ), )+\
    mdb.models['Model-1'].rootAssembly.instances['Part-Bottom-CLT-1'].faces.getSequenceFromMask(
    mask=('[#10 ]', ), )+\
    mdb.models['Model-1'].rootAssembly.instances['Part-Middle-CLT-1'].faces.getSequenceFromMask(
    mask=('[#10 ]', ), )+\
    mdb.models['Model-1'].rootAssembly.instances['Part-Trans2-cut-1'].faces.getSequenceFromMask(
    mask=('[#10000 ]', ), )+\
    mdb.models['Model-1'].rootAssembly.instances['Part-Top-CLT-cut-1'].faces.getSequenceFromMask(
    mask=('[#40000 ]', ), )+\
    mdb.models['Model-1'].rootAssembly.instances['Part-Concrete-Top-1'].faces.getSequenceFromMask(
    mask=('[#2000 ]', ), ), name='Set-Symmetry')
mdb.models['Model-1'].rootAssembly.makeIndependent(instances=(
    mdb.models['Model-1'].rootAssembly.instances['Part-Trans2-cut-1'],
    mdb.models['Model-1'].rootAssembly.instances['Part-Concrete-Top-1']))
mdb.models['Model-1'].ConstrainedSketch(gridSpacing=164.29, name='__profile__',
    sheetSize=6571.91, transform=
    mdb.models['Model-1'].rootAssembly.MakeSketchTransform(
    sketchPlane=mdb.models['Model-1'].rootAssembly.instances['Part-Bottom-CLT-1'].faces[3],
    sketchPlaneSide=SIDE1,
    sketchUpEdge=mdb.models['Model-1'].rootAssembly.instances['Part-Bottom-CLT-1'].edges[11],
    sketchOrientation=RIGHT, origin=(225.0, -20.0, 1627.5)))
mdb.models['Model-1'].rootAssembly.projectReferencesOntoSketch(filter=
    COPLANAR_EDGES, sketch=mdb.models['Model-1'].sketches['__profile__'])
mdb.models['Model-1'].sketches['__profile__'].Line(point1=(1522.5, 225.0),
    point2=(1522.5, -225.0))
mdb.models['Model-1'].sketches['__profile__'].VerticalConstraint(addUndoState=
```

```
    False, entity=mdb.models['Model-1'].sketches['__profile__'].geometry[6])
mdb.models['Model-1'].sketches['__profile__'].CoincidentConstraint(
    addUndoState=False, entity1=
    mdb.models['Model-1'].sketches['__profile__'].vertices[5], entity2=
    mdb.models['Model-1'].sketches['__profile__'].geometry[2])
mdb.models['Model-1'].rootAssembly.PartitionFaceBySketch(faces=
    mdb.models['Model-1'].rootAssembly.instances['Part-Bottom-CLT-1'].faces.getSequenceFromMask(
    ('[#8 ]', ), ), sketch=mdb.models['Model-1'].sketches['__profile__'],
    sketchUpEdge=
    mdb.models['Model-1'].rootAssembly.instances['Part-Bottom-CLT-1'].edges[11])
del mdb.models['Model-1'].sketches['__profile__']
mdb.models['Model-1'].rootAssembly.Set(edges=
    mdb.models['Model-1'].rootAssembly.instances['Part-Bottom-CLT-1'].edges.getSequenceFromMask(
    ('[#1 ]', ), ), name='Set-2')
mdb.models['Model-1'].rootAssembly.Surface(name='Surf-Concrete-bottom',
    side1Faces=
    mdb.models['Model-1'].rootAssembly.instances['Part-Concrete-Top-1'].faces.getSequenceFromMask(
    ('[#1fff ]', ), ))
mdb.models['Model-1'].rootAssembly.Surface(name='Surf-Top-CLT-1', side1Faces=
    mdb.models['Model-1'].rootAssembly.instances['Part-Top-CLT-cut-1'].faces.getSequenceFromMask(
    mask=('[#a13c89 ]', ), )+\
    mdb.models['Model-1'].rootAssembly.instances['Part-Trans2-cut-1'].faces.getSequenceFromMask(
    mask=('[#1ff ]', ), ))
mdb.models['Model-1'].rootAssembly.Surface(name='Surf-Top-CLT-2', side1Faces=
    mdb.models['Model-1'].rootAssembly.instances['Part-Top-CLT-cut-1'].faces.getSequenceFromMask(
    ('[#84202 ]', ), ))
mdb.models['Model-1'].rootAssembly.Surface(name='Surf-Trans1-1', side1Faces=
    mdb.models['Model-1'].rootAssembly.instances['Part-Trans2-cut-1'].faces.getSequenceFromMask(
    ('[#5c00 ]', ), ))
mdb.models['Model-1'].parts['Part-Top-CLT-cut'].Set(cells=
    mdb.models['Model-1'].parts['Part-Top-CLT-cut'].cells.getSequenceFromMask((
    '[#f ]', ), ), name='Set-3')
mdb.models['Model-1'].parts['Part-Top-CLT-cut'].sectionAssignments[0].setValues(
    region=mdb.models['Model-1'].parts['Part-Top-CLT-cut'].sets['Set-3'])
mdb.models['Model-1'].parts['Part-Top-CLT-cut'].materialOrientations[0].setValues(
    additionalRotationField='', additionalRotationType=ROTATION_NONE, angle=
    0.0)
del mdb.models['Model-1'].parts['Part-Top-CLT-cut'].materialOrientations[0]
mdb.models['Model-1'].parts['Part-Top-CLT-cut'].MaterialOrientation(
    additionalRotationType=ROTATION_NONE, axis=AXIS_1, fieldName='', localCsys=
    None, orientationType=GLOBAL, region=Region(
    cells=mdb.models['Model-1'].parts['Part-Top-CLT-cut'].cells.getSequenceFromMask(
```

```
    mask=('[#f ]', ), )), stackDirection=STACK_3)
mdb.models['Model-1'].parts['Part-Bottom-CLT'].materialOrientations[0].setValues(
    additionalRotationField='', additionalRotationType=ROTATION_NONE, angle=
    0.0)
mdb.models['Model-1'].parts['Part-Middle-CLT'].materialOrientations[0].setValues(
    additionalRotationField='', additionalRotationType=ROTATION_NONE, angle=
    0.0)
mdb.models['Model-1'].parts['Part-Trans-1'].materialOrientations[0].setValues(
    additionalRotationField='', additionalRotationType=ROTATION_ANGLE, angle=
    90.0, axis=AXIS_2, orientationType=SYSTEM)
mdb.models['Model-1'].parts['Part-Trans2-cut'].MaterialOrientation(
    additionalRotationField='', additionalRotationType=ROTATION_ANGLE, angle=
    90.0, axis=AXIS_2, fieldName='', localCsys=None, orientationType=SYSTEM,
    region=Region(
    cells=mdb.models['Model-1'].parts['Part-Trans2-cut'].cells.getSequenceFromMask(
    mask=('[#1 ]', ), )), stackDirection=STACK_3)
mdb.models['Model-1'].rootAssembly.regenerate()
del mdb.models['Model-1'].boundaryConditions['BC-Displacement']
mdb.models['Model-1'].rootAssembly.Surface(name='Surf-11', side1Faces=
    mdb.models['Model-1'].rootAssembly.instances['Part-Concrete-Top-1'].faces.getSequenceFromMask(
    ('[#4000 ]', ), ))
mdb.models['Model-1'].Pressure(amplitude=UNSET, createStepName='Step-1',
    distributionType=UNIFORM, field='', magnitude=0.00512, name=
    'Load-qload-bfloor', region=
    mdb.models['Model-1'].rootAssembly.surfaces['Surf-11'])
mdb.models['Model-1'].interactions['Int-5'].setValues(adjustMethod=NONE,
    bondingSet=None, enforcement=SURFACE_TO_SURFACE, initialClearance=OMIT,
    sliding=SMALL, supplementaryContact=SELECTIVE, thickness=ON)
mdb.models['Model-1'].interactions['Int-4'].setValues(adjustMethod=NONE,
    bondingSet=None, enforcement=SURFACE_TO_SURFACE, initialClearance=OMIT,
    sliding=SMALL, supplementaryContact=SELECTIVE, thickness=ON)
mdb.models['Model-1'].rootAssembly.Surface(name='Surf-Trans1-2', side1Faces=
    mdb.models['Model-1'].rootAssembly.instances['Part-Trans2-cut-1'].faces.getSequenceFromMask(
    ('[#8000 ]', ), ))
mdb.models['Model-1'].interactions['Int-3'].setValues(adjustMethod=NONE,
    bondingSet=None, enforcement=SURFACE_TO_SURFACE, initialClearance=OMIT,
    sliding=SMALL, supplementaryContact=SELECTIVE, thickness=ON)
mdb.models['Model-1'].interactions['Int-2'].setValues(adjustMethod=NONE,
    bondingSet=None, enforcement=SURFACE_TO_SURFACE, initialClearance=OMIT,
    sliding=SMALL, supplementaryContact=SELECTIVE, thickness=ON)
mdb.Job(atTime=None, contactPrint=OFF, description='', echoPrint=OFF,
    explicitPrecision=SINGLE, getMemoryFromAnalysis=True, historyPrint=OFF,
```

```
    memory=90, memoryUnits=PERCENTAGE, model='Model-1', modelPrint=OFF,
    multiprocessingMode=DEFAULT, name='Job-bfloor-otherdir-5layers',
    nodalOutputPrecision=SINGLE, numCpus=1, numGPUs=0, queue=None,
    resultsFormat=ODB, scratch='', type=ANALYSIS, userSubroutine='', waitHours=
    0, waitMinutes=0)
mdb.models['Model-1'].rootAssembly.PartitionCellByPlaneThreePoints(cells=
    mdb.models['Model-1'].rootAssembly.instances['Part-Concrete-Top-1'].cells.getSequenceFromMask(
    ('[#1 ]', ), ), point1=
    mdb.models['Model-1'].rootAssembly.instances['Part-Top-CLT-cut-1'].vertices[31]
    , point2=
    mdb.models['Model-1'].rootAssembly.instances['Part-Top-CLT-cut-1'].vertices[12]
    , point3=
    mdb.models['Model-1'].rootAssembly.instances['Part-Top-CLT-cut-1'].vertices[30])
mdb.models['Model-1'].rootAssembly.PartitionCellByPlaneThreePoints(cells=
    mdb.models['Model-1'].rootAssembly.instances['Part-Trans2-cut-1'].cells.getSequenceFromMask(
    ('[#1 ]', ), ), point1=
    mdb.models['Model-1'].rootAssembly.instances['Part-Trans2-cut-1'].vertices[6]
    , point2=
    mdb.models['Model-1'].rootAssembly.instances['Part-Trans2-cut-1'].vertices[19]
    , point3=
    mdb.models['Model-1'].rootAssembly.instances['Part-Trans2-cut-1'].vertices[7])
mdb.models['Model-1'].rootAssembly.seedPartInstance(deviationFactor=0.1,
    minSizeFactor=0.1, regions=(
    mdb.models['Model-1'].rootAssembly.instances['Part-Bottom-CLT-1'],
    mdb.models['Model-1'].rootAssembly.instances['Part-Trans-2-1'],
    mdb.models['Model-1'].rootAssembly.instances['Part-Top-CLT-cut-1'],
    mdb.models['Model-1'].rootAssembly.instances['Part-Trans2-cut-1'],
    mdb.models['Model-1'].rootAssembly.instances['Part-Concrete-Top-1']), size=
    20.0)
mdb.models['Model-1'].rootAssembly.generateMesh(regions=(
    mdb.models['Model-1'].rootAssembly.instances['Part-Bottom-CLT-1'],
    mdb.models['Model-1'].rootAssembly.instances['Part-Trans-2-1'],
    mdb.models['Model-1'].rootAssembly.instances['Part-Top-CLT-cut-1'],
    mdb.models['Model-1'].rootAssembly.instances['Part-Trans2-cut-1'],
    mdb.models['Model-1'].rootAssembly.instances['Part-Concrete-Top-1']))
mdb.models['Model-1'].rootAssembly.deleteMesh(regions=(
    mdb.models['Model-1'].rootAssembly.instances['Part-Bottom-CLT-1'],
    mdb.models['Model-1'].rootAssembly.instances['Part-Trans-2-1'],
    mdb.models['Model-1'].rootAssembly.instances['Part-Top-CLT-cut-1'],
    mdb.models['Model-1'].rootAssembly.instances['Part-Trans2-cut-1'],
    mdb.models['Model-1'].rootAssembly.instances['Part-Concrete-Top-1']))
mdb.models['Model-1'].rootAssembly.seedPartInstance(deviationFactor=0.1,
```

```
    minSizeFactor=0.1, regions=(
    mdb.models['Model-1'].rootAssembly.instances['Part-Bottom-CLT-1'],
    mdb.models['Model-1'].rootAssembly.instances['Part-Trans-2-1'],
    mdb.models['Model-1'].rootAssembly.instances['Part-Middle-CLT-1'],
    mdb.models['Model-1'].rootAssembly.instances['Part-Top-CLT-cut-1'],
    mdb.models['Model-1'].rootAssembly.instances['Part-Trans2-cut-1'],
    mdb.models['Model-1'].rootAssembly.instances['Part-Concrete-Top-1']), size=
    20.0)
mdb.models['Model-1'].rootAssembly.generateMesh(regions=(
    mdb.models['Model-1'].rootAssembly.instances['Part-Bottom-CLT-1'],
    mdb.models['Model-1'].rootAssembly.instances['Part-Trans-2-1'],
    mdb.models['Model-1'].rootAssembly.instances['Part-Middle-CLT-1'],
    mdb.models['Model-1'].rootAssembly.instances['Part-Top-CLT-cut-1'],
    mdb.models['Model-1'].rootAssembly.instances['Part-Trans2-cut-1'],
    mdb.models['Model-1'].rootAssembly.instances['Part-Concrete-Top-1']))
```